



**Mononuclear Ruthenium Complexes Bearing N-Donor and  
NHC Ligands: Structure and Oxidative Catalysts.**

Hai-Jie Liu

Doctoral Thesis

Programa de Doctorat en Química

Dr. Lluís Escriche Martínez and Dr. Xavier Sala Román

Departament de Química

Facultat de Ciències

2014

Memòria presentada per aspirar al Grau de Doctor en Química per Hai-Jie Liu

Hai-Jie Liu

Vist i plau

Dr. Lluís Escriche Martínez  
Departament de Química  
Facultat de Ciències  
Universitat Autònoma de Barcelona

Dr. Xavier Sala Román  
Departament de Química  
Facultat de Ciències  
Universitat Autònoma de Barcelona

Bellaterra, 06 de novembre de 2014

## ACKNOWLEDGEMENTS

This thesis resumes all the work of my years in UAB but without the help of all the people who have shared the time with me, I would never be able to perform a single sentence of this thesis. For this reason I would like to thank to all of them for their important contribution to my Ph.D. inside and outside UAB.

My deepest gratitude goes first to Dr. Lluís Escriche, my supervisor, for his constant encouragement and guidance. Without his consistent and illuminating instruction, this thesis could not have reached its present form.

Second, I would like to express my heartfelt gratitude to Dr. Xavier Sala, my second supervisor, who led me into the world of ruthenium chemistry and oxidative catalysis. His careful and beneficial guidance, timely advice and frequent encouragement throughout the entire three years has helped me walk through all the stages of achieving the Doctor Degree. I have benefited greatly from his patience, encouragement and excellent guidance and also I am deeply moved by his serious attitude towards academic work.

I also would like to give my thanks to Dr. Jordi García-Antón and Dr. Roger Bofill, who gave me considerable help by means of suggestion, comments and criticism.

I would like to express my warmest gratitude to Prof. Antoni Llobet for giving to me the opportunity of being part of his group several times and also for providing me with valuable advice and access to the related resources on my experiments and thesis.

I also owe my sincere gratitude to Dr. Joan Aguiló and Dr. Laia Francàs who gave me valuable help for many of the experiments. I will also thank Pau Nolis for his kind help of assigning all the NMR spectrums.

Besides, I wish to say “Thanks!” to the other members and also friends of the lab Rosa Conzález, Marcos Gil, Jonathan De Tovar, Bing Jiang, Jordi Creus and Javi Heras, for their direct and indirect help to work out problems during the difficult time of all the work.

My thanks would also go to all the other tutors and teachers in the inorganic chemistry department.

Special thanks should go to my friends Dani Peral, Dani Herrera, Mercedes Cordon, Katia Samper, Selene Gil, Yang-Chun Xin, Tong Liu, Liu He, He-Lan Zhang, Yuan-Yuan Lu et al. who have put considerable time and effort in helping me deal with problems both in the lab and in daily life.

I am also deeply indebted to my beloved parents and my fiancé Qin Liu, for their loving considerations and great confidence in me all through these years, especially Qin, who has accompanied me through tough times during the three years.

I would also like to thank Universitat Autònoma de Barcelona for providing the opportunity and all the facilities.

Finally, the work performed in the present doctoral thesis has been possible thanks to the funding of:

Chinese Scholarship Council

MINECO CTQ2011-26440

# TABLE OF CONTENTS

<b>TABLE OF CONTENTS .....</b>	<b>III</b>
<b>Glossary of Terms and Abbreviations .....</b>	<b>V</b>
<b>Chapter I. General Introduction.....</b>	<b>1</b>
I.1. Carbene Chemistry .....	1
I.1.1. Carbenes: History and Properties.....	1
I.1.2. N-Heterocyclic Carbenes (NHCs) .....	3
I.2. Ruthenium and its role in oxidative catalysis .....	6
I.2.1. Ruthenium coordination chemistry.....	6
I.2.2. Artificial photosynthesis with ruthenium complexes.....	8
I.3. Alkene Epoxidation Catalyzed by Ruthenium Complexes.....	15
I.3.1. Nonasymmetric epoxidation catalyzed by ruthenium Complexes.....	16
I.3.2. Asymmetric epoxidation catalyzed by ruthenium Complexes .....	26
I.4.1. Stereospecific epoxidation catalyzed by ruthenium Complexes.....	34
I.4. References .....	36
<b>Chapter II. Objective.....</b>	<b>45</b>
<b>Chapter III. New Ru(II) Complexes bearing N and C-donor Ligands: Synthesis, Characterization and Catalytic Performance .....</b>	<b>47</b>
III.1. Introduction .....	47
III.2. Results and discussion.....	54
III.2.1. Synthesis and Structural Characterization of the CNNC Ligand L1 <sup>2+</sup> .....	54
III.2.2. Synthesis of Complexes C1-Cl/OH <sub>2</sub> , C2-Cl/OH <sub>2</sub> , C3-Cl/OH <sub>2</sub> and C4-Cl/OH <sub>2</sub> .....	57

III.2.3. Breakage of Ligand L1 <sup>2+</sup> .....	59
III.2.4. Characterization of the Complexes .....	60
III.2.5. Water Oxidation .....	85
III.2.6. Epoxidation of Alkenes .....	87
III.3. Conclusions .....	96
III.4. Experimental Section.....	97
III.5. References .....	105
III.6. Supporting Information .....	110
<b>Chapter IV. Enantioselective Alkene Epoxidation Catalyzed by Ru Carbene Chiral Polypyridyl Complexes.....</b>	<b>146</b>
IV.1. Introduction .....	146
IV.2. Results and Discussion.....	150
IV.2.1. Synthesis and characterization of [Ru <sup>III</sup> (L2)Cl <sub>3</sub> ].....	150
IV.2.2. Synthesis and Characterization of C5-Cl/OH <sub>2</sub> .....	151
IV.2.3. Asymmetric Epoxidation of Different Alkenes .....	157
IV.3. Conclusions .....	160
IV.4. Experimental Section .....	160
IV.5. References .....	164
IV.6. Supporting Information.....	167
<b>Chapter V. Conclusions .....</b>	<b>175</b>

## Glossary of Terms and Abbreviations

1D	Monodimensional
2D	Bidimensional
bpea	N,N-bis(pyridin-2-ylmethyl)ethanamine
bpy	2,2'-bipyridine
COSY	Correlation Spectroscopy
CV	Cyclic Voltammetry
d	Doublet
DCE	1,2-dichloroethane
DCM	Dichloromethane
dcp	1,4-dichlorophthalazine
DFT	Density Functional Theory
DMF	N,N-dimethylformamide
DMSO	Dimethyl sulfoxide
DOSY	Diffusion spectroscopy
DPV	Differential pulse voltammetry
E	Potential
E <sub>0</sub>	Standard potential
E <sub>1/2</sub>	Half-wave potential
ESI-MS	Electrospray Ionization Mass
GC	Gas chromatography
HMBC	Heteronuclear Multiple Bond Correlation Spectroscopy
HSQC	Heteronuclear single quantum coherence spectroscopy
IPrOH	Isopropanol
J	Coupling constant
M	Molar
m/z	Mass-to-Charge ratio
MeOH	Methanol
MLCT	Metal-to-ligand charge transfer
MS	Mass Spectrometry

NHC	N-Heterocycle Carbene
NMR	Nuclear Magnetic Resonance
NOESY	Nuclear Overhauser effect spectroscopy
PCET	Proton Coupled Electron Transfer
py	Pyridine
ROESY	Rotating frame nuclear Overhauser effect spectroscopy
s	Singlet
SSCE	Sodium Saturated Calomel Electrode
t	Triplet
TBAH	Tetra(N-butyl)ammonium hexafluorophosphate
TOCSY	Total Correlation Spectroscopy
TOF	Turn Over Frequency
TON	Turn Over Number
tpm	Tri(1H-pyrazol-1-yl)methane
trpy	2,2':6',2''-terpyridine
UV-vis	Ultraviolet-visible spectroscopy
vs.	versus
$\delta$	Chemical shift
$\lambda$	Wavelength
$\mu$	Ionic force
$\Sigma$	Sum



# Chapter I. General Introduction

## I.1. Carbene Chemistry

### I.1.1. Carbenes: History and Properties

The existence and important role of carbenes as transient intermediates in several reactions had been conceived by scientists long time before their authentic discovery.<sup>1,2</sup> In the late 1950s, the early chemistry of carbenes was studied by Skell and coworkers and a carbene intermediate was proposed to take part in the addition reaction of carbon atom into a carbon-carbon double bond.<sup>3</sup> Before 1960 carbenes were considered too reactive to be isolated. A key breakthrough came in 1962 when Fischer and coworkers introduced carbenes into inorganic and organometallic chemistry reporting the reactivity and stability of the tungsten carbene complex (C1), which was the first reported carbene-containing transition-metal complex (Figure 1).<sup>4</sup>

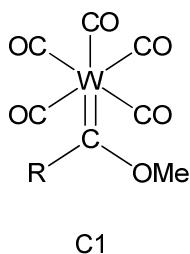


Figure 1. Drawing of the tungsten carbene complexes C1.

Carbenes are neutral compounds featuring a divalent carbon atom with only six electrons in its valence shell. The form of a prototype carbene is  $:CR_1R_2$ , where the carbon atom can be either linear or bent, each geometry describable by a certain degree of hybridization. Therefore, electronically, carbenes can be described either as singlet or triplet species. In singlet carbenes the carbon atoms are  $sp^2$ -hybridised with one  $sp^2$  orbital occupied by a lone pair of electrons while the other two orbitals connect with the external substituents with a bond angle comprised between 100 and 110°.

Furthermore, an empty p-orbital is perpendicular to the plane of the  $sp^2$ -orbitals (Figure 2a). However, in triplet carbenes, the two unpaired electrons could be either a  $sp^2$ -hybrid or a linear  $sp$ -hybrid, in which cases the two free electrons either occupy one  $sp^2$ -orbital and one p-orbital (Figure 2b) or occupy two p-orbitals (Figure 2c). Bond angles are in this case between  $136$  and  $180^\circ$ .<sup>1</sup>

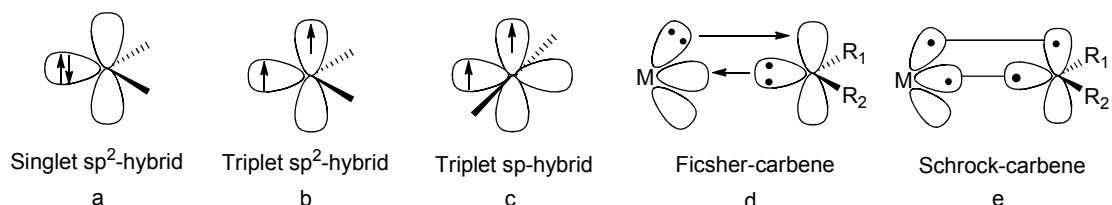


Figure 2. Electronic configurations of carbenes.

The ground-state spin multiplicity is a fundamental feature that dictates their reactivity.<sup>5</sup> Indeed, singlet carbenes feature a filled and a vacant orbital, and therefore, they should possess an ambiphilic character. On the other hand, triplet carbenes have two singly occupied orbitals and are generally regarded as diradicals.

The carbene ground-state multiplicity is related to the relative energy of the  $\sigma$  and  $p_\pi$  orbitals. The singlet ground state is favored by a large  $\sigma$ - $p_\pi$  separation,<sup>6</sup> similarly to what happens with the crystal-field theory and high or low-spin configurations. Therefore, the steric and electronic properties of the carbene substituents will be key for its ground-state multiplicity and, therefore, its reactivity.

Carbenes are usually used as ligands in organometallic chemistry given their interesting and modular electronic properties and stability. Fischer-carbenes and Schrock-carbenes are two major different patterns of carbene organometallic complexes. The formers have singlet ground-state multiplicity and are electrophilic at the carbon atom (Figure 2d). Accordingly, they prefer low oxidation state metals which are usually found in middle and late transition metals such as for example, Fe(0), Mo(0) or Cr(0). On the other hand, Schrock-carbenes (Figure 2e) are considered as triplet carbenes and prefer high oxidation states of the early transition metals like for instance Ti(IV) or Ta(V).<sup>7,8</sup>

### I.1.2. N-Heterocyclic Carbenes (NHCs)

Whereas the majority of carbenes are short-lived reactive intermediates, this picture does not hold for N-heterocyclic carbenes (NHCs), as reported in 1962 by Wanzlick.<sup>9</sup> In 1968 the parallel works of Öfele<sup>10</sup> and Wanzlick<sup>11</sup> described organometallic chromium and mercury complexes where NHCs were used as ligands for transition metals (**C2** and **C3**, Figure 3). Later, the research was continued by Lappert and Stone in the early 1970s.<sup>12</sup> After that, surprisingly, the field of NHCs as ligands in transition metal chemistry remained nearly dormant for the following 20 years. In 1991, a report by Arduengo and coworkers reported the isolation and extraordinary stability of the crystalline NHC ligand **L1** (Figure 3).<sup>13</sup> This first isolated carbene invoked people's enthusiasm for the investigation of NHCs as ligands in organometallic compounds.<sup>14</sup>

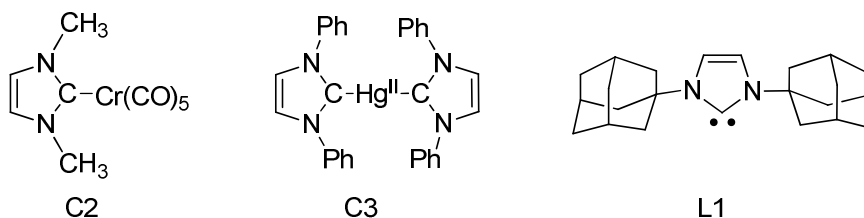
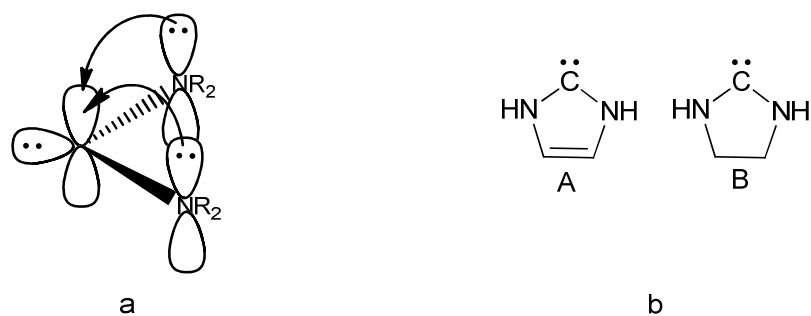
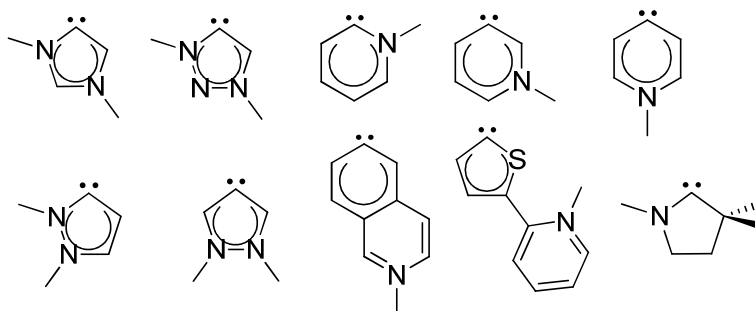


Figure 3. Structure of the carbene **C2**, **C3** and **L1**.

The interest on understanding the structure, reactivity and electronic properties of NHCs arise from the fact that, despite being neutral molecules, they are one of the strongest Lewis bases and nucleophilic molecules known.<sup>15</sup> NHCs are stabilized by their nitrogen atoms in the singlet-state (Fischer carbenes) while the unfavored triplet-state species is normally 70-80 kcal/mol higher in energy (Figure 4).<sup>16</sup> In addition, aromatic carbenes (in fact pseudo-aromatic given the predominance of the carbonic over the ylidic resonance structures,<sup>17</sup> Figure 4bA) are more stable than those none aromatic (Figure 4bB). These ligands are excellent  $\sigma$ -donors and therefore form rather strong metal-carbon bonds. Furthermore, their corresponding transition-metal complexes are often stable under ambient conditions.<sup>15</sup>



Recently a new family of ligands has been developed; the so-called “abnormal/mesoionic carbenes” in which the word “mesoionic” indicates that no heteroatom is located in the one or two vicinal positions to the carbene carbon atom (Figure 5).<sup>18</sup> Most of the mesoionic carbenes belong to the family of NHCs. For example in 2002 Crabtree and coworkers reported the first mesoionic metallation of imidazolium salts (**C4** in Figure 6). The reaction of the iridium polyhydride  $\text{IrH}_5(\text{PPh}_3)_2$  with pyridine-functionalized imidazolium salt afforded the iridium (III) complex **C4** in which the central metal ion was bounded to the mesoionic carbene position.<sup>19</sup> Later, other transition-metal complexes of Os, Pd, Ru, Rh including mesoionic carbene NHC ligands were also discovered.<sup>20,21</sup>



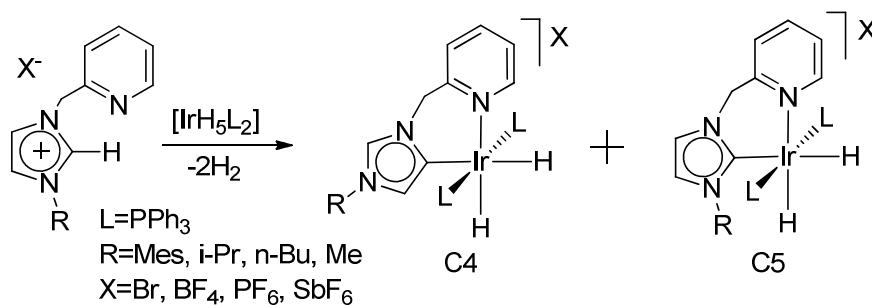


Figure 6. Synthetic process of the mesoionic metallation carbenes C4.

Complexes containing NHC coordinating ligands, no matters in their normal or mesoionic character, had seen wide applications in different areas of catalysis such as olefin metathesis,<sup>22</sup> hydrogenation of alkenes and alkynes,<sup>23</sup> transfer hydrogenation,<sup>24</sup> activation of C-H bonds,<sup>25</sup> as well as a wide set of oxidative transformations.<sup>26</sup>

Pd-NHC complexes, which have been deeply investigated during the last two decades, are one of the most prominent and fruitful catalytic families within this species. For instance, they were used as efficient catalysts for the aerobic oxidation of alcohols.<sup>27</sup>

Other transition metals such as Rh, Au, Ir and Ru also have been commonly and successfully employed in combination with NHCs for catalytic applications. The Rh NHC complexes, both normal (C6) and mesoionic (C7) ones, reported by Albrecht and coworkers in 2012 were introduced as excellent catalysts in the reaction of hydrolytic oxidation of dimethylphenylsilane to siloxane and silanol.<sup>28</sup> Au, which was normally considered inert also manifests good catalytic reactivity when coordinated with NHC ligands. An example is the C9 complex presented by the same group in 2013 showed excellent catalytic reactivity in the synthesis of oxazoline.<sup>29</sup> The Ir NHC complex C10 supported on silica was found to be capable of initiating the hydrogen transformation reaction.<sup>30</sup> In 2012 Stephen and coworkers reported the Ru NHC complex C11 catalyzing olefin selective hydrogenation reaction effectively.<sup>31</sup>

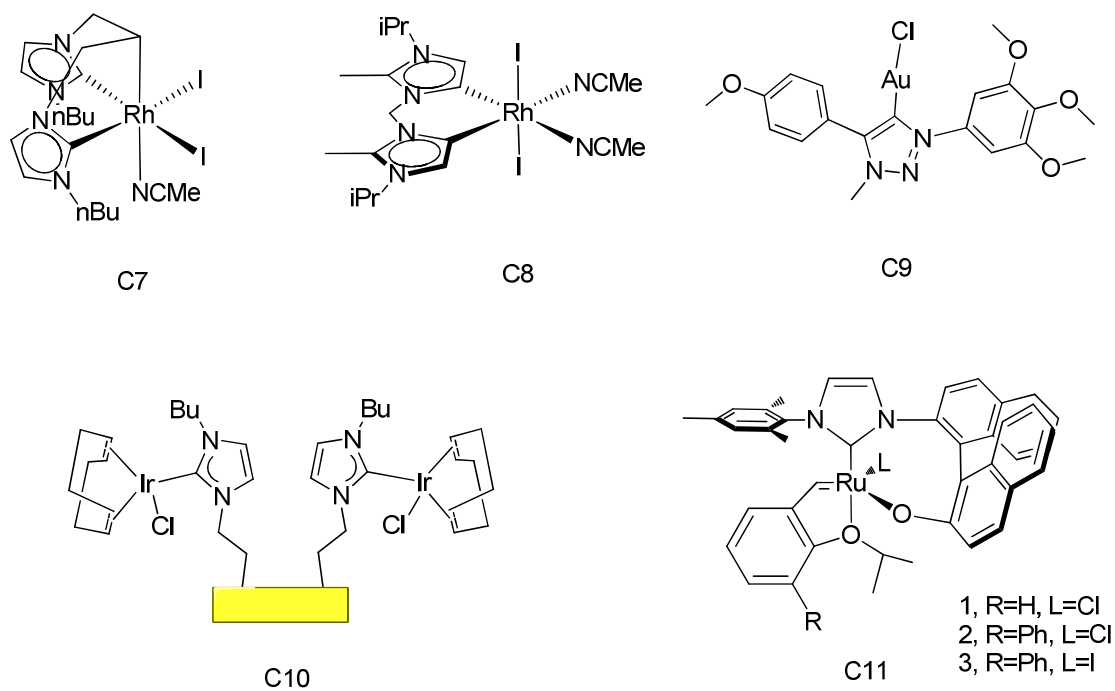


Figure 7. Drawing of C7 to C11.

## I.2. Ruthenium and its role in oxidative catalysis

The unique catalytic properties of Ru-carbene complexes stated in the previous section not only arise from the carbene type of ligands but also from the particular features of the Ru metal ion. Catalytic applications of Ru complexes have widely increased its scope and efficiency during the past few decades. Therefore, in the following subsections of this introduction we will focus on two of these catalytic processes where Ru-based catalysts play an important role: water oxidation and the epoxidation of alkenes.

### I.2.1. Ruthenium coordination chemistry

Coordination chemistry deals with the interactions of organic and inorganic ligands with metal centers. However, it is not strictly restricted to classical inorganic chemistry, also playing a key role on the study of supramolecular interactions and biomaterials.<sup>32</sup> Researchers are not only interested in their geometrical structure, electronic configuration or properties of the coordinating bonds but also pay much attention to the

application of these compounds in a wide variety of fields such as catalysis,<sup>33</sup> optics,<sup>34</sup> hydrometallurgical extraction,<sup>35</sup> medical and biomedical research,<sup>36</sup> semiconductors and nanomaterials,<sup>37</sup> among others.<sup>34</sup>

Nearly all transition metals have been employed in the area of coordination chemistry. Ruthenium, with the electronic configuration  $4d^75s^1$ , shows unique properties and displays the widest range of oxidation states among transition metals, ranging from -2 in  $[\text{Ru}(\text{CO})_2]^{2-}$  to +8 in  $\text{RuO}_4$ .<sup>38</sup> In addition, Ru compounds possess a high electron transfer capacity and a great ability to stabilize reactive metal species such as oxo-metals and metal-carbene complexes. Therefore, the wide range of oxidation states accessible along with the different coordination geometries available and the capacity of stabilizing highly-reactive metal species provides an interesting scenario for Ru complexes to be used as catalysts. Consequently, they have found application in many different fields, such as hydrogenation,<sup>39</sup> oxidation,<sup>40</sup> nucleophilic addition to C-C multiple bonds and C-C bond formation,<sup>41</sup> regioselective reductions<sup>42</sup> etc.

Due to the particular electrochemical properties of Ru complexes, an interesting situation emerges within the redox chemistry of these complexes. With one water molecule directly bonded to the metal centre, the successive oxidations from Ru(II) to Ru(IV) are accompanied by a sequential proton loss generating a proton-coupled electron transfer (PCET)<sup>43</sup> process and the corresponding properties would be affected by proton exchange (Figure 8). The Ru(III/II) and Ru(IV/III) redox processes will be pH dependent and will be shifted to lower potentials when a drop in the medium acidity takes place, attributing to the fact that higher oxidation states tend to be more acidic. This important property makes Ru-aqua complexes critical in the area of oxidation catalysis, especially in water oxidation and alkene epoxidation.

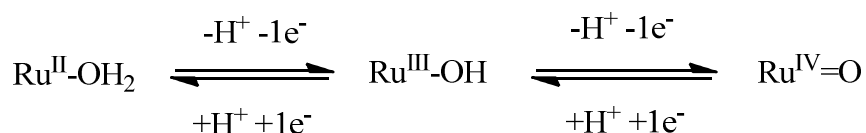


Figure 8. Ru proton-coupled electron transfer (PCET) process.

## I.2.2. Artificial photosynthesis with ruthenium complexes

Nowadays, the exploration of cheap and sustainable energy source is urgently needed for the welfare of our society in the near future.<sup>44</sup> However, only 2 % of all renewable energies used nowadays comes from solar energy thus the development of artificial systems to mimic the natural process is necessary and shows huge potentials.<sup>45</sup>

Nature has been harvesting sunlight as an energy source through the photosynthesis with the help of green plants, algae and cyanobacteria. The formation of dioxygen which comes from water oxidation is the most critical in the process of photosynthesis. In nature, water oxidation is promoted by the  $\mu$ -oxido- $\text{Mn}_4\text{Ca}$  cluster shown in Figure 9, the so-called oxygen-evolving complex (OEC) of Photosystem II (PS II),<sup>46</sup> the structure of which has been recently reported at 1.9 Å resolution.<sup>47</sup>

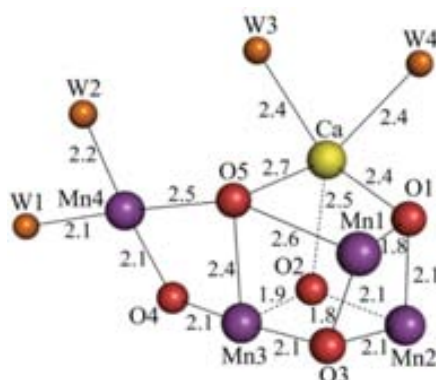
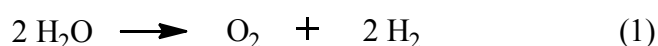


Figure 9. Structure of  $\mu$ -oxido- $\text{Mn}_4\text{Ca}$  cluster.<sup>47</sup>

In order to mimic nature one of the most feasible proposals is to split water into oxygen and hydrogen (Equation 1). Since water does not interact directly with the electromagnetic radiation emitted by sunlight, the overall redox process is divided into the extraction of protons and electrons (Equation 2) and the formation hydrogen (Equation 3).





The Ru-aqua are good candidate to mimic the natural process of water splitting initiated by Photosystem II.

These processes can be assembled in a three-component photo-electrochemical cell (PEC) as illustrated in Figure 10 in which the three process, light harvesting, water oxidation and proton reduction should be separated.<sup>48</sup> In order to assemble the three components into a robust single cell, a proton-exchange membrane (PEM) is mandatory which allows the diffusion of protons to the cathode while at the same time, physically separates the anodic and the cathodic compartments. (Figure 10)

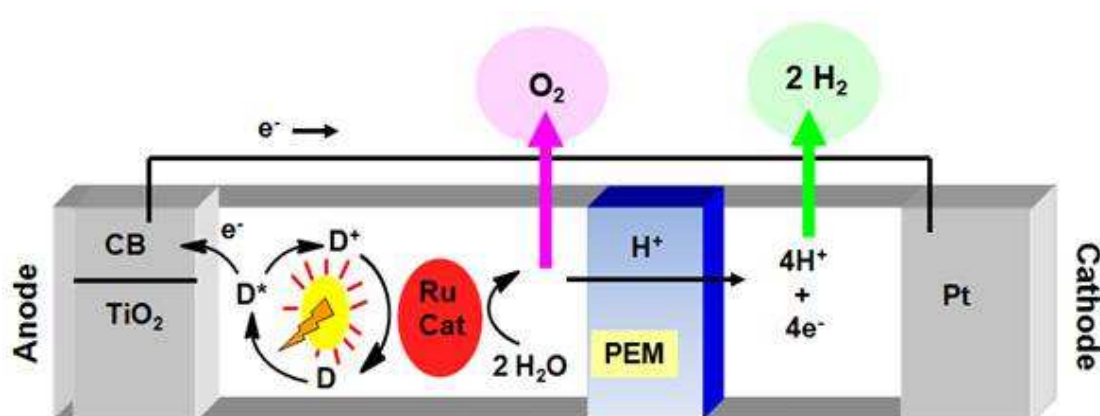


Figure 10. The three-component photo-electrochemical cell (PEC).<sup>49</sup>

### I.2.2.1. Water Oxidation Catalyzed by Dinuclear Ruthenium Complexes

The first reported Ru complex capable of oxidizing water to dioxygen, the so-called *blue dimer* (*cis,cis*-[(bpy)<sub>2</sub>(H<sub>2</sub>O)Ru(μ-O)Ru(H<sub>2</sub>O)(bpy)<sub>2</sub>]<sup>4+</sup>, **C12** in Figure11), was developed in 1982 by the group of T. J. Meyer.<sup>50</sup> However, its flexible μ-oxo bridge of reduced stability and prone to reductive cleavage hampered its stability under catalytic conditions.<sup>51</sup> Quite low TON (13.2) and TOF (0.24 min<sup>-1</sup>) values were reported under optimized conditions and by means of Ce(IV) as sacrificial oxidant.<sup>52</sup> However, this pioneering work was inspiring for later researchers that used similar strategies based on the inclusion of two Ru-aqua/oxo groups in a single molecule to efficiently extract four protons and four electrons from two water molecules and form an O-O bond.

Llobet and coworkers developed in 2004 a new and more efficient Ru dinuclear complex for water oxidation, *in,in*-{[Ru<sup>II</sup>(trpy)H<sub>2</sub>O]<sub>2</sub>(μ-bpp)}<sup>3+</sup> (*in,in*-Ru-bpp, **C13** in

Figure 11) using the bis(2-pyridyl)-3,5-pyrazolate anionic bridge (bpp) as backbone.<sup>53,54</sup> The result of these improvements is that through the full redox cycle the ligand would hold the Ru assembly intact, forming dioxygen faster and avoiding catalyst decomposition. Therefore, under optimized conditions, the TON and TOF increased to 512 and 0.78 min<sup>-1</sup>, respectively,<sup>55</sup> and the proposed mechanism assumes that the oxygen-oxygen bond is formed by means of an intramolecular mechanism.<sup>56</sup>

In 2007 Thummel and coworkers developed a family of Ru dinuclear complexes (**C14** in Figure 11) containing bis-tridentate polypyridine type of ligands as bridging scaffolds and substituted pyridines as complementary axial ligands. Those possessing -OCH<sub>3</sub> pyridine substituents manifested better catalytic performance and TON values were further increased to 689.<sup>57</sup>

Later on, the group of Sun developed a new Ru dinuclear complex with a pyridazine containing bridging ligand including lateral carboxylic groups (**C15** in Figure 11).<sup>58</sup> Modification of the bridging ligand by replacing the pyridazine scaffold by a phthalazine group (**C16** in Figure 11) results in a dramatic increase of the TON values from 1690 to 10400. **C16** is still nowadays the best performing Ru-based dinuclear water oxidation catalyst using Ce(IV) as sacrificial oxidant.

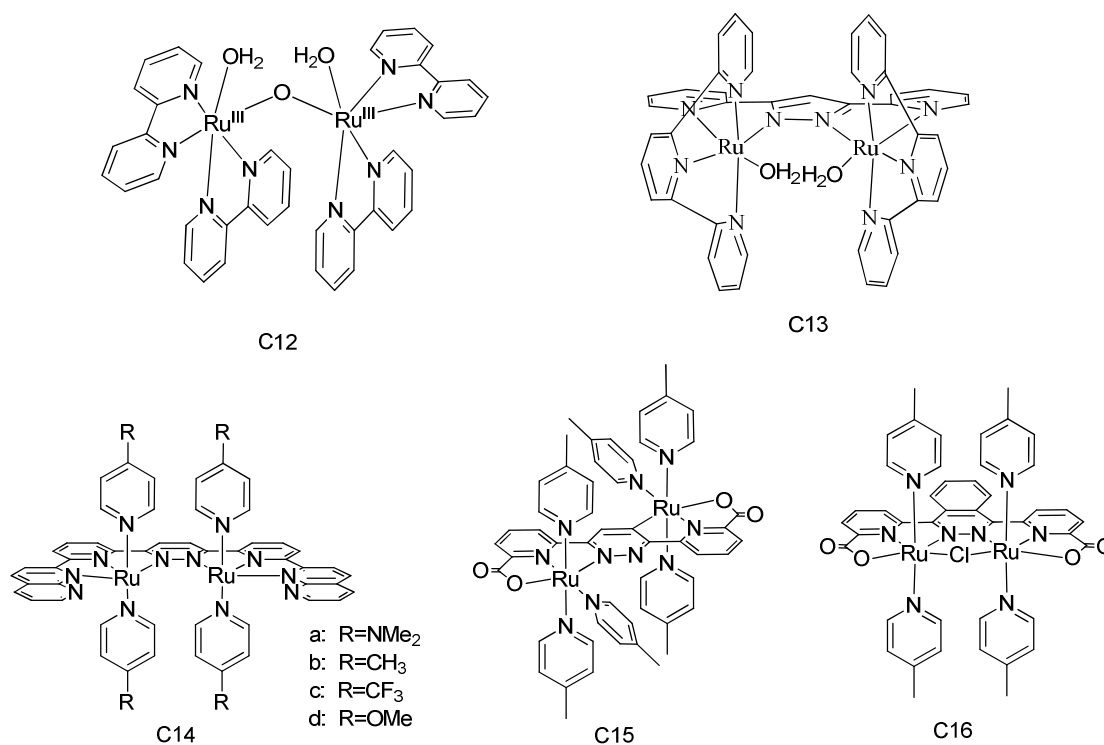


Figure 11. Drawing of C12, C13, C14, C15 and C16.

### I.2.2.2. Water Oxidation Catalyzed by Mononuclear Ruthenium Complexes

In 2005 Thummel and coworkers developed a series of non-aqua  $\text{Ru}^{\text{II}}\text{N}_6$  complexes such as  $[\text{Ru}(\text{dpp})(4\text{-Me-py})_2]^{2+}$  (C17 in Figure 13) and  $[\text{Ru}(\text{trpy})(4\text{-Me-py})_3]^{2+}$  (C18 in Figure 13) which also exhibited water oxidation capacity with TON values up to 416,<sup>59</sup> using the, called water nucleophilic attack (WNA) mechanism, which was also supported by density functional theory (DFT) calculations.<sup>60</sup>

Later on, the Meyer's group synthesized a  $\text{RuN}_5\text{-OH}_2$  complex<sup>61</sup> and proved that a  $\text{Ru}(\text{V})$  oxo species which will oxidize water into dioxygen is involved in the WNA process while the rate determining step is the decomposition of  $[\text{Ru}^{\text{IV}}\text{OO}]^{2+}$  species.

Sun and coworkers also synthesized a set of mononuclear Ru complexes bearing [2,2'-bipyridine]-6,6'-dicarboxylic acid and pyridine-2,6-dicarboxylic acid as ligand (C19 to C21).<sup>62</sup> (Figure 13) An interesting point of this work was the isolation and X-ray characterization of a seven coordinated intermediate (Figure 12), providing compelling

evidence of its existence and implication on the oxidation of water with Ru-based mononuclear species.<sup>63</sup>

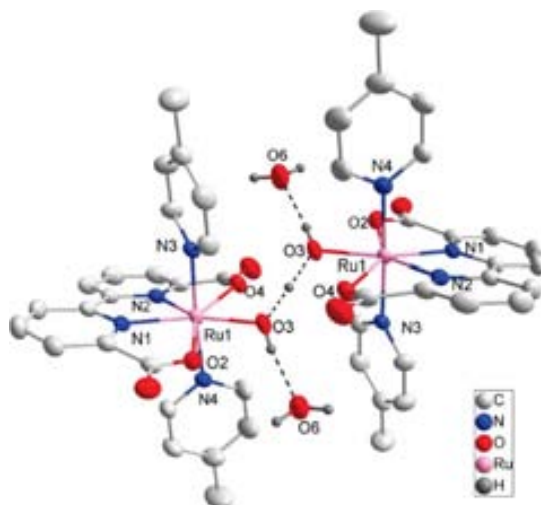


Figure 12. Crystal structure of the seven coordinated intermediate.<sup>63</sup>

Recently the catalytic activity of the Ru mononuclear complex  $[\text{Ru}(\text{bda})(\text{isoq})_2]$  ( $\text{H}_2\text{bda}$ =2,2'-bipyridine-6,6'-dicarboxylic acid;  $\text{isoq}$ =isoquinoline) (**C22** in Figure 13) toward water oxidation was described by Sun and Llobet.<sup>64</sup> This catalyst is really a breakthrough in water oxidation exhibiting TON about 8360 and  $\text{TOF} = 303 \text{ s}^{-1}$  when using  $\text{Ce}(\text{IV})$  as sacrificial oxidant, which are close to the reaction rate of the  $\mu$ -oxido- $\text{Mn}_4\text{Ca}$  cluster of photosystem II ( $\text{TOF} = 100\text{-}400 \text{ s}^{-1}$ ).

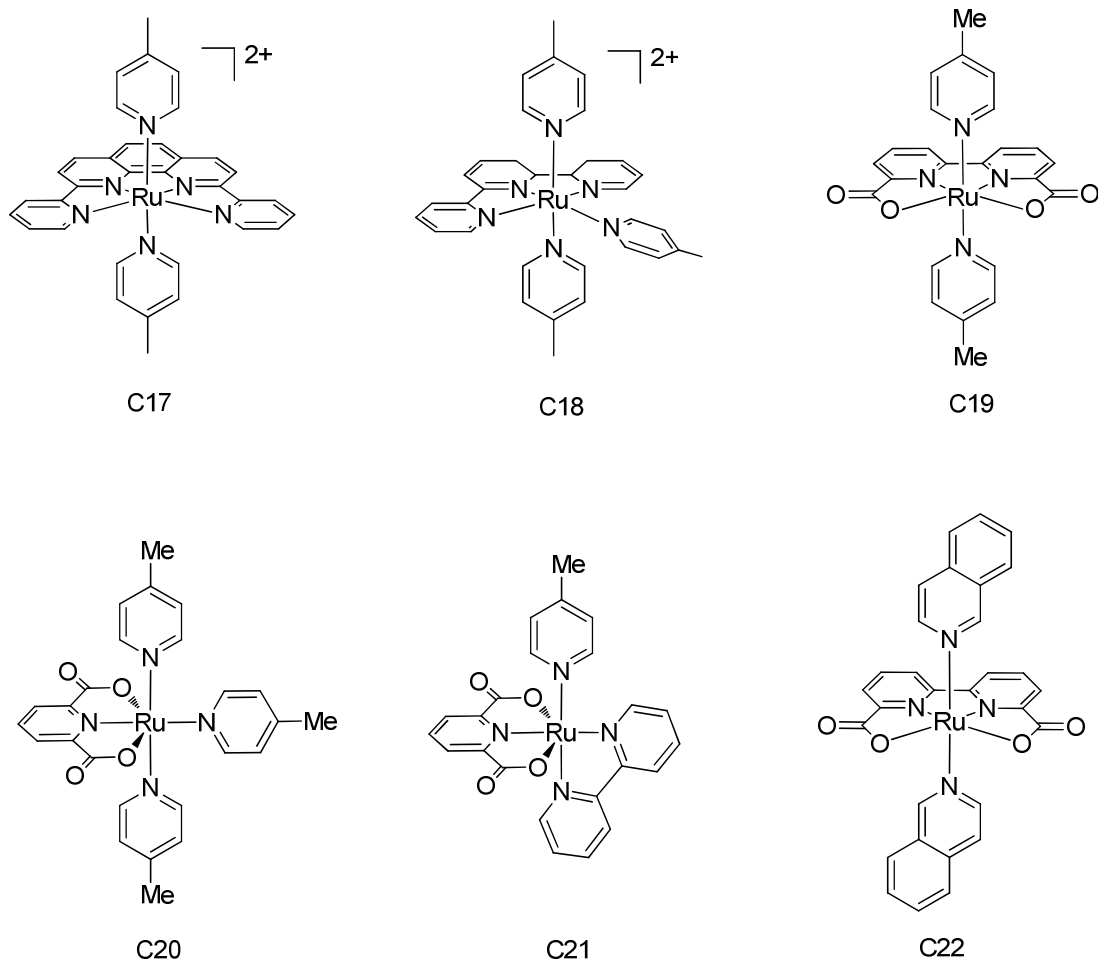


Figure 13. Structure of Ru mononuclear complexes C17 to C22.

### 1.2.2.3. Water Oxidation Catalyzed by Heterogeneous Ru Complexes

When Ru complexes were anchored onto solid surfaces through chemical bonds the catalyst-catalyst degradation observed in homogeneous media would be blocked. Furthermore, the immobilization of Ru complexes provides a much easier proposal to introduce the water oxidation catalyst in a real photoelectrochemical cell for the photoreduction of hydrogen. Consequently, different strategies have been developed to do this immobilization onto solid surfaces of thin films, mesoporous solids and nanomaterials.

To design efficient heterogeneous systems, some requirements should be fulfilled by the chosen support and the grafting methodologies:

- 1) The surface-catalyst system must be stable under highly oxidative catalytic conditions.
- 2) The system must be resistant towards strong acidic conditions.
- 3) The electron transfer from catalyst to electrode must be enough efficient to ensure efficient redox catalysis.

In fact, as early as 2007, Meyer and coworkers began to immobilize Ru complexes onto surfaces of ITO, TiO<sub>2</sub>, ZrO<sub>2</sub> and SnO<sub>2</sub>. However the extent of catalytic activity is limited (TON values lower than 3) due to the weak cohesion between the substrate and the catalyst.<sup>65</sup> Later on they improved the system and new complexes were anchored onto FTO<sup>66</sup> and TiO<sub>2</sub><sup>67</sup> surfaces *via* phosphonate linkage. The TON reached up to 11000 and 28000 respectively.

Later Sun and coworkers reported the covalent immobilization of one of their catalysts to functionalized carbon surfaces (**C23** in Figure 14).<sup>68</sup> The hybrid system resulted in a maximum TOF value of 1.6 s<sup>-1</sup> when an overpotential of 0.7 V was introduced.

From 2009 our group began to immobilize the Ru bpp dinuclear complex onto TiO<sub>2</sub> surfaces by the chemical modification of the Hbpp backbone with different functional groups. The first attempt was made introducing a methylenebenzoic acid in the pyrazole ring (**C24** in Figure 14).<sup>69</sup> The complex was successfully anchored in the solid support and the catalyst produced relative amounts of oxygen, but also remarkable amounts of CO<sub>2</sub> suggesting the degradation of the surrounding organic ligands under the highly oxidative and acidic media, leading to the subsequent catalytic deactivation. Nevertheless, this research sets up a basis for further insides in the anchoring strategies.

More recently, our group has developed a family of Ru-Hbpp complexes containing charged pyridylic rings on the trpy auxiliary ligands (**C25** in Figure 14). The presence of the positively charged ligand was expected to favour the electrostatic interaction between different solid support and the complex. Following this idea Ru-catalyst was immobilized onto silica, FTO-Nafion and FTO-TiO<sub>2</sub>.<sup>70</sup> However CO<sub>2</sub> was also generated during the catalytic cycles, which justifies the leaching of the complex observed after several hours. The data collected before the deactivation of the catalysts

showed that the supported Silica and FTO-Nafion catalysts exhibit good stability while the one immobilized on FTO-Nafion has better oxidation capacity.

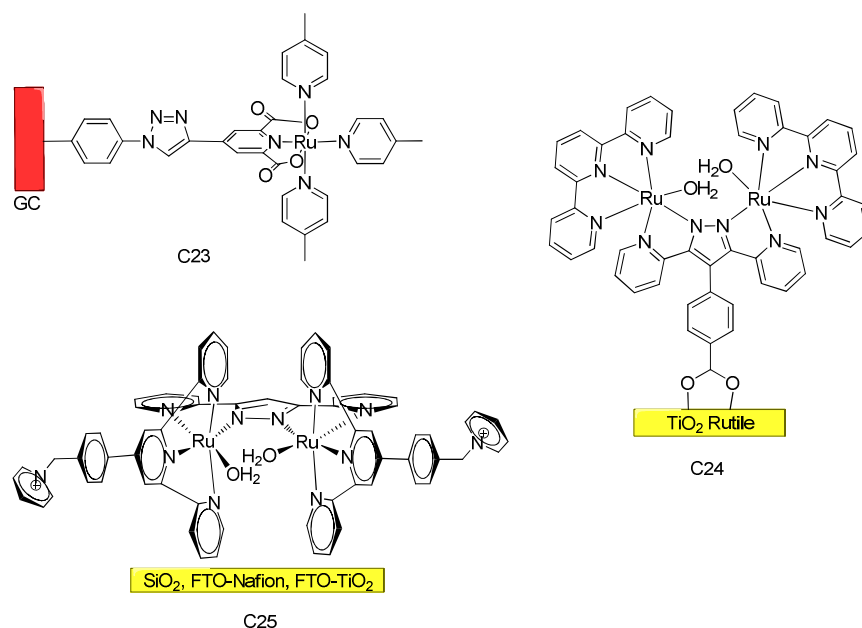


Figure 14. Drawing of heterogeneous Ru system **C23**, **C24** and **C25**.

### I.3. Alkene Epoxidation Catalyzed by Ruthenium Complexes.

As the development of synthetic and material chemistry, the production of epoxides has seen increasing importance during the past few decades. From 1970s both metal oxides and coordination metal complexes had been introduced as catalysts for the alkene epoxidation. Nearly each transition metal has been investigated thoroughly by researchers, such as Mn, Mo, Ti, Cu and Zr etc. Asymmetric alkene epoxidation is a critical area to produce wide variety of different epoxides and Nobel Prize was given to Barry Sharpless in 2001 for the honor of his great contribution in the field of asymmetric epoxidation. Since Ru oxo species always manifest excellent oxidation capacity, investigations on Ru complexes for alkene epoxidation has become a top research field. Herein, the introduction is divided into nonasymmetric epoxidation and asymmetric epoxidation part.

### I.3.1. Nonsymmetric epoxidation catalyzed by ruthenium Complexes

The discussion of nonsymmetric alkene epoxidation is made up classifying the reported works in those that no previous isolation of the active complex is done (Balavoine's method), and the procedures using Ru porphyrin complexes, Ru Schiff base complexes and Ru polypyridyl complexes.

#### I.3.1.1. Nonsymmetric alkene epoxidation using Balavoine's Method

In the area of alkene epoxidation, traditional ruthenium inorganic compound catalysts always lead to the oxidative cleavage of the double bond and very little amount of epoxide was obtained. Balavoine and coworkers considered that good electron donating ligands would moderate the oxidizing power of the  $\text{RuCl}_3/\text{NaIO}_4$  system thus the yield of the epoxide might be increased. Instead of synthesizing ruthenium complexes they added such ligands directly into the solution (Figure 15) and the product was separated by column chromatography.<sup>71</sup>

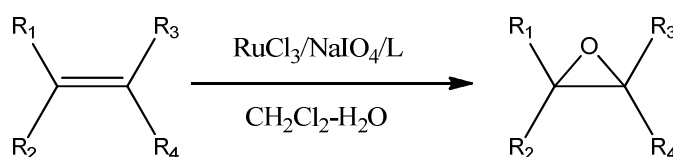


Figure 15. Balavoine's method for Ru epoxidation.

Initially, the ligand introduced by Balavoine and coworkers was bpy (2,2'-bipyridine).<sup>71</sup> Using this system they tested a series of substrate such as *trans*-stilbene, cyclohexene, cyclooctene, norbornylene etc. with the yield differed from 10% (cyclohexane) to 83% (*trans*-stilbene). Later in the same group, this method was employed with different substituents, phenanthrolines as ligands (L2, Figure 16) and the trail alkene was *trans*-stilbene.<sup>72</sup> The results varied depending on different ligands, but it was evidenced that the more electron donating ones, like L2-c slowed down the reaction rate while increased the selectivity and the yield of the epoxides.



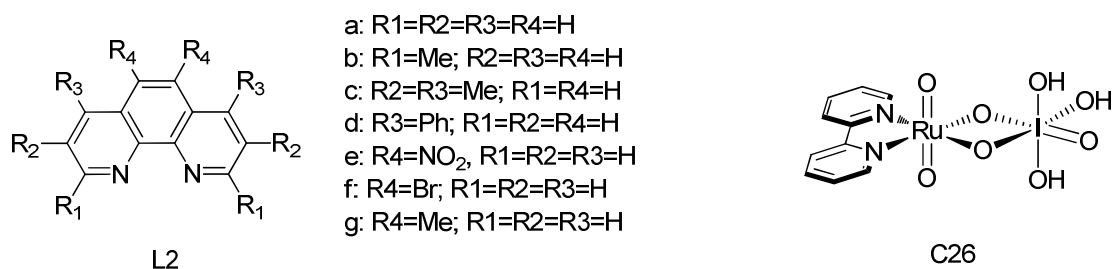


Figure 16. Structure of **L2** and **C26**.

Balavoine and coworkers speculated that the active species in the processes was a Ru(IV)-oxo intermediate,<sup>73</sup> an assumption similar to that made by Meyer and coworkers for the catalytic alkene epoxidation using trpy-bpy and bpy-py Ru complexes. In 1995, Griffith and coworkers attempted to clarify whether or not the Ru(IV)-oxo was the active species for Balavoine's method<sup>74</sup> using RuCl<sub>3</sub>/bpy reagent and the complex of *trans*-[Ru(H<sub>2</sub>O)<sub>2</sub>(bpy)<sub>2</sub>]<sup>2+</sup> in different experiences. They did not find the active species, but separated the complex [RuO<sub>2</sub>(bpy){IO<sub>3</sub>(OH)<sub>3</sub>}]·1.5H<sub>2</sub>O (**C26**, Figure 16) which showed similar catalytic capacity towards epoxidation as *trans*-[Ru(H<sub>2</sub>O)<sub>2</sub>(bpy)<sub>2</sub>]<sup>2+</sup>.<sup>74,75</sup>

In 1996, Sheldon and coworkers studied the alkene epoxidation under similar conditions but using Ru(dmsO)<sub>4</sub>Cl<sub>2</sub> in place of RuCl<sub>3</sub> in CH<sub>2</sub>Cl<sub>2</sub> with t-BuOOH as terminal oxidant. The results showed that the Ru(dmsO)<sub>4</sub>Cl<sub>2</sub>/pymox (pymox: (5-phenyl-2-(pyridin-2-yl)oxazol-4-yl)methanol) system was the best catalyst for most of the alkenes.<sup>76</sup>

### I.3.1.2. Nonsymmetric alkene epoxidation with Ru porphyrin complexes

The Ru porphyrin complexes have constituted an important field of catalysts for the epoxidation of alkenes. In 1984, John Groves's group developed the dioxo complex: [Ru<sup>VI</sup>(TMP)(O)<sub>2</sub>] (TMP: tetramesitylporphyrinato) (**C27**, Figure 17).<sup>77</sup> The alkene epoxidation proceeded in a Ru(VI)– Ru(II) cycle with the help of O<sub>2</sub>, but, the yield was not so high (45.6% for the norbornene). The same complex was studied by Bernd Scharbert's group in 1995 with the substrate of propene and oct-1-ene.<sup>78</sup> They found that the partial oxidation of the substrates generate CO, which forms Ru<sup>II</sup>(TMP)CO species and deactivate the catalyst. In 2003, Haruo Inoue and coworkers reported that the Ru<sup>II</sup>(TMP)CO complex (**C27** coordinated by CO) could be used as a photosensitizer

for alkene epoxidation with high quantum yield and selectivity. Isotope labeling experiments confirmed that the oxygen atom of the epoxide came from one water molecule.<sup>79</sup>

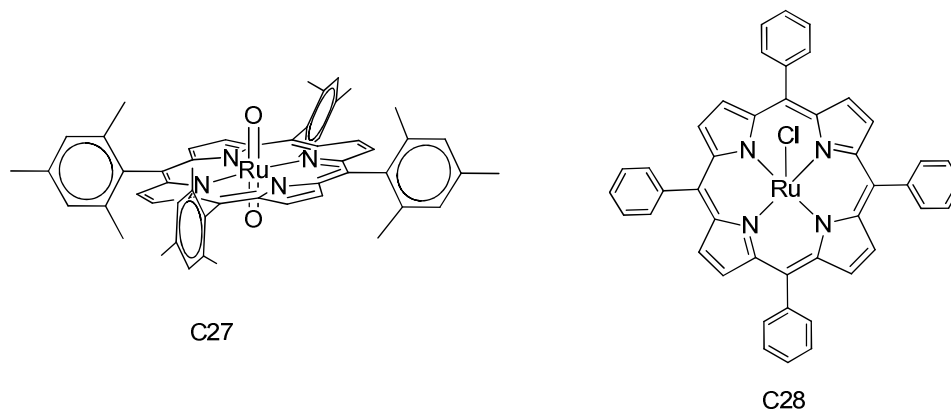


Figure 17. Structure of the porphyrin complexes **C27** and **C28**.

In 1996, Tsunehiko Higuchi's group used a Ru porphyrin complex based on the model of cytochrome P450 on the epoxidation of different alkenes and proved that the oxygen of the epoxide came from the oxidant, 2,6-dichloropyridine N-oxide (Cl<sub>2</sub>pyNO). They also proved that oxidants containing electron donating substitutes, manifested higher epoxidation capacity under the same condition.<sup>80</sup>

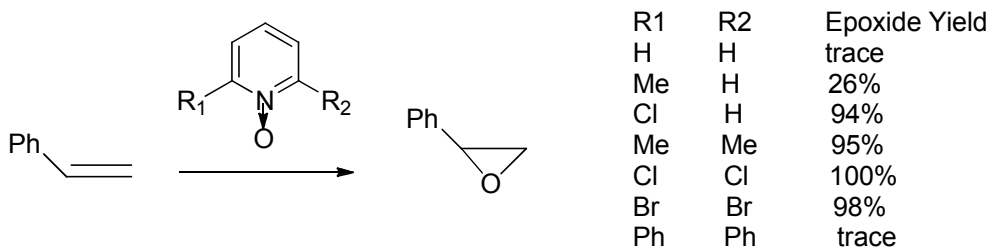


Figure 18. Epoxidation of styrene by pyridine N-oxide with different substitutes.

In 2010 Hongbing Ji and coworkers used the complex **C28** (Figure 17) as catalyst for the epoxidation of cyclohexene under mild conditions with an 86% of conversion and 85% of yield.<sup>81</sup>

### I.3.1.3. Nonasymmetric alkene epoxidation with Ru Schiff base complexes

The relatively simple synthetic procedures used in the preparation of the Schiff base ligands make the study of their Ru complexes one especially interesting area in the field of the Ru catalysis.

As early as 1989, Chi-Ming Che's group studied a family of Ru salen complexes with the general formula  $[\text{Ru}^{\text{III}}(\text{salen})(\text{X})(\text{Y})]^n$  [ $n = -1$ ,  $(\text{X})(\text{Y}) = (\text{CN})_2$ ;  $n = 0$ ,  $(\text{X})(\text{Y}) = (\text{PPh}_3)(\text{PBu}_3)$ ,  $(\text{PPh}_3)(\text{py})$ ;  $n = 1$ ,  $(\text{X})(\text{Y}) = (\text{PPh}_3)(\text{N}_3)$ ,  $(\text{PPh}_3)(\text{TsO})$  (TsO = tosylate anion)] as catalyst in the epoxidation of different olefins, but the yield was comparatively low as the substrates favored the oxidative cleavage of the double bonds.<sup>82</sup>

In 2003 Henrique E. Toma and coworkers synthesized the complex **C29** (Figure 19) in which the Cl substitute could be exchanged into aqua molecule<sup>83</sup> and used to catalyze the epoxidation of cyclohexene with a selectivity of the 95%.<sup>84</sup>

In 2009 the group of Debabrata Chatterjee studied as catalysts the family of complexes **C30** to **C33** (Figure 19). The epoxide yield was not so high with most of selectivity lower than 50%. However they proposed that a  $[\text{Ru}^{\text{IV}}-\text{O}(\text{tBu})-\text{O}\cdot]$  radical species was the catalytically active intermediate in the experimental condition.<sup>85</sup>

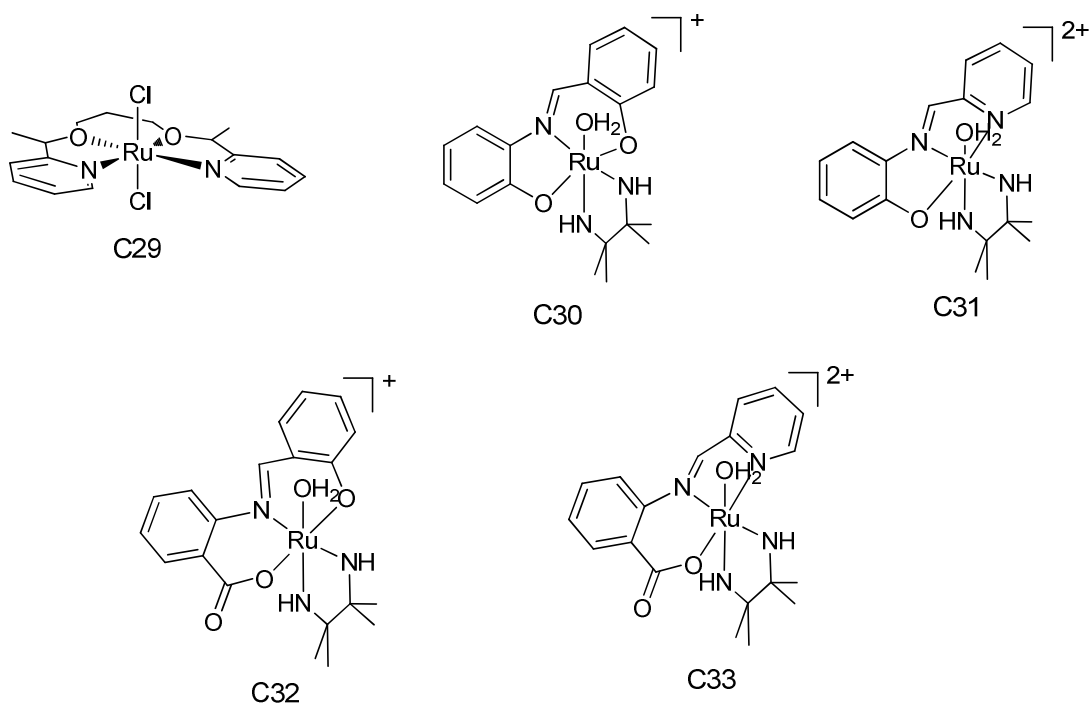


Figure 19. Structure of Ru Schiff base complexes **C29** to **C33**.

In 2009, the Mirkhani's group used as epoxidation catalyst a Ru(III) salophen complex (salophen: 2,2'-((1E,1'E)-(1,2-phenylenebis(azanylylidene)) bis(methanylylidene)) diphenol) which was then successfully supported onto a polymer, polystyrene.<sup>86</sup> The best results were obtained using NaIO<sub>4</sub> as terminal oxidant, with 100% of conversion and selectivity for cyclooctene, indene, heptene and dodec-1-ene.

Also in 2009 by Koichiro Jitsukawa and coworkers reported a Ru complex with tetradentate BABP (6,6-bis(benzoylamino)-2,2-bipyridine) ligand which was then immobilized onto FSM surface (a mesoporous silica, folded-sheet mesoporous material) with different methodologies and used as catalyst in the epoxidation of cyclooctene. The yields obtained with different terminal oxidants was comparatively low (less than 30%).<sup>87</sup>

#### **1.3.1.4. Nonasymmetric alkene epoxidation with Ru polypyridyl complexes**

Ru polypyridyl complexes are of great significance since they are coordinatively stable both in higher and lower oxidation states and a wide variety of oxidation states could be seen in a comparatively narrow potential range. Normally, Ru oxo complexes

containing polypyridyl ligands are known to be effective oxidation species especially for alkene epoxidation.

The first Ru polypyridyl complexes used for alkene epoxidation, the  $[(\text{bpy})_2(\text{py})\text{Ru}(\text{OH}_2)]^{2+}$  and  $[(\text{trpy})(\text{bpy})\text{Ru}(\text{OH}_2)]^{2+}$ . (trpy = 2,2':6',2''-terpyridine; bpy = 2,2'-bipyridine), were developed by the Thomas Meyer's group in 1986. Styrene, trans-stilbene and cis-stilbene were chosen as trial alkenes with co-oxidant of NaOCl. Although the conversion and selectivity were lower compared with later complexes, this study was considered as the steppingstone for successive researches.<sup>88</sup>

In 1987, Chi-Ming Che and coworkers used the  $[\text{Ru}^{\text{IV}}(\text{chbae})(\text{PPh}_3)(\text{py})]$  complex in the epoxidation of cyclohexene and styrene but the yield were only 10.3% and 7.3% respectively.<sup>89</sup> During the same year, the Che's group reported the use of *trans*- $[\text{Ru}^{\text{III}}(\text{phen})_2(\text{OH})(\text{OH}_2)]^{2+}$  and *trans*- $[\text{Ru}^{\text{III}}(\text{bpy})_2(\text{OH})(\text{OH}_2)]^{2+}$  complexes to catalyze the epoxidation with a number of alkenes and both the conversion and selectivity increased a lot (53.7% and 44.4% respectively for cyclohexene). They supposed that an intermediate of *trans*- $[\text{Ru}^{\text{IV}}(\text{bpy})_2\text{O}(\text{OH}_2)]^{2+}$  formed as active species during the catalytic reaction.<sup>90</sup>

In 1988 Mario Bressan and coworkers used the complexes,  $[\text{Ru}(\text{DPP})_2\text{Cl}]^+$  and  $[\text{Ru}(\text{PPY})_2\text{Cl}]^+$ , [DPP = 1,3-bis(diphenylphosphino)propane, PPY = 1-(diphenylphosphino)-(2-pyridyl)ethane] as catalysts, and reported that norbornene and cyclooctene showed the best selectivity while alkenes bearing aromatic substituents revealed the lowest. In addition, linear alkenes were selectively but called for longer time to react. A Ru(IV) oxo complex was considered to be the active species which was proved by isotopic exchange experiment.<sup>91</sup>

In 1994 Russell Drago's group used the complexes, *cis*- $[\text{Ru}(\text{dmp})_2(\text{S})_2]^{2+}$  (S = H<sub>2</sub>O; CH<sub>3</sub>CN) (dmp = 2,9-dimethyl-1,10-phenanthroline) as catalyst in front of norbornene in acetonitrile, with a selectivity of 94% for 2,3-epoxynorbornane. Further studies of this reaction indicated a free-radical mechanism in which H atom abstraction was the rate-determining step.<sup>92</sup>

The  $[\text{Ru}^{\text{II}}(\text{trpy})(\text{pic})(\text{H}_2\text{O})]^+$  complex (pic: picolinic acid) (**C34**) (Figure 21) was synthesized in 2006 by Debabrata Chatterjee and coworkers. Epoxidation of various

alkenes (styrene and substituted styrenes, stilbenes, cyclohexene, 1,2-dihydronaphthalene) had been studied for this complex in presence of t-BuOOH as terminal oxidant. The complex showed the best epoxidation capacity towards 4-Methoxystyrene (59% of yield).<sup>93</sup>

A series of Ru carbene complexes were reported in 2006 by Llobet's group (**C35** to **C37** in Figure 21). From the Pourbaix Diagram they were able to distinguish the Ru complexes experiencing a one-electron process or a two-electron process in aqueous solution. Complexes favoring two-electron processes showed better performance and selectivity in epoxidation than complexes favoring one-electron processes as it is illustrated in Table 1.<sup>94</sup>

Ru complex	epoxide yield%	cis (mM)	trans (mM)	cis/trans
$[\text{Ru}^{\text{II}}(\text{CNC})(\text{bpy})(\text{OH}_2)]^{2+}$	19.3	8.5	3.1	2.7
<i>trans</i> - $[\text{Ru}^{\text{II}}(\text{CNC})(\text{CN})(\text{OH}_2)]^{2+}$	33.7	20.2	trace	only cis
<i>cis</i> - $[\text{Ru}^{\text{II}}(\text{CNC})(\text{CN})(\text{OH}_2)]^{2+}$	22.0	13.2	—	only cis

Table 1. Alkene epoxidation catalyzed by **C35**, **C36** and **C37**.

In 2008 Olivier Hamelin and coworkers used as epoxidation catalyst towards cyclooctene the  $[\text{Ru}(\text{L5pyr})(\text{CH}_3\text{CN})]^{2+}$  complex (L5pyr = 2,6-bis-(6-ethyl-2,2'-bipyridyl)-pyridine). Comparison of the activity with regard to  $[\text{Ru}(\text{bpy})_2(\text{CH}_3\text{CN})_2]^{2+}$  and  $[\text{Ru}(\text{bpy})_2(\text{py})(\text{CH}_3\text{CN})]^{2+}$  confirmed that the addition of a fifth pyridine ligand in the coordination sphere improved the efficiency of the catalyst, with yield of 80% and TON of 40.<sup>95</sup>

In 2009 Mallayan Palaniandavar and coworkers synthesized the  $[\text{Ru}(\text{ntb})\text{Cl}_2]^+$  and  $[\text{Ru}(\text{mntb})\text{Cl}_2]^+$  [ntb: tris-(benzimidazol-2-ylmethyl)amine; mntb: tris(N-methylbenzimidazol-2-ylmethyl)amine complexes (**L3**) (Figure 21)]. The epoxidation essays proved that the formation of  $[\text{Cl}(\text{ntb}/\text{mntb})\text{Ru}-\text{O}-\text{O}-\text{CO}-\text{C}_6\text{H}_4\text{Cl}]^+$  and  $[\text{Cl}(\text{ntb}/\text{mntb})\text{Ru}-\text{O}-\text{O}-\text{tBu}]^+$  species are responsible for the oxidation activity. In addition, it illustrated that the electronic and steric effects of tripodal 4N ligands contributed to catalyze the effective oxidative transformation of organic compounds.<sup>96</sup>

In 2010 Mizuki Tada and coworkers supported successfully a Ru complex onto SiO<sub>2</sub> surface (**C38** in Figure 20) and assayed the epoxidation of alkenes showing high TONs for *trans*-stilbene (TON=2,100,000) and cyclopentene (TON=1,020,000) which were among the highest TONs reported in the field of metallic alkene epoxidation. The fact was attribute to the addition of isobutylaldehyde which forms the intermediate **Int-1** (Figure 20) which would reduce the reaction barrier significantly and the result was supported by DFT calculations.<sup>97</sup>

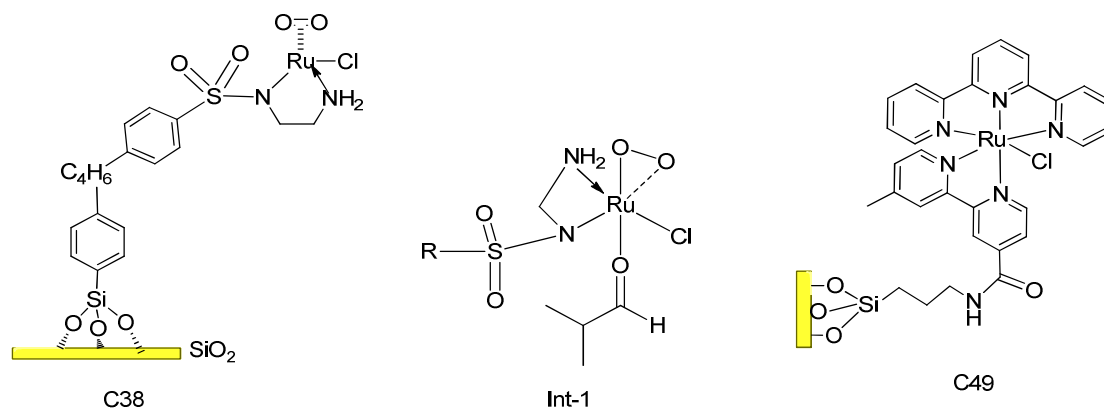


Figure 20. Structure of **C38**, **Int-1** and **C49**.

In 2010 Isabel Romero and coworkers reported the family of complexes with anionic and neutral N-donor ligands, **C39** to **C41** (Figure 21) and the alkene epoxidation was tested towards different substrates. They discovered that steric effects didn't play a major role while electronic effects strongly dominate the reactivity. The **C39** had the highest  $E^\circ(\text{IV}/\text{II})$  redox potential thus the reactivity was the highest for the major of the alkenes.<sup>98</sup>

More recently, the same group used the carbene complexes **C42** to **C44** (Figure 21) in the epoxidation of different alkenes, with high conversion and selectivities (>90% in most cases). **C43** was also tested in ionic liquid which was considered as the first example of Ru-based system for epoxidation catalysis under these conditions. The system displayed excellent reusability as well as a highly remarkable effectiveness and selectivity for the epoxide products.<sup>99</sup>

In 2011 G. K. Lahiri's group reported the *cis* and *trans* Ru isomers **C45** and **C46** (Figure 21) and established that the *cis*-isomer is an excellent catalyst for alkene epoxidation

while the *trans*-isomer was almost inactive even under the same conditions. The fact was supported by DFT calculations.<sup>100</sup>

In 2012, Nicolai Burzlaff and coworkers presented the Ru dicarbonyl complexes: **C47** and **C48** (Figure 21) which were employed as catalysts in the epoxidation of cyclohexene. Different co-oxidant had been studied for the two complexes with PhIO showing the best activity (the yield was 68.6% and TON was 20.6).<sup>101</sup>

The [Ru(terpy)(bpy)]<sup>2+</sup> complex was immobilized onto the surface of SiO<sub>2</sub> through a pseudo-peptide bond (**C49** in Figure 20) by Louloudi and coworkers in 2012. The catalytic epoxidation ability of the heterogeneous system was studied and cyclooctene gave the highest epoxide product (70% of yield).<sup>102</sup>

Recently in 2013, Llobet's group synthesized the Ru dinuclear complex **C50**. Their catalytic epoxidation performance and the results were especially good for cyclohexene with TON 1580 and TOF 40.6 min<sup>-1</sup>. They also reported that alkenes with electron donor substituent showed better reactivity than those with electron withdrawer groups.<sup>103</sup>

In 2013, the group of Goutam Lahiri used as catalyst the complex, **C51** (Figure 21) and a wide variety of alkenes had been introduced as epoxidation substrates. The results showed that terminal alkenes were the most effective substrates towards the epoxidation process except for styrene which turned out to be "over-oxidized". In addition, Ru-oxo species was considered to be the active intermediate and this was supported by DFT calculation.<sup>104</sup>



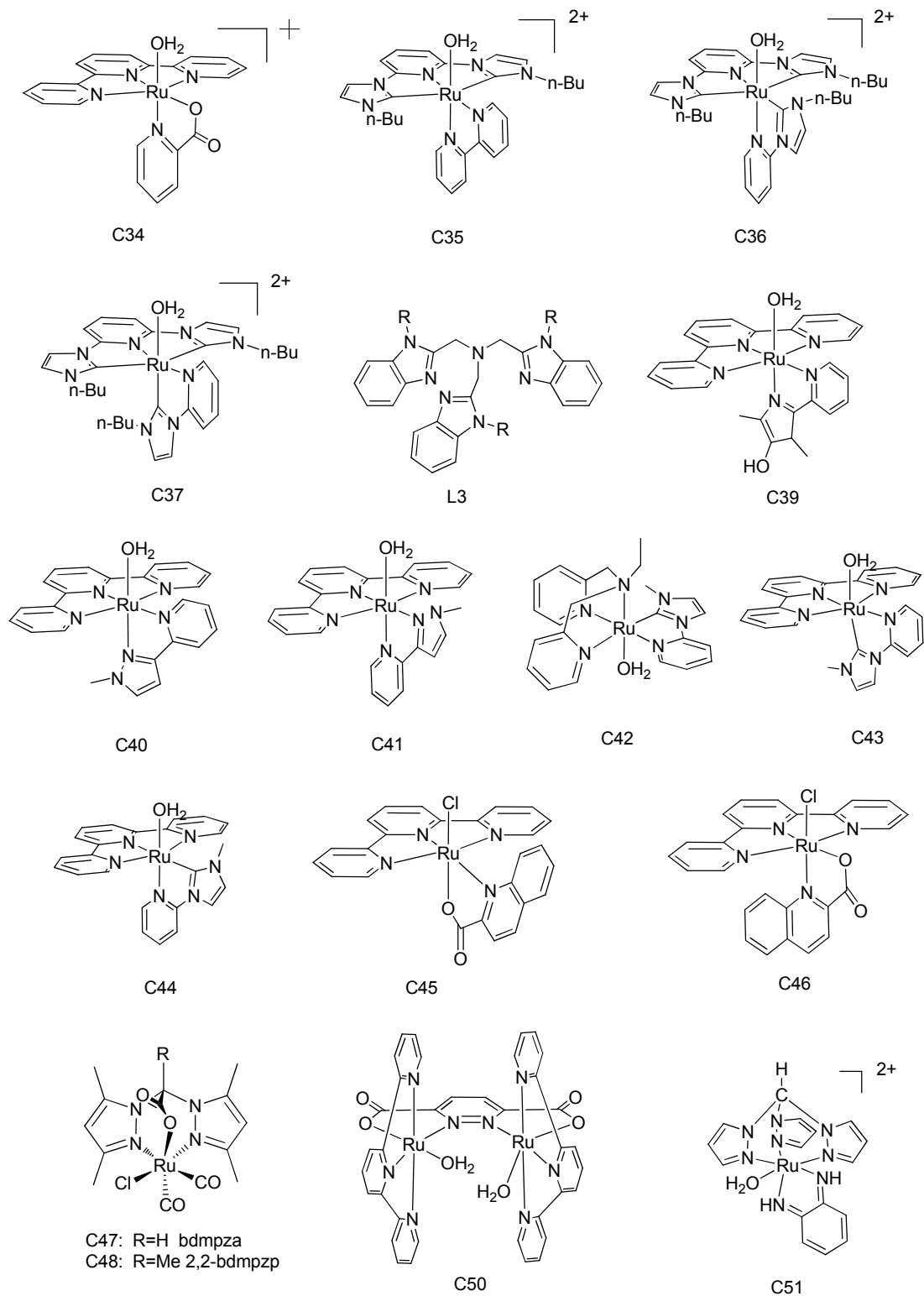


Figure 21. Drawing of C34, to C37, L3, C39 to C48, C50 and C51.

### I.3.2. Asymmetric epoxidation catalyzed by ruthenium Complexes

The catalyst for asymmetric alkene epoxidation which can be found in the literature were classified following the same scheme used for the nonasymmetric systems.

#### I.3.2.1. Asymmetric alkene epoxidation using Balavoine's Method

In 1993, Li-Xin Dai's group introduced a group of chiral 2-pyridyl-oxazolines ligands (**L4** in Figure 22) into Balavine's system to catalyze the epoxidation of *trans*-stilbene and 1-phenyl-cyclohexene. Although the highest enantiomeric excess (ee) was only 21% this was the first catalytic asymmetric epoxidation system using chiral N-donor bidentate ligand and RuCl<sub>3</sub> as catalyst. The proposed mechanism assumed that ruthenium complex was first oxidized forming a chiral Ru oxo intermediate and then an oxene was transferred to the carbon-carbon double bond with the help of the Ru oxo species.<sup>105</sup>

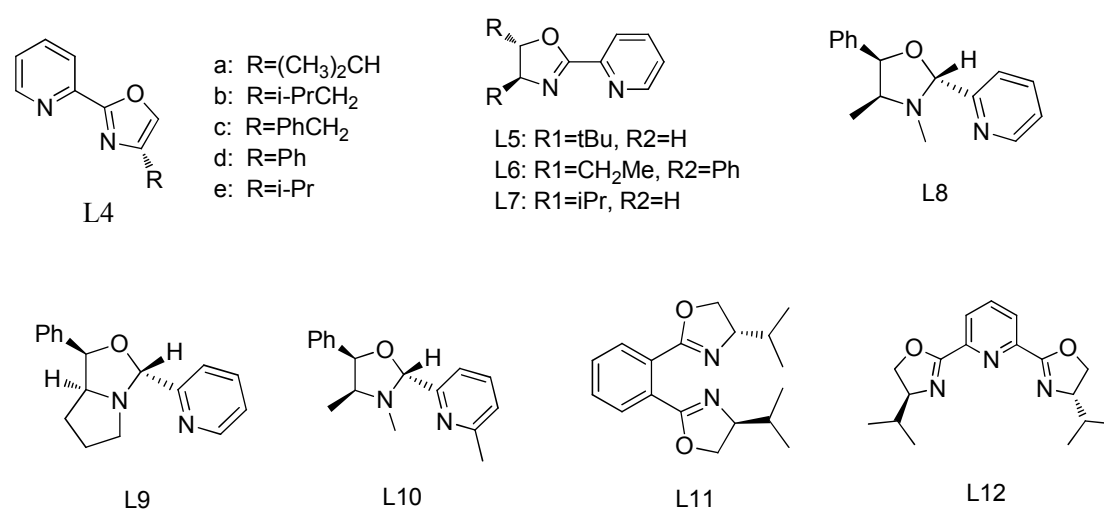


Figure 22. Structure of L4 to L12.

Later in 1995, B. Waegella and coworkers used a set of Ru complexes with oxazolidines derivatives (**L5-L12** in Figure 22) in the epoxidation of *trans*-stilbene. Although the ee of the epoxide obtained were pretty low with most of the substrates they discovered that the yield and selectivity were much higher for **L5** to **L10** compared with the **L11** and **L12**. They proposed that for the stereostructural reasons, **L5** to **L10** were pronged to

form *trans* ruthenium complexes while *cis* ruthenium complexes were easily formed with **L11** and **L12**.<sup>106</sup>

In 1998, Andreas Pfaltz's group introduced bis(dihydrooxazolyphenyl) oxalamide as ligands into Balavine's procedure to catalyze epoxidation of *trans*-stilbene and *trans*-1-phenylpropene. The result increased significantly with ee 69% and 58% for *trans*-stilbene and *trans*-1-phenylpropene respectively.<sup>107</sup>

### **I.3.2.2. Asymmetric alkene epoxidation with Ru porphyrin complexes**

In 1996 Zeev Gross and coworkers synthesized a homochiral ruthenium dioxo porphyrin complex **C52** (Figure 23) which was applied on the epoxidation of styrene. The best results were initially obtained using Cl<sub>2</sub>pyNO as terminal oxidants,<sup>108</sup> and subsequent modifications of the initial conditions increased significantly the conversion.<sup>109</sup> Although the ee was not the highest compared with other metalloporphyrin catalyst<sup>110</sup> this research was considered as the first utilization of homochiral ruthenium porphyrin as enantioselective epoxidation catalyst. The porphyrin scaffold was further modified with other chiral groups (**C53**, **C54** in Figure 23) by Zeev Gross' group and they obtained better ee (81%) and turnover number (551) for styrene.<sup>111</sup>

The substituent chiral R in the **C52-C54** complexes was also modified with cyclohexane auxiliaries (**L13**, Figure 23) by Gérard Simonneaux's group, but this new complexes didn't increase the yield and the highest ee was only 35%.<sup>112</sup>

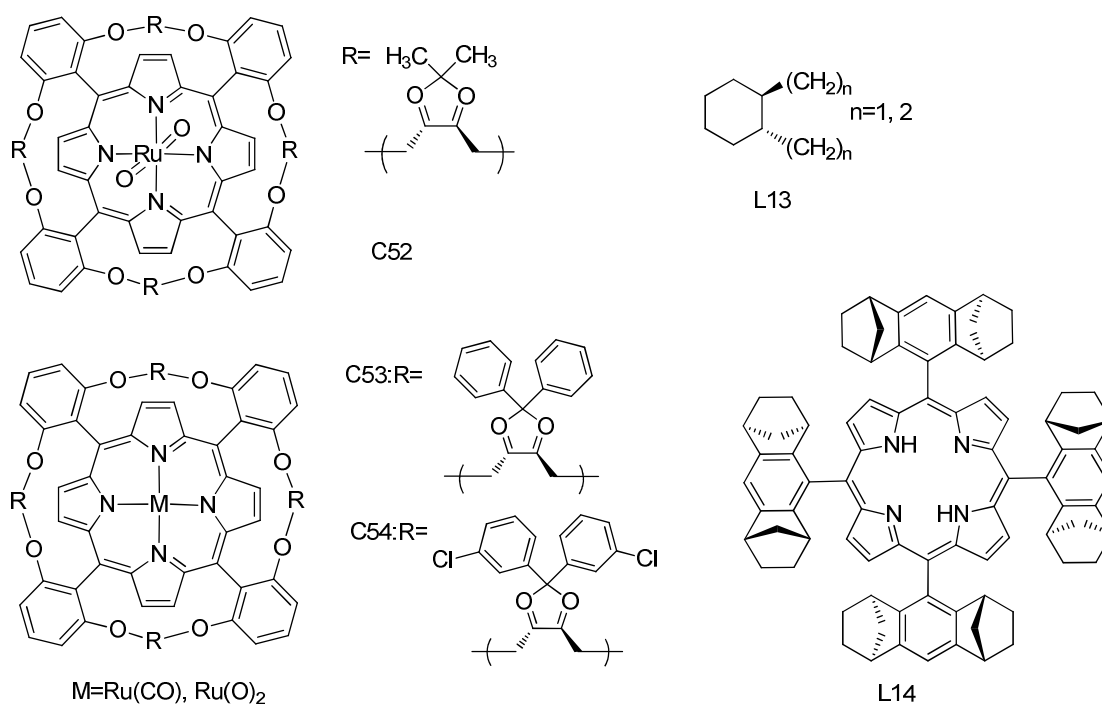


Figure 23. Drawing of **C52**, **C53**, **C54** and **L13**, **L14**.

As early as 1991 Ronald Halterman and coworkers had synthesized a manganese complex with a porphyrin ligand bearing four chiral anthracene derivatives (**L14**, Figure 23).<sup>113</sup> In 1997, A. Berkessel and coworkers changed the coordinated metal into Ru forming  $[\text{Ru}^{\text{II}}(\text{L14})\text{CO}]$  which was employed to catalyze the alkene epoxidation with different substrates achieving ee of 77% in some cases.<sup>114</sup> Che's group replaced CO by two Cl atoms coordinated onto the ruthenium centre (**C55** in Figure 24) making the charge of ruthenium increased from II to IV.<sup>115</sup> When styrene was introduced as trial alkene for epoxidation the turnover number reached up to 2190 and the ee to 69%.<sup>115</sup> Further modification of the complex resulted in dioxo group coordinated perpendicularly to the porphyrin planner forming which in the case of *cis*- $\beta$ -methylstyrene achieved a 73% of ee.<sup>116,117</sup>

The dichloro derivative of **C52**, the complex **C55** and the complex **C56** (Figure 24) were supported into a sol-gel matrix forming a heterogeneous catalyst system which exhibited good activity for the styrene epoxydation with TON's around 10000.<sup>115</sup> The good catalytic activity manifested by the immobilized chiral ruthenium porphyrin complexes induced to the Che's group to integrate these systems into ordered mesoporous molecular sieves MCM-41 and MCM-48. The catalytic activity in the

epoxydation of different alkenes exhibited TON from 3030 to 13450 and ee from 43% to 77%.<sup>118</sup> The related complexes **C57** (Figure 24) were also attached to a polymer of Melt-Processible Rubber (MPR)<sup>119</sup> giving epoxidation yields ranging from 62% to 98%.

The chiral groups of **C56** and **C57** were further modified by Berkessel and coworkers (**C58** and **C59** in Figure 24) and the catalytic experiences showed that **C58d** was the best catalyst for the tested alkenes, reaching TON's of 14200 for epoxidation while the ee value was about 80%.<sup>120</sup>

Recently, Thorsten Bach's group developed the new Ru chiral porphyrin complex **C60** (Figure 24) and used it as catalyst in the epoxidation of 3-vinylquinolone obtaining a 95% of yield and ee and 71% of yield. The fact was attributed to the formation of a set of hydrogen bonds between the substrate and the indol moiety of the complex which strongly influence their activity and the enantioselectivity. Later they expended the substrate to other derivatives of 3-vinylquinolone and the results also gave evidence to the former conclusion.<sup>121,122</sup>

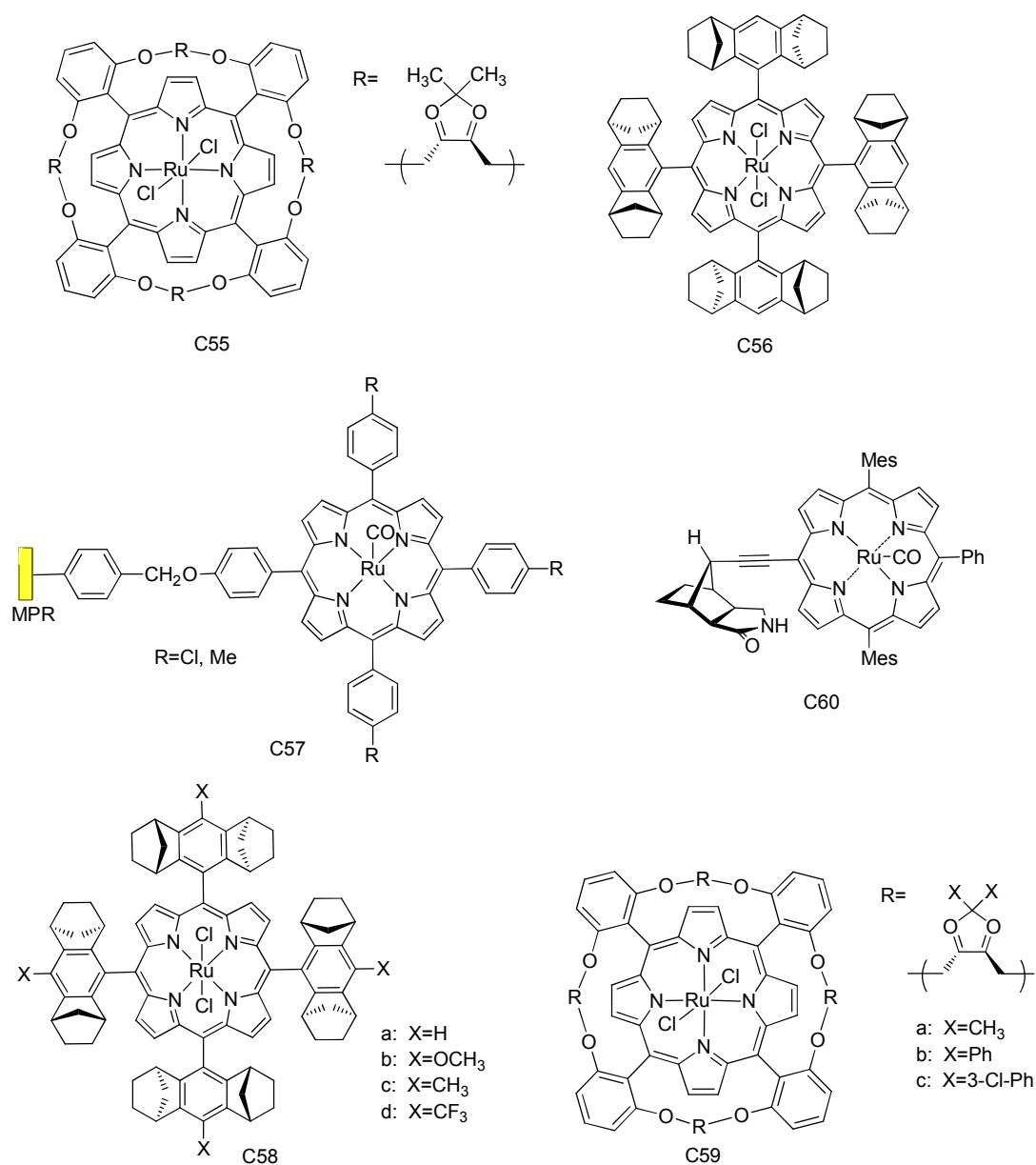


Figure 24. Drawing of Ru porphyrin complexes C55 to C60.

### I.3.2.3. Asymmetric alkene epoxidation with Ru Schiff base complexes.

In 1994 R. Kureshy and coworkers developed the family of chiral Ru(II) Schiff base complexes, C61-7 and C61-8 which were studied as epoxidation catalysts towards a series of styrene derivatives obtaining ee ranging from 45% to 80%.<sup>123</sup> In 1999 the same group completed the family of C61 complexes (Figure 25). The complexes were used as catalysts for enantioselective epoxidation of 1,2-dihydronaphthalene and the

results revealed that catalysts bearing electron donating substituents favored the enantioselectivity.<sup>124</sup> Later the same group synthesized similar Ru complexes (**C62**, Figure 25) and similar conclusion had been achieved.<sup>125</sup>

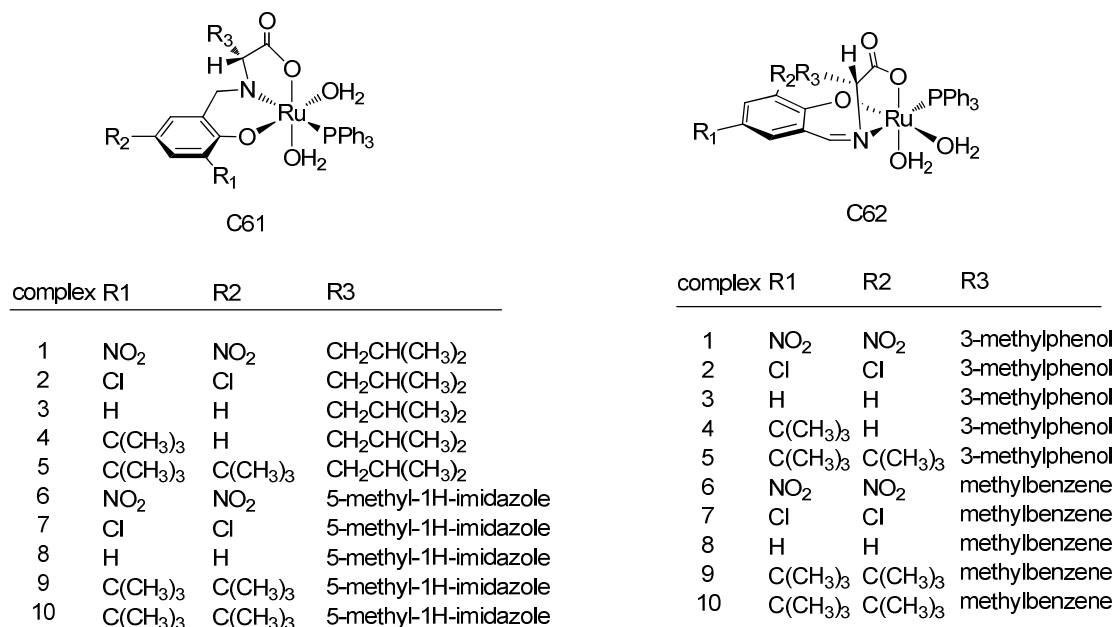


Figure 25. Structure of **C61** and **C62**.

The Ru-(nitrosyl) complex **C63** (Figure 26) synthesized by Tsutomu Katsuki's group in 2001 also manifested good ability in asymmetric epoxidation of different alkenes with conversions and ee exceeding 90%.<sup>126</sup>

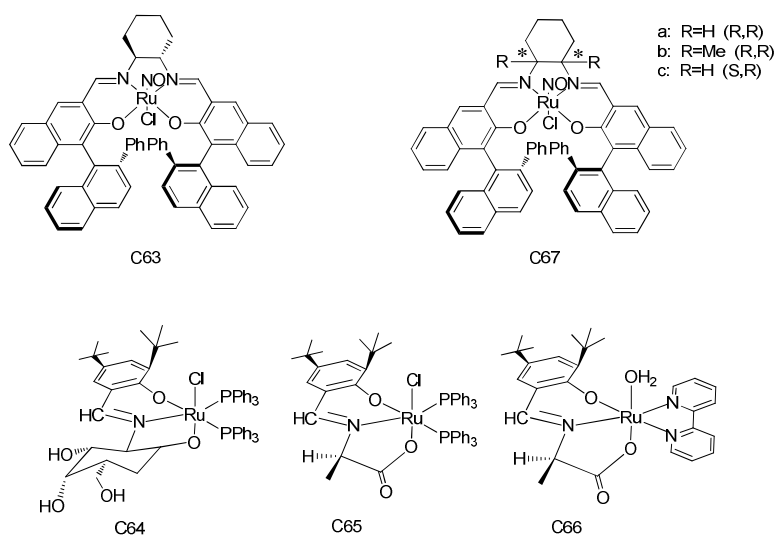


Figure 26. Drawing of **C63** to **C67**.

In 2006 a serie of Ru(III) complexes containing a sugar-based ligand was developed by Jacques Muzart's group (**C64** to **C66** in Figure 26). Different substrates were effectively converted to their organic epoxides in the 70–95% ee at ambient temperature, giving **C64** the best results under the used experimental conditions.<sup>127</sup>

Later, Antonio Mezzetti and coworkers synthesized a family of Ru Tetradentate P<sub>2</sub>N<sub>2</sub> complexes which were employed as catalysts for the epoxidation of styrene and its derivatives obtaining a 42% of ee.<sup>128</sup> Former researches indicated when O<sub>2</sub> was employed as co-oxidant the yield of epoxide was comparatively low.<sup>119</sup> These results differ to that reported in 2010 by the group of T. Katsuki which developed a set of Ru salen complexes (**C67**, Figure 26) which catalyzed epoxidation of conjugated *cis*- $\beta$ -methylstyrene olefins and its derivatives with O<sub>2</sub> obtaining both excellent yield and ee.<sup>129</sup>

#### **I.3.2.4. Asymmetric alkene epoxidation using Ru polypyridyl complexes**

One of the most commonly used catalysts for the enantioselective epoxidation of alkenes was the Ru pyridinedicarboxylate complexes, the first of which (**C68**, Figure 27) were developed in 1997 by the Hisao Nishiyama's group. Using *trans*-stilbene as trail substrate. Since the meridional tridentate connected structure of dicarboxylate pyridine on the complexes was rigid enough, the oxazolic moiety maintained the chiral environment during the catalysis inducing the enantioselection.<sup>130</sup>

In 2003, the same complexes were further studied by M. Beller and coworkers. They amplified the variety of alkenes and researched in more detail about the reaction conditions increasing the ee to 71% in optimized situation.<sup>131</sup> In 2004, the same group synthesized the family of complexes **C69** to **C71** (Figure 27). The alkene epoxidation using these complexes gave yields and ee higher than 90% and 50% respectively.<sup>132</sup>

From 2005, M. Beller's group developed a "library" of Ru pyridinedicarboxylate complexes based on the Ru(pybox)(pydic) and Ru(pybdi)(pydic) (pybdi = 2,6-bis(4,5-dihydro-1H-imidazol-2-yl)pyridine). Some selective examples are shown in Figure 27 (**C72** to **C77**). Each complex had been introduced to the alkene epoxidation and gave excellent catalytic capacity and selectivity.<sup>133</sup>



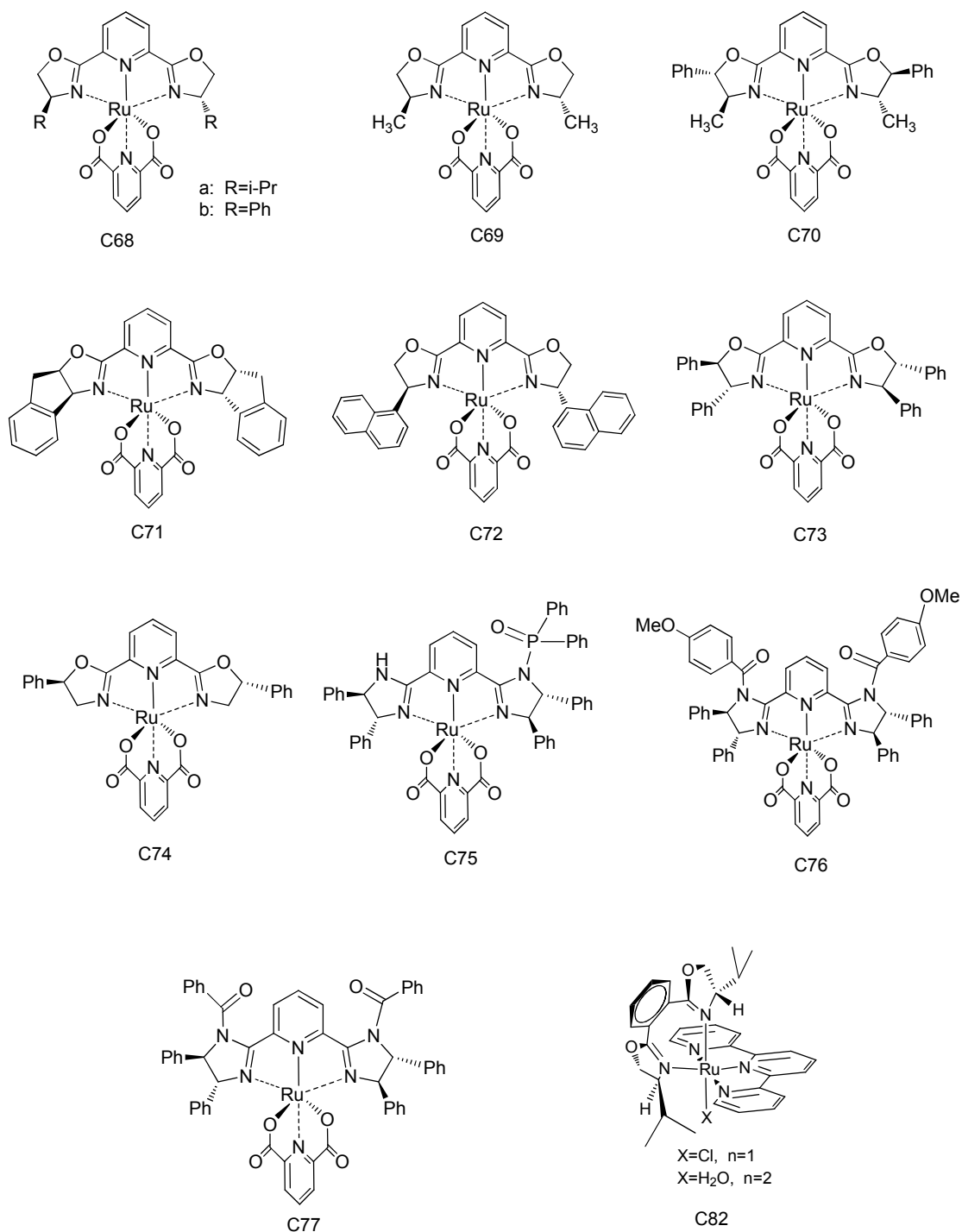


Figure 27. Drawing of **C68** to **C77** and **C82**.

In 2007 X. Sala and coworkers synthesized the  $C_2$  symmetric Ru complex bearing a trpy and oxazoline ligands **C82** (Figure 27). Styrene and *trans*-stilbene were used as trial alkenes showing low values for the enantioselective epoxidation (less than 10%). Since the catalytic reaction took place in the region of the planar trpy ligand, the

stereogenic center in the oxazoline ligand only had little effect on the orientation of the substrate.<sup>134</sup>

#### I.4.1. Stereospecific epoxidation catalyzed by ruthenium Complexes

Stereospecific alkene epoxidation catalyzed by Ru has been another important research field during the past few decades. One of the examples of stereospecific epoxidation was the complex **C83** (Figure 28) synthesized in 1997 by S. Chandrasekaran and coworkers. They studied the epoxidation of complex alkenes like the 4-vinylcyclohex-1-ene, limonene and  $\Delta^5$ -unsaturated steroids with very good stereoselectivity (88%-96%).<sup>135</sup>

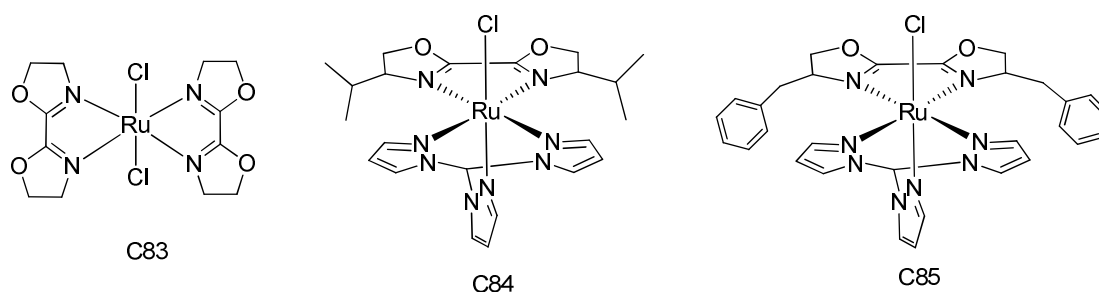


Figure 28. Drawing of **C83**, **C84** and **C85**.

The Thorsten Bach's group recently used the Ru chiral porphyrin complex **C60** (Figure 24) in the epoxidation of a diolefin derivative of the 3-vinylquinolone (Figure 29). The product ratio 1:2 with **C60** was 91:9 while with other achiral Ru catalyst a ratio of 62:38 was obtained.<sup>121,122</sup>

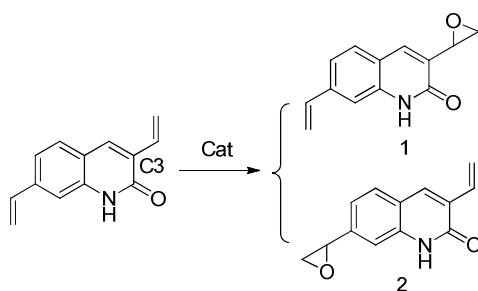


Figure 29. Stereospecific epoxidation of the derivatives of 3-vinylquinolone by **C60**.

In 2011, I. Romero and coworkers reported the new Ru-tmp complexes (**C84** and **C85**, Figure 28). The two catalysts showed significant difference in regioselectivity towards the epoxidation of 4-vinylcyclohexene. The complex **C85** leads to the regioselective oxidation at the ring alkene position, whereas **C84** resulted in the oxidation at the terminal position. Although the energy differences between the two possible products, the energy barrier for the intermediate of the two catalytic systems agreed with the observed difference in reactivity.<sup>136</sup>

## I.4. References

---

- <sup>1</sup> Kirmse, W. *Carbene Chemistry*, Academic Press, New York, **1964**.
- <sup>2</sup> Hine, J. *Divalent Carbon*, The Ronald Press Company, New York, **1964**.
- <sup>3</sup> Skell, P. S.; Sandler, S. R. *J. Am. Chem. Soc.* **1958**, 80 (8), 2024.
- <sup>4</sup> Fischer, E. O. and Maasböl, A. *Angew. Chem. Int. Ed.* **1964**, 3(8), 580.
- <sup>5</sup> Schuster, G. B. *Adv. Phys. Org. Chem.* **1986**, 22, 311.
- <sup>6</sup> Hoffman, R. *J. Am. Chem. Soc.* **1968**, 90, 1475.
- <sup>7</sup> Arduengo, A. J.; Harlow, R. L. and Kline, M. *J. Am. Chem. Soc.* **1991**, 113, 361.
- <sup>8</sup> Crabtree, R. H. *The Organometallic Chemistry of the Transition Metals*, 4th edition, Wiley-Interscience, New Jersey, **2005**.
- <sup>9</sup> Wanzlick, H. W. *Angew. Chem. Int. Ed.* **1962**, 1(2), 75.
- <sup>10</sup> Öfele, K; *J. Organomet. Chem.* **1968**, 12, 42.
- <sup>11</sup> Wanzlick, H.W. and Schönherr, H.J. *Angew. Chem. Int. Ed.* **1968**, 7, 141.
- <sup>12</sup> a) Gründemann, S.; Kovacevic, A.; Albrecht, M.; Faller Robert, J. W. and Crabtree, H. *Chem. Commun.* **2001**, 2274. b) Öfele, K. *J. Organomet. Chem.* **1968**, 12, 42.
- <sup>13</sup> Arduengo, A. J.; Harlow, R. L. and Kline, M. *J. Am. Chem. Soc.* **1991**, 113, 361.
- <sup>14</sup> a) Diez-Gonzalez, S. *N-Heterocyclic Carbenes: From Laboratory Curiosities to Efficient Synthetic Tools*, Royal Society of Chemistry, UK, **2010**. b) Nolan, S. P. *N-Heterocyclic Carbenes in Synthesis*, Wiley VCH, Weinheim, **2006**. c) Catherine S.J. Cazin, *N-Heterocyclic Carbenes in Transition Metal Catalysis and Organocatalysis*, Springe, London (UK), **2011**. d) Moss, R. A. and Doyle. M. P. *Contemporary Carbene Chemistry*, Wiley-Blackwell, New Jersey (USA), **2013**.
- <sup>15</sup> Herrmann, W. A. and Köcher, C. *Angew. Chem. Int. Ed.* **1997**, 36, 2162.
- <sup>16</sup> Lee, M.; Hu, C. *Organometallics* **2004**, 23, 976.
- <sup>17</sup> Diez-Gonzalez, S. *N-Heterocyclic Carbenes: From Laboratory Curiosities to Efficient Synthetic Tools*, Royal Society of Chemistry, UK, **2010**.

- 
- <sup>18</sup> Schuster, O.; Yang, L. R.; Raubenheimer, H. G. and Albrecht, M. *Chemical Review*, **109**(8), **2009**, 3445.
- <sup>19</sup> Gründemann, S.; Kovacevic, A.; Albrecht, M.; Faller, J. W. and Crabtree, R. H. *J. Am. Chem. Soc.* **2002** 124 10473.
- <sup>20</sup> a) Eguillor, B.; Esteruelas, M. A.; Oliván, M.; Puerta, M. *Organometallics* **2008**, *27*, 445. b) Heckenroth, M.; Kluser, E.; Neels, A.; Albrecht, M. *Dalton Trans.* **2008**, 6242. c) Ellul, C. E.; Mahon, M. F.; Saker, O.; Whittlesey, M. K. *Angew. Chem. Int. Ed.* **2007**, *46*, 6343. b) Crittall, M. R.; Ellul, C. E.; Mahon, M. F.; Saker, O.; Whittlesey, M. K. *Dalton Trans.* **2008**, 4209.
- <sup>21</sup> a) Gomez, M.; Kisenyi, J. M.; Sunley, G. J.; Maitlis, P. M. *J. Organomet. Chem.* **1985**, 296, 197. b) Fanizzi, F. P.; Sunley, G. J.; Wheeler, J. A.; Adams, H.; Bailey, N. A.; Maitlis, P. M. *Organometallics* **1990**, *9*, 131.
- <sup>22</sup> a) Weskamp, T.; SchaRenmann, W. C.; Spiegler, M.; Herrmann, W. A. *Angew. Chem. Int. Ed.* **1998**, *37*, 2490. b) Scholl, M.; Ding, S.; Lee, C. W. and Grubbs, R. H. *Org. Lett.* **1999**, *1*, 953. c) Garber, S. B.; Kingsbury, J. S. and Hoveyda, A. H. *J. Am. Chem. Soc.* **2000**, *122*, 8168. d) Araki, K.; Kuwata, S. and Ikariya, T. *Organometallics*, **2008**, *27*, 2176.
- <sup>23</sup> Clinton L. Lund, Michael J. Sgro, Renan Cariou, and Douglas W. Stephan. *Organometallics*, **2012**, *31*, 802.
- <sup>24</sup> Cheng, Y; Lu, X. Y; Xu, H. J.; Li, Y. Z.; Chen, X. T. and Xue, Z. L. *Inorg. Chem. Acta*, **2010**, 363, 430.
- <sup>25</sup> a) Prince, B. M. and Cundari, T. R. *Organometallics*, **2012**, *31* (3), 1042. b) Whittlesey, M. K., and Williams, J. M. J. *J. Am. Chem. Soc.*, **2007**, *129*, 1987.
- <sup>26</sup> a) Sigman, M. S. et al. *J. Org. Chem.* **2005**, *70*, 3343. b) Crabtree, R.H. and Persis, E. *Organometallics*, **2003**, *22*, 1110. c) Herrmann, W. A. and Strassner, T. *Angew. Chem. Int. Ed.* **2002**, *41*, 1745. d) Hartwig, J. F. et al. *J. Am. Chem. Soc.* **2001**, *123*, 8410.
- <sup>27</sup> Schultz, M. J.; Hamilton, S. S.; Jensen, D. R. and Sigman, M. S. *J. Org. Chem.* **2005**, *70*, 3343.
- <sup>28</sup> Krüger, A. and Albrecht, M. *Chem. Eur. J.*, **2012**, *18*, 652.

- 
- <sup>29</sup> Canseco-Gonzalez, D.; Petronilho, A.; Mueller-Bunz, H.; Ohmatsu, K.; Ooi, K. and Albrecht, M. *J. Am. Chem. Soc.*, **2013**, 135, 13193.
- <sup>30</sup> Modugno, G.; Monney, A.; Bonchio, M.; Albrecht, M. and Carraro, M. *Eur. J. Inorg. Chem.*, **2014**, 2356.
- <sup>31</sup> Clinton L. Lund, Michael J. Sgro, Renan Cariou, and Douglas W. Stephan. *Organometallics*, **2012**, 31, 802.
- <sup>32</sup> Mc Cleverty, J. and Meyer, T. J. *Comprehensive Coordination Chemistry II. From Biology to Nanotechnology*, Vol 9, *Applications of Coordination Chemistry* Elsevier, Amsterdam, **2003**.
- <sup>33</sup> Bofill, R.; García-Antón, J.; Escriche, L.; Sala, X. and Llobet, A. *Comprehensive Inorganic Chemistry II*, Oxford, Elsevier, **2013**.
- <sup>34</sup> Haas, K. L. and Franz, K. J. *Chem. Rev.* **2009**, 109, 4921.
- <sup>35</sup> Jones, C. and Thornback, J. *Medicinal Applications of Coordination Chemistry*, The Royal Society of Chemistry **2007**.
- <sup>36</sup> Safarzadeh, M. S.; Bafghi, M.S. D.; Moradkhani, M. O. *Minerals Engineering*, **2007**, 20, 211.
- <sup>37</sup> Holder, E.; Langeveld, B. W. and Schubert, U. S. *Adv. Mater.* **2005**, 17, 1109.
- <sup>38</sup> Bruneau, C. *Ruthenium catalysts and fine chemistry*, Springer-Verlag, Berlin, **2004**.
- <sup>39</sup> Trost, B. M.; and Pinkerton, A. B. *J. Am. Chem. Soc.* **1999**, 121, 4068.
- <sup>40</sup> Trost, B. M.; Pinkerton, A. B. and Kremzow, D. *J. Am. Chem. Soc.* **2000**, 122, 12007.
- <sup>41</sup> Shing, T. K.; Tai, V. W. and Tam, E. K. *Angew. Chem. Int. Ed.* **1994**, 33, 2312.
- <sup>42</sup> Grela, K.; Harutyunyan, S. and Michrowska, A. *Angew. Chem. Int. Ed.* **2002**, 114, 4038.
- <sup>43</sup> Sala, X.; Escriche, L.; Llobet, A.; et al. *Acc. Chem. Res.* **2014**, 47(2), 504.
- <sup>44</sup> Armaroli, N.; Balzani, V. *Angew. Chem. Int. Ed.* **2007**, 46, 52.
- <sup>45</sup> *Annual Energy Review*, Energy Information Administration. Department of Energy, US. September, **2012**.

- 
- <sup>46</sup> a) Najafpour, M. M.; Ehrenberg, T.; Wiechen, M. and Kurz, P. *Angew. Chem. Int. Ed.* **2010**, *49*, 2233. b) La Ganga, G.; Puntoriero, F.; Campagna, S.; Bazzan, I.; Berardi, S.; Bonchio, M.; Sartorel, A.; Natali, M. and Scandola, F. *Faraday Discuss.*, **2012**, 155, 177.
- <sup>47</sup> a) Ferreira, K. N.; Iverson, T. M.; Maghlaoui, K.; Barber, J. and Iwata, S. *Science*, **2004**, *303*, 1831. (b) Umena, Y.; Kawakami, K.; Shen, J.R. and Kamaiya, N. *Nature*, **2011**, *473*, 55.
- <sup>48</sup> a) Francàs, L.; Sala, X.; Benet-Buchholz, J.; Escriche, L.; Llobet, A. *ChemSusChem* **2009**, *2*, 321. b) Herrero, C.; Quaranta, A.; Leibl, W.; Rutherford, A.W.; Aukauloo, A. *Energy Environ. Sci.* **2011**, *4*, 2353. c) Gust, D.; Moore, T.A.; Moore, A.L. *Acc. Chem. Res.* **2009**, *42*, 1890. d) Herrero, C.; Lassalle-Kaiser, B.; Leibl, W.; Rutherford, A.W.; Aukauloo, A. *Coord. Chem. Rev.* **2008**, *252*, 456-468.
- <sup>49</sup> PhD Thesis of Laia Francàs
- <sup>50</sup> Gestern, S. W.; Samuels, G. J.; Meyer, T. J. *J. Am. Chem. Soc.* **1982**, *104*, 4029.
- <sup>51</sup> Lebeau, E. L.; Adeyemi, S. A.; Meyer, T. J. *Inorg. Chem.* **1998**, *37*, 6476.
- <sup>52</sup> a) Nagoshi, K.; Yamashita, S.; Yagi, M.; Kaneko, M. *J. Mol. Catal. A: Chem.* **1999**, *144*, 71. b) Collin, J. P.; Sauvage, J. P. *Inorg. Chem.* **1986**, *25*, 135.
- <sup>53</sup> Sens, C.; Romero, I.; Rodríguez, M.; Llobet, A.; Parella, T.; Benet-Buchholz, J. *J. Am. Chem. Soc.* **2004**, *126*, 7798.
- <sup>54</sup> a) Bozoglian, F.; Romain, S.; Ertem, M.Z.; Todorova, T.K.; Sens, C.; Mola, J.; Rodríguez, M.; Romero, I.; Benet-Buchholz, J.; Fontrodona, X.; Cramer, C.J.; Gagliardi, L.; Llobet, A. *J. Am. Chem. Soc.* **2009**, *131*, 15176. b) Sala, X.; Romero, I.; Rodríguez, M.; Escriche, L.; Llobet, A. *Angew. Chem. Int. Ed.* **2009**, *48*, 2842. c) Planas, N.; Christian, J. G.; Mas-Marzà, E.; Sala, X.; Fontrodona, X.; Maseras, F.; Llobet, A. *Chem. Eur. J.* **2010**, *16*, 7965.
- <sup>55</sup> a) García-Antón, J.; Bofill, R.; Escriche, L.; Llobet, A. and Sala, X. *Eur. J. Inorg. Chem.*, **2012**, 4763. b) Bofill, R.; García-Antón, J.; Escriche, L.; Sala, X. and Llobet, A. *Comprehensive Inorganic Chemistry II*, Oxford, Elsevier, **2013**.

- 
- <sup>56</sup> Bozoglian, F.; Romain, S.; Ertem, M. Z.; Todorova, T. K.; Sens, C.; Mola, J.; Rodríguez, M.; Romero, I.; Benet-Buchholz, J.; Fontrodona, X.; Cramer, C. J.; Gagliardi, L. and Llobet, A. *J. Am. Chem. Soc.* **2009**, 131, 15176.
- <sup>57</sup> Deng, Z.; Tseng, H. W.; Zong, R.; Wang, D.; Thummel, R. *Inorg. Chem.* **2008**, 47, 1835.
- <sup>58</sup> a) Xu, Y.; Åkermark, T.; Gyollai, V.; Zou, D.; Eriksson, L.; Duan, L.; Zhang, R.; Åkermark, B.; Sun, L. *Inorg. Chem.* **2009**, 48, 2717. b) Xu, Y.; Fischer, A.; Duan, L.; Tong, L.; Gabrielsson, E.; Åkermark, B.; Sun, L. *Angew. Chem. Int. Ed.* **2010**, 49, 8934.
- <sup>59</sup> a) Tseng, H. W.; Zong, R.; Muckerman, J. T.; Thummel, R. *Inorg. Chem.* **2008**, 47, 11763. b) Zhang, G.; Zong, R.; Tseng, H.-W.; Thummel, R. P. *Inorg. Chem.* **2008**, 47, 990. c) Zong, R.; Thummel, R. P. *J. Am. Chem. Soc.* **2005**, 127, 12802.
- <sup>60</sup> Tseng, H. W.; Zong, R.; Muckerman, J. T.; Thummel, R. *Inorg. Chem.* **2008**, 47, 11763.
- <sup>61</sup> Concepcion, J. J.; Jurss, J. W.; Templeton, J. L.; Meyer, T. J. *J. Am. Chem. Soc.* **2008**, 130, 16462.
- <sup>62</sup> Duan, L.; Xu, Y.; Gorlov, M.; Tong, L.; Andersson, S.; Sun, L. *Chem. Eur. J.* **2010**, 16, 4659.
- <sup>63</sup> Duan, L.; Fischer, A.; Xu, Y.; Sun, L. *J. Am. Chem. Soc.* **2009**, 131, 10397.
- <sup>64</sup> Duan, L.; Bozoglian, F.; Mandal, S.; Stewart, B.; Privalov, T.; Llobet, A.; Sun, L. *Nat. Chem.* **2012**, 4, 418.
- <sup>65</sup> Liu, F.; Cardolaccia, T.; Hornstein, B. J.; Schoonover, J. R.; Meyer, T. J. *J. Am. Chem. Soc.*, **2007**, 129, 2446.
- <sup>66</sup> a) Chen, Z. F.; Concepcion, J. J.; Jurss, J. W. and Meyer, T. J. *J. Am. Chem. Soc.* **2009**, 131, 15580. b) Concepcion, J. J.; Jurss, J. W.; Hoertz, P. G. and Meyer, T. J. *Angew. Chem. Int. Ed.* **2009**, 48, 9473.
- <sup>67</sup> Concepcion, J. J.; Jurss, J. W.; Brennaman, M. K.; Hoertz, P. G.; Patrocinio, A. O.; Iha, N. Y.; Templeton, J. L. and Meyer, T. J. *Acc. Chem. Res.* **2009**, 42, 1954.
- <sup>68</sup> Tong, L.; Göthelid, M.; Sun, L. *Chem. Commun.*, **2012**, 48, 10025.



- 
- <sup>69</sup> Francas, L.; Sala, X.; Benet-Buchholz, J.; Escriche, L.; Llobet, A. *ChemSusChem* **2009**, 2(4), 321.
- <sup>70</sup> Aguiló, J.; Francàs, L.; Liu, H. J.; Llobet, A.; Escriche, L.; Sala, X.; et al. *Catal. Sci. Technol.* **2014**, 4,190.
- <sup>71</sup> Balavoine, G.; Eskenazi, C.; Meunieret, F.; Riviere, H. *Tetrahedron Letters*, **1984**, 25, 3187.
- <sup>72</sup> Eskenazi, C.; Balavoine, G.; Meunier, F.; Riviere, H. *J. Chem. Soc., Chem. Commun.*, **1985** 1111.
- <sup>73</sup> Balavoine, G.; Eskenazi, C.; Meunier, F.; Riviere, H. *Tetrohedron Lett.* **1984**, 25, 3187.
- <sup>74</sup> Bailey, A. J.; Griffith, W. P. and Savageb, P. D. *J. Chem. Soc. Dalton Trans.* **1995**, 3537.
- <sup>75</sup> Bailey, A. J. and Williams, D. J. *J. Chem. Soc., Chem. Commun.*, **1994**, 1833.
- <sup>76</sup> Barf, G. A.; Van den Hoek, D. and Sheldon, R. A. *Tetrahedron*, **1999**, 52, 12971.
- <sup>77</sup> a) Groves, J. T. and Quinn, R. *J. Am. Chem. Soc.* **1985**, 5790. b) Groves, J. T.; Quinn, R. *Inorg. Chem.* **1984**, 23, 3846.
- <sup>78</sup> Scharbert, B.; Zeisberger, E.; Paulus, E. *Journal of Organometallic Chemistry*, **1995**,143.
- <sup>79</sup> Funyu, S.; Isobe, T.; Takagi, S.; Tryk, D. A. and Inoue, H. *J. Am. Chem. Soc.* **2003**, 125, 5734.
- <sup>80</sup> Higuchi, T.; Hirobe, M. *Journal of Molecular Catalysis A Chemical* **1996**, 113, 403.
- <sup>81</sup> Zhou, X. T.; Ji, H. B. *Chemical Engineering Journal*, **2010**, 156, 411.
- <sup>82</sup> Leung, W. H. and Che, C. M. *Inorganic Chemistry*, **1989**, 28, 4619.
- <sup>83</sup> Campbell, T. G. and Urbach, F. L. *Inorg. Chem.* **1973**, 12, 1836.
- <sup>84</sup> De Souza, V. R.; Nunes, G. S.; Rocha, R. C.; Toma, H. E. *Inorganica Chimica Acta* **2003**, 348 50.
- <sup>85</sup> Chatterjee, D. *Journal of Molecular Catalysis A Chemical.* **2009**, 310, 174.

- 
- <sup>86</sup> Hatefi, M.; et al. *Applied Catalysis A General*, **2009**, 370, 66.
- <sup>87</sup> Okumuraa, T.; et al. *Journal of Molecular Catalysis A Chemical*. **2009**, 307, 51.
- <sup>88</sup> J. Meyer, T. J.; et. al. *Inorg. Chem.* **1986**, 25, 1514.
- <sup>89</sup> Che, C. M.; Cheng, W. K.; Leung, W. H. and Makb, T. C. *J. Chem. Soc., Chem. Commun.*, **1987**, 418.
- <sup>90</sup> Che, C. M.; Leung, W. H. and Poon. C. K.; *J. Chem. Soc., Chem. Commun.*, **1987**, 173.
- <sup>91</sup> Bressan, M. and Morvillo, A. *Inorg. Chem.* **1989**, 28, 950.
- <sup>92</sup> Goidstein, A. S.; Beer, R. H. and Drago, R. S. *J. Am. Chem. Soc.*, **1994**, 116, 2424.
- <sup>93</sup> Chatterjee, D. et al. *Polyhedron*, **2007**, 26, 178.
- <sup>94</sup> Masllorens, E.; Llobet, A. et al. *J. Am. Chem. Soc.*, **2006**, 128, 5306.
- <sup>95</sup> Hamelin, O. et al. *Inorganic Chemistry*, **2008**, 14, 6413.
- <sup>96</sup> Murali, M.; Mayilmurugan, R. and Palaniandavar, M. *Eur. J. Inorg. Chem.*, **2009**, 3238.
- <sup>97</sup> Tada, M.; Muratsugu, S.; Kinoshita, M.; Sasaki, T. and Iwasawa, T. *J. Am. Chem. Soc.*, **2010**, 132, 713.
- <sup>98</sup> Dakkach, M. and Llobet, A.; et al. *Inorg. Chem.* **2010**, 49, 7072.
- <sup>99</sup> a) Dakkach, M.; Parella, T.; Atlamsani, A.; Romero, I. and Rodriguez, M. *Adv. Synth. Catal.* **2011**, 353, 231. b) Dakkach, M.; Atlamsani, A.; Parella, T.; Romero, I. and Rodríguez, M. *Inorg. Chem.* **2013**, 52, 5077.
- <sup>100</sup> Dutta, A.; et al. *Inorg. Chem.* **2011**, 50, 1775.
- <sup>101</sup> Türkoglu, G.; et al. *Organometallics*, **2012**, 31, 2166.
- <sup>102</sup> Papafotiou, F.; et al. *Polyhedron*, **2013**, 52, 634.
- <sup>103</sup> Di Giovanni, C.; Vaquer, L.; Sala, X. and Llobet, A. *Inorg. Chem.* **2013**, 52, 4335.
- <sup>104</sup> Agarwala, H.; et al. *Dalton Trans.*, **2013**, 42, 3721.
- <sup>105</sup> Yang, R. Y. and R. Y. and Dai, L. X. *Journal of Molecular Catalysis*, **1994**, 87, Ll.

- 
- <sup>106</sup> Augier, C.; Malara, L.; Lazzeri, V. and Waegell, B. *Tetrahedron, Letters*, **1995**, 36(48), 8775.
- <sup>107</sup> End, N. and Pfaltz, A. *Chem. Commun.*, **1998**, 589.
- <sup>108</sup> Gross, Z.; Ini, S.; Kapon, M. and Cohen, S. *Tetrahedron Letters*, **1996**, 37(40), 7325.
- <sup>109</sup> Gross, Z. and Ini, S. *J. Org. Chem.* **1997**, 62, 5514.
- <sup>110</sup> Coilman, J. P.; Lee, V. J.; Kellen-Yuen, C. J.; Zhang, X.; Ibers, J. A.; Brauman, J. I. *J. Am. Chem. Soc.*, **1995**, 117, 692.
- <sup>111</sup> a) Gross, Z. and Ini, S. *Org. Lett.*, **1999**, 1(13) 2077. b) Gross, Z. and Ini, S. *J. Org. Chem.*, **1997**, 62, 5514.
- <sup>112</sup> Le Maux, P.; Lukas, M. and Simonneaux, G. *Journal of Molecular Catalysis A Chemical*, **2003**, 206, 95.
- <sup>113</sup> Halterman, R. L. and Jan, S. T. *J. Org. Chem.*, **1991**, 56, 5253.
- <sup>114</sup> Berkessel, A. and Frauenkron, M. *J. Chem. Soc., Perkin Trans.*, **1997**, 2265.
- <sup>115</sup> Zhang, R.; Yu, W. Y.; Wong, K. Y. and Che, C. M. *J. Org. Chem.*, **2001**, 66, 8145.
- <sup>116</sup> Lai, T. S.; Kwong, H. L.; Zhang, R. and Che, C. M. *J. Chem. Soc., Dalton Trans.*, **1998**, 3559.
- <sup>117</sup> Lai, T. S.; Zhang, R.; Cheung, K. K.; Kwong, H. L. and Che, C. M. *Chem. Commun.*, **1998**, 1583.
- <sup>118</sup> Zhang, J. L.; Liu, Y. L. and Che, C. M. *Chem. Commun.*, **2002**, 2906.
- <sup>119</sup> Yu, X. Q.; Huang, J. S.; Yu, W. Y. and Che, C. M. *J. Am. Chem. Soc.*, **2000**, 122, 5337.
- <sup>120</sup> Berkessel, A.; Kaiser, P. and Lex, J. *Chem. Eur. J.*, **2003**, 9, 4746.
- <sup>121</sup> Fackler, P.; Berthold, C.; Voss, F. and Bach, T. *J. Am. Chem. Soc.*, **2010**, 132, 15911.
- <sup>122</sup> Fackler, P.; Huber, S. M. and Bach, T. *J. Am. Chem. Soc.*, **2012**, 134, 12869.
- <sup>123</sup> R. I.; Khan, N. H. and Abdi, S. H. R. *Journal of Molecular Catalysis A Chemical*, **1995**, 96, 117.
- <sup>124</sup> Kureshy, R. I.; et al. *Journal of Molecular Catalysis A Chemical*, **1999**, 150, 163.

- 
- <sup>125</sup> Kureshy R. I. ; et al. *Journal of Molecular Catalysis A Chemical*, **1999**, 150, 175.
- <sup>126</sup> Nakata, K.; Takeda, T. Mihara, J.; Katsuki, T. *Chem. Eur. J.*, **2001**, 17, 7.
- <sup>127</sup> a) Anilkumar, G. et al. *Tetrahedron Asymmetry*, **2005**, 16, 3536. b) Chatterjee, D.; et al. *Journal of Molecular Catalysis A Chemical*, **2006**, 255, 283.
- <sup>128</sup> a) Stoop, R. M. and Mezzetti, A. *Green Chemistry*, **1999**, 39. b) Stoop, R. M.; Bachmann, S. and Mezzetti, A. *Organometallics*, **2000**, 19, 4117.
- <sup>129</sup> Tanaka, H. et al.; *J. Am. Chem. Soc.*, **2010**, 132, 12034.
- <sup>130</sup> Nishiyama, H.; Shimada, T.; Itoh, H.; Sugiyama, H. and Motoyama, Y. *Chem. Commun.*, **1997**, 1863.
- <sup>131</sup> Tse, M. K.; Bhor, S.; Klawonn, M.; Dobler, C. and Beller, M. *Tetrahedron Letters.*, **2003**, 7479.
- <sup>132</sup> Bhor, S.; Tse, M. K.; Klawonn, M.; Dobler, C.; Magerlein, W. and Beller, M. *Adv. Synth. Catal.* **2004**, 346, 263.
- <sup>133</sup> a) Beller, M.; et al. *Journal of Organometallic Chemistry*, **2006**, 691, 4419. b) Anilkumar, G.; et al. *Tetrahedron Asymmetry*, **2005**, 3536. c) Tse, M. K.; Bhor, S.; Klawonn, M.; Anilkumar, G.; Jiao, H. J.; Spannenberg, A.; Hugl, H. and Beller, M. *Chem. Eur. J.*, **2006**, 12, 1875. d) Tse, M. K.; Bhor, S.; Klawonn, M.; Hugl, H. and Beller, M. *Angew. Chem. Int. Ed.*, **2004**, 43, 5255. e) Bhor, S.; Anilkumar, G.; Tse, M. K.; Klawonn, M.; Bitterlich, B.; Grotevendt, A. and Beller, M. *Org. Lett.*, **2005**, 7(16), 3393.
- <sup>134</sup> Sala, X.; Serrano, I.; Romero, I.; Llobet, A.; et al. *Eur. J. Inorg. Chem.*, **2007**, 5207.
- <sup>135</sup> a) Kesavan, V. and Chandrasekaran, S. *J. Org. Chem.*, **1998**, 63, 6999. b) Kesavan, V. and Chandrasekaran, S. *J. Chem. Soc., Perkin Trans.*, **1997**, 1, 3115.
- <sup>136</sup> Serrano, I.; Poater, A.; Parella, T.; Llobet, A.; Rodríguez, M. and Romero, I. *Inorg. Chem.*, **2011**, 50, 6044.

## Chapter II. Objective

Artificial photosynthesis is nowadays attempted by means of the splitting of water driven by sunlight. This reaction would lead to the sustainable production of hydrogen and this would serve as a solution for the critical energy situation our society is nowadays facing. However, as explained in Chapter I, the oxidation of water (one of the semi-reaction of water splitting) is still a major challenge the scientific community is facing. On the other hand, as also summarized in Chapter I, the catalytic epoxidation of alkenes in a really efficient and stereoselective manner is still one of the aims of the scientific community. Thereby, the preparation of redox catalysts to contribute to the advance of these two technologically relevant transformations is the general goal of this Thesis. The following particular goals were initially intended.

### I.

The feasible preparation of N-heterocyclic carbenes (NHCs), which has extraordinarily grow up during the last years together with the interesting properties of this compounds when used as ligands in very diverse catalytic systems, pushed us to the development of ligands of this kind to be applied in Ru catalyzed oxidation reactions. Thus, the main goal of this chapter is to synthesize and characterize a new set of hybrid N/C-donor ligands and the evaluation of their effect on the electrochemical properties and catalytic activity of the corresponding mono- and dinuclear ruthenium complexes. For this purpose, the combination of the dinucleating tetradentate NHC ligand **L1** with several tridentate N-donor ligands such as trpy, bpea or tpm is proposed.

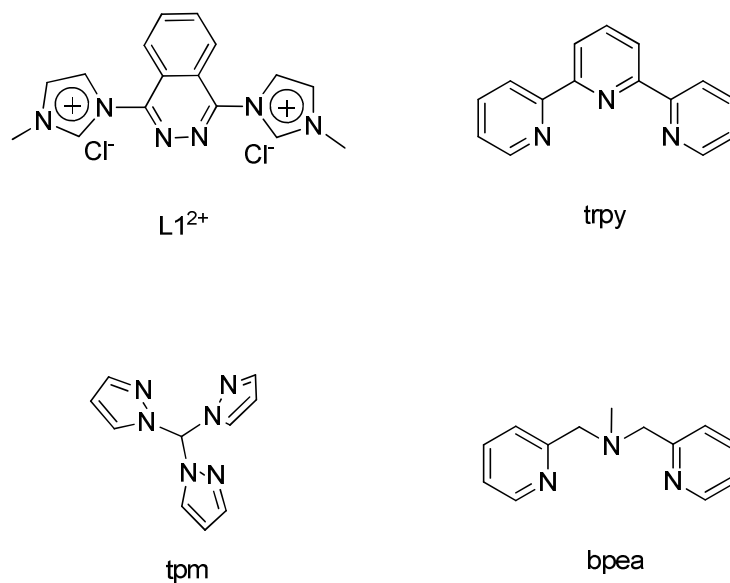


Chart 1. Drawing of the NHC (**L1<sup>2+</sup>**) and N-donor (trpy, bpea and tpm) ligands proposed to be combined with Ru in Chapter I.

## II.

In spite of the intensive investigation in the area of asymmetric alkene epoxidation catalyzed by organometallic compounds, few Ru chiral complexes have been reported containing NHC ligands. Therefore, the second goal of this project is to introduce chirality to the Ru carbene complexes prepared in the first part of the Thesis and the study of the capacity of obtained complexes in the enantioselective epoxidation of alkenes. For this purpose, the use of chiral polypyridylic ligands arising from the monoterpene chiral pool is proposed. Therefore, the [4,5]pinene-trpy ligand **L2** (Chart 2) will be used to replace trpy in the best performing complexes previously prepared and the enantioselective alkene epoxidation capacity of the new chiral complexes prepared will be thoroughly analyzed

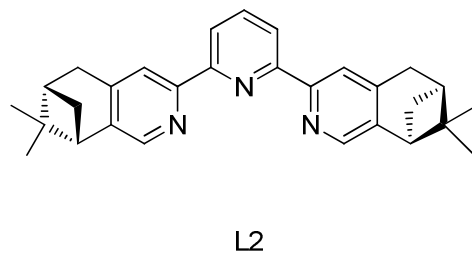


Chart 2. Drawing of the [4,5]pinene-trpy ligand **L2**.

## Chapter III.

# New Ru(II) Complexes bearing N and C-donor Ligands: Synthesis, Characterization and Catalytic Performance

### III.1. Introduction

As indicated in Chapter I research on carbene organometallic compounds, particularly those bearing NHCs as ligands, as well as their catalytic application is one of the fast developing areas in Chemistry.<sup>1</sup> Among them, Ru-based NHC complexes have played (and still play) a key role as efficient catalysts for important transformations such as olefin metathesis or the hydrogenation of olefins.<sup>2,3</sup> Therefore, for instance, in 1998 Herrmann and coworkers reported a Ru carbene complex coordinated by two monodentate IMes ligands (**1**, Figure 1) which manifested excellent catalytic properties in the olefin metathesis reaction.<sup>4</sup> Recently in 2012, Stephan and coworkers presented the Ru NHC complex **2** as an efficient catalyst for the hydrogenation of a wide range of functional olefins.<sup>5</sup> As Ru cover a wide range of accessible oxidation states (from -2 in  $[\text{Ru}(\text{CO})_2]^{2-}$  to +8 in  $\text{RuO}_4$ ), Ru complexes are redox active and much of their applications relate to redox catalysis. Therefore, Ru NHC complexes have also found relevant application in the fields of water oxidation and the epoxidation of alkenes. Figure 1 shows a selection of relevant catalysts for these two transformations. Complex **3** reported by Meyer and coworkers is a typical example for water oxidation<sup>6</sup> while compounds **4** and **5** (reported by Rodríguez and Romero, and Llobet, respectively) are representative compounds for the stereoselective epoxidation of alkenes<sup>7,8</sup>

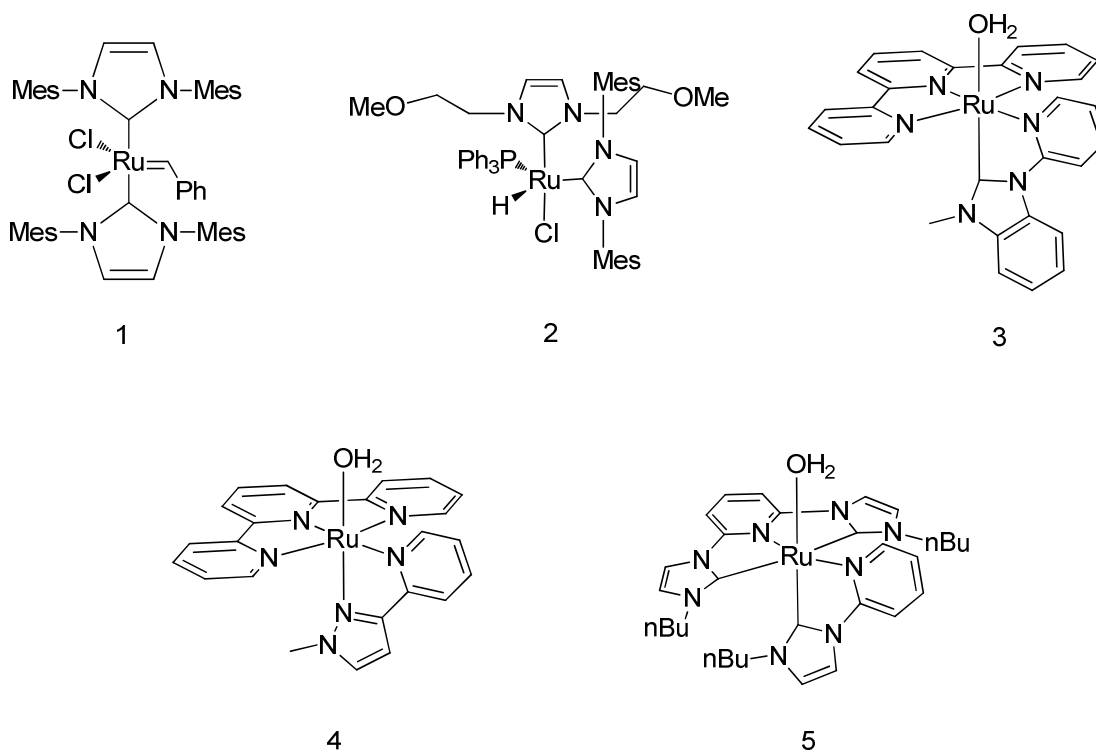
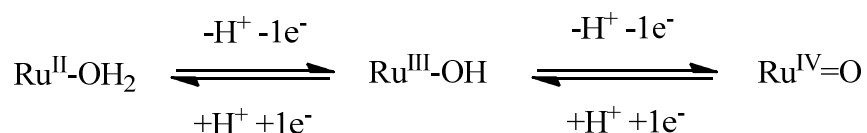


Figure 1. Drawing of complexes **1** to **5**.

When designing catalysts for redox processes such as the epoxidation of alkenes, controlling the oxidative power and the accessibility and stability of the oxidation states involved in the catalytic cycle is of paramount importance for the selectivity of the catalyzed reaction. In the case of Ru complexes, redox potentials are clearly (and quite predictively) influenced by the electronic properties of the ligands. In general, in the presence of electron-withdrawing ligands low oxidation states (such as Ru(II)) are stabilized and the redox potentials increase. On the contrary, when electron-donating ligands are employed high oxidation states (such as Ru(III) or Ru(IV)) are stabilized and hence, the redox potentials decrease.<sup>9</sup>

When a water molecule is directly coordinated to the metal centre, the redox properties of the Ru-aqua complexes are affected by proton exchange. The successive  $1e^-$  oxidations taking place from Ru(II) to Ru(IV) are accompanied by a sequential loss of protons favored by the enhanced acidity of the bounded aqua ligand. Therefore, proton coupled electron transfer (PCET) takes place and the oxidation of the initial  $Ru^{II}-OH_2$  species to high oxidation states becomes fairly accessible (Scheme 1).





Scheme 1. Proton-coupled electron transfer (PCET) process characteristic of Ru-aqua complexes.

As a consequence of this behavior, the redox potentials of the aqua complexes are directly correlated with the pH of the medium in such a way that, if pH increases, the Ru(III/II) and Ru(IV/III) couples are shifted to lower potentials. This dependence of redox potential and pH is reflected in the Nernst equation, in which, for a monoprotic and monoelectronic transfer, the redox couple half wave potential diminishes in 59 mV by every pH unit increased.

PCET is also responsible of the observed dramatic stabilization of the Ru(IV) species in the aqua-containing complex. This stabilization is promoted by the proton loss; *i.e.* by the loss of a positive charge, maintaining the total charge of the complex, and by a  $\sigma$  and  $\pi$  donation of the oxo group to the electron deficient metal center. Stabilization of Ru(IV) as the oxo complex causes the near overlap of Ru(IV/III) and Ru(III/II) potentials. There is an important implication in reactivity in this closeness of the redox potentials, being Ru(IV), thermodynamically, nearly as good two-electron oxidant as one-electron oxidant. This avoids radicalary reaction pathways of high energy and reactivity usually generated by monoelectronic transfers.<sup>10,11</sup>

To better understand the influence of the electronic properties of a given ligand set around a Ru-OH<sub>2</sub> core on the relative stability of the different oxidation states of the complex, Meyer and coworkers represented a plot based on the evolution of the redox potentials difference between the Ru(III/II) and Ru(IV/III) couples,  $\Delta E_{1/2}$ , with the sum of the so-called Lever parameters ( $\Sigma E_L$ ) for the surrounding ligands (Figure 2). This plot suggests that if a  $\Sigma E_L$  close to 1.06 V is obtained, Ru(III) would be unstable with respect to disproportionation to Ru(II) and Ru(IV) and, therefore, bi-electronic transfers would be favored for these species.<sup>12</sup> By successively increasing the NHC content in the surrounding ligands of a Ru-OH<sub>2</sub> core (thus decreasing the overall  $\sigma$ -donating or  $\pi$ -acceptor character of the whole set of non-aqua ligands with regards to complexes 8 and 9 in Figure 2, respectively), Llobet and coworkers proved in 2006 that bi-electronic

transfers could be favored (see the Pourbaix diagram of the  $[\text{Ru}(\text{CNC})(\text{CN})(\text{OH}_2)]^{2+}$  (**5**) complex in Figure 3) and that they were key for the achievement of high stereoselectivities in the epoxidation of *cis* olefins.<sup>8</sup> Similarly, the Ru-OH<sub>2</sub> complex (**4**) developed later on by Rodriguez, Romero and co-workers following the same strategy is also a two-electron oxidant.<sup>7</sup>

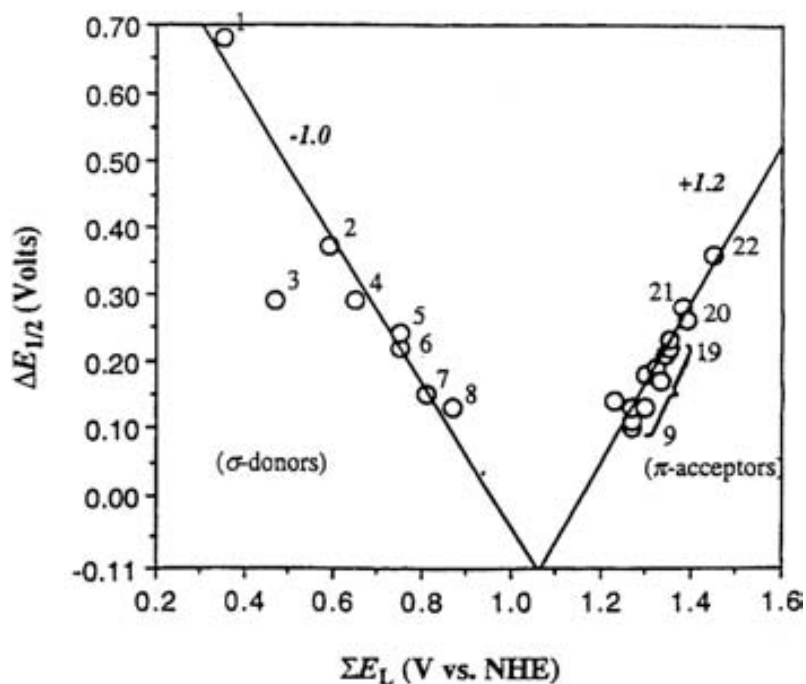


Figure 2. Meyer-Lever plot representing  $\Delta E_{1/2}$  vs  $\Sigma E_L$ . Complex **8** is  $[\text{Ru}(\text{tpy})(\text{tmen})(\text{H}_2\text{O})]^{2+}$  (tmen = 2,3-diamino-2,3-dimethylbutane) and **9** is  $[\text{Ru}(\text{tpy})(\text{phen})(\text{H}_2\text{O})]^{2+}$  (phen = phenanthroline).

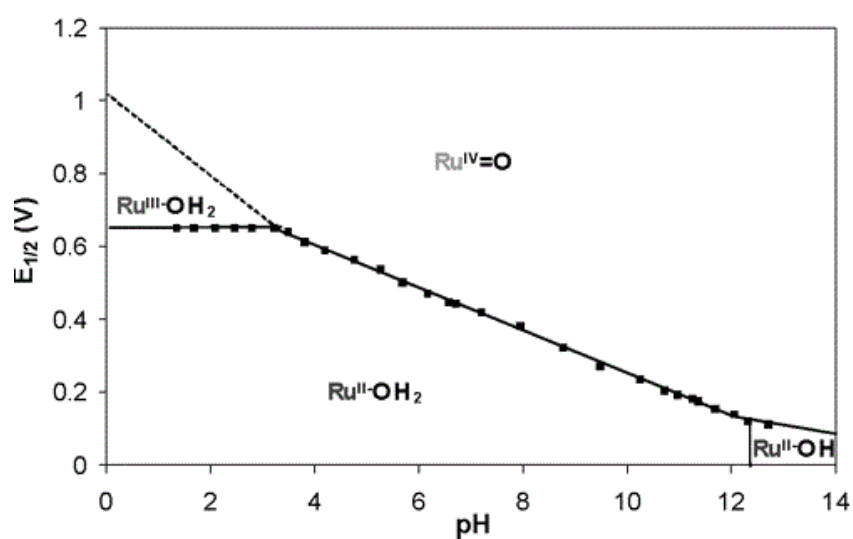
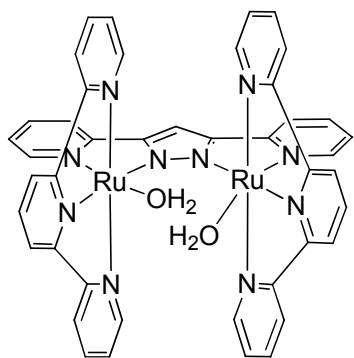
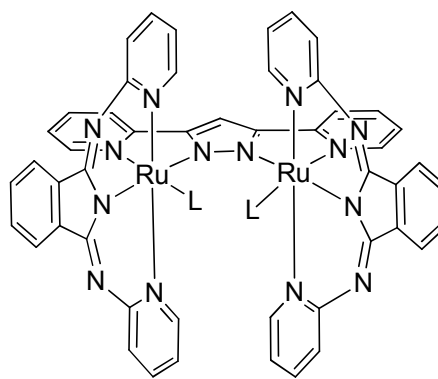


Figure 3. Pourbaix diagram of  $[\text{Ru}(\text{CNC})(\text{CN})(\text{OH}_2)]^{2+}$  (**5**).

As is the case of the above examples, most of the research related to redox catalysis using Ru compounds is based on mononuclear complexes since they are generally easily accessible from a synthetic point of view.<sup>13</sup> However, during the past few years researchers began to emphasize the distinctive and sometimes superior performance of bimetallic catalysts based on this transition metal.<sup>14</sup> The fine-tuning of the relative disposition of the two Ru-OH<sub>2</sub> active sites by means of the geometry imposed by a rigid bridging ligand can allow the two metals to cooperate through space. Moreover, the bridging ligand can also act as an electronic communicator between them.<sup>13</sup> A paradigmatic example of this is the Ru-Hbpp family of complexes (see for example **6** and **7** in Figure 4) developed by Llobet and co-workers.<sup>15</sup> The rich water oxidation chemistry of this type of catalysts originates from the intrinsic geometry imposed by the bpp- bridge, which favors the cooperative behavior of the two closely placed Ru atoms. Similar examples were later presented by Sun and co-workers with complexes **8** and **9** in Figure 4. Complex **8**, which geometrically allows the two metals to cooperate through space, is a fairly superior water oxidation catalyst compared with the less symmetric **9**.<sup>16,17</sup>

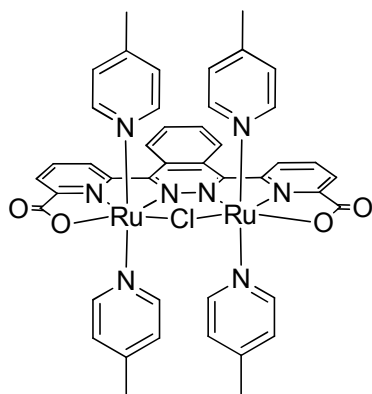


6

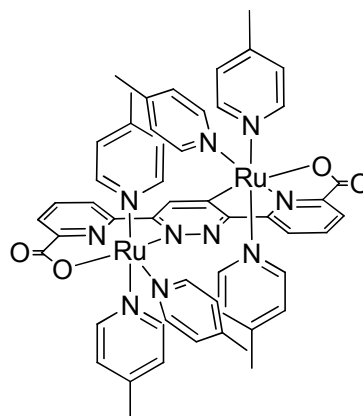


L=Py, 4-Me-Py, 3,5-Me<sub>2</sub>-Py,  
4-CF<sub>3</sub>-Py, MeCN or L+L=MeCOO

7



8



9

Figure 4. Drawing of dinuclear complexes **6** to **9**.

Taking into account all the aforementioned results we envisaged in this Chapter the preparation of a set of dinuclear Ru complexes bearing a bis-NHC bridge in combination with different facial and meridional tridentate auxiliary ligands to be used as redox catalyst. This should lead to a family of complexes with different dispositions of the Ru-aqua/oxo active sites (and therefore distinct cooperative capacities) that could benefit from the electronic communication of the two Ru centers, the rigidity of the bridging ligand and the smooth reaching of high oxidation states facilitated by the donor properties of the NHC moieties. For this purpose, 1,6-(1-methylimidazole)phthalene (**L1**<sup>2+</sup>) was chosen as bridging ligand and combined with different [Ru<sup>III</sup>(T)Cl<sub>3</sub>] (T = trpy, tpm and bpea, trpy = 2,2':6',2"-terpyridine, tpm = tris(pyrazol-1-yl)methane, bpea = N,N-bis(pyridin-2-ylmethyl)ethanamine) metal precursors. However, the instability

of the bridging ligand under synthetic conditions lead to unexpected mononuclear compounds with general formula  $cis$ -[Ru(PhthaPz-R)(trpy)X] $^{n+}$  (X = Cl, n = 1, X = H<sub>2</sub>O, n = 2 ; R = Methyl, Isopropyl; PhthaPz = 1,6-(1-methylimidazole)phthalene), [Ru(PhthaPz-R)(tpm)X] $^{n+}$ , (R = Methyl) and  $trans, fac$ -[Ru(PhthaP-R)(bpea)X] $^{n+}$  (R = Methyl) that were also interesting species when employed in redox catalysis. We here on present the synthesis, characterization and water oxidation and alkene epoxidation ability of the set of obtained complexes.

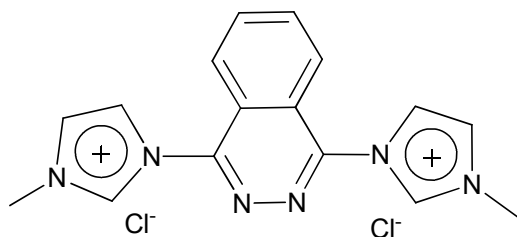


Chart 1. Drawing of ligand **L1**(Cl)<sub>2</sub>

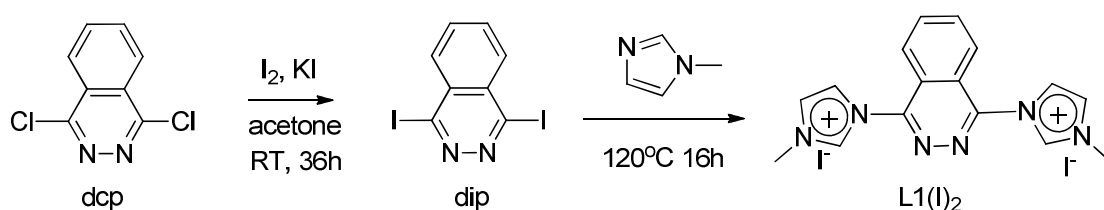
## III.2. Results and discussion

### III.2.1. Synthesis and Structural Characterization of the CNNC Ligand $L1^{2+}$

The tetradentate dinucleating CNNC bridging ligand  $L1^{2+}$  (see Chart 1 above) has been successfully synthesized and characterized by means of NMR spectroscopy, ESI-MS, Elemental Analysis as well as X-ray crystallography.

#### III.2.1.1. Synthesis of Ligand $L1^{2+}$

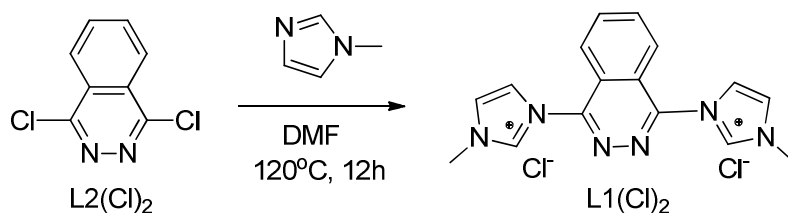
$L1(Cl)_2$  and  $L1(PF_6)_2$  were obtained following a modified procedure with regards to the one reported by Meyer and co-workers.<sup>18</sup> In general, this type of NHC ligands is prepared by the nucleophilic attack of an imidazole scaffold to a 1,4-dichlorophthalazine (dcp) skeleton. The reaction was initially attempted, as reported,<sup>18</sup> in a melt of the neat reactants. However, this procedure ended up with the formation of several by-products, which prevented the isolation of the pure ligand. Therefore, the chlorido groups on dcp were exchanged into iodine derivatives,<sup>19</sup> thus obtaining the 1,4-diiodophthalazine (dip, Scheme 1), which was further reacted with 1-methylimidazole under solvent-free conditions yielding the  $L1(I)_2$  ligand in moderate yields (40%) as a white powder (Scheme 2).



Scheme 2. Synthetic procedure of  $L1(I)_2$ .

Polar aprotic solvents such as DMF or DMSO are polar enough to dissolve the starting reactants and tend to favor the nucleophilic attack. Therefore, a second and more convenient (one step) synthetic method was then developed by employing 1,4-dichlorophthalazine and DMF as solvent, which resulted in shorten reaction times and higher yields (Scheme 3). The insolubility of  $L1(Cl)_2$  in DMF allowed the easy isolation

of the ligand by simple filtration and subsequent washing with diethyl ether. The yield of **L1(Cl)<sub>2</sub>** improved to 75%.



Scheme 3. Synthetic procedure of **L1(Cl)<sub>2</sub>**.

### III.2.1.2. Characterization of **L1<sup>2+</sup>**

**L1(Cl)<sub>2</sub>**, **L1(PF<sub>6</sub>)<sub>2</sub>** and **L1(I)<sub>2</sub>** have been characterized by means of the usual structural and spectroscopic techniques: 1D and 2D NMR, MS and X-ray crystallography (see the Experimental Section below).

#### III.2.1.2.1 NMR Spectroscopy

Nuclear Magnetic Resonance (NMR) spectroscopy for **L1<sup>2+</sup>** has been carried out both in acetone-*d*<sub>6</sub> (**L1(PF<sub>6</sub>)<sub>2</sub>**) and methanol-*d*<sub>4</sub> (**L1(Cl)<sub>2</sub>**). Both 1D (<sup>1</sup>H, <sup>13</sup>C) and 2D (COSY and HSQC) experiments were necessary to characterize the structure of the ligand in solution (see Figure 5 and Figure S1 in the Supporting Information). All the resonances displayed could be unambiguously assigned based on their integrals, multiplicity and the *C*<sub>2v</sub> symmetry of the ligand in solution. For **L1<sup>2+</sup>**, both H5 and H6 (or H3 and H4) display a doublet of doublets with a mirror effect which is in agreement with the typical AA'BB' (5463 in our case) pattern of this kind of system<sup>20</sup> as shown in the inset of Figure 5. The singlet appearing at very low fields in acetone-*d*<sub>6</sub> (Figure 5a) can be assigned to the imidazolic protons C(9) and C(13) in accordance with the high electron-withdrawing effect of the two heteroatoms they have in alpha, as previously reported for similar ligands.<sup>21</sup> However, the integral of this resonance at 9.9 ppm sharply decrease (up to only 5% of the expected integral) when the <sup>1</sup>H NMR spectrum of **L1(Cl)<sub>2</sub>** is recorded in methanol-*d*<sub>4</sub> (Figure 5b), showing the fast exchange rate of these acidic protons with the protic solvent.

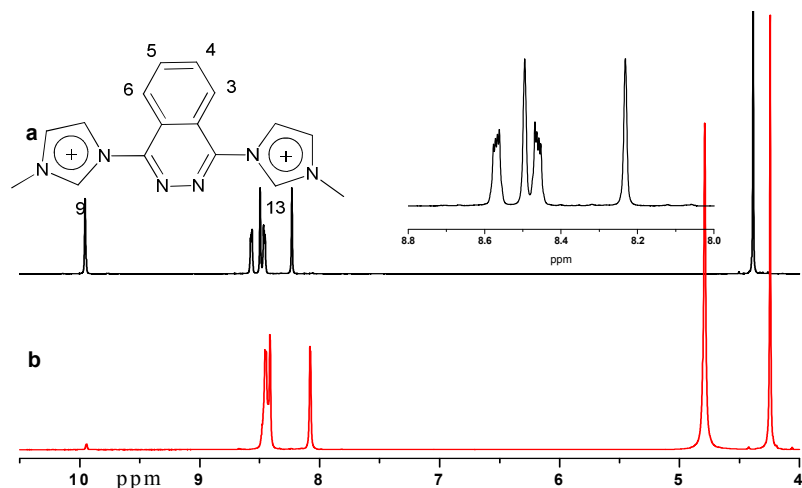


Figure 5.  $^1\text{H}$  NMR spectrum of  $\text{L1}(\text{PF}_6)_2$  in acetone- $d_6$  (a), and  $\text{L1}(\text{Cl})_2$  in MeOD (b). Inset: zoom of the aromatic region of  $\text{L1}(\text{PF}_6)_2$ .

### III.2.1.2.2. X-ray Crystal Structure of $\text{L1}(\text{PF}_6)_2$

Suitable crystals for X-ray diffraction analysis were obtained by slow diffusion of diethyl ether into a solution of  $\text{L1}(\text{PF}_6)_2$  in acetone. The ORTEP plot for the cationic moiety of  $\text{L1}^{2+}$  together with its corresponding atom labeling scheme are shown in Figure 6. Acquisition and crystallographic data are reported in Table S1 in the Supporting Information. It is worth mentioning that the steric congestion of both five membered rings (specially protons at C(13) and C(11)) with the central phthalazine moiety (protons at C(3) and C(6)) place the three scaffolds in different planes, being the angle between them of about  $53^\circ$  (see Figure S2 in the Supporting Information).





Figure 6. ORTEP plot of the crystal structure for  $L1^{2+}$ . Ellipsoids at 50% probability.

### III.2.2. Synthesis of Complexes $C1-Cl/OH_2$ , $C2-Cl/OH_2$ , $C3-Cl/OH_2$ and $C4-Cl/OH_2$

The synthesis of the chlorido and aqua complexes  $C1-Cl/OH_2$ ,  $C2-Cl/OH_2$ ,  $C3-Cl/OH_2$ , and  $C4-Cl/OH_2$  was carried out according to the usual procedures of our research group for this kind of complexes.<sup>22</sup> Besides  $L1^{2+}$ , we have chosen trpy, tpm and bpea (trpy = 2,2':6',2''-terpyridine, tpm = tri(1H-pyrazol-1-yl)methane, bpea = N,N-bis(pyridin-2-ylmethyl)ethanamine) as auxiliary ligands given their polypyridylic (and usually rugged) nature and their ability to fine-tune both the electronic (given the different type of N-donor sites) and geometric (*fac* vs. *mer*) properties of Ru-OH<sub>2</sub> species.<sup>23</sup> The ligands tpm and bpea were prepared following the reported methodologies while trpy was obtained commercially.<sup>24,25</sup>

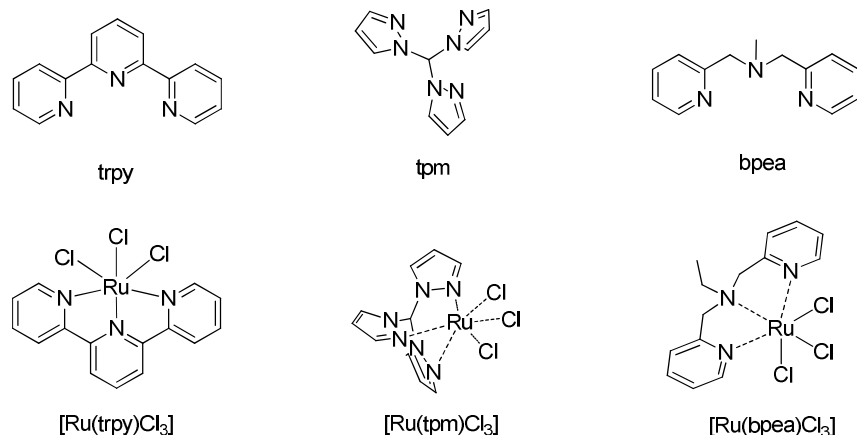
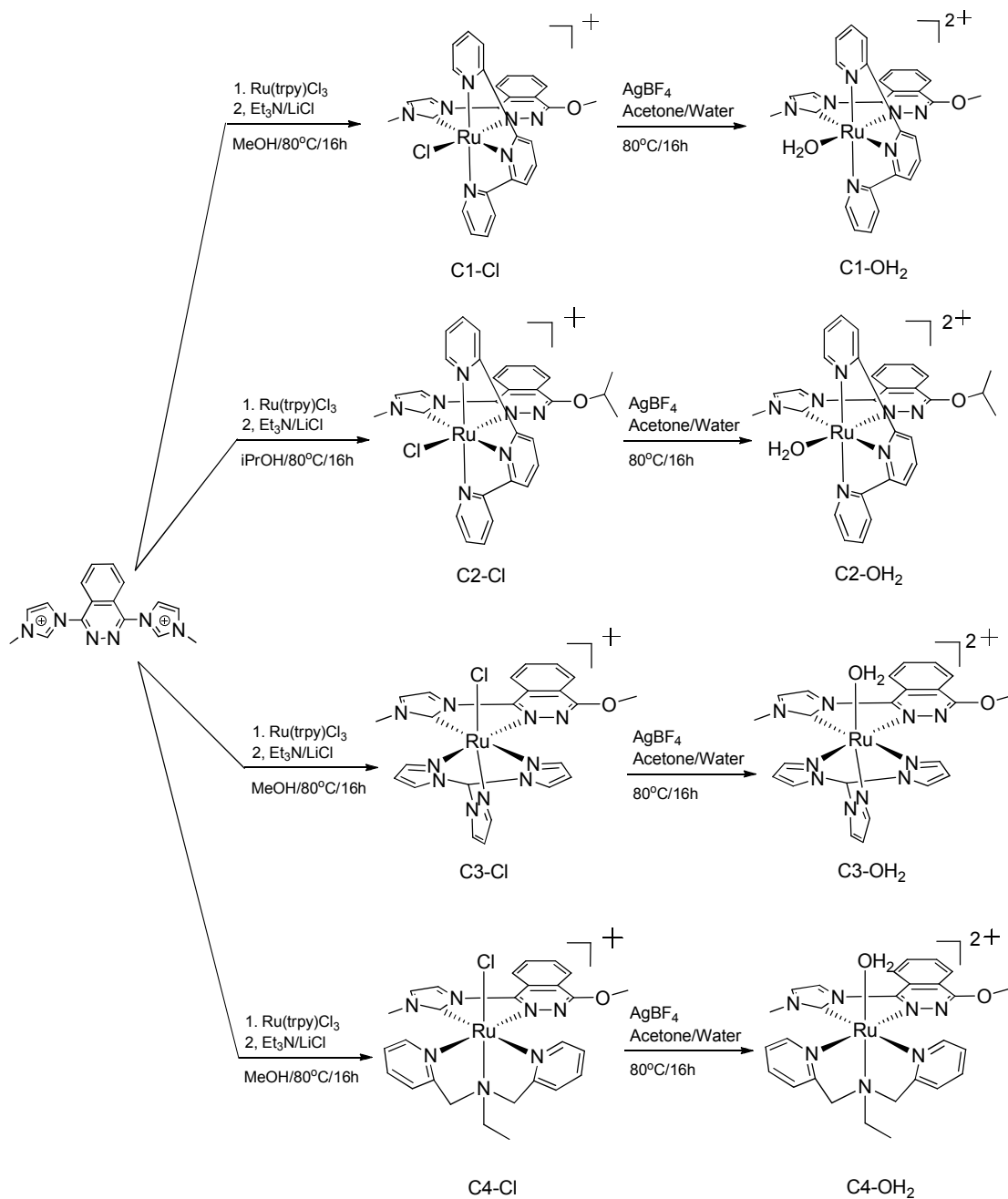


Figure 7. Drawing of the ligands trpy, tpm, bpea and precursors  $[\text{Ru}(\text{trpy})\text{Cl}_3]$ ,  $[\text{Ru}(\text{tpm})\text{Cl}_3]$  and  $[\text{Ru}(\text{bpea})\text{Cl}_3]$  employed in this work.

Different Ru complexes of general formula  $[\text{Ru}^{\text{III}}(\text{T})\text{Cl}_3]$  ( $\text{T} = \text{trpy}$ ,  $\text{bpea}$  or  $\text{tpm}$ , see Figure 7 above), where the tridentate N-donor ligands adopt either facial or meridional coordination geometries around the central metal ion have been used as precursors to introduce the dinucleating CNNC ligand  $\text{L1}^{2+}$ .<sup>26,27,28</sup> Following previously reported synthetic strategies reported by our group,<sup>29,30</sup> 2 molar equivalents of  $[\text{Ru}^{\text{III}}(\text{T})\text{Cl}_3]$  were mixed with  $\text{L1}^{2+}$ , triethylamine ( $\text{Et}_3\text{N}$ ) as reducing agent and  $\text{LiCl}$  to ensure the presence of a labile site in the generated complexes. After hot filtration, addition of a few drops of aqueous  $\text{NH}_4\text{PF}_6$  to the crude solution and partial solvent evaporation under vacuum a brown-orange precipitate appeared in all cases. However, despite bimetallic species with different relative arrangements of the Ru-Cl sites were expected, the mononuclear complexes **C1-Cl** (*cis*- $[\text{Ru}^{\text{II}}(\text{PhthaPz-Ome})(\text{trpy})\text{Cl}]\text{PF}_6$ ), **C2-Cl** (*cis*- $[\text{Ru}^{\text{II}}(\text{PhthaPz-Ipro})(\text{trpy})\text{Cl}]\text{PF}_6$ ), **C3-Cl** ( $[\text{Ru}^{\text{II}}(\text{PhthaPz-Ome})(\text{tpm})\text{Cl}]\text{PF}_6$ ) and **C4-Cl** (*trans, fac*- $[\text{Ru}^{\text{II}}(\text{PhthaPz-Ome})(\text{bpea})\text{Cl}]\text{PF}_6$ ) were obtained under the reaction conditions employed (see section III.2.3 below). The subsequent synthesis of the corresponding aqua complexes involved the presence of silver tetrafluoroborate ( $\text{AgBF}_4$ ), which promotes the decoordination of the chlorido ligand (silver chloride is formed as a grey-white precipitate), thus allowing the coordination of the water molecule. After  $\text{AgCl}$  filtration, acetone was slowly evaporated under vacuum. The counter ion could be easily exchanged from  $\text{BF}_4^-$  to  $\text{PF}_6^-$  by adding excess  $\text{NH}_4\text{PF}_6(\text{aq})$  into the aqueous solution obtaining the whole set of  $[\text{Ru}-\text{OH}_2](\text{PF}_6)_2$  type of complexes as orange-red

precipitates. Scheme 4 shows the whole synthetic procedure followed for the synthesis of the four complexes.

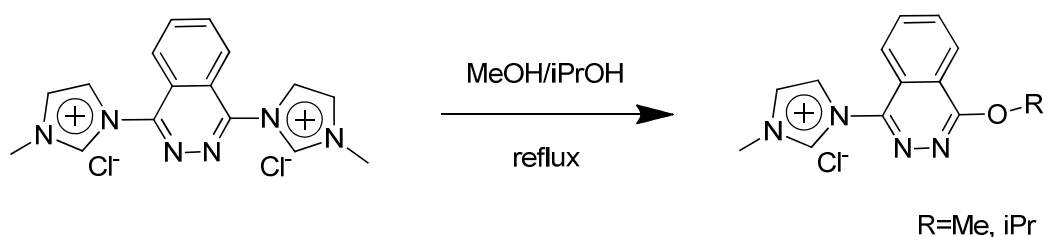


Scheme 4. Synthetic procedure for C1-Cl/OH<sub>2</sub>, C2-Cl/OH<sub>2</sub>, C3-Cl/OH<sub>2</sub> and C4-OH<sub>2</sub>.

### III.2.3. Breakage of Ligand L1<sup>2+</sup>

The formation of the mononuclear complexes shown in Scheme 3 above originates from the breakage of the dinucleating CNNC Ligand L1<sup>2+</sup> under the reaction conditions

employed. Although ligand  $L1^{2+}$  (no matter  $L1(PF_6)_2$  or  $L1Cl_2$ ) shows excellent stability in air and also in solutions of acetone and methanol at room temperature,  $L1^{2+}$  decomposes when refluxed overnight in methanol as proved by  $^1H$  NMR and Mass Spectrometry (MS), which confirmed the replacement of one imidazole ring of  $L1^{2+}$  by a methoxy group. The proposed process is illustrated in Scheme 4. Other researchers have previously reported similar decomposition processes by using related CNNC ligands in nucleophilic protic solvents.<sup>31, 32, 33</sup> Isopropanol, with increased steric hindrance and therefore less nucleophilic character, was then tested as solvent for the coordination of  $L1^{2+}$  to the Ru metal ion. However, the same process was observed, with decomposition of the tetradentate ligand and formation of a mononuclear complex. As a result, the new ligands PhthaPz-OMe (abbreviated as CN-OMe, from methanol) and PhthaPz-iPrO (CN-iPrO from isopropanol) are obtained from  $L1^{2+}$  and coordinated to the Ru metal ion.



Scheme 5. Proposed nucleophilic process leading to the breakage of  $L1^{2+}$ .

The decomposition of the  $L1^{2+}$  tetradentate ligand can also be explained from an electronic point of view. When  $L1^{2+}$  coordinates to a first electrophilic Ru(II) ion there is a flow of electron-density from this ligand to the metal center and, therefore, the nucleophilic attack of a MeOH or iPrOH solvent molecule is still more favored.

### III.2.4. Characterization of the Complexes

The structure of the above-depicted mononuclear complexes was confirmed either by spectroscopic (1D and 2D NMR and UV-vis), spectrometric (ESI-MS), electrochemical (CV and DPV) and analytical (Elemental Analysis) techniques as will be shown in the following sections.

### III.2.4.1. NMR Spectroscopy

Nuclear Magnetic Resonance experiments have been carried out for the diamagnetic compounds **C1-Cl/OH<sub>2</sub>**, **C2-Cl/OH<sub>2</sub>**, **C3-Cl/OH<sub>2</sub>** and **C4-Cl/OH<sub>2</sub>**. Both 1D (<sup>1</sup>H and <sup>13</sup>C) and 2D (TOCSY, ROESY, HSQC and HMBC) NMR experiments have proven to be mandatory tools in order to structurally characterize these compounds in solution (see Figures S3 to S10 in the Supporting Information).

In analogy to what is observed with other tetradentate dinucleating bridging ligands such as Hbpp (3,5-Bis(2-pyridyl)pyrazole)<sup>34</sup> or phthalazin-bis(triazole),<sup>35</sup> a family of dinuclear complexes with general formula [Ru<sub>2</sub><sup>II</sup>(T)<sub>2</sub>(μ-Cl)(μ-L1)]<sup>3+</sup> (T = trpy, bpea or tpm) was expected when combining (under the reaction conditions shown in Scheme 3 above) the CNNC ligand **L1**<sup>2+</sup> with the three precursors shown in Figure 7. However, when the obtained precipitates were subjected to <sup>1</sup>H NMR analysis the obtained resonances, integrals and coupling constants corresponded with those expected for a mononuclear complex. Furthermore, DOSY NMR experiments (Figure 8 shows the diffusion spectrum of **C1-Cl** as a representative example) excluded the presence of mixed mono- and dinuclear species.

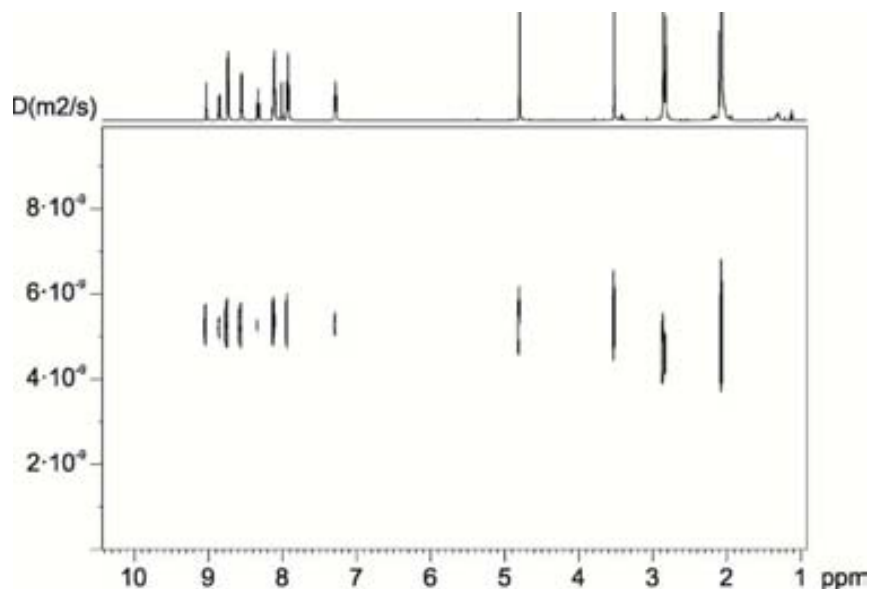


Figure 8. DOSY NMR spectrum of **C1-Cl** in acetone-d<sub>6</sub>.

The loss of the “ABBA” spin-spin coupling pattern in the <sup>1</sup>H NMR spectrum of **C1-Cl** (Figure 9) perfectly agrees with the reduced symmetry of **L1**<sup>2+</sup> after nucleophilic



isopropyl group and the protons on C(27), C(28) and C(24) of the trpy ligand as well as between the methyl group of the imidazole ring and the proton on C(21) of the trpy ligand, this clearly identifying the *cis* disposition of the **C2-Cl** complex. The same conclusion could be extracted from the ROESY NMR spectra of **C1-Cl**, being the isomer obtained also *cis* in nature.

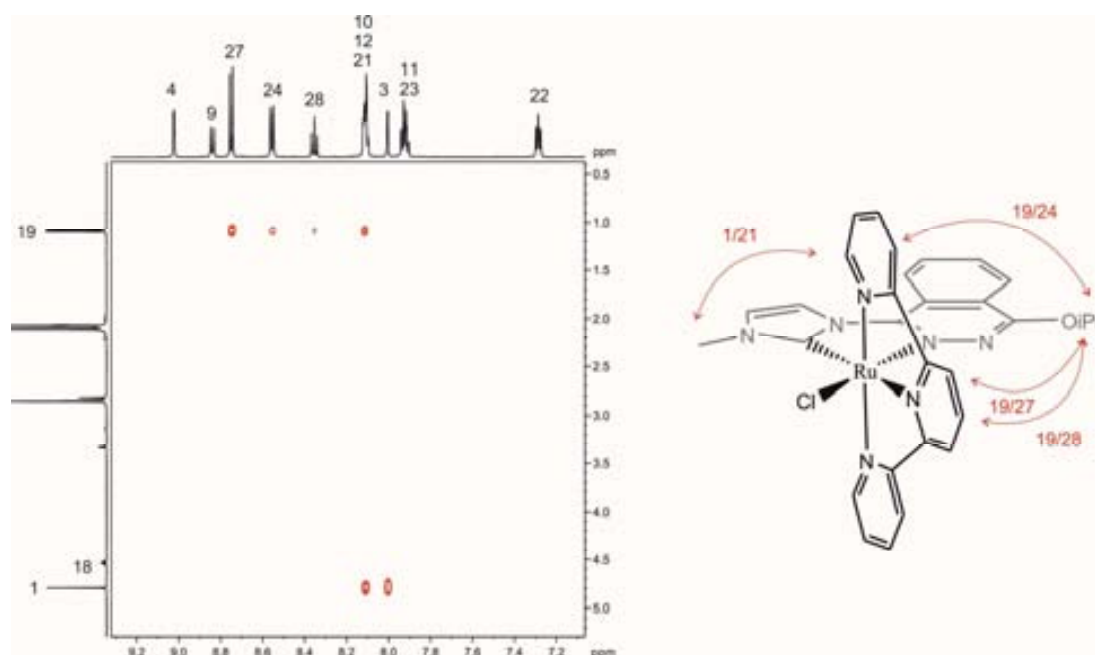


Figure 10. Selective 2D ROESY NMR spectrum of **C2-Cl** in acetone- $d_6$  and schematic drawing of the observed interactions. .

Due to the  $C_3$  symmetry of the tpm ligand, which coordinates in a facial manner, no isomeric mixtures are expected for complex **C3-Cl**. This can be corroborated in the obtained  $^1\text{H}$  NMR spectrum shown in Figure 11. The  $C_1$  symmetry of the complex converts the whole set of protons in different resonances and a complex spectrum is obtained. The assignment of each resonance to a single proton was carried out by means of the 2D (HSQC, HMBC, ROESY and TOSCY) spectra shown in Figures S5.

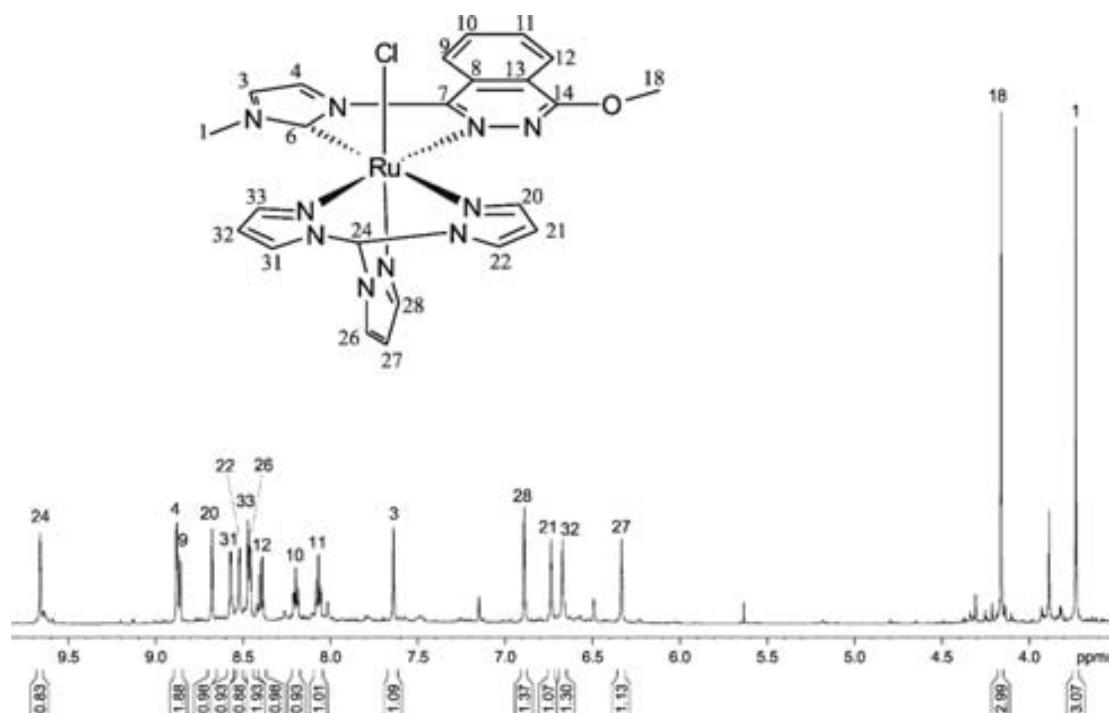


Figure 11. <sup>1</sup>H-NMR of **C3-Cl** in acetone-d<sub>6</sub> and its corresponding proton assignment.

Similar to **C3-Cl**, no symmetry is observed in the <sup>1</sup>H NMR spectrum of **C4-Cl**. Due to its flexibility, the tridentate bpea ligand is able to potentially coordinate the central metal both facially and meridionally.<sup>36</sup> Therefore, in combination with a non-symmetric bidentate ligand such as PhthaPz-OMe, seven potential stereoisomers can be obtained.<sup>37,38</sup> A drawing of these seven potential isomers as well as the notation used for each of them is shown in Figure 12. The letters a-g following the name of the complex will be used from now on to identify these isomers through the text. The notation *fac* and *mer* refers to the facial or meridional disposition of the bpea ligand whereas *up* and *down* indicates the relative orientation of the ethyl group of bpea with regards to the chlorido ligand upon coordination. Both steric and electronic interactions between the ligands coordinated to the metal center play a key role in the degree of the isomeric mixture synthetically obtained. However, in the synthesis of **C4-Cl**, just the *trans, fac* isomer is formed. Hydrogen bondind interactions between the proton alpha to the pyridylic nitrogens of bpea and the chlorido ligand dramatically stabilize a *trans, fac* conformation lowering the energy of the system and stabilizing the molecular geometry. This strong stabilitzation of the *trans, fac* isomer has already been reported and thoroughly studied by means of theoretical DFT calculations for similar Ru-based



systems.<sup>39</sup> The predominance of these hydrogen-bonding interactions over other factors for stabilizing and selectively obtaining the *trans,fac* isomer in a series of related complexes has been recently established by our research group.<sup>40</sup>

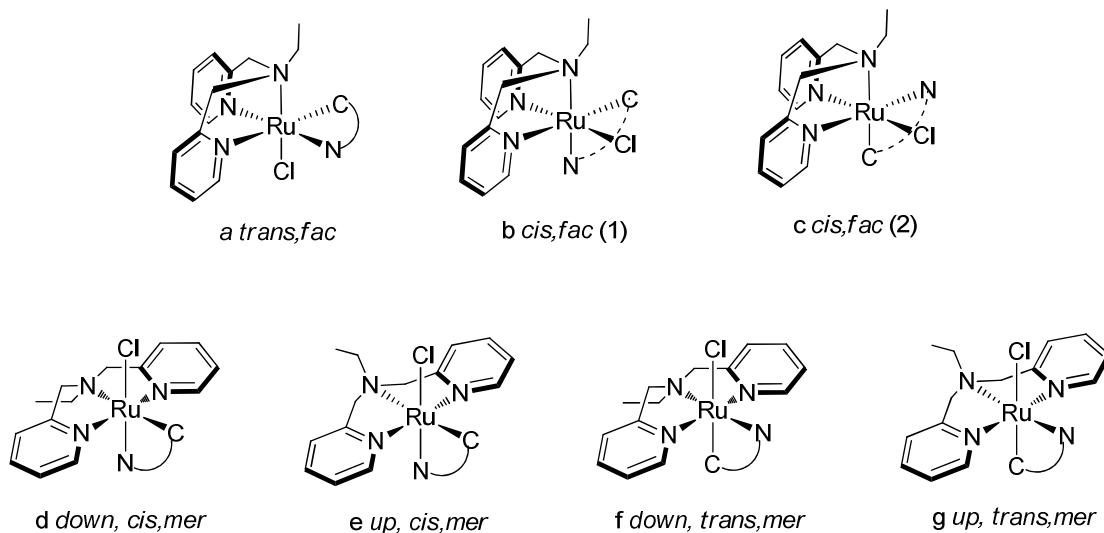


Figure 12. Possible diastereoisomers for Complex **C4-Cl**.

The *trans,fac* assignment for the pure **C4-Cl** species obtained was corroborated by NMR spectroscopy. When this complex was subjected to selective 2D NOESY NMR, key interactions unambiguously revealed the *trans, fac* nature of the obtained species (see Figure 13 and Figure S6 in the Supporting Information). Therefore, interaction between the protons of C(1) and C(20) C(21), C(18) and C(34) as well as interaction between the chlorido ligand and the protons of C(20) and C(34) could be witnessed, that confirming the *trans,fac* nature of the **C4-Cl** species.

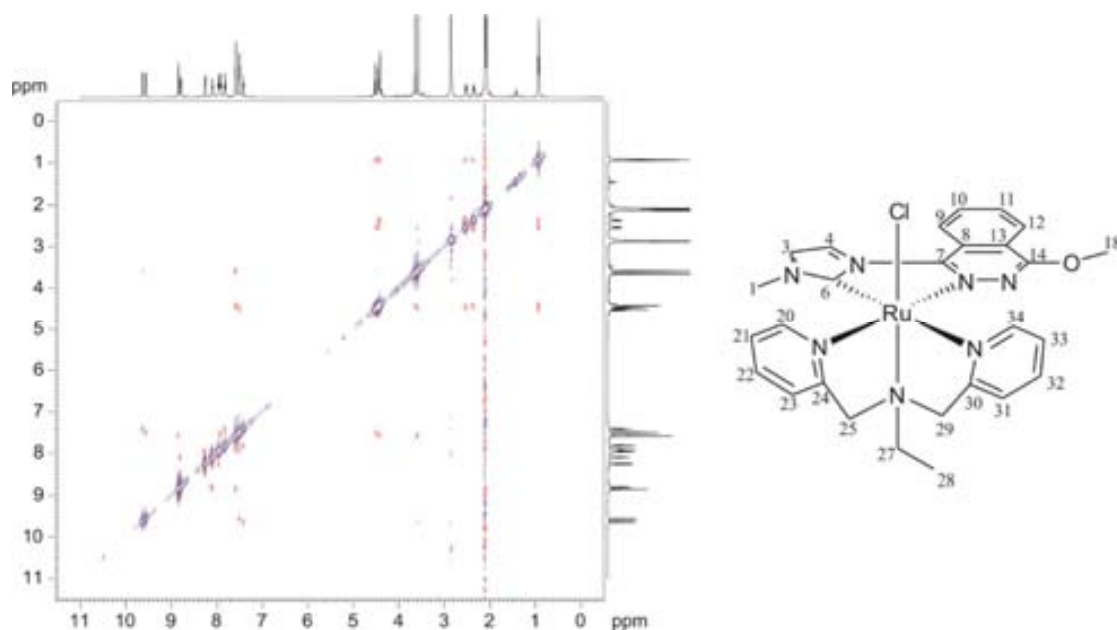


Figure 13. Selective 2D NOESY NMR in acetone- $d_6$  and numbering scheme of **C4-Cl**

Therefore, summarizing, from a geometrical point of view the four complexes prepared can be classified into two groups: **C1-Cl** and **C2-Cl** as meridional species, and **C3-Cl** and **C4-Cl** as facial compounds.

As expected, replacement of a chlorido ligand by a water molecule in these families of complexes induces significant chemical shift displacements. This is exemplified by the **C1-Cl/OH<sub>2</sub>**  $^1\text{H}$  NMR couple show in Figure 14, where mainly protons close to these monodentate ligands such as those on C(26), C(27) and C(22) are affected. Similar displacements of the chemical shifts were observed for the **C2-Cl/OH<sub>2</sub>** couple as illustrated in Figure S4 in the Supporting Information. Both complexes maintain the *cis* conformation after the coordination of the aqua ligand.

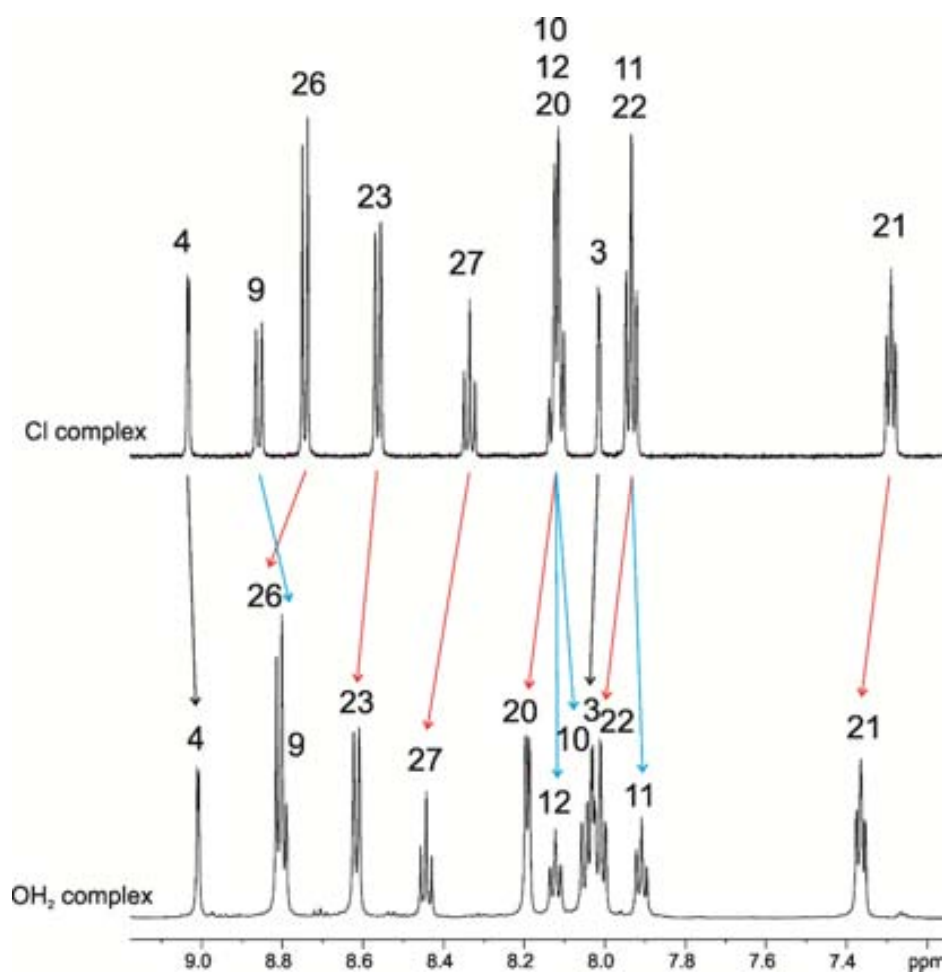


Figure 14. Aromatic region of the <sup>1</sup>H NMR spectrum of C1-Cl and C1-OH<sub>2</sub> in acetone-d<sub>6</sub>.

Complexes C3-OH<sub>2</sub> and C4-OH<sub>2</sub> also maintain their original conformation in solution after water coordination as can be deduced from the NMR spectra shown in Figures S9 and S10 in the Supporting Information.

The four aqua complexes prepared are soluble in water. However, it is worth to mention that when the meridional complexes C1-OH<sub>2</sub> and C2-OH<sub>2</sub> are dissolved in this solvent, they slowly decompose. Figure 15 displays the spectral changes of C1-OH<sub>2</sub> dissolved in D<sub>2</sub>O and left at room temperature during one week. Although the transformation process as well as the final structure of the compound/s formed is still not clear, their instability in water and the rate at which this decomposition takes place are key factors for the posterior study of the electrochemical and catalytic properties of these complexes in this solvent (see below). On the other hand, complexes C3-OH<sub>2</sub> and C4-

OH<sub>2</sub> are stable in water, as shown by the invariable appearance of their NMR spectra in D<sub>2</sub>O (see Figure S11 in the Supporting Information).

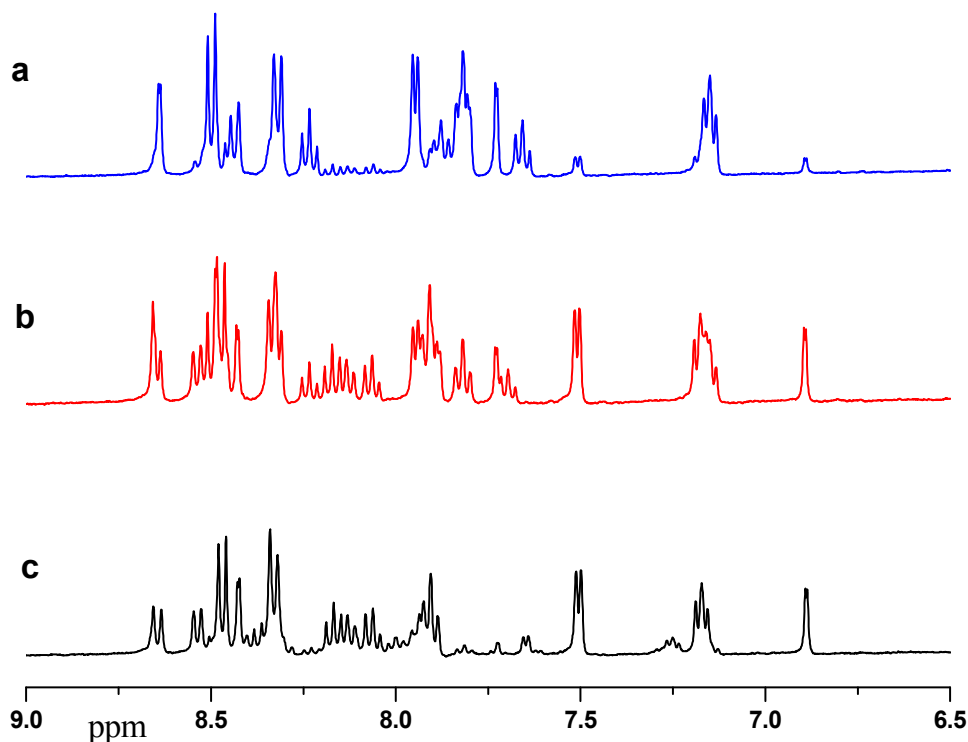


Figure 15. Structural transformation of C1-OH<sub>2</sub> in water solution, a) C1-OH<sub>2</sub> freshly dissolved in D<sub>2</sub>O, b) C1-OH<sub>2</sub> dissolved in D<sub>2</sub>O for 48hs, c) C1-OH<sub>2</sub> dissolved in D<sub>2</sub>O for 7 days.

#### III.2.4.2. X-ray Crystal Structure

Suitable crystals for X-ray diffraction analysis of C4-Cl were obtained by slow diffusion of diethyl ether into a solution of C4-Cl in methanol. Figure 16 displays an ORTEP plot for the cationic moiety of this complex as well as its corresponding atom labeling scheme. A selection of the more relevant bond distances and angles is reported in Table 1. Acquisition and crystallographic data is reported in the Supporting Information (Table S2).

The Ru(II) ion adopts a distorted octahedral geometry with bond distances and angles that resemble to analogous complexes reported in earlier literature.<sup>41</sup> The Ru carbene

bond distance (1.962Å) is shorter than the Ru-N bonds (more than 2Å). The bond angles N(1)-Ru(1)-Cl(1) (171.63°), N(2)-Ru(1)-Cl(1) (94.92°) and N(3)-Ru(1)-Cl(1) (90.90°) show the facial coordination of the tridentate N-donor bpea ligand to the Ru metal center. The Ru-Cl bond appears *trans* to the Ru-carbene bond, which reveals the *trans, fac* conformation of the C4-Cl complex in agreement with its structure in solution determined by NMR spectroscopy (see section III.2.4.1 above). Furthermore, it can be observed that the imidazole and the phthalazine rings do not lay exactly on the same plane. Instead, there is a torsion angle of 16°. However, this angle is obviously shorter with regard to the one observed for the free ligand, which was of 53° (see Figure 6 above). The methoxy group is nearly on the same plane of the phthalazine skeleton since the observed torsion angle C(30)-O(1)-C(16)-N(5) is only of 1.9°. Further, instead of the 90° expected for an ideal octahedral geometry, the N(1)-Ru(1)-N(3) and N(1)-Ru(1)-N(2) angles are, respectively, of 81.15° and 81.68° due to the formation of two five-membered rings when the bpea ligand coordinates to the central Ru ion. In addition, a clear hydrogen-bonding interaction is observed between the pyridyl protons of the bpea ligand on C(12) and C(13) and the chlorido ligand (2.7Å). This electronic interaction is responsible for the strong stabilization of the *trans, fac* isomer and of its pure attainment during the synthetic procedure.

Furthermore, C4-Cl crystallizes in a small unit cell containing two independent complex molecules and two PF<sub>6</sub> anions. The two PF<sub>6</sub> anions locate in the center of the cell while the two complex molecules on the two sides of the PF<sub>6</sub> anions (Figure 16b).

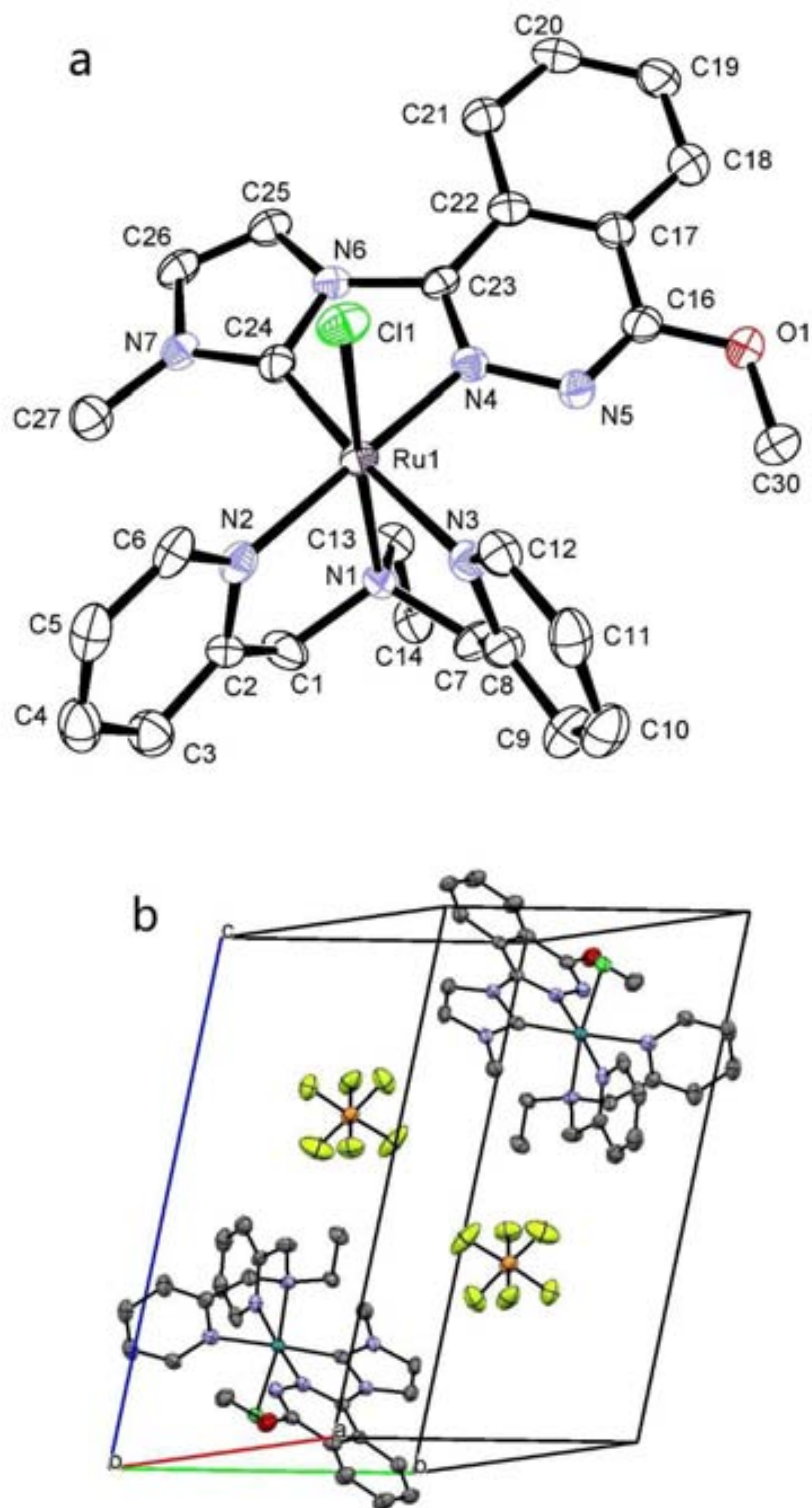


Figure 16. ORTEP plot of (a) the cationic moiety of C4-Cl and (b) its unit cell.

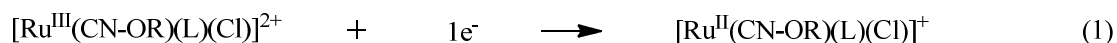
Table 1. Selected interatomic distances (Å) and angles (°) for complex **C4-Cl**

BOND DISTANCES			
Ru(1)-C(24)	1.962(4)	Ru(1)-N(1)	2.130(4)
Ru(1)-N(4)	2.014(4)	Ru(1)-N(3)	2.139(4)
Ru(1)-N(2)	2.066(4)	Ru(1)-Cl(1)	2.4088(12)
ANGLES			
C(24)-Ru(1)-N(4)	77.44(16)	N(4)-Ru(1)-Cl(1)	88.04(11)
C(24)-Ru(1)-N(2)	101.35(16)	N(2)-Ru(1)-N(1)	81.68(15)
C(24)-Ru(1)-N(1)	98.55(16)	N(2)-Ru(1)-N(3)	83.78(13)
C(24)-Ru(1)-N(3)	174.78(16)	N(2)-Ru(1)-Cl(1)	94.92(12)
C(24)-Ru(1)-Cl(1)	89.60(13)	N(1)-Ru(1)-N(3)	81.15(14)
N(4)-Ru(1)-N(2)	176.80(15)	N(1)-Ru(1)-Cl(1)	171.63(10)
N(4)-Ru(1)-N(1)	95.54(14)	N(3)-Ru(1)-Cl(1)	90.90(11)
N(4)-Ru(1)-N(3)	97.38(14)		

### III.2.4.3. Electrochemistry

The redox properties of the eight complexes described in the present work have been investigated in terms of CV and DPV. The electrochemistry of the **C1-C4-Cl** complexes is reported in dichloromethane (DCM) and that of the aqua complexes **C1-C4-OH<sub>2</sub>** in both DCM and aqueous solutions at diverse pH values (from pH=0 to 14).

The CVs for the chlorido complexes in DCM are shown in Figure 17 and exhibit single reversible waves at different potentials corresponding to the following process:



L = trpy, tpm or bpea R = Me or iPr

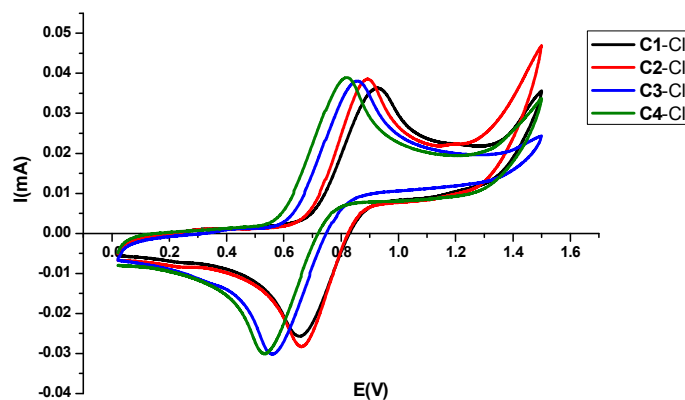
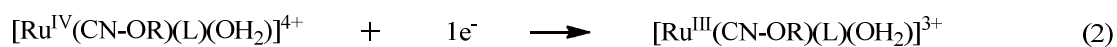


Figure 17. Cyclic Voltammetry of **C1-Cl**, **C2-Cl**, **C3-Cl** and **C4-Cl** in DCM (0.1 M TBAPF<sub>6</sub>) at a scan rate of 100 mv/s and using glassy carbon as working electrode and SSCE as reference electrode.

As usual for this type of Ru-aqua complexes, Ru(III/II) processes are not observed in DCM. Therefore, the reversible waves shown in Figure 18 correspond to the following Ru(IV/III) process:



L = trpy, tpm or bpea R = Me or iPr

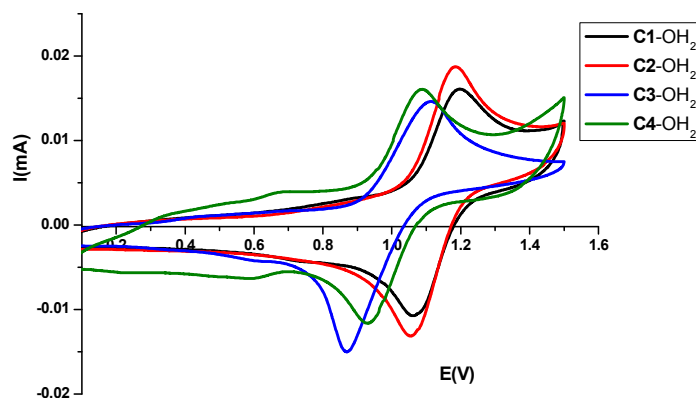


Figure 18. Cyclic Voltammetry of **C1-OH<sub>2</sub>**, **C2-OH<sub>2</sub>**, **C3-OH<sub>2</sub>** and **C4-OH<sub>2</sub>** in DCM (0.1 M TBAPF<sub>6</sub>) at a scan rate of 100 mv/s and using glassy carbon as working electrode and SSCE as reference electrode.



Given the high similarity of the structural and chemical surroundings of the Ru metal ion in the meridional complexes **C1-Cl/OH<sub>2</sub>** and **C2-Cl/OH<sub>2</sub>** (being the only difference among them a OMe or OiPr substituent in a quite remote position), the redox chemistry of both chlorido and aqua complexes is very similar when studied in DCM (see Figures 17 and 18 and Table 2). However, a clear downshift of the E<sub>1/2</sub> is observed for the facial derivatives **C3-Cl/OH<sub>2</sub>** and **C4-Cl/OH<sub>2</sub>** when compared with their corresponding meridional counterparts. This is in agreement with the higher σ-donating and lower π-acceptor capacity of both the imidazole rings (**C3-Cl/OH<sub>2</sub>**) and the aliphatic N (**C4-OH<sub>2</sub>**) with regards to the pyridyl scaffolds of the trpy ligand. The observed decrease in the redox potentials is in the range of 80-120 mV (see Table 2).

Table 2. Redox potentials of **C1-Cl/OH<sub>2</sub>** to **C4-Cl/OH<sub>2</sub>** in DCM (0.1 M TBAPF<sub>6</sub>).

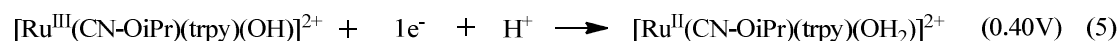
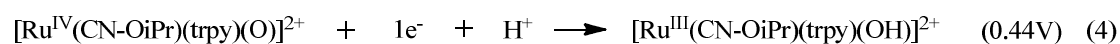
	<b>C1-Cl/OH<sub>2</sub></b>	<b>C2-Cl/OH<sub>2</sub></b>	<b>C3-Cl/OH<sub>2</sub></b>	<b>C4-Cl/OH<sub>2</sub></b>
E <sub>1/2</sub> (III/II) (Cl)	0.79V	0.78V	0.71V	0.68V
E <sub>1/2</sub> (IV/III) (OH <sub>2</sub> )	1.11V	1.11V	0.99V	1.02V

In order to further understand the redox behavior of the four Ru-OH<sub>2</sub> complexes, their electrochemical properties have also been extensively investigated by means of CV and DPV in aqueous solutions with pH range from 0 to 14.

For complex **C2-OH<sub>2</sub>** at pH=1, the single reversible wave observed (see the CV and DPV shown in Figures 19 and 20, respectively) is assigned to the following one electron process:



At pH=8, two very close redox processes can be observed in the CV and DPV (Figure 19 and Figure 20, respectively) that are assigned to the following electrochemical processes:



As shown in Equations 4 and 5 for complex  $C2-OH_2$  the presence of the aqua group enables a PCET (proton coupled electron transfer) process. The simultaneous removal of electrons and protons facilitates the access to high oxidation states by preventing the built up of columbic charge in the complex. That makes the two redox processes to occur at comparatively low potentials and in a rather narrow potential range. The stability region of the Ru(III) species is quite small, as evidenced by the fact that the two reversible waves observed are only 40 mV apart.

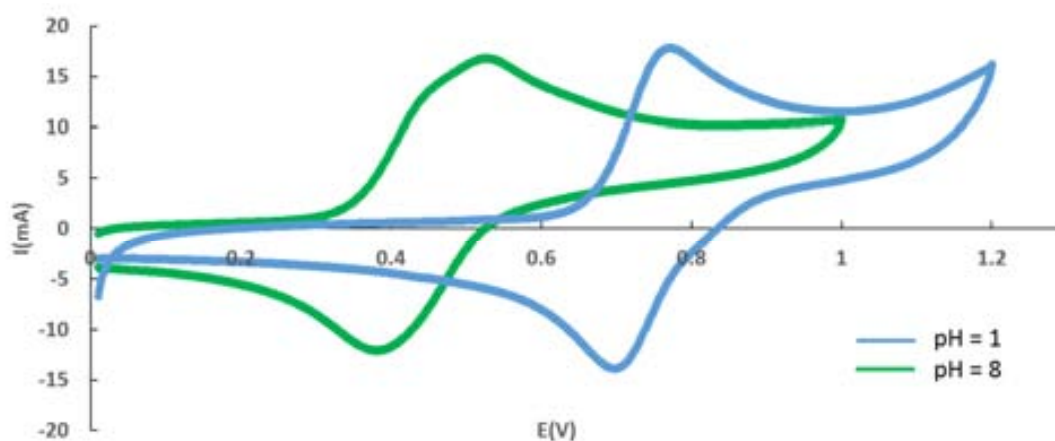


Figure 19. CV of  $C2-OH_2$  in pH=1 water (triflic acid buffer) and pH=8 (phosphate buffer) at 100 mV/s scan rate. Glassy carbon is used as working electrode and the potential is measured vs. SSCE.

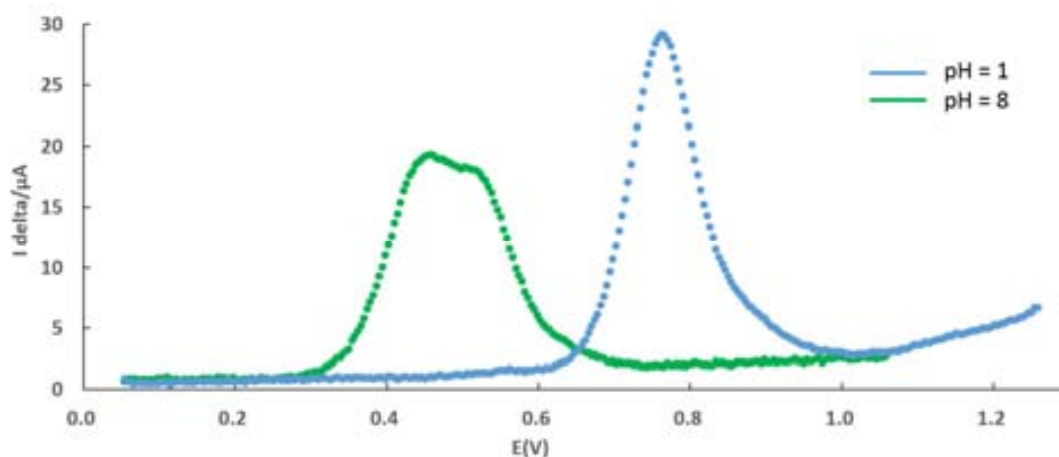


Figure 20. DPV of  $C2-OH_2$  in pH=1 water (triflic acid buffer) and pH=8 (phosphates buffer) at 20 mV/s scan rate. Glassy carbon is used as working electrode and the potential is measured vs. SSCE.

The simultaneous removal of protons and electrons taking place in ruthenium aqua complexes such as the ones here described provokes the pH-dependence of their redox potentials. This dependence is usually reflected in the so-called Pourbaix diagrams and the results obtained for complex  $C2-OH_2$  are displayed in Figure 21.

From pH=7 to pH=11 two independent one-electron redox processes that take place with simultaneous proton transfer are observed. The corresponding lines present a slope of approximately 59 mV per pH unit, as expected for a one-electron one-proton transfer (see equations 4 and 5 above).<sup>42</sup> At lower pH, only the Ru(III/II) couple can be observed. The diminishment or disappearance of the Ru(IV/III) redox couple in CV experiments is quite common for aqua complexes and is assumed to be caused by slow heterogeneous electron-transfer kinetics from the solution to the electrode surface.<sup>43</sup> The stability regions for species having different proton composition are indicated in the diagram along with the pKa values for Ru(III) and Ru(II) aqua complexes, which are around 2.8 and 11.0, respectively.

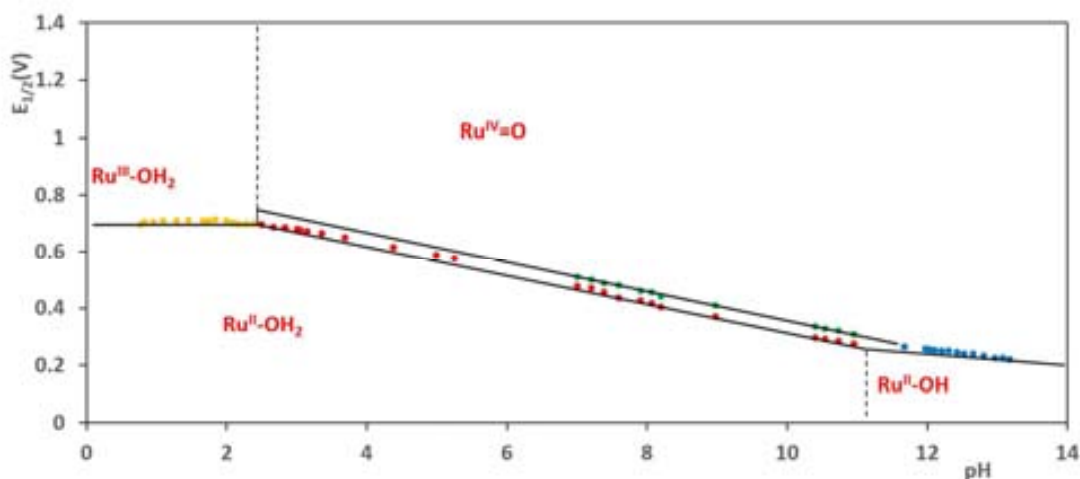
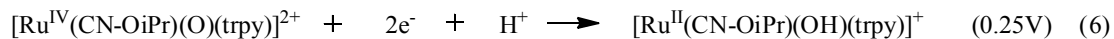


Figure 21. A plot of  $E_{1/2}$  vs. pH (Pourbaix Diagram) for complex **C2-OH<sub>2</sub>**. The pH/potential regions of stability for the various oxidation states and their dominant proton compositions are indicated by using abbreviations such as Ru<sup>II</sup>-OH<sub>2</sub>, for example, for [Ru<sup>II</sup>(CN-OiPr)(OH<sub>2</sub>)(trpy)]<sup>2+</sup>.

The vertical dashed lines in the various E/pH regions show the pKa values.

From pH=11.5, the redox decreasing slope changes and the reversible wave is assigned as a different type of PCET process taking place in alkaline solution:



As expected given the almost identical coordination environment, similar redox behavior was observed for **C1-OH<sub>2</sub>** in aqueous solution. Therefore, the electrochemical study of this complex (CVs, DPVs and Pourbaix Diagram) is shown as Supporting Information in Figures S12-S14.

The redox properties in aqueous solution of the facial aqua complex **C3-OH<sub>2</sub>** are particularly different. At pH=1, the single reversible wave observed in both CV and DPV (Figures 22 and 23, respectively) is assigned to the following one electron process:



The redox potentials of the Ru(III/II) couple measured at pH=1 are shifted cathodically by 120 mV with regard to **C1-OH<sub>2</sub>** and **C2-OH<sub>2</sub>** due to the stronger electron donating character of the tpm ligand presented in **C3-OH<sub>2</sub>**. Similarly to in **C2-OH<sub>2</sub>** and **C1-OH<sub>2</sub>**, a cathodic shift of the redox potentials is observed when the pH increase due to PCET.

From pH=1.85 to pH=11.13 a single two-electron redox processes that take place with simultaneous proton transfer is observed. The corresponding line present a slope of approximately 59 mV per pH unit (see the corresponding Pourbaix Diagram in Figure 24), as expected for the two-electron two-proton transfer shown in equation (8).

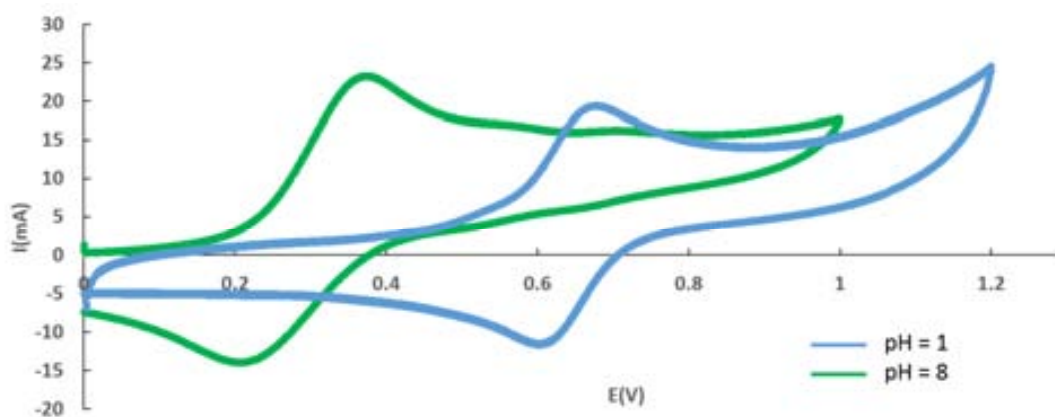
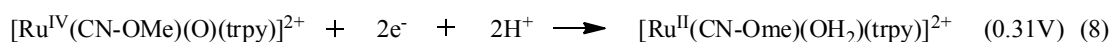


Figure 22. CV of C3-OH<sub>2</sub> in water pH=1 (triflic acid buffer) and pH=8 (phosphates buffer) at 100 mV/s scan rate. Glassy carbon is used as working electrode and the potential is measured vs. SSCE.

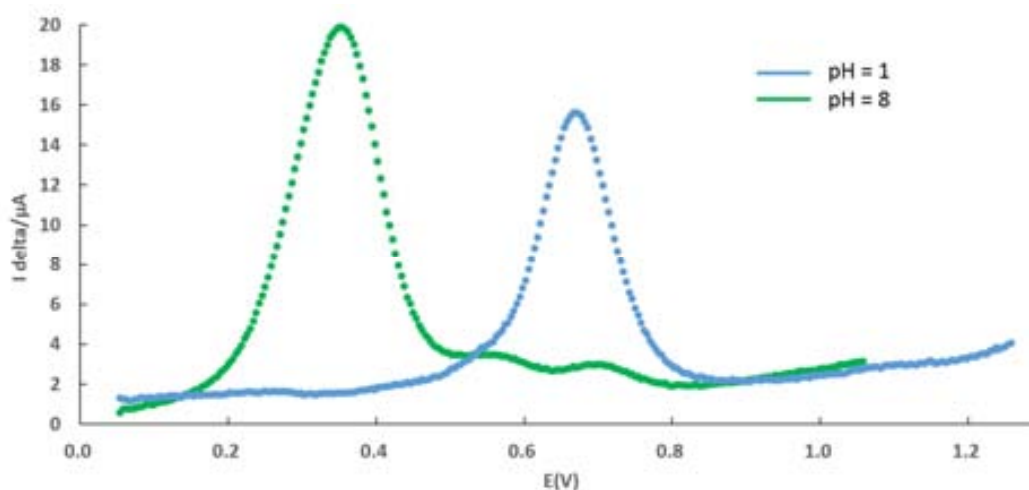


Figure 23. DPV of C3-OH<sub>2</sub> in water pH=1 (triflic acid buffer) and pH=8 (phosphate buffer) at 20 mV/s scan rate. Glassy carbon is used as working electrode and the potential is measured vs. SSCE.

The stability regions for species having different proton composition are indicated in the Pourbaix diagram shown in Figure 24 along with the pKa values for Ru(III) and Ru(II), which are around 1.8 and 11.2.

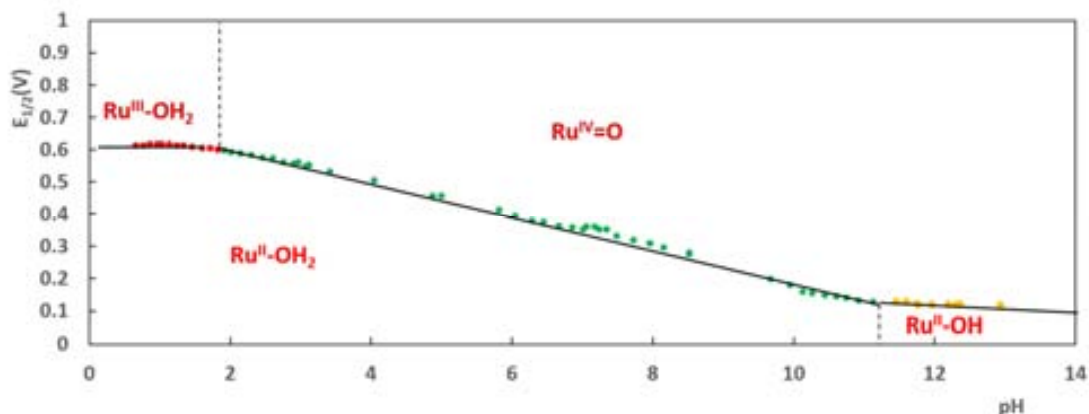


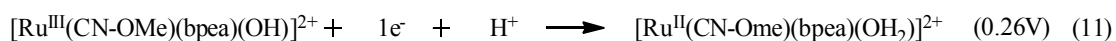
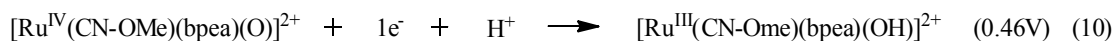
Figure 24. A plot of  $E_{1/2}$  vs. pH (Pourbaix Diagram) for complex C3-OH<sub>2</sub>. The pH/potential regions of stability for the various oxidation states and their dominant proton compositions are indicated by using abbreviations such as Ru<sup>II</sup>-OH<sub>2</sub>, for example, for [Ru<sup>II</sup>(CN-OMe)OH<sub>2</sub>(tpm)]<sup>2+</sup>.

The vertical solid lines in the various E/pH regions show the pKa values.

Dramatically different is the observed redox behavior of C4-OH<sub>2</sub>. At pH=1, the sole reversible wave that appears in the CV and DPV (Figure 25 and Figure 26) is assigned as the following one electron process:



At pH=8, two redox processes could be observed as illustrated in the CV and DPV respectively shown in Figures 25 and 26, which are assigned to the following electrochemical reactions:



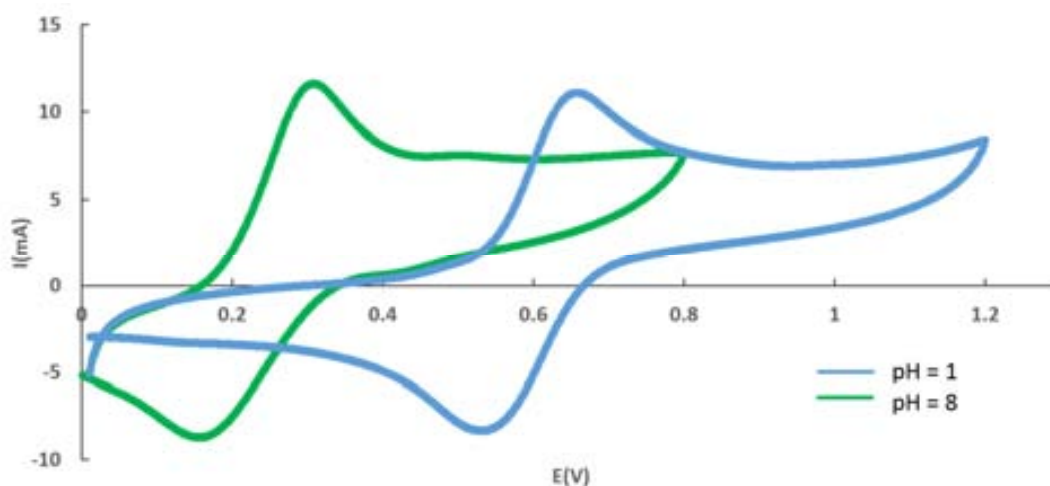


Figure 25. CV of C4-OH<sub>2</sub> in water pH=1 (triflic acid buffer) and pH=8 (phosphates buffer) at 100 mV/s scan rate. Glassy carbon is used as working electrode and the potential is measured vs. SSCE.

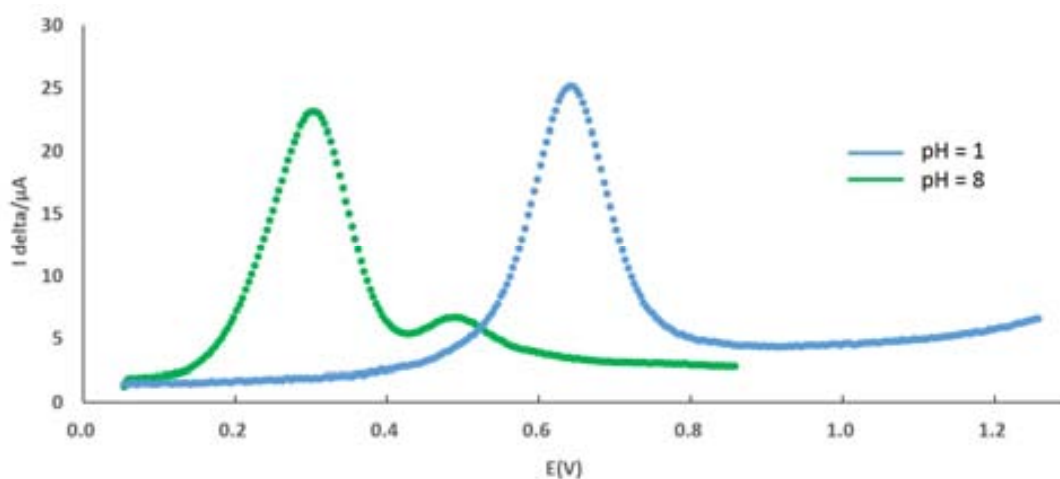


Figure 26. DPV of C4-OH<sub>2</sub> in water pH=1 (triflic acid buffer) and pH=8 (phosphates buffer) at 20 mV/s scan rate. Glassy carbon is used as working electrode and the potential is measured vs. SSCE.

The  $\Delta E_{1/2}$  value ( $\Delta E_{1/2}$ , defined as the difference between  $E_{1/2}(\text{IV/III})$  and  $E_{1/2}(\text{III/II})$ , which defines the zone of stability of oxidation state III), is here quite large and about 200 mV at pH=8 (see Table 3). As can be observed in the Pourbaix Diagram shown in Figure 27, from pH=6 to pH=13 two independent one-electron redox processes take place with simultaneous proton transfer. The corresponding lines present a slope of

approximately 59 mV per pH unit, as expected for a one-electron one-proton transfer (see equations 10 and 11 above).<sup>44</sup> At lower pH, only the Ru(III/II) couple can be observed as also observed for **C1-OH<sub>2</sub>** and **C2-OH<sub>2</sub>** and already commented above.<sup>45</sup> The stability regions for species having different proton composition are indicated in the diagram along with the pK<sub>a</sub> values for Ru(III) and Ru(II), which are around 1.2 and 11.2, respectively.

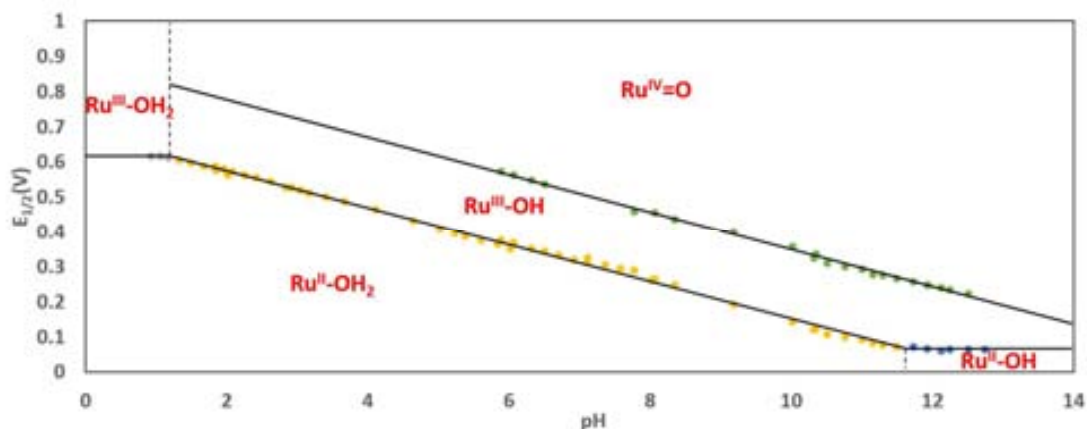


Figure 27. A plot of  $E_{1/2}$  vs. pH (Pourbaix Diagram) for complex **C4-OH<sub>2</sub>**. The pH/potential regions of stability for the various oxidation states and their dominant proton compositions are indicated by using abbreviations such as Ru<sup>II</sup>-OH<sub>2</sub>, for example, for [Ru<sup>II</sup>(CN-OMe)OH<sub>2</sub>(bpea)]<sup>2+</sup>.

The vertical solid lines in the various E/pH regions show the pK<sub>a</sub> values.

In summary, from an electronic point of view (see Table 3 for a summary of the redox properties of the four complexes), complex **C3-OH<sub>2</sub>** favors bi-electronic processes ( $\Delta E_{1/2} \leq 0$ ) while for complex **C4-OH<sub>2</sub>** mono-electronic transfers are clearly preferred ( $\Delta E_{1/2} = 200$  mV). **C1-OH<sub>2</sub>** and **C2-OH<sub>2</sub>** are a situation in between, where the region of stability of the Ru(III) species is rather small ( $\Delta E_{1/2} = 40$  mV) but still present.

The Pourbaix Diagrams of the four aqua complexes have also allowed the tentative assignment of the pK<sub>a1</sub> and pK<sub>a2</sub> values of the four aqua complexes that are also listed in Table 3. The aqua groups on **C4-OH<sub>2</sub>** (bpea) and **C3-OH<sub>2</sub>** (tpm) are clearly more acidic than those of their meridional (trpy) counterparts given the less  $\pi$ -acceptor and higher  $\sigma$ -donor character of the tridentate facial ligands.



Table 3. Redox potentials and pKa values obtained for the aqua complexes C1-OH<sub>2</sub> to C4-OH<sub>2</sub>

	pH=1	pH=8		pKa <sub>1</sub>	pKa <sub>2</sub>
	Ru (III/II)	Ru (IV/III)	Ru (III/II)		
C1-OH <sub>2</sub>	0.71	0.46	0.42	3.0	11.5
C2-OH <sub>2</sub>	0.71	0.44	0.40	2.8	11.0
C4-OH <sub>2</sub>	0.62	0.46	0.26	1.2	11.7
		Ru (IV/II)			
C3-OH <sub>2</sub>	0.62	0.31		1.8	11.2

#### III.2.4.4. UV-vis Spectroscopy

The UV-vis spectra of the eight complexes have been recorded in methanol and are displayed in Figure 28. Two regions could be observed for all the four complexes; one region between 260 nm and 350 nm (between 260 nm and 325 nm for C4-Cl/OH<sub>2</sub>) with very intense bands is due to intraligand  $\pi$  to  $\pi^*$  transitions of the coordinated ligands. A second region is between 350 nm and 550 nm (between 325 nm and 550 nm in the case of C4-Cl/OH<sub>2</sub>), where unsymmetrical broad typical metal-to-ligand charge transfer (MLCT) bands appear that could be tentatively assigned to  $d\pi(\text{Ru})$  to  $\pi^*$  N-ligands transitions.<sup>46,47</sup>

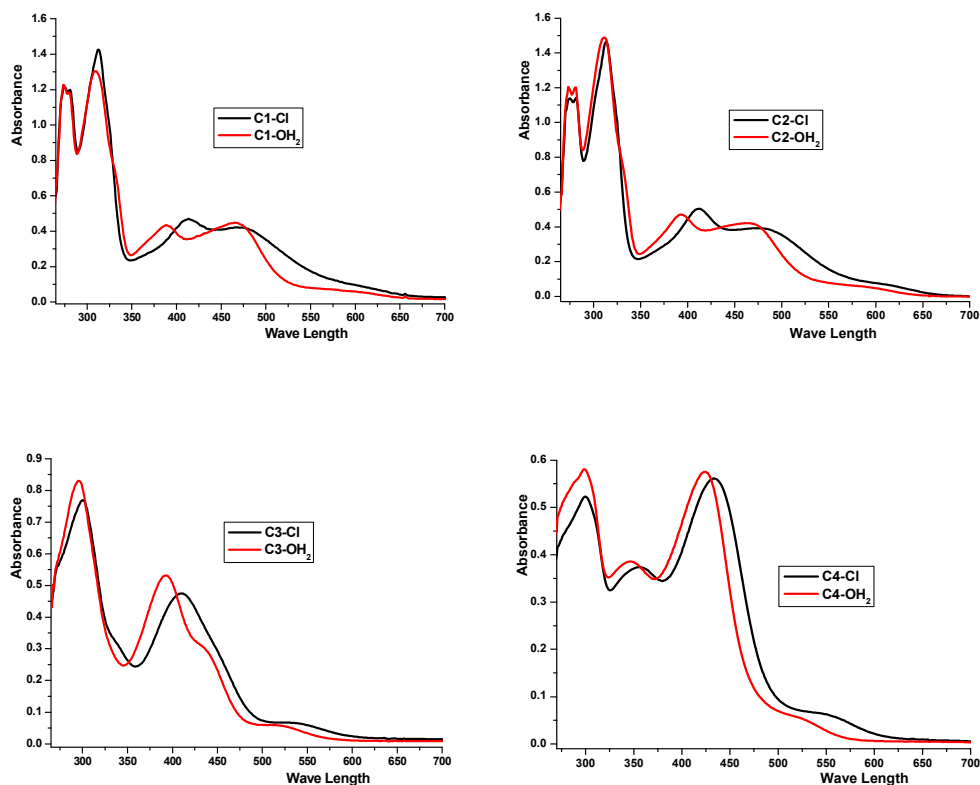


Figure 28. UV-vis spectra for **C1-Cl**/ $\text{OH}_2$  to **C4-Cl**/ $\text{OH}_2$  complexes in 50  $\mu\text{M}$  MeOH solutions.

The electronic nature of the monodentate ligand influences the energies of the transitions involving orbitals with  $d(\text{Ru})$  character to some extent. The MLCT bands for the Ru-aqua complexes are blue-shifted with regards to those of their Ru-Cl counterparts due to the relative stabilization of the  $d\pi(\text{Ru})$  levels provoked by the non- $\pi$ -donor character of the aqua ligand.<sup>48</sup>

### III.2.4.5. Spectrophotometric titration of **C1-OH<sub>2</sub>** to **C4-OH<sub>2</sub>** with $\text{Ce}^{\text{IV}}$

To further confirm the mono- or bi-electronic nature of the redox processes assigned in the electrochemical section above, and once recorded the electronic absorption features of the set of aqua complexes **C1-OH<sub>2</sub>** to **C4-OH<sub>2</sub>** at the Ru(II) oxidation state, we have performed their redox spectrophotometric titration at  $\text{pH}=1$  by using  $\text{Ce}(\text{IV})$  as chemical oxidant. The sets of spectra obtained are shown in Figure 29 (**C1-OH<sub>2</sub>** and **C4-OH<sub>2</sub>**) and in Figure S15 of the Supporting Information (**C2-OH<sub>2</sub>** and **C3-OH<sub>2</sub>**).

For **C1-OH<sub>2</sub>**, **C2-OH<sub>2</sub>** and **C3-OH<sub>2</sub>**, the evolution of the spectra along the addition of 2 equivalents of Ce(IV) leads to a featureless UV-vis spectrum characteristic of Ru<sup>IV</sup>=O species.<sup>错误!未定义书签。</sup> A pair of isosbestic points appear throughout the whole titration at  $\lambda = 370$  and 600 nm for **C1-OH<sub>2</sub>**, at  $\lambda = 370$  and 600 nm for **C2-OH<sub>2</sub>** and at  $\lambda = 355$  and 480 nm for **C3-OH<sub>2</sub>**, thus indicating the direct 2-electron transformation of Ru(II) to Ru(IV) at this pH.<sup>49</sup>

Radically different is the behavior of complex **C4-OH<sub>2</sub>**. A first set of isosbestic points at  $\lambda = 340$  and 550 nm is observed after the addition of the first Ce<sup>IV</sup> equivalent (Figure 29b). However, a second and different pair of isosbestic points, now at  $\lambda = 288$  and 420 nm, are observed when a second equivalent of this oxidant is added (Figure 29c). This sequential oxidation behavior clearly indicates the stability of the Ru(III) oxidation state in aqueous solution and therefore, the preference of this complex for mono-electronic process.

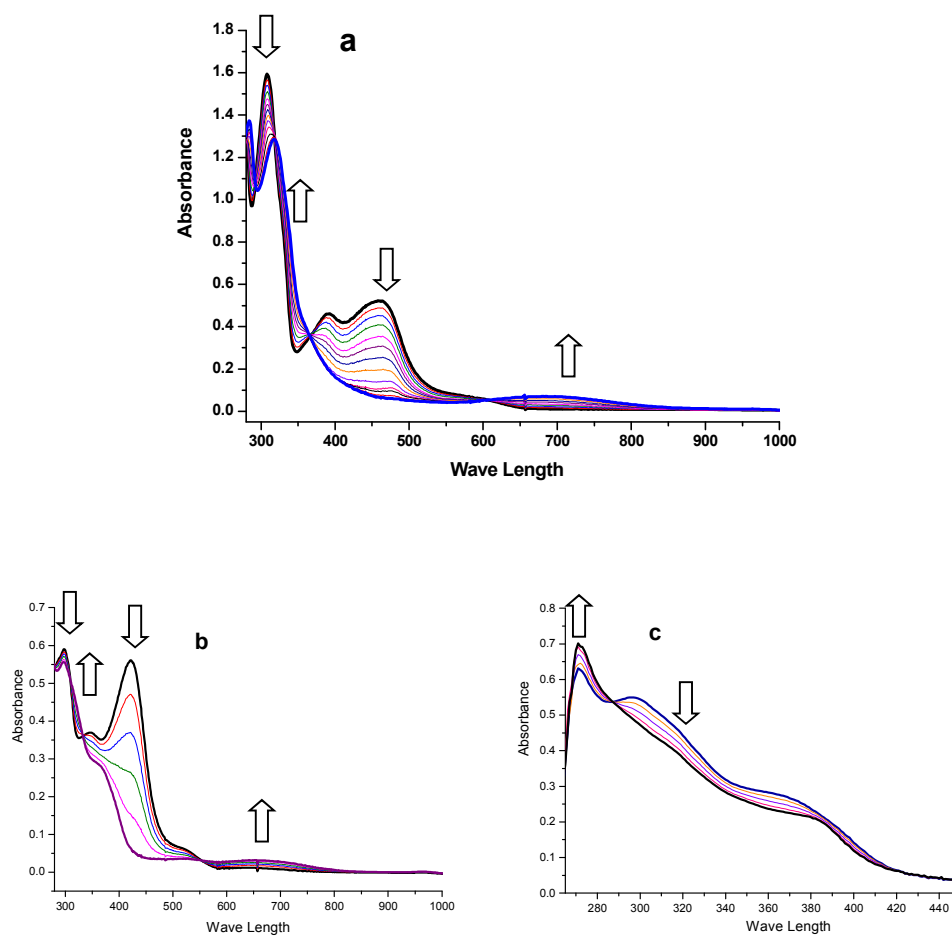


Figure 29. Redox spectrophotometric titrations performed by sequential addition of 3  $\mu\text{L}$  of a 10  $\mu\text{M}$  solution of  $\text{Ce}^{\text{IV}}$  (up to 2 equivalents) to 3 mL of a 50  $\mu\text{M}$  solutions of **C1-OH<sub>2</sub>** and **C4-OH<sub>2</sub>** in 0.1 M HCl. a) Two equivalents of  $\text{Ce}^{\text{IV}}$  added to the **C1-OH<sub>2</sub>** solution, b) One equivalent of  $\text{Ce}^{\text{IV}}$  added to the **C4-OH<sub>2</sub>** solution, c)  $\text{Ce}^{\text{IV}}$  added to the **C4-OH<sub>2</sub>** solution from one to two equivalents.

The results of the spectrophotometric titrations of the four Ru-aqua complexes are in agreement with the conclusions previously extracted from their electrochemical analysis and further confirm the Pourbaix diagrams proposed above (See Figures 21, 24 and 27 and Figure S15 in the Supporting Information).

### III.2.5. Water Oxidation

The capacity of the four aqua complexes (**C1-OH<sub>2</sub>** to **C4-OH<sub>2</sub>**) to oxidize water to dioxygen was initially tested electrochemically. For this purpose, the CVs and DPVs of the four complexes were recorded in aqueous solution (pH=1 and pH=7), at different scan rates and until redox potentials high enough to reach the oxidation states potentially able to oxidize water. However, no significant electrocatalytic water oxidation waves were observed (see Figure S16). Therefore, at least electrochemically and in the time scale of the electrocatalytic experiments carried out, the catalysts do not behave as efficient water oxidation catalysts.

Nevertheless, the four synthesized aqua complexes were tested as potential catalysts towards the oxygen evolution from water in the presence of  $(\text{NH}_4)_2\text{Ce}^{\text{IV}}(\text{NO}_3)_6$  as sacrificial oxidant. The total gas evolved was manometrically measured (Figure 30) and its composition in terms of  $\text{O}_2:\text{CO}_2$  ratio was analyzed by means of on-line Mass Spectrometry (Figure 31).

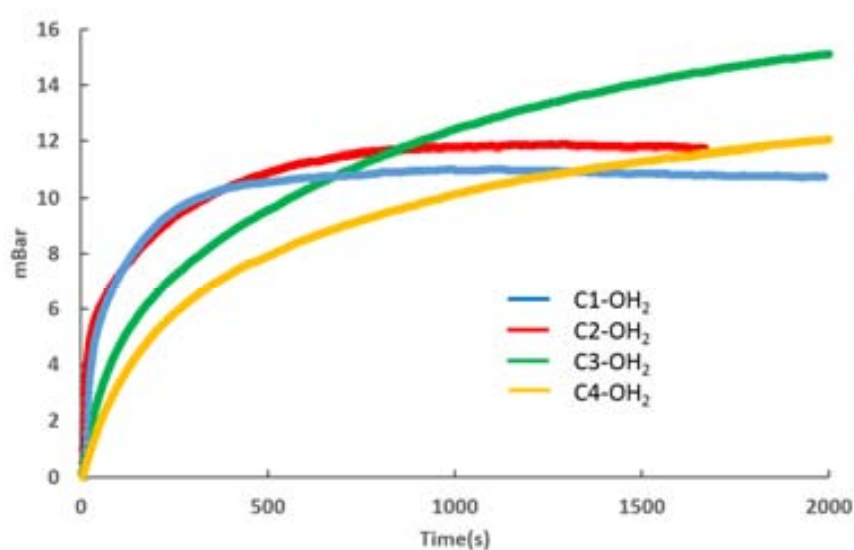


Figure 30. Manometric profile of evolved gases for complexes **C1-OH<sub>2</sub>** to **C4-OH<sub>2</sub>** in a pH=1 aqueous solution and using  $(\text{NH}_4)_2\text{Ce}^{\text{IV}}(\text{NO}_3)_6$  as sacrificial oxidant.

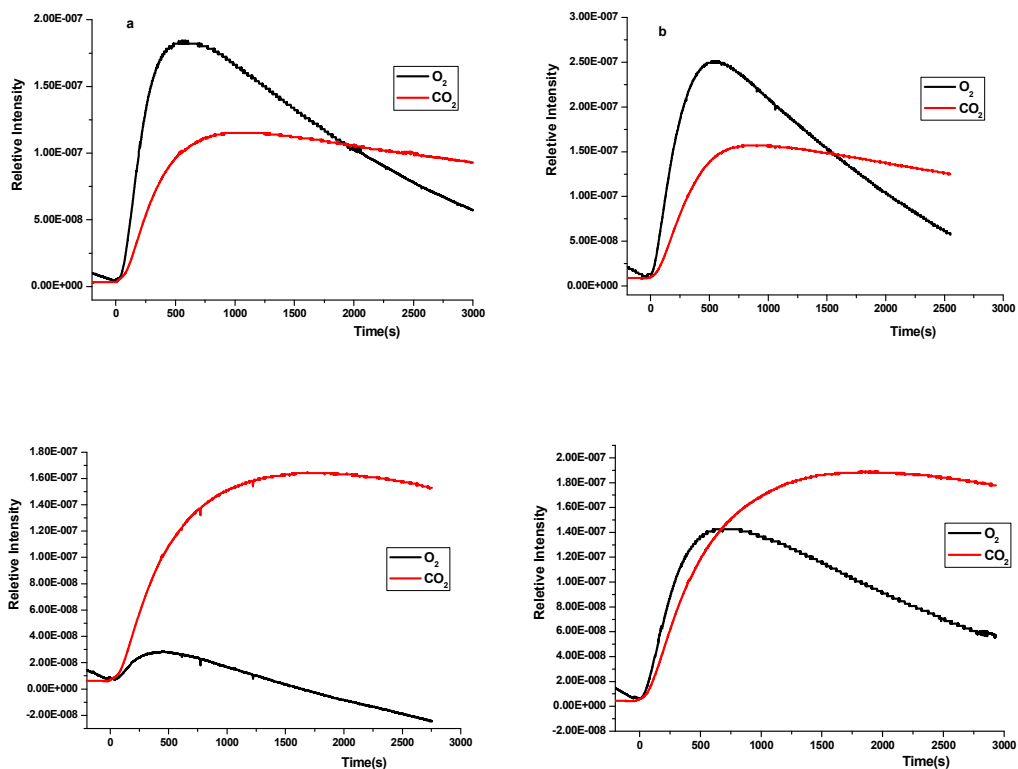


Figure 31. Mass Spectrometry profile of the generated gases upon oxidative treatment with  $((\text{NH}_4)_2\text{Ce}^{\text{IV}}(\text{NO}_3)_6)$  of: a) **C1-OH<sub>2</sub>**, b) **C2-OH<sub>2</sub>**, c) **C3-OH<sub>2</sub>**, d) **C4-OH<sub>2</sub>**.

In the presence of 100 equivalents of  $\text{Ce}^{\text{IV}}$  at  $\text{pH}=1$ , complex **C3-OH<sub>2</sub>** generated more gas ( $\approx 15$  mBar) after 30 min of reaction than the other three complexes (Figure 30). In general, and only considering the amount of generated gas, facial complexes are superior to their meridional counterparts (see Figure 30). However when the profile of the generated gases is analyzed by on-line MS (Figure 31) **C3-OH<sub>2</sub>** has the lowest  $\text{O}_2:\text{CO}_2$  ratio (1:5.5), followed by **C4-OH<sub>2</sub>** with 1:1.4, (Figure 31c-d). The  $\text{O}_2:\text{CO}_2$  ratio was much higher for **C1-OH<sub>2</sub>** and **C2-OH<sub>2</sub>** (1:0.6, see Figure 31a-b). Therefore, despite still poor, the stability of the meridional trpy-based complexes **C1-C2-OH<sub>2</sub>** is clearly higher than that of their facial (tpm or bpea) counterparts **C3-C4-OH<sub>2</sub>** that easily get oxidized in the harsh reaction conditions of water oxidation. This is clearly reflected in Figure 32 where the profile of  $\text{O}_2$  evolution of the four aqua complexes can be compared.

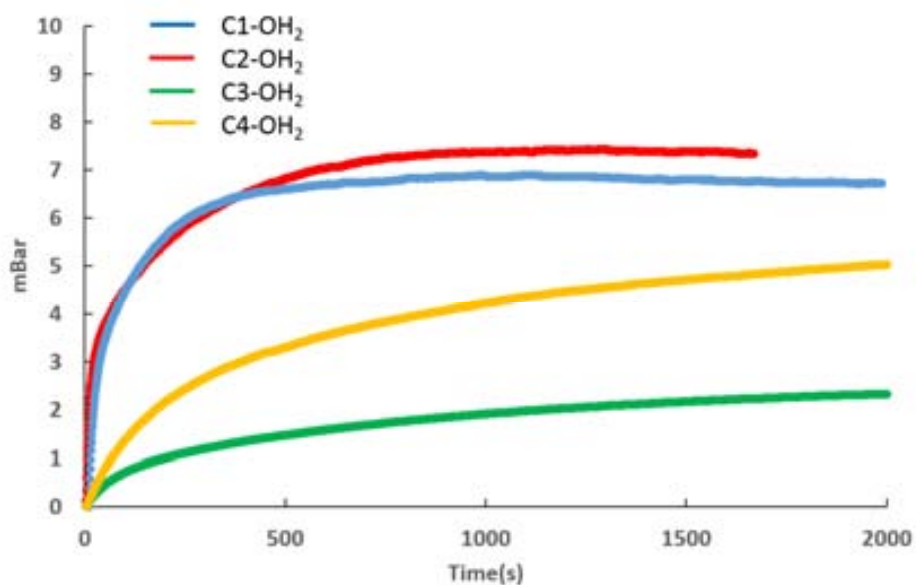


Figure 32. Profile of oxygen evolution at pH=1 employing  $(\text{NH}_4)_2\text{Ce}^{\text{IV}}(\text{NO}_3)_6$  as sacrificial oxidant.

Catalyst-catalyst intermolecular oxidative degradation involving  $\text{Ru}^{\text{IV}}=\text{O}$  species<sup>50</sup> or the direct degradation of the complexes by the highly oxidant  $\text{Ce}^{\text{IV}}$  are considered as the potential origin of the evolved  $\text{CO}_2$ . In our system, the only relevant differences between the four evaluated complexes are the tridentate ligands employed. Therefore, tpm and bpea (both containing aliphatic carbon atoms prone to be easily oxidized in the harsh catalytic conditions employed) quickly decompose under catalytic conditions generating big amounts of  $\text{CO}_2$  that arise from ligand oxidation. However, and given that a great number of robust water oxidation catalysts containing the trpy ligand have been reported,<sup>51</sup> the observed evolution of  $\text{CO}_2$  from **C1-C2-OH<sub>2</sub>** clearly reflects the weakness of PhthaPz-OR family of ligands under oxidative conditions.

## III.2.6. Epoxidation of Alkenes

### III.2.6.1. Electrocatalytic Alkene Epoxidation

The capacity of the prepared aqua complexes of electrocatalytically epoxide *cis*- $\beta$ -methylstyrene as model substrate has been investigated by means of cyclic voltammetry.

All the experiments were performed in dichloromethane under well-controlled concentration of both catalysts and substrate. A glassy carbon electrode was used as the working electrode, a platinum wire as the auxiliary electrode and SSCE as the reference electrode; all the CVs were recorded at a scan rate of 100 mV/s.

Figure 33 shows successive cyclic voltammograms of a 0.5 mM solution of C1-OH<sub>2</sub> in dichloromethane with increasing concentrations of *cis*- $\beta$ -methylstyrene. When the alkene is present, important electrocatalytic currents assigned to its oxidation are observed with 1.2 V vs. SSCE as onset potential.

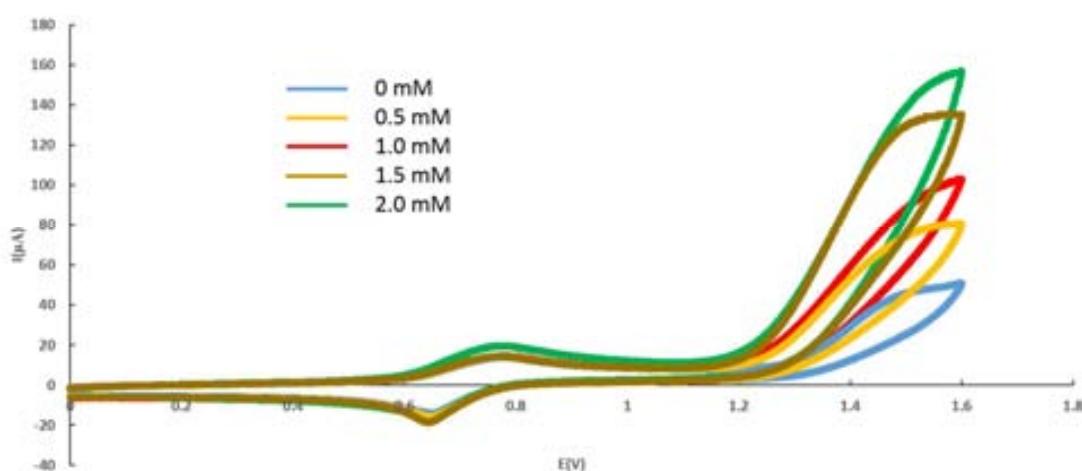


Figure 33. Successive cyclic voltammograms of a 0.5mM solution of C1-OH<sub>2</sub> in DCM (0.1M TBAPF<sub>6</sub>) at increasing concentrations of *cis*- $\beta$ -methylstyrene. Working electrode: glassy carbon; counter electrode: Pt; reference electrode: Hg/Hg<sub>2</sub>SO<sub>4</sub>; scan rate: 100 mV/s. Starting at 0 V toward positive potentials.

The rate constant value  $k$  for the electrocatalytic epoxidation could be estimated from the plots of the  $i_{\text{cat}}$  vs. the square root of the substrate concentration according to equation 12:<sup>52</sup>

$$i_{\text{cat}} = nFA[\text{cat}]D^{1/2}k^{1/2}[\text{sub}]^{1/2} \quad (12)$$

where  $i_{\text{cat}}$  is the current intensity in the presence of *cis*- $\beta$ -methylstyrene,  $n$  is the number of electrons involved in the catalysis,  $F$  is the Faraday constant,  $A$  is the surface area of the working electrode in cm<sup>2</sup> ( $A$  is 0.07 cm<sup>2</sup> in this experiment),  $[\text{cat}]$  is the



concentration of catalyst in mM,  $D$  is the diffusion coefficient of the catalyst in  $\text{cm}^2/\text{s}$ , and  $[\text{sub}]$  is the concentration of *cis*- $\beta$ -methylstyrene in mM.

The plot of  $i_{\text{cat}}$  vs.  $[\text{sub}]^{1/2}$  shows a linear trend with the increasing concentration of substrate and under kinetic control conditions the slope is proportional to  $k^{1/2}$ . Figure 34 shows the plot of  $i_{\text{cat}}$  vs.  $[\text{sub}]^{1/2}$  for **C1-OH<sub>2</sub>**.

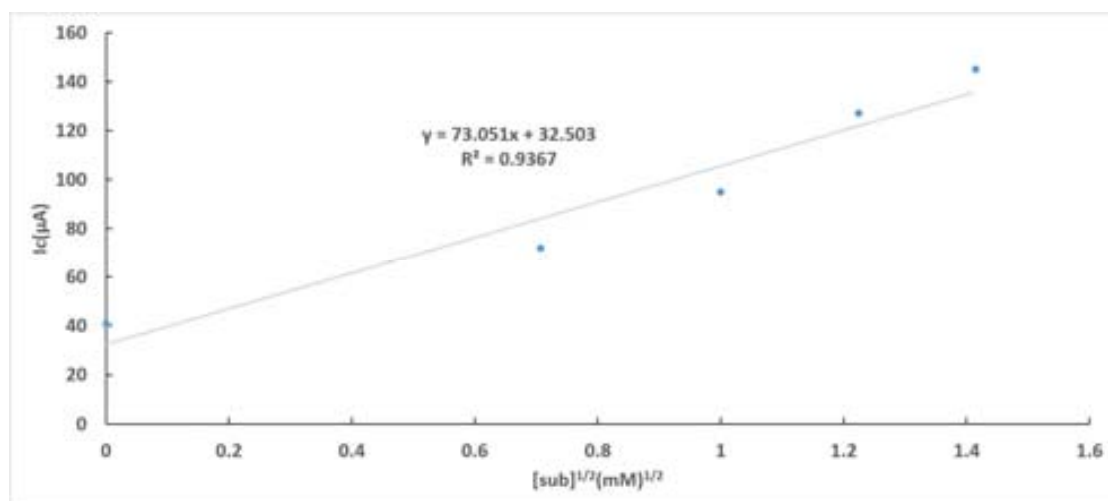


Figure 34. Dependence of  $i_{\text{cat}}$  vs.  $[\text{sub}]^{1/2}$ . Experimental conditions: **C1-OH<sub>2</sub>** (0.5mM),  $[\text{sub}] = 0\text{-}2.0\text{mM}$ , DCM (0.1 M TBAPF<sub>6</sub>), working electrode: glassy carbon; counter electrode: Pt; reference electrode: SSCE; scanning rate: 100 mV/s.

In order to estimate the value of the rate constant, the diffusion coefficient  $D$  was calculated from the peak current prior the addition of the substrate according to the following equation<sup>52</sup>:

$$i_p = (2.69 \cdot 10^5) n^{3/2} A D^{1/2} [\text{cat}] \nu^{1/2} \quad (13)$$

where  $i_p$  is the current intensity at 1.6 V,  $n$  is the number of electrons involved in the electrochemical process,  $A$  is the surface area of the working electrode in  $\text{cm}^2$ ,  $D$  is the diffusion coefficient of the catalyst in  $\text{cm}^2/\text{s}$ ,  $[\text{cat}]$  is the concentration of catalyst in mM and  $\nu$  is the scan rate in V/s.

If a linear relationship for  $i_p$  vs.  $\nu^{1/2}$  is obtained, the slope is proportional to  $AD^{1/2}$ . As shown in Figure 35 for **C1-OH<sub>2</sub>** the plot of  $i_p$  vs. the square root of the scan rate presented a good linear trend for a range of scan rate from 20 mV/s to 200 mV/s.

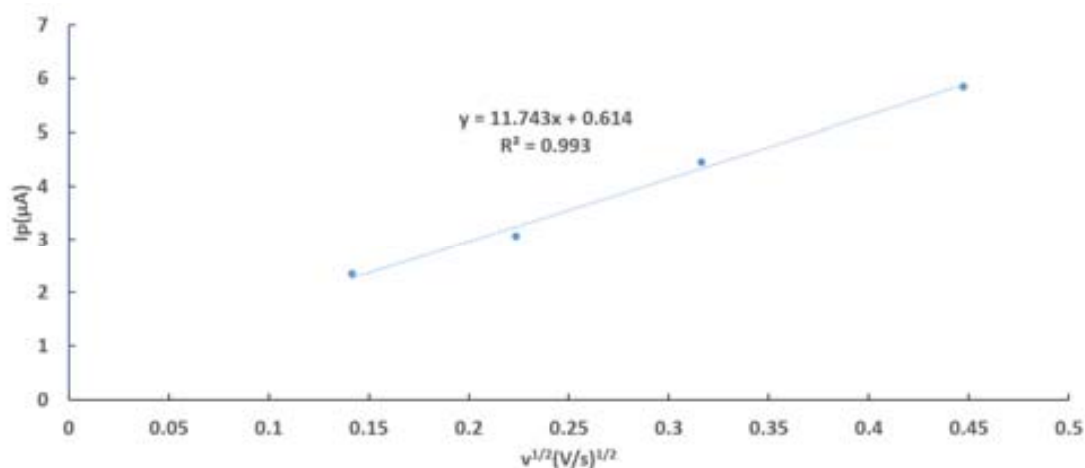


Figure 35. Dependence of  $i_p$  vs.  $v^{1/2}$ . Experimental conditions: **C2-OH<sub>2</sub>** (0.5mM)  $v = 20$ -200V/s, DCM (0.1 M TBAPF<sub>6</sub>), working electrode: glassy carbon; counter electrode: Pt; reference electrode: SSCE.

The electrocatalytic epoxidation capacity of **C3-OH<sub>2</sub>** and **C4-OH<sub>2</sub>** with regards to *cis*- $\beta$ -methylstyrene was also tested and the corresponding figures and plots obtained are presented in the Supporting Information (Figures S17 to S22).

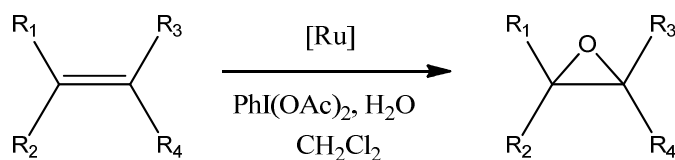
From equations 12 and 13 and their combination both the diffusion coefficient factor  $D$  and rate constant  $k$  of the three tested complexes were calculated for the electrocatalytic epoxidation of *cis*- $\beta$ -methylstyrene in dichloromethane. The values obtained are shown in Table 4.

Table 4. Diffusion coefficient factor ( $D$ ) and rate constant ( $k$ ) for complexes **C1-OH<sub>2</sub>**, **C3-OH<sub>2</sub>** and **C4-OH<sub>2</sub>**.

	<b>C1-OH<sub>2</sub></b>	<b>C3-OH<sub>2</sub></b>	<b>C4-OH<sub>2</sub></b>
$D$ (cm <sup>2</sup> /s)	$2 \cdot 10^{-4}$	$2 \cdot 10^{-4}$	$1.1 \cdot 10^{-4}$
$k$ (M <sup>-1</sup> s <sup>-1</sup> )	576	441	961

### III.2.6.2. Chemical Alkene Epoxidation

The four aqua complexes, **C1-C4-OH<sub>2</sub>** have been also tested with regards to their ability to epoxidize alkenes (Scheme 6) when chemically triggered with PhIO(OAc)<sub>2</sub>. The catalytic reactions have been carried out following the conditions exposed in Table 5, while the most relevant results are displayed in Table 6.



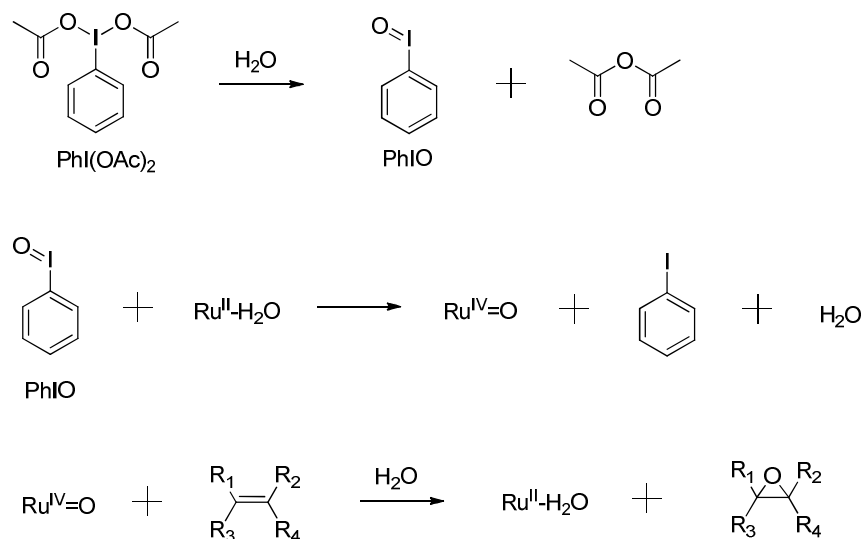
Scheme 6. Alkene epoxidation catalyzed by Ru complexes.

Table 5. Reaction conditions for the epoxidation of alkenes with **C1-C4-OH<sub>2</sub>**. The final volume is  $\approx$  1.47 mL.

Species	mmols	Concentration (M)	Ratio cat:X
Cn-OH <sub>2</sub> *	2.5E-03	1.7E-03	—
Alkene	2.5	1.7	1000
1,1'-biphenyl	1	0.7	800
(diacetoxyiodo)benzene	5	3.4	2000
water	5	3.4	2000

\* n=1, 2, 3, 4

A vial containing 1 mL of 1,2-dichloroethane (DCE) as solvent, (diacetoxyiodo)benzene as co-oxidant, 1,1'-biphenyl as internal standard, the catalyst, and the alkene substrate was stirred at room temperature. The excess of water is mandatory to ensure the generation of PhIO from PhI(OAc)<sub>2</sub>.<sup>53,54</sup> Scheme 7 summarizes the set of reactions that occur during the catalytic epoxidation of alkenes for the proposed system. The products of each catalytic reaction have been analyzed by GC and identified by comparison of the retention times obtained with those of commercial samples and GC-MS.

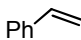
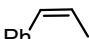
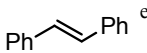
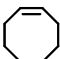


Scheme 7. Summary of the reactions taking place in the catalytic epoxidation of alkenes with the four aqua complexes described in this Chapter.

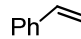
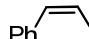
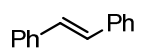
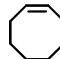
The catalytic activity of the four complexes towards alkene epoxidation was initially tested and optimized for the epoxidation of *cis*- $\beta$ -methylstyrene and GC and GC-MS monitored the reaction evolution. The catalytic reaction was carried out at room temperature with a catalyst: substrate: PhI(OAc)<sub>2</sub> ratio of 1: 1000: 2500. Afterwards, other alkenes as styrene, *trans*-stilbene and cyclooctene were studied for each of the four aqua complexes under the same reaction conditions. The gathered results obtained for all the alkenes tested are shown in Table 6.

Table 6. Results of epoxidation on different alkenes catalyzed by the four aqua complexes, a) **C1-OH<sub>2</sub>**, b) **C2-OH<sub>2</sub>**, c) **C3-OH<sub>2</sub>**, d) **C4-OH<sub>2</sub>**. Reaction conditions: complexes ( $2.5 \cdot 10^{-3}$  mmols, final concentration 0.85 mM), DCE (1mL), substrate (2.5 mmols, 1.7 M), PhI(OAc)<sub>2</sub> (5 mmols, 3.4 M), H<sub>2</sub>O (5 mmols, 3.4 M), 1,1'-byphenil (1 mmol, 0.68 M), final volume  $\approx$  1.47 mL.

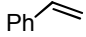
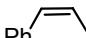
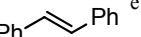
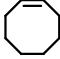
a)

Entry	Substrate	Time (min)	Substrate Conversion (%) <sup>a</sup>	[Epoxide], M; (Selectivity, %) <sup>b</sup>	TON/TOF <sup>c</sup>
1		240	42	0.34; (19)	194/0.8
2		525	100	1.42; (82) <sup>d</sup>	840/1.6
3		540	100	1.19; (67)	680/1.3
4		480	100	1.63; (91)	930/2

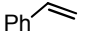
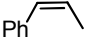
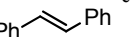
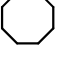
b)

Entry	Substrate	Time (min)	Substrate Conversion (%) <sup>a</sup>	[Epoxide], M; (Selectivity, %) <sup>b</sup>	TON/TOF <sup>c</sup>
1		180	29	0.34; (19)	191/0.9
2		620	100	1.43; (80) <sup>d</sup>	816/1.3
3		540	100	1.04; (58)	596/1.1
4		430	99	1.65; (92)	946/2.2

c)

Entry	Substrate	Time (min)	Substrate Conversion (%) <sup>a</sup>	[Epoxide], M; (Selectivity, %) <sup>b</sup>	TON/TOFi <sup>c</sup>
1		120	23	0.11; (6)	60/0.5
2		1410	97	0.95; (53) <sup>d</sup>	545/0.4
3		510	90	0.26; (15)	148/0.3
4		2400	100	1.32; (74)	756/0.3

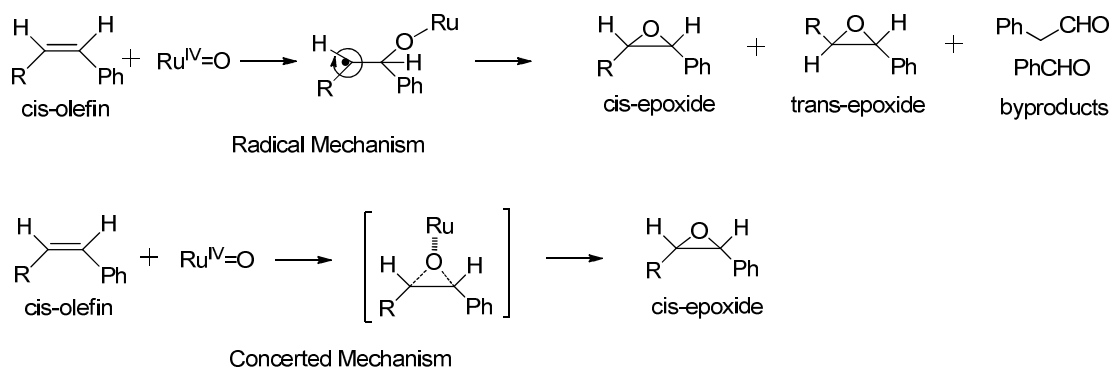
d)

Entry	Substrate	Time (min)	Substrate Conversion (%) <sup>a</sup>	[Epoxide], M; (Selectivity, %) <sup>b</sup>	TON/TOFi <sup>c</sup>
1		240	21	0.49; (2.6)	27/0.1
2		990	99	1.20; (67) <sup>d</sup>	687/0.7
3		720	91	0.24; (13)	136/0.2
4		2520	100	1.65; (92)	940/0.4

<sup>a</sup> Substrate conversion =  $\{([substrate]_i - [substrate]_f) / [substrate]_i\} * 100$ . <sup>b</sup> Epoxide selectivity =  $\{[epoxide]_f / ([substrate]_i - [substrate]_f)\} * 100$ . <sup>c</sup> TON with regard to epoxide; TOFi = TON/min. <sup>d</sup> *cis* epoxide. <sup>e</sup> DCE volum is 5ml.

As can be observed in entry 2 of Table 6(c), the system: **C1-OH<sub>2</sub>** 1.7mM, *cis*- $\beta$ -methylstyrene 1.7M, PhI(OAc)<sub>2</sub> 3.4M, H<sub>2</sub>O 3.4 M in DCE gives 1.42 M *cis*- $\beta$ -

methylstyrene epoxide which represent a TON of 840 with regard to the initial catalyst in 525 minutes. The conversion of the initial substrate is 100% and the selectivity in epoxide is 82%. The activity of the four aqua complexes tested in the epoxidation of different alkenes is also reported in Table 6. As a general trend, complexes where direct bi-electronic transfers between Ru(II) and Ru(IV) species are favored (those where Ru(III) is unstable with regards to disproportionation) give higher epoxide yields, therefore, an increased selectivity of the oxidation process. It is well known that bi-electronic catalysts drive epoxidation reactions to concerted pathways (see Scheme 8). This avoids the generation of radicalary intermediates of high energy that usually end up reducing the selectivity of the whole process by the generation of a wide set of byproducts. This is the trend observed for **C1-C2-OH<sub>2</sub>** (see Table 6a-b). However, comparatively lower epoxidation capacity (both lower conversions and selectivities are gathered with regards to **C1-C2-OH<sub>2</sub>** even at much longer reaction times) is observed for **C3-OH<sub>2</sub>**, also a catalyst favoring bi-electronic processes (Table 6c). Two conceivable reasons are: 1) the tpm ligand is prone to be oxidized in the employed reaction conditions, thus progressively lowering the catalyst loading with time and b) the steric bulkiness of the tpm ligand difficult and modify the interaction between the substrates and the active site of the catalyst, that lowering the catalytic reaction and modifying the obtained reaction products. Other information extracted from Table 6 shows that studied aqua complexes perform much better with substrates containing electron-donor groups than with those bearing electron-withdrawer substituents. Therefore, the best results are gathered for *cis*-cyclooctene for each of the complexes whereas the poorest values are obtained for styrene and, specially, *trans*-stilbene. *Trans*-stilbene also suffers from potential steric effects due to the bulkiness of its two phenyl rings. Another interesting feature observed from the systems studied in this work is the stereospecific nature of the catalytic process. For the whole set of aqua complexes, when *cis*- $\beta$ -methylstyrene is employed as substrate, no *cis/trans* isomerization takes place. Therefore, if catalysts favoring bi-electronic pathways can potentially go through a concerted oxene insertion to the alkene double bond (Scheme 8, bottom), ring closure must be faster than C-C rotation in the radical intermediates proposed for catalysts such as **C4-OH<sub>2</sub>** that proceed through mono-electronic transfers (Scheme 8, top).



Scheme 8. Radicalary and concerted mechanisms for the epoxidation of alkenes with Ru complexes.

### III.3. Conclusions

A new dinucleating CNNC tetradentate ligand (**L1**<sup>2+</sup>) has been synthesized and thoroughly characterized in solution (1D and 2D NMR) and in the solid state (X-ray diffraction analysis). Attempts of coordinating this ligand to [Ru(T)Cl<sub>3</sub>] (T = trpy, tpm, bpa) type of precursors in nucleophilic protic solvents such as MeOH or iPrOH lead to ligand breakage (C-N bond scission due to the nucleophilic attack of a solvent molecule) and the consequent formation of four new Ru mononuclear complexes with general formula: *out*-[Ru(PhthaPz-R)(trpy)X]<sup>n+</sup> (X = Cl, n = 1, X = H<sub>2</sub>O, n = 2; R = Methyl, Isopropyl; PhthaPz = 1-(1-methylimidazole)phthalene), [Ru(PhthaPz-R)(tpm)X]<sup>n+</sup>, (R = Methyl, tpm = Tris(pyrazol-1-yl)methane) and *trans, fac*-[Ru(PhthaPz-R)(bpa)X]<sup>n+</sup> (R = Methyl, bpa = N,N-bis(pyridin-2-ylmethyl)ethanamine), respectively termed **C1**-Cl/OH<sub>2</sub>, **C2**-Cl/OH<sub>2</sub>, **C3**-Cl/OH<sub>2</sub> and **C4**-Cl/OH<sub>2</sub>. The four complexes have been thoroughly characterized in solution by means of spectroscopic (1D and 2D NMR and UV-vis) and electrochemical techniques (CV and DPV) and in the solid state (X-ray diffraction analysis) for the **C4**-Cl case. A Structural transformation of **C1**-OH<sub>2</sub> and **C2**-OH<sub>2</sub> when dissolved in water is observed by NMR spectroscopy. However, complexes **C3**-OH<sub>2</sub> and **C4**-OH<sub>2</sub> are stable in this solvent. From an electronic point of view, a nice regulation of the stability regions of the different oxidation states have been obtained by the different ligand combinations, thus going from **C4**-OH<sub>2</sub> where Ru(III) is clearly stable and mono-electronic transfers are favored to **C3**-OH<sub>2</sub> where this oxidation state is instable with regard to disproportionation to



Ru(II) and Ru(IV). All this passing from complexes **C1-C2-OH<sub>2</sub>** that represent an intermediate situation with a narrow range of Ru(III) stability.

The catalytic performance of the four Ru-OH<sub>2</sub> complexes has been analyzed with regards to the chemically driven water oxidation reaction and the chemically and electrochemically triggered epoxidation of alkenes. With regards to water oxidation, the four aqua complexes show poor stability due to ligand oxidation under the harsh reaction conditions and the consequent evolution of CO<sub>2</sub> together with O<sub>2</sub>. Higher O<sub>2</sub>:CO<sub>2</sub> ratios are observed for the trpy-based complexes **C1-OH<sub>2</sub>** and **C2-OH<sub>2</sub>** given the more robust character of this fully aromatic ligand when compared with tpm and bpea (**C3-OH<sub>2</sub>** and **C4-OH<sub>2</sub>**, respectively). With regards to the epoxidation of alkenes, complexes favoring two-electronic processes showed better performance and selectivity compared with those favoring one-electronic processes. The comparatively lower oxidation capacity of complex **C3-OH<sub>2</sub>** potentially originates from the oxidative degradation of the tpm ligand under the conditions used or/and due to the steric bulkiness of this facial ligand. Alkenes containing electron-donor groups performed better than those bearing electron-withdrawers. In addition, when *cis*- $\beta$ -methylstyrene is employed as substrate, no *cis/trans* isomerization takes place, therefore leading to stereospecific epoxidation processes.

### III.4. Experimental Section

**Materials:** All reagents used in the present work were obtained from Sigma Aldrich Chemical Co. and were used without further purification. Reagent-grade organic solvents were obtained from Scharlab. RuCl<sub>3</sub>·3H<sub>2</sub>O was supplied by Alfa Aesar. The starting ligands tri(1H-pyrazol-1-yl)methane (tpm) and N,N-bis(pyridin-2-ylmethyl)ethanamine (bpea) were prepared as described in the literature.<sup>55,56</sup> The synthetic manipulations were routinely performed under nitrogen atmosphere using Schlenk flask and vacuum-line techniques.

**Instrumentation and Measurements:** UV-vis spectroscopy was carried out by a HP8453 spectrometer using 1 cm quartz cells. NMR spectroscopy was performed on a

Bruker DPX 250 MHz, DPX 360 MHz, DPX 400 MHz, DPX 500 MHz or a DPX 600 MHz spectrometer. Samples were run in MeOD, DCM-d<sub>2</sub> or acetone-d<sub>6</sub> with internal references. Elemental analyses were performed using a Carlo Erba CHMS EA-1108 instrument from the Chemical Analysis Service of the Universitat Autònoma de Barcelona (CAS-UAB). Electrospray ionization Mass Spectrometry (ESI-MS) experiments were performed on a HP298s gas chromatography (GC-MS) system from the CAS-UAB. Cyclic voltammetry and differential pulse voltammetry experiments were performed on the Bio Logic Science Instrument SP-150 potentiostat using a three-electrode cell. A glassy carbon electrode (7 mm diameter) was employed as working electrode while platinum wire as auxiliary electrode and a SSCE as a reference electrode. Working electrodes were polished with 0.05 micron Alumina paste and washed with distilled water and acetone before each measurement. The complexes were dissolved in acetonitrile, methanol or dichloromethane solutions of 0.1 M ionic strength containing the necessary amount of n-Bu<sub>4</sub>NPF<sub>6</sub> (TABH) as supporting electrolyte. For the electrochemical analysis performed in water, the complexes were dissolved in pH=1 triflic acid solution or solutions of phosphoric buffer for other pHs with ionic strength of 0.1 M. The pH values were increased or reduced by adding drops of 0.1 M NaOH solution or the pH=1 triflic acid solution. E<sub>1/2</sub> values here presented were estimated from CV experiments from the average of the oxidative and reductive peak potentials (E<sub>p,a</sub> + E<sub>p,c</sub>)/2. The electrocatalysis of alkene epoxidation was carried out in dichloromethane (0.1M TBAPF<sub>6</sub>) at increasing concentrations of *cis*- $\beta$ -methylstyrene with glassy carbon as working electrode and Hg/Hg<sub>2</sub>SO<sub>4</sub> as the reference electrode. The CVs were recorded at scan rate of 100 Mv/s. For chemical catalysis of alkene epoxidation, the introduced substrates and the corresponding epoxides were separated and analyzed through Gas Chromatography HP 5890 PACKARD SERIES II.

On-line manometry measurements were performed on a Testo 521 differential pressure manometer with an operating range of 1 to 100 hPa and accuracy within 0.5% of the measurement, coupled to thermostatted reaction vessels for dynamic monitoring of the headspace pressure above each reaction. On-line monitoring of the gas evolution was carried out on a Pfeiffer Omnistar GSD 301C mass spectrometer. Typically, a degassed vial of 16.04 mL containing a suspension of the catalysts in a 0.1 M triflic acid (1.5 mL) was connected to the apparatus capillary tubing. Subsequently, the previously degassed

solution of Ce<sup>IV</sup> (0.5 mL) at pH=1 (triflic acid, 100 equiv.) was injected by a Hamilton gastight syringe, and the reaction was dynamically monitored. A response ratio of 1: 2 was observed when equal concentrations of dioxygen and carbon dioxide were injected which was used for the calculation of their relative concentrations.

### X-ray Crystal Structure Determination

Crystals of **L1**<sup>2+</sup> were grown by slow diffusion of diethyl ether into a solution of **L1**(PF<sub>6</sub>)<sub>2</sub> in acetone. Crystals of **C4-Cl** were prepared by slow diffusion of diethyl ether on a solution of **C4-Cl** in methanol.

### Data collection

**Structure Solution and Refinement** For this, SHELXTL was used. The crystal data parameters of **L1**<sup>2+</sup> and **C4-Cl** are listed in Table S1 and S2. The structure of **L1**<sup>2+</sup> and **C4-Cl** were analyzed by the program ORTEP and Mercury.

### Synthetic Preparations

*1,4-bis(1-methylimidazolium-1-yl)phthalazine dichloride (L1(Cl)<sub>2</sub>):* To a evacuated Schlenk flask a mixture of 1,4-dichlorophthalazine (dcp) (990 mg, 0.5 mol) and 1-methylimidazole (2.050 g 3 mol) were dissolved into 2 ml of DMF. The mixture was stirred under nitrogen atmosphere at 120°C for 4 hours. A white precipitate appeared in the reaction crude, which was filtered off, washed with DMF and diethyl ether and dried under vacuum. Yield: 1.26 g (70%). <sup>1</sup>H-NMR (400Hz, acetone-d<sub>6</sub>, 298K) δ=9.95 (s, 2H, H6, H6'), 8.57 (dd, 2H, J<sub>9-10</sub> = 6.2, 3.0 Hz, H9, H9'), 8.50 (s, 2H, H4, H4'), 8.46 (dd, 2H, J<sub>10-9</sub> = 6.3, 3.0 Hz, H10, H10'), 8.23 (s, 2H, H3, H3'), 4.39 (m, 6H, H1). <sup>13</sup>C-NMR (400Hz, acetone-d<sub>6</sub>, 298K) δ=150.65 (C7), 138.44 (C6), 136.50 (C10), 125.28 (C3), 124.16 (C9), 124.08 (C8), 123.57 (C4), 36.84 (C1).

*cis-[Ru<sup>II</sup>(PhthaPz-Ome)(trpy)Cl]PF<sub>6</sub> (C1-Cl):* [Ru(trpy)Cl<sub>3</sub>] (130 mg, 0.3 mmol), 1,4-bis(1-methylimidazolium-1-yl)phthalazine dichloride (**L1**(Cl)<sub>2</sub>) (73 mg, 0.2 mmol) and LiCl (38 mg 0.9 mmol) were mixed in a round bottom flask and dry methanol (20 mL) was added as solvent. Triethylamine (121 mg, 166 μL, 1.2 mmol) was added to the solution and the mixture was refluxed at 80°C for 16 hours. After cooling to room

temperature, the reaction crude was filtered through celite<sup>®</sup> to remove the black solid formed and then 20 drops of saturated NH<sub>4</sub>PF<sub>6</sub> aqueous solution were added to the filtrate. The solution was concentrated under vacuum until about 10 mL, when a brown precipitate appeared. The precipitate was filtered off, washed with diethyl ether and dried under vacuum. Yield: 62 mg, (41%). <sup>1</sup>H-NMR (600 MHz, CD<sub>2</sub>Cl<sub>2</sub>) δ=8.63 (d, 1H, *J*<sub>4-3</sub> = 2.4 Hz, H4), 8.53 (d, 1H, *J*<sub>9-10</sub> = 8.7 Hz, H9), 8.37 (d, 2H, *J*<sub>26-27</sub> = 8.1 Hz, H26), 8.22 (d, 2H, *J*<sub>23-22</sub> = 8.0 Hz, H23), 8.18 (t, 1H, *J*<sub>27-26,26'</sub> = 8.1 Hz, H27), 8.12 (d, 1H, *J*<sub>12-11</sub> = 8.1 Hz, H12), 8.07 (m, 1H, H10), 7.94 (d, 2H, *J*<sub>20-21</sub> = 5.3 Hz, H20), 7.85 (t, 1H, *J*<sub>11-10,12</sub> = 7.6 Hz, H11), 7.82 (t, 2H *J*<sub>22-21,23</sub> = 7.8, Hz, H22), 7.69 (d, 1H *J*<sub>3-4</sub> = 2.4 Hz, H3), 7.20 (m, 2H, H21), 4.78 (s, 3H, H1), 3.47 (s, 3H, H18). <sup>13</sup>C-NMR (600 MHz, CD<sub>2</sub>Cl<sub>2</sub>) 200.66 (C6), 158.75 (C24), 158.43 (C14), 156.51 (C20), 155.50 (C25), 151.45 (C7), 136.59 (C22), 135.43 (C27), 133.91 (C10), 132.29 (C11), 126.88 (C21), 125.83 (C3), 124.51 (C12), 122.95 (C23), 121.16 (C26), 121.00 (C8), 120.20 (C9), 119.51 (C13), 118.77 (C4), 54.61 (C18), 38.15 (C1). UV/vis (methanol): λ<sub>max</sub> (ε)= 281 (11988), 313 (14247), 413 (4700), 475 (4332). ESI-MS (MeOH): *m/z* = 610.1 ([M-PF<sub>6</sub>-1]). Elemental analysis (%) found C, 37.66; H, 2.69; N, 10.95. Calcd for C<sub>28</sub>H<sub>24</sub>ClF<sub>12</sub>N<sub>7</sub>OP<sub>2</sub>Ru: C, 37.33; H, 2.68; N, 10.88.

*cis*-[Ru<sup>II</sup>(PhthaPz-Ipro)(trpy)Cl]PF<sub>6</sub> (C2-Cl): [Ru(trpy)Cl<sub>3</sub>] (130 mg, 0.3 mmol), 1,4-bis(1-methylimidazolium-1-yl)phthalazine dichloride (L1(Cl)<sub>2</sub>) (73 mg, 0.2 mmol) and LiCl (38 mg 0.9 mmol) were mixed in a round bottom flask and dry isopropanol (20 mL) was added as solvent. Triethylamine (121 mg, 166 μL, 1.2 mmol) was added to the solution and the mixture was refluxed at 80°C for 16 hours. After cooling to room temperature, the reaction crude was filtered through celite<sup>®</sup> to remove the black solid formed and 20 drops of saturated aqueous NH<sub>4</sub>PF<sub>6</sub> were added to the filtrate. The solvent was then totally removed in a rotary evaporator and the brown solid obtained was re-dissolved in methanol. The mixture was filtered through celite<sup>®</sup> and methanol was removed from the filtrate under vacuum until about 10 mL left. During this process a brown precipitate appeared, which was filtered off, washed with diethyl ether and dried under vacuum. Yield: 55 mg (35% yield) <sup>1</sup>H-NMR (600 MHz, acetone-d<sub>6</sub>, 298K) δ=9.02 (d, 1H *J*<sub>4-3</sub> = 2.4 Hz, H4), 8.84 (d, 1H, *J*<sub>9-10</sub> = 9.0 Hz, H9), 8.75 (d, 2H, *J*<sub>27-28</sub> = 8.1 Hz, H27), 8.57 (d, 2H, *J*<sub>24-23</sub> = 15.8 Hz, H24), 8.35 (t, 1H, *J*<sub>28-27,27'</sub> = 8.1 Hz, H28), 8.11 (m, 4H, *J*<sub>21-22</sub> = 7.2, H21; *J*<sub>12-11</sub> = 4.8, H12; *J*<sub>10-9,11</sub> = 3.8 Hz, H10), 8.00 (d, 1H, *J*<sub>3-</sub>

$\delta$  = 2.4 Hz, H3), 7.92 (m, 3H, H11, H23), 7.29 (ddd, 1H,  $J_{22-21,23,24}$  = 7.0, 5.6, 1.2 Hz, H22), 4.79 (s, 3H, H1), 4.54 (m, 1H, H18).  $^{13}\text{C}$ -NMR (600 MHz, acetone- $d_6$ , 298K) 200.91 (C6), 159.08 (C25), 157.41 (C14), 156.82 (C21), 155.61 (C26), 151.44 (C7), 136.70 (C23), 135.48 (C28), 133.82 (C10), 132.09 (C11), 126.85 (C22), 126.03 (C3), 124.30 (C12), 123.13 (C24), 121.64 (C27), 121.28 (C8), 120.94 (C9), 119.61 (C13), 119.14 (C4), 70.79 (C18), 37.48 (C1), 20.96 (C19). UV/vis (methanol):  $\lambda_{\text{max}}$  ( $\epsilon$ ) = 276 (11315), 314 (14616), 413 (5036), 479 (3889). ESI-MS (MeOH):  $m/z$  = 638.1 ([M-PF $_6$ -1]).

*[Ru(PhthaPz-Ome)(tpm)Cl]PF $_6$  (C3-Cl)*: [Ru(tpm)Cl $_3$ ] (130 mg, 0.3 mmol), 1,4-bis (1-methylimidazolium-1-yl)phthalazine dichloride (L1(Cl) $_2$ ) (73 mg, 0.2 mmol) and LiCl (38 mg 0.9 mmol) were mixed in a round bottom flask and dry methanol (20 mL) was added as solvent. Triethylamine (121 mg, 166  $\mu\text{L}$ , 1.2 mmol) was added to the solution and the mixture was refluxed at 80°C for 16 hours. After cooling to room temperature, the reaction crude was filtered through celite<sup>®</sup> to remove the black solid formed and 20 drops of saturated aqueous NH $_4$ PF $_6$  were added to the filtrate. The methanolic solution was concentrated in a rotary evaporator until about 10 mL and a brown precipitate was obtained. The precipitate was filtered off, washed with diethyl ether and dried under vacuum. Yield: 88 mg (60%)  $^1\text{H}$ -NMR (600 MHz, acetone- $d_6$ , 298K)  $\delta$  = 9.66 (s, 1H, H24), 8.88 (d, 1H,  $J$  = 2.3 Hz, H4), 8.87 (d, 1H,  $J$  = 8.6 Hz, H9), 8.68 (d, 1H,  $J_{20-21}$  = 1.6 Hz, H20), 8.57 (d, 1H,  $J_{31-32}$  = 2.3 Hz, H31), 8.52 (d, 1H,  $J_{22-21}$  = 2.2 Hz, H22), 8.47 (d, 1H,  $J_{33-32}$  = 1.7 Hz, H33), 8.46 (d, 1H,  $J_{26-27}$  = 2.5 Hz, H26), 8.39 (d, 1H,  $J_{12-11}$  = 8.0 Hz, H12), 8.20 (t, 1H,  $J_{10-9,11}$  = 7.3 Hz, H10), 8.07 (t, 1H,  $J_{11-10,12}$  = 7.6 Hz, H11), 7.64 (d, 1H,  $J_{3-4}$  = 2.3 Hz, H3), 6.89 (d, 1H,  $J_{28-27}$  = 1.9 Hz, H28), 6.74 (s, 1H, H21), 6.67 (s, 1H, H32), 6.33 (t, 1H,  $J_{27-26,28}$  = 2.4 Hz, H27), 4.16 (s, 3H, H18), 3.73 (s, 3H, H1).  $^{13}\text{C}$ -NMR (600 MHz, acetone- $d_6$ , 298K) 157.87 (C14), 151.40 (C7), 149.12 (C33), 146.71 (C28), 146.66 (C20), 134.70 (C26), 133.97 (C31), 133.75 (C10), 132.43 (C22), 132.27 (C11), 124.89 (C3), 124.34 (C12), 121.57 (C8), 121.28 (C9), 120.17 (C13), 119.63 (C4), 108.41 (C32), 108.27 (C27), 107.51 (C21), 76.77 (C24), 55.04 (C18), 36.27 (C1). UV/vis (methanol):  $\lambda_{\text{max}}$  ( $\epsilon$ ) = 302 (7799), 410 (4745). ESI-MS (MeOH):  $m/z$  = 591.1 ([M-PF $_6$ -1]).

*trans, fac*-[Ru(*PhthaPz-Ome*)(*bpea*)Cl]PF<sub>6</sub> (**C4-Cl**): [Ru(*bpea*)Cl<sub>3</sub>] (130 mg, 0.3 mmol), 1,4-bis(1-methylimidazolium-1-yl)phthalazine dichloride (**L1(Cl)**)<sub>2</sub> (73 mg, 0.2 mmol) and LiCl (38 mg 0.9 mmol) were mixed in a round bottom flask and dry methanol (20 mL) was added as solvent. Triethylamine (121 mg, 166 μL, 1.2 mmol) was added to the solution and the mixture was refluxed at 80°C for 16 hours. After cooling to room temperature, the reaction crude was filtered through celite<sup>®</sup> to remove the black solid formed and 20 drops of saturated aqueous NH<sub>4</sub>PF<sub>6</sub> were added to the filtrate. The methanolic solution was concentrated in a rotary evaporator until about 10 mL left and a brown precipitate appeared. The precipitate was filtered, washed with diethyl ether and dried under vacuum. Yield: 68 mg (45%). <sup>1</sup>H-NMR (600 MHz, acetone-d<sub>6</sub>, 298K) δ=9.63 (d, 1H, *J*<sub>20-21</sub> = 5.3 Hz, H20), 9.56 (d, 1H, *J*<sub>34-33</sub> = 5.0 Hz, H34), 8.84 (s, 1H, H4), 8.79 (d, 1H, *J*<sub>9-10</sub> = 8.3 Hz, H9), 8.25 (d, 1H, *J*<sub>12-11</sub> = 8.0 Hz, H12), 8.12 (t, 1H, *J*<sub>10-9,11</sub> = 7.5 Hz, H10), 7.97 (t, 1H, *J*<sub>11-10,12</sub> = 7.6 Hz, H11), 7.92 (t, 1H, *J*<sub>32-31,33</sub> = 7.3 Hz, H32), 7.82 (t, 1H, *J*<sub>22-21,23</sub> = 7.4 Hz, H22), 7.58 (d, 2H, *J*<sub>3-4,31-32</sub> = 10.2 Hz, H3, H31), 7.50 (m, 1H, *J*<sub>23-22,33-32,34</sub> = 7.3 Hz, H23, H33), 7.41 (t, 1H, *J*<sub>21-20,22</sub> = 6.5 Hz, H21). 4.52-4.42 (m, 4H, H26, H29) 3.65 (s, 3H, H18), 3.58 (s, 3H, H1), 2.53 (td, 1H, *J*<sub>27-27',28</sub> = 13.8, 6.8 Hz, H27), 2.35 (td, 1H, *J*<sub>27'-27,28</sub> = 13.7, 6.8 Hz, H27'), 0.91 (m, 3H, H28). <sup>13</sup>C-NMR (600 MHz, acetone-d<sub>6</sub>, 298K) 204.97 (C6), 67.49 (C25), 66.09 (C29), 61.96 (C27), 53.89 (C18), 35.45 (C1), 7.98 (C28), 161.42 (C20), 160.02 (C34), 158.07 (C14), 151.65 (C24), 150.15 (C13), 149.42 (C30), 136.55 (C32), 125.73 (C22), 133.74 (C10), 131.47 (C11), 125.00 (C3), 124.30 (C12), 123.63 (C21), 123.13 (C33), 121.52 (C8), 121.01 (C23), 120.70 (C9), 120.64 (C31), 119.44 (C7), 118.85 (C4). UV/vis (methanol): λ<sub>max</sub> (ε)= 299 (5226), 434 (5612). ESI-MS (MeOH): *m/z* = 604.1 ([M-PF<sub>6</sub>-1]).

*cis*-[Ru<sup>II</sup>(*PhthaPz-Ome*)(*trpy*)(OH<sub>2</sub>)](PF<sub>6</sub>)<sub>2</sub> (**C1-OH<sub>2</sub>**): **C1-Cl** (120 mg, 0.16 mmol) was dissolved in a mixture of acetone and water (acetone: water = 1: 3, 40 mL). AgBF<sub>4</sub> (109 mg, 0.56 mmol) was added into the solution, which was then refluxed at 90°C for 4 hours. After cooling to room temperature, the reaction crude was filtered through celite<sup>®</sup> to remove the black solid formed. The brown solution was concentrated under vacuum until about 20 mL left, followed by centrifugation (10.000r/m, 10min) to remove the potential colloidal silver still remaining. To the clear red solution 20 drops of saturated aqueous NH<sub>4</sub>PF<sub>6</sub> solution were added and the precipitate formed was filtered off, washed with diethylether and dried under vacuum. Yield: 91 mg (65%) <sup>1</sup>H-

NMR (600 MHz, acetone- $d_6$ , 298K) 9.01 (d, 1H,  $J_{4-3} = 2.4$  Hz, H4), 8.80 (d, 2H,  $J_{26-27} = 7.4$  Hz, H26), 8.78 (d,  $J_{9-10} = 8.7$  Hz, H9), 8.62 (d, 2H,  $J_{23-22} = 8.0$  Hz, H23), 8.44 (t, 2H,  $J_{27-26,26'} = 8.1$  Hz, H27), 8.19 (d, 2H,  $J_{20-21} = 5.0$  Hz, H20), 8.12 (t, 1H,  $J_{10-9,11} = 19.9$  Hz, H10), 8.04-8.00 (m, 4H, H12, H3, H22), 7.91 (t, 1H,  $J_{11-10,12} = 7.5$  Hz, H11), 7.37 (m, 2H, H21), 4.56 (s, 3H, H1), 3.46 (s, 3H, H18).  $^{13}\text{C}$ -NMR (600 MHz, acetone- $d_6$ , 298K) 200.62 (C6), 159.47 (C24), 158.01 (C14), 157.82 (C20), 156.41 (C25), 153.08 (C7), 138.22 (C22), 137.65 (C27), 134.20 (C10), 132.83 (C11), 127.53 (C21), 126.29 (C3), 124.05 (C12), 123.85 (C23), 122.38 (C26), 121.12 (C9), 120.90 (C8), 119.57 (C14), 119.21 (C3), 54.43 (C18), 36.55 (C1). UV/vis (methanol):  $\lambda_{\text{max}}$  ( $\epsilon$ ) = 275 (12189), 309 (13040), 388 (4338), 467 (4474). ESI-MS (MeOH):  $m/z = 594.1$  ([M-2PF $_6$ ]).

*cis*-[Ru<sup>II</sup>(PhthaPz-Ipro)(trpy)(OH $_2$ )]PF $_6$  (C2-OH $_2$ ): C2-Cl (120mg, 0.15 mmol) was dissolved in a 40 mL mixture of acetone and water (1:3). AgBF $_4$  (109 mg, 0.56 mmol) was then added to the solution, which was then refluxed at 90°C for 4 hours. After cooling to room temperature, the reaction crude was filtered through celite<sup>®</sup> to remove the silver chloride formed. The brown filtrate was then concentrated in a rotary evaporator until about 20 mL, followed by centrifugation (10.000 r/m, 10 min) to remove the remaining solids. To the clear red solution 20 drops of a saturated aqueous NH $_4$ PF $_6$  solution were added. The brown precipitate formed was filtered off, washed with diethyl ether and dried under vacuum. Yield: 91 mg (65%)  $^1\text{H}$ -NMR (600 MHz, acetone- $d_6$ , 298K)  $\delta$ =9.03 (d, 2H,  $J = 2.4$  Hz, H4), 8.84 (d, 2H,  $J_{27-28} = 6.7$  Hz, H27), 8.81 (d, 1H,  $J_{9-10} = 8.7$  Hz, H9). 8.63 (d, 2H,  $J_{24-23} = 8.0$  Hz, H24), 8.50 (t, 1H,  $J_{28-27,27'} = 8.1$  Hz, H28), 8.23 (dd, 2H,  $J_{21-22,23} = 10.5, 5.6$  Hz, H21), 8.13 (d, 1H,  $J_{3-4} = 8.5$  Hz, H3), 8.10 (t, 1H,  $J_{23-22,24} = 8.7$  Hz, H23), 7.93 (t, 1H,  $J_{11-10,12} = 7.6$  Hz, H11), 7.38 (ddd, 1H,  $J_{22-21,23,24} = 7.0, 5.6, 1.2$  Hz, H22), 4.58 (s, 3H, H1), 4.49 (dt, 1H,  $J_{18-19,19'} = 12.3, 6.2$  Hz, H18), 1.07 (d, 6H,  $J_{19-18} = 6.2$  Hz, H19).  $^{13}\text{C}$ -NMR (600 MHz, acetone- $d_6$ , 298K) 200.66 (C6), 159.47 (C25), 157.96 (C21), 157.31 (C14), 156.32 (C26), 152.73 (C7), 138.23 (C23), 137.53 (C28), 134.05 (C10), 132.74 (C11), 127.63 (C22), 126.16 (C3), 124.24 (C12), 123.77 (C24), 122.47 (C27), 121.15 (C8), 121.07 (C9), 119.80 (C13), 119.62 (C4), 70.98 (C18), 36.39 (C1), 20.90 (C19). UV/vis (methanol):  $\lambda_{\text{max}}$  ( $\epsilon$ ) = 280 (12006), 311 (14895), 392 (4700), 463 (4220). ESI-MS (MeOH):  $m/z = 622.1$  ([M-2PF $_6$ ]).

*[Ru(PhthaPz-Ome)(tpm)(OH<sub>2</sub>)](PF<sub>6</sub>)<sub>2</sub> (C3-OH<sub>2</sub>):* C3-Cl (120 mg, 0.16 mmol) was dissolved in a 40 mL mixture of acetone and water (1:3). AgBF<sub>4</sub> (109 mg, 0.56 mmol) was added into the solution that was then refluxed at 90°C for 4 hours. After cooling to room temperature, the reaction crude was filtered through celite<sup>®</sup> to remove the silver chloride formed. The brown filtrate was then concentrated in a rotary evaporator until about 20 mL, followed by centrifugation (10.000 r/m 10 min) in order to remove the remaining solids. To the clear red solution 20 drops of a saturated aqueous NH<sub>4</sub>PF<sub>6</sub> solution were added. The brown precipitate formed was filtered off, washed with diethyl ether and dried under vacuum. Yield: 76 mg (55%) <sup>1</sup>H-NMR (600 MHz, acetone-d<sub>6</sub>, 298K) δ=9.90 (s, 1H, H24), 8.99 (d, 1H, *J* = 2.4 Hz, H4), 8.97 (d, 1H, *J* = 8.5 Hz, H9), 8.83 (d, 1H, *J* = 1.7 Hz, H20), 8.72 (t, 1H, *J*<sub>31-32</sub> = 4.9 Hz, H31), 8.67 (d, 1H, *J*<sub>22-21</sub> = 2.7 Hz, H22), 8.57 (t, 1H, *J*<sub>33-32</sub> = 4.2 Hz, H33), 8.53 (d, 1H, *J*<sub>26-27</sub> = 5.5 Hz, H26), 8.47 (d, 1H, *J*<sub>12-11</sub> = 8.1 Hz, H12), 8.29 (tt, 1H, *J*<sub>10-9,11</sub> = 14.2, 7.1 Hz, H10), 8.17 (t, 1H, *J*<sub>11-10,12</sub> = 7.7 Hz, H11), 7.74 (d, 1H, *J*<sub>3-4</sub> = 2.3 Hz, H3), 6.85 (m, *J*<sub>21-20,22</sub> = 24 Hz, *J*<sub>28-27</sub> = 22 Hz H21, H28), 6.80 (t, 1H, *J*<sub>32-31,33</sub> = 2.5 Hz, H32), 6.35 (dt, 1H, *J*<sub>27-26,28</sub> = 5.1, 2.5 Hz, H27), 4.20 (s, 3H, H18), 3.74 (s, 1H, H1). <sup>13</sup>C-NMR (600 MHz, acetone-d<sub>6</sub>, 298K) 200.22 (C6), 158.58 (C14), 152.76 (C7), 148.70 (C33), 148.04 (C28), 147.06 (C20), 135.74 (C26), 134.89 (C31), 134.17 (C10), 133.64 (C22), 133.40 (C11), 125.84 (C3), 124.48 (C12), 122.02 (C9), 121.75 (C8), 120.96 (C13), 120.61 (C4), 109.06 (C32), 108.69 (C27), 108.04 (C21). 76.61 (C24), 55.38 (C18), 36.65 (C1). UV/vis (methanol): λ<sub>max</sub> (ε) = 295 (8297), 392 (5315). ESI-MS (MeOH): *m/z* = 575.1 ([M-2PF<sub>6</sub>]).

*trans, fac-[Ru(PhthaP-Ome)(bpea)(OH<sub>2</sub>)](PF<sub>6</sub>)<sub>2</sub> (C4-OH<sub>2</sub>):* C4-Cl (120 mg, 0.16 mmol) was dissolved in a 40 mL mixture of acetone and water (1: 3). AgBF<sub>4</sub> (109 mg, 0.56 mmol) was then added into the solution, which was refluxed at 90°C for 4 hours. After cooling to room temperature, the reaction crude was filtered through celite<sup>®</sup> to remove the silver chloride formed. The brown solution was concentrated in a rotary evaporator until about 20 mL, followed by centrifugation (10.000r /m, 10 min) to remove the remaining solids. To the clear red solution 20 drops of a saturated aqueous NH<sub>4</sub>PF<sub>6</sub> solution were added. The precipitate formed was filtered off, washed with diethyl ether and dried under vacuum. Yield: 96 mg (68%) <sup>1</sup>H-NMR (600 MHz, acetone-d<sub>6</sub>, 298K) δ=8.99 (d, 1H, *J* = 2.4 Hz, H4), 8.96 (d, 1H, *J* = 5.3 Hz, H20), 8.93 (m, 2H, H34, H9). 8.36 (d, 1H, *J* = 8.1 Hz, H12), 8.23 (m, 1H, H10), 8.08 (t, 1H, *J*<sub>11-</sub>



$_{10,12} = 7.6$  Hz, H11), 7.99 (td, 1H,  $J_{22-21,23} = 7.8, 1.4$  Hz, H22), 7.88 (td, 1H,  $J_{32-31,33} = 7.4, 1.7$  Hz, H32), 7.72 (d, 1H,  $J_{3-4} = 2.4$  Hz, H3), 7.67 (d, 1H,  $J_{23-22} = 7.9$  Hz, H23), 7.57 (m, 1H, H21), 7.55 (d, 1H,  $J_{31-32} = 7.9$  Hz, H31), 7.50 (t, 1H,  $J_{33-32,34} = 6.6$  Hz, H33), 4.57-4.40 (m, 4H, H29, H25), 3.71 (s, 3H, H1), 3.65 (s, 3H, H18), 2.34 (m, 2H, H7), 0.91 (dd, 3H,  $J_{28-27,27'} = 9.2, 5.0$  Hz, H28).  $^{13}\text{C}$ -NMR (600 MHz, acetone- $d_6$ , 298K) 202.85 (C6), 161.20 (C30), 159.56 (C24), 158.81 (C14), 151.85 (C7), 149.37 (C34), 147.67 (C20), 137.42 (C22), 136.72 (C32), 134.06 (C10), 132.67 (C11), 125.82 (C3), 124.41 (C12), 124.30 (C33), 123.78 (C21), 121.63 (C8), 121.54 (C31), 121.49 (C23), 121.35 (C9), 120.47 (C13), 119.89 (C4), 67.89 (C29), 67.29 (C25), 62.80 (C27), 54.19 (C18), 35.89 (C1), 7.97 (C28). UV/vis (methanol):  $\lambda_{\text{max}}$  ( $\epsilon$ ) = 299 (5810), 423 (5753). ESI-MS (MeOH):  $m/z = 588.1$  ( $[\text{M}-2\text{PF}_6]$ ).

## Acknowledgements

The NMR assignment of the ligands and complexes were analyzed with the help of Pau Nolis from Universitat Autònoma de Barcelona (UAB). The experiments of water oxidation presented in section III.2.5. and electrocatalytic epoxidation of alkenes in section III.2.6.1 were performed during an stay in the group of Prof. Antoni Llobet at the Institut Català d'Investigació Química (ICIQ) under the supervision of Dr. Laia Francàs.

## III.5. References

- 
- <sup>1</sup> Herrmann, W. A. and Köcher, C. *Angew. Chem. Int. Ed.* **1997**, 36, 2162.
  - <sup>2</sup> Bruneau, C. *Ruthenium catalysts and fine chemistry* Springer-Verlag, Berlin, **2004**.
  - <sup>3</sup> a) Trost, B. M. and Pinkerton, A. B. *J. Am. Chem. Soc.* **1999**, 121, 4068. b) Trost, B. M.; Pinkerton, A. B. and Kremzow, D. *J. Am. Chem. Soc.* **2000**, 122, 12007. c) Shing,

---

T. K.; Tai, V. W. and Tam, E. K. *Angew. Chem. Int. Ed.* **1994**, 33, 2312. d) Grela, K.; Harutyunyan, S. and Michrowska, A. *Angew. Chem. Int. Ed.* **2002**, 114, 4038.

<sup>4</sup> Weskamp, T.; SchaRenmann, W. C.; Spiegler, M.; Herrmann, W. A. *Angew. Chem. Int. Ed.* **1998**, 37, 2490.

<sup>5</sup> Clinton L. Lund, Michael J. Sgro, Renan Cariou, and Douglas W. Stephan. *Organometallics*, **2012**, 31, 802.

<sup>6</sup> Chen, Z. F.; Concepcion, J. J. and Meyer, T. J. *Dalton Trans.*, **2011**, 40, 3789.

<sup>7</sup> Dakkach, M. and Llobet, A.; et al. *Inorg. Chem.* **2010**, 49, 7072.

<sup>8</sup> Masllorens, E.; Rodriguez, M.; Romero, I.; Roglans, A.; Parella, T.; Benet-Buchholz, J.; Poyatos, M. and Llobet, A. *J. Am. Chem. Soc.* **2006**, 128, 5306.

<sup>9</sup> a) Dovletoglou, A.; Adeyemi, S. A.; Meyer, T. J. *Inorg. Chem.* **1996**, 35, 4120. b) Ph.D Thesis of Lydia Vaquer. Universitat Rovira i Virgili, **2011**.

<sup>10</sup> Masllorens, E.; Rodriguez, M.; Romero, I.; Roglans, A.; Parella, T.; Benet-Buchholz, J.; Poyatos, M.; Llobet, A. *J. Am. Chem. Soc.* **2006**, 128, 5306.

<sup>11</sup> a) Richard Keene, F. *Coordination Chemistry Reviews* **1999**, 187, 121. b) Meyer, T. J. *J. Electrochem. Soc.* **1984**, 131, 221C.

<sup>12</sup> Dovletoglou, A.; Adeyemi, S. A.; Meyer, T. J. *Inorg. Chem.* **1996**, 35, 4120.

<sup>13</sup> Duan, L.; Araujo, C. M.; Ahlquist, M. S. G. and Sun, L. *PNAS*, **2012**, 109, 15584.

<sup>14</sup> a) Di Giovanni, C.; Poater, A.; Benet-Buchholz, J.; Cavallo, L.; Solà, M.; Llobet, A. *Chem. Eur. J.* **2014**, 20, 3898. b) Di Giovanni, C.; Vaquer, L.; Sala, X.; Benet-Buchholz, J. and Llobet, A. *Inorg. Chem.* **2013**, 52, 4335. c) Aguiló, J.; Naeimi, A.; Bofill, R.; Mueller-Bunz, H.; Llobet, A.; Escriche, L.; Sala, X.; Albrecht, M. *New. J. Chem.* **2014**, 38, 1980. d) Planas, N.; Christian, G. J.; Mas-Marza, E.; Sala, X.; Fontrodona, X.; Maseras, F.; Llobet, A. *Chem. Eur. J.* **2010**, 16, 7965. Sens, C.; Romero, I.; Rodríguez, M.; Llobet, A.; Parella, T.; Benet-Buchholz, J. *J. Am. Chem. Soc.* **2004**, 126, 7798.

<sup>15</sup> a) Sens, C.; Romero, I.; Rodríguez, M.; Llobet, A.; Parella, T.; Benet-Buchholz, J.; *J. Am. Chem. Soc.* **2004**, 126, 7798. b) Planas, N.; Christian, J. G.; Mas-Marzà, E.; Sala, X.; Fontrodona, X.; Maseras, F.; Llobet, A.; *Chem. Eur. J.* **2010**, 16, 7965. c) García-

---

Antón, J.; Bofill, R.; Escriche, L.; Llobet, A. and Sala, X. *Eur. J. Inorg. Chem.* **2012**, 4775.

<sup>16</sup> Xu, Y.; Åkermark, T.; Gyollai, V.; Zou, D.; Eriksson, L.; Duan, L.; Zhang, R.; Åkermark, B.; Sun, L. *Inorg. Chem.* **2009**, *48*, 2717.

<sup>17</sup> Xu, Y.; Fischer, A.; Duan, L.; Tong, L.; Gabrielsson, E.; Åkermark, B.; Sun, L. *Angew. Chem. Int. Ed.* **2010**, *49*, 8934.

<sup>18</sup> Scheele, U. J.; Dechert, S. and Meyer, F. *Tetrahedron Letters* **2007**, *48*, 8366.

<sup>19</sup> Hirsch, A.; and G. Orphan, D. G.; *Canadian Journal of Chemistry* **1966**, *44*, 1551.

<sup>20</sup> Aguiló, J.; Naeimi, A.; Bofill, R.; Mueller-Bunz, H.; Llobet, A.; Escriche, L.; Sala, X.; Albrecht, M. *New J. Chem.* **2014**, *38*, 1980.

<sup>21</sup> a) Van Veldhuizen, J.; Campbell, J.; Giudici, R. and Hoveyda, A. *J. Am. Chem. Soc.* **2005**, *127*, 6877. b) Truscott, B.; Klein, R. and Kaye, T. P.; *Tetrahedron Letters* **2010**, *51*, 5041.

<sup>22</sup> Vaquer, L.; Sala, X.; Benet-Buchholz, J. and Llobet, A. *Inorg. Chem.* **2013**, *52*, 4335.

<sup>23</sup> Serrano, I.; Sala, X.; Plantalech, E.; Rodríguez, M.; Romero, I.; Jansat, S.; Gomez, M.; Parella, T.; Stoeckli-Evans, H.; Solans, X.; *Inorg. Chem.* **2007**, *46*, 5381.

<sup>24</sup> Reger, D. L.; Grattan, T. C.; Brown, K. J.; Little, C. A.; Lamba, J. J. S.; Rheingold, A. L.; Sommer, R. D. *J. Organomet. Chem.*, **2000**, *607*, 120.

<sup>25</sup> Pal, S.; Chan, M. K. and Armstrong, W. H. *J. Am. Chem. Soc.* **1992**, *114*, 6398.

<sup>26</sup> Sullivan, B. P.; Calvert, J. M. and Meyer, T. J. *Inorg. Chem.* **1980**, *19*, 1404.

<sup>27</sup> Salierno, M.; Fameli, C. and Etchenique, R. *Eur. J. Inorg. Chem.* **2008**, 1125.

<sup>28</sup> Serrano, I.; Rodríguez, M. and Romero, I. *Inorg. Chem.* **2006**, *45*, 2644.

<sup>29</sup> Sens, C.; Romero, I.; Rodríguez, M.; Llobet, A.; Parella, T.; Benet-Buchholz, J. *J. Am. Chem. Soc.* **2004**, *126*, 7798.

<sup>30</sup> García-Antón, J.; Bofill, J.; Escriche, L.; Llobet, A. and Sala, X. *Eur. J. Inorg. Chem.* **2012**, 4775.

<sup>31</sup> Liu, X. L. and Chen, W. Z. *Organometallics*, **2012**, *31*, 6614.

- 
- <sup>32</sup> Chen, C.; Qiu, H. Y.; Chen, W. Z. And Wang, D. Q. *J. Organomet. Chem.* **2008**, 693, 3273.
- <sup>33</sup> Ye, J. S.; Zhang, X. M.; Chen, W. Z. and Shimada, S. *Organometallics*, **2008**, 27, 4166.
- <sup>34</sup> Sens, C.; Romero, I.; Rodríguez, M.; Llobet, A.; Parella, T.; Benet-Buchholz, J.; *J. Am. Chem. Soc.* **2004**, 126, 7798.
- <sup>35</sup> Planas, N.; Christian, J. G.; Mas-Marzà, E.; Sala, X.; Fontrodona, X.; Maseras, F.; Llobet, A.; *Chem. Eur. J.* **2010**, 16, 7965.
- <sup>36</sup> Mola, J.; Romero, I.; Rodríguez, M.; Bozoglian, F.; Poater, A.; Solà, M.; Parella, T.; Benet-Buchholz, J.; Fontrodona, X.; and Llobet, A. *Inorg. Chem.*, **2007**, 46, 10707.
- <sup>37</sup> Dakkach, M.; Parella, T.; Atlamsani, A.; Romero, I. and Rodríguez, M. *Adv. Synth. Catal.* **2011**, 353, 231.
- <sup>38</sup> Dakkach, M.; Atlamsani, A.; Parella, T.; Romero, I. and Rodríguez, M. *Inorg. Chem.* **2013**, 52, 5077.
- <sup>39</sup> a) Vaquer, L.; De Tovar, J.; García-Antón, J.; Llobet, A.; Sala, X., *Inorg. Chem.* **2013**, 52, 4985. b) Dakkach, M.; Atlamsani, A.; Parella, T.; Romero, I. and Rodríguez, M. *Inorg. Chem.* **2013**, 52, 5077.
- <sup>40</sup> a) Sala, X.; Poater, A.; Von Zelewsky, A.; Parella, T.; Fontrodona, X.; Romero, I.; Sola, M.; Rodríguez, M.; Llobet, A. *Inorg. Chem.* **2008**, 47, 8016. b) Ye, J. S.; Zhang, X. M.; Chen, W. Z. and Shimada, S. *Organometallics*, **2008**, 27, 4166.
- <sup>41</sup> Laurent, F.; Plantalech, E.; Donnadiou, B.; Jimenez, A.; Hernández, F.; Martínez-Ripoll, M.; Biner, M.; Llobet, A. *Polyhedron*, **1999**, 18, 3321.
- <sup>42</sup> Bard, A. J. and Faulkner, L. R. *Electrochemical Methods: Fundamentals and Applications* 2<sup>nd</sup> Edition, John Wiley & Sons, New York, **2001**.
- <sup>43</sup> a) Dobson, J. C.; Meyer, T. J. *Inorg. Chem.* **1988**, 27, 3283-3291. b) Cabaniss, G. E.; Diamantis, A. A.; Murphy, W. R.; Linton, R. W.; Meyer, T. J. *J. Am. Chem. Soc.* 1985, 107, 1845-1853.
- <sup>44</sup> Bard, A. J. and Faulkner, L. R. *Electrochemical Methods: Fundamentals and Applications* 2<sup>nd</sup> Edition, John Wiley & Sons, New York, **2001**.

- 
- <sup>45</sup> a) Dobson, J. C.; Meyer, T. J. *Inorg. Chem.* **1988**, *27*, 3283-3291. b) Cabaniss, G. E.; Diamantis, A. A.; Murphy, W. R.; Linton, R. W.; Meyer, T. J. *J. Am. Chem. Soc.* **1985**, *107*, 1845-1853.
- <sup>46</sup> Rodríguez, M.; Romero, I.; Llobet, A. *Inorg. Chem.* **2001**, *40*, 4150.
- <sup>47</sup> Takeuchi, K. J.; Thompson, M. S.; Pipes, D. W.; Meyer, T. J. *Inorg. Chem.* **1984**, *23*, 1845.
- <sup>48</sup> Shriver, D. F. and Atkins, P. W. *Inorganic Chemistry*; Oxford University Press, **2012**.
- <sup>49</sup> a) Francas, L.; Sala, X.; Benet-Buchholz, J.; Escriche, L.; Llobet, A. *ChemSusChem* **2009**, *2*(4), 321. b) Dakkach, M.; Parella, T.; Atlamsani, A.; Romero, I. and Rodríguez, M. *Adv. Synth. Catal.* **2011**, *353*, 231.
- <sup>50</sup> Francas, L.; Sala, X.; Escudero-Adan, E.; Benet-Buchholz, J.; Escriche, L.; Llobet, A. *Inorg. Chem.* **2011**, *50*(7), 2771.
- <sup>51</sup> a) Francàs, L.; Sala, X.; Benet-Buchholz, J.; Escriche, L.; Llobet, A. *ChemSusChem* **2009**, *2*, 321. b) Aguiló, J.; Francàs, L.; Liu, H. J.; Llobet, A.; Escriche, L.; Sala, X.; et al. *Catal. Sci. Technol.* **2014**, *4*, 190.
- <sup>52</sup> Bard, A. J.; Faulkner, L. R. *Electrochemical Methods: fundamentals and applications*, Dianhuaxue Bianjibu **2001**, *7*, 255.
- <sup>53</sup> In, J. H.; Park, S. E.; Song, R. and Nam, W. *Inorg. Chim. Acta* **2003**, *343*, 373.
- <sup>54</sup> Sala, X.; Santana, N.; Serrano, I.; Plantalech, E.; Romero, I.; Rodríguez, M.; Llobet, A.; Jansat, S.; Gómez, M.; Fontrodona, X. *Eur. J. Inorg. Chem.* **2007**, 5207.
- <sup>55</sup> Reger, D. L.; Grattan, T. C.; Brown, K. J.; Little, C. A.; Lamba, J. J. S.; Rheingold, A. L.; Sommer, R. D. *J. Organomet. Chem.*, **2000**, *607*, 120.
- <sup>56</sup> Pal, S.; Chan, M. K. and Armstrong, W. H. *J. Am. Chem. Soc.* **1992**, *114*, 6398.

## III.6. Supporting Information

NMR

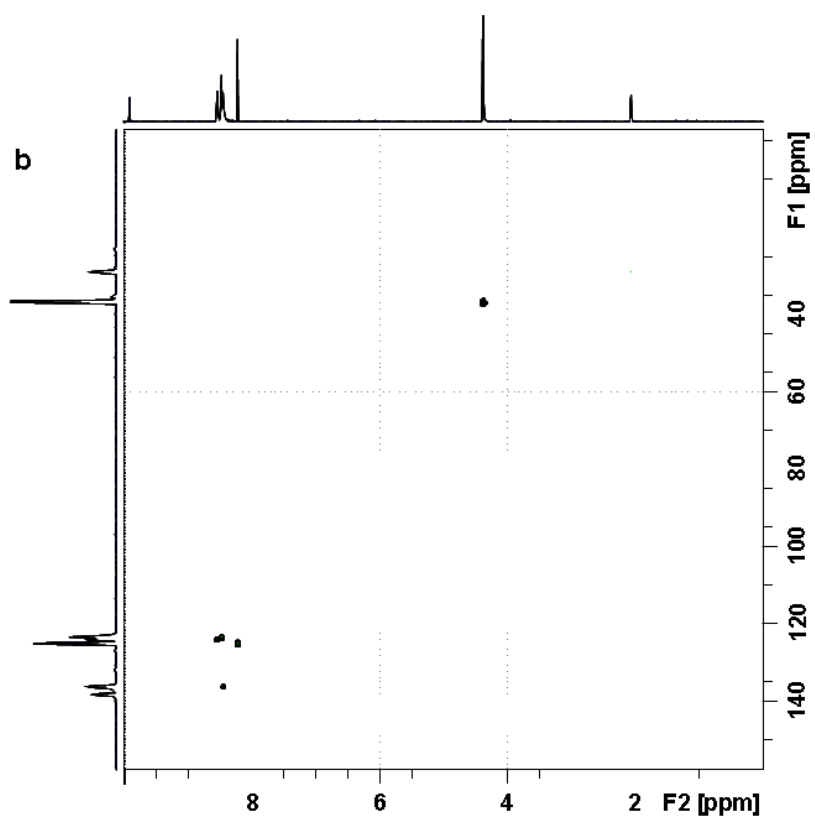
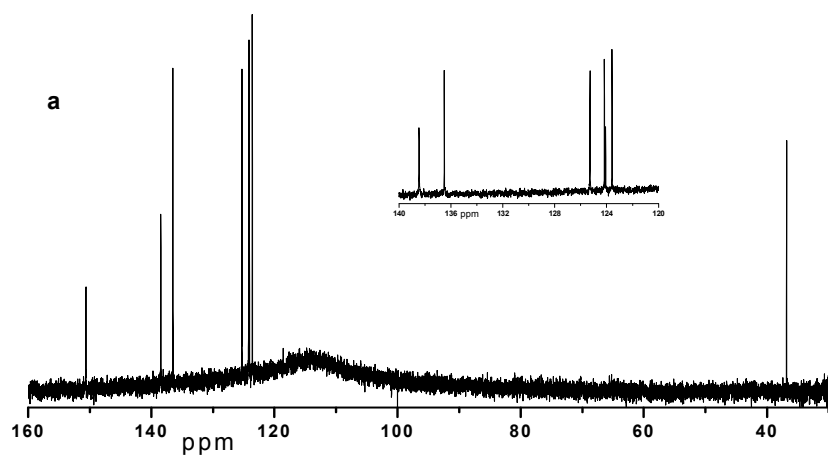
X-ray

Electrochemistry

Spectrophotometric titration with  $\text{Ce}^{\text{IV}}$

Water Oxidation

Figure S1. 1D and 2D NMR spectra of Ligand  $L1^{2+}$  (600 MHz, 298K, acetone- $d_6$ ): a)  $^{13}C$  NMR, b) HSQC, b) HMBC



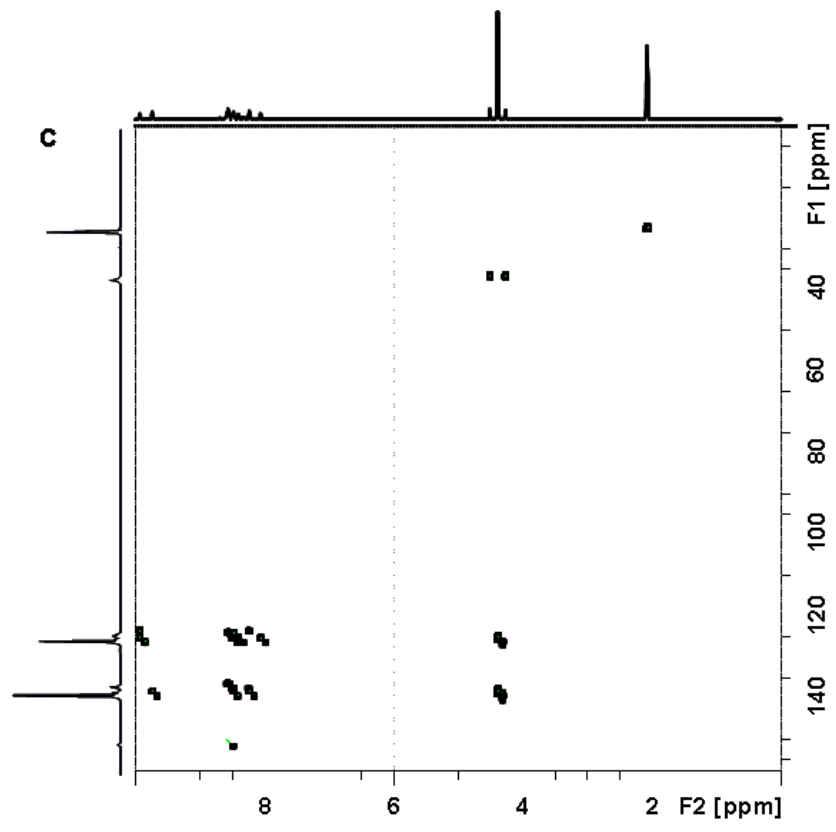




Table S1. Crystallographic data for **L1**(PF<sub>6</sub>)<sub>2</sub>

Empirical formula	C <sub>16</sub> H <sub>16</sub> F <sub>12</sub> N <sub>6</sub> P <sub>2</sub>
Formula weight	582.29
Temperature	298(2) K
Wavelength	0.71073 Å
Crystal system	Monoclinic
Space group	P2(1)/c
Unit cell dimensions	a = 17.64(6) Å    α = 90° b = 12.59(4) Å    β = 101.23(7) ° c = 18.67(6) Å    γ = 90°
Volume	4065(22) Å <sup>3</sup>
Z	8
Calculated density	1.903 Mg/m <sup>3</sup>
Absorption coefficient	0.344 mm <sup>-1</sup>
F(000)	2336
Crystal size	0.30 × 0.30 × 0.25 mm <sup>3</sup>
Theta range for data collection	1.96 to 29.66°
Limiting indices	-24 ≤ h ≤ 24, -17 ≤ k ≤ 17, -25 ≤ l ≤ 25
Reflections collected / unique	68116 / 11227 [R(int) = 0.2510]
Completeness to theta = 29.66	97.7 %
Absorption correction	Empirical
Max. and min. transmission	1.0 and 0.388546
Refinement method	Full-matrix least-squares on F <sup>2</sup>
Data / restraints / parameters	11227 / 0 / 649
Goodness-of-fit on F <sup>2</sup>	1.016
Final R indices [I > 2σ(I)]	R <sub>1</sub> = 0.0940, wR <sub>2</sub> = 0.2072
R indices (all data)	R <sub>1</sub> = 0.3097, wR <sub>2</sub> = 0.2912
Largest diff. peak and hole	0.592 and -0.387 e.Å <sup>-3</sup>

Figure S2. The angle between the plane of two imidazoles and the phthalazine scaffold from the crystal structure of **L1**(PF<sub>6</sub>)<sub>2</sub>.

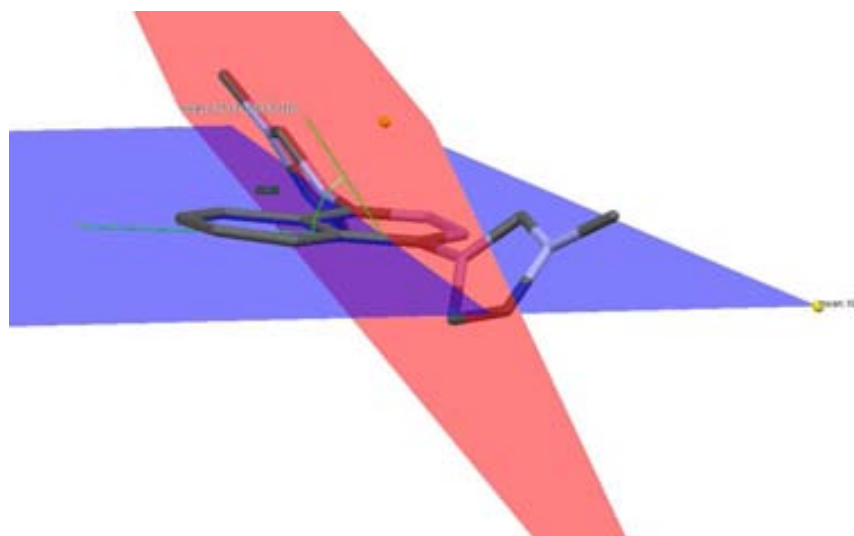
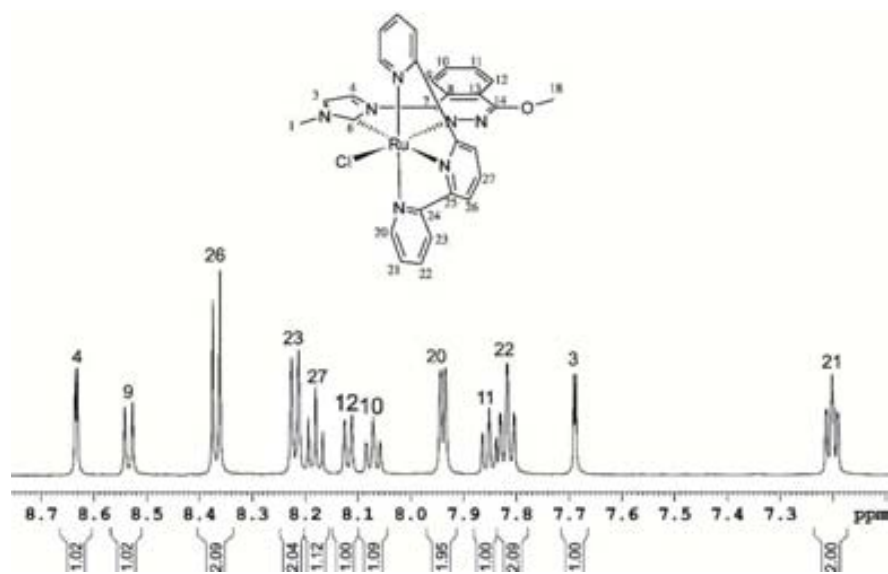
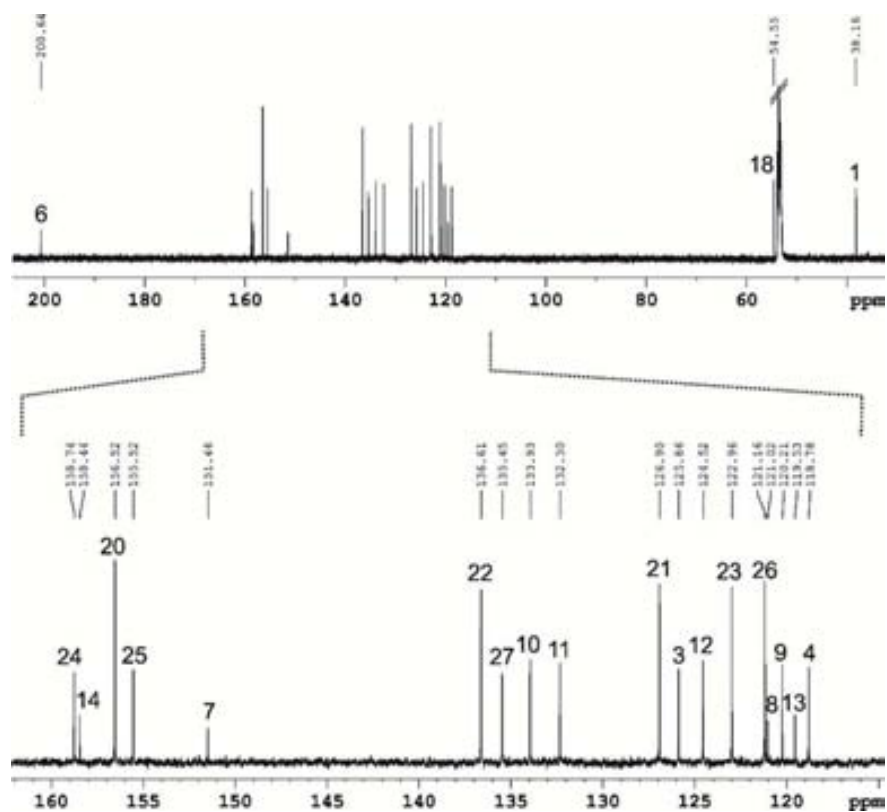


Figure S3. 1D and 2D NMR spectra of **C1**-Cl (600 MHz, 298K, CD<sub>2</sub>Cl<sub>2</sub>): a) <sup>1</sup>H NMR, b) <sup>13</sup>C NMR, c) HSQC, d) HMBC

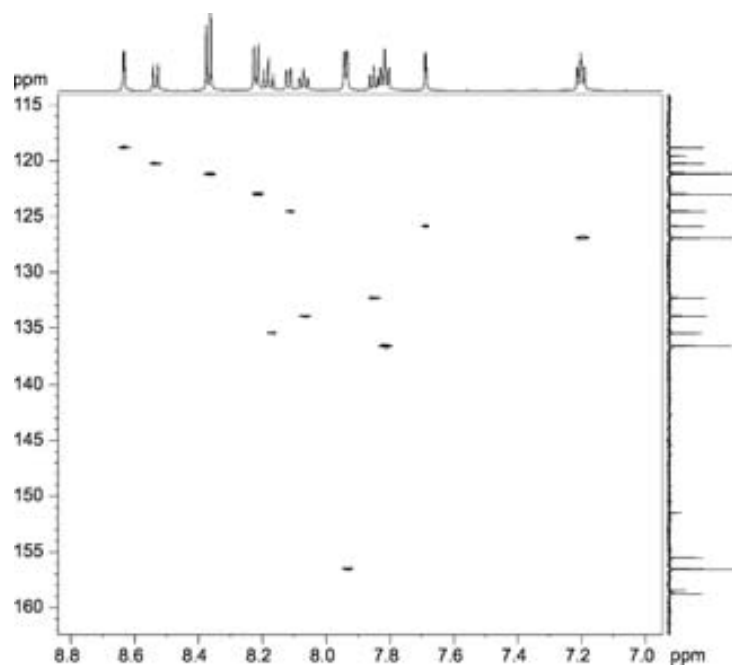
a)



b)



c)



d)

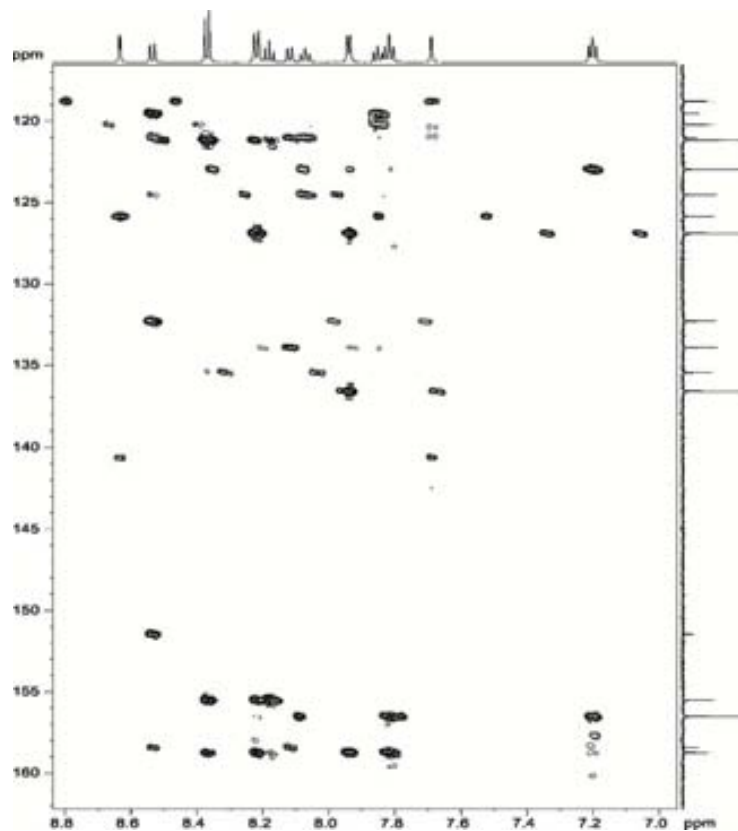
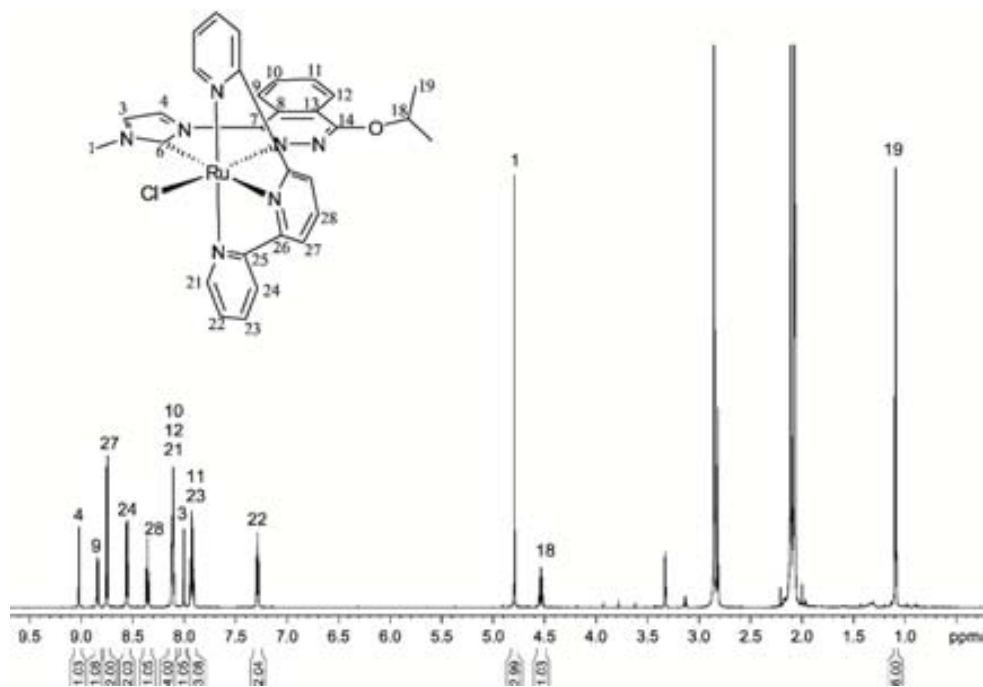
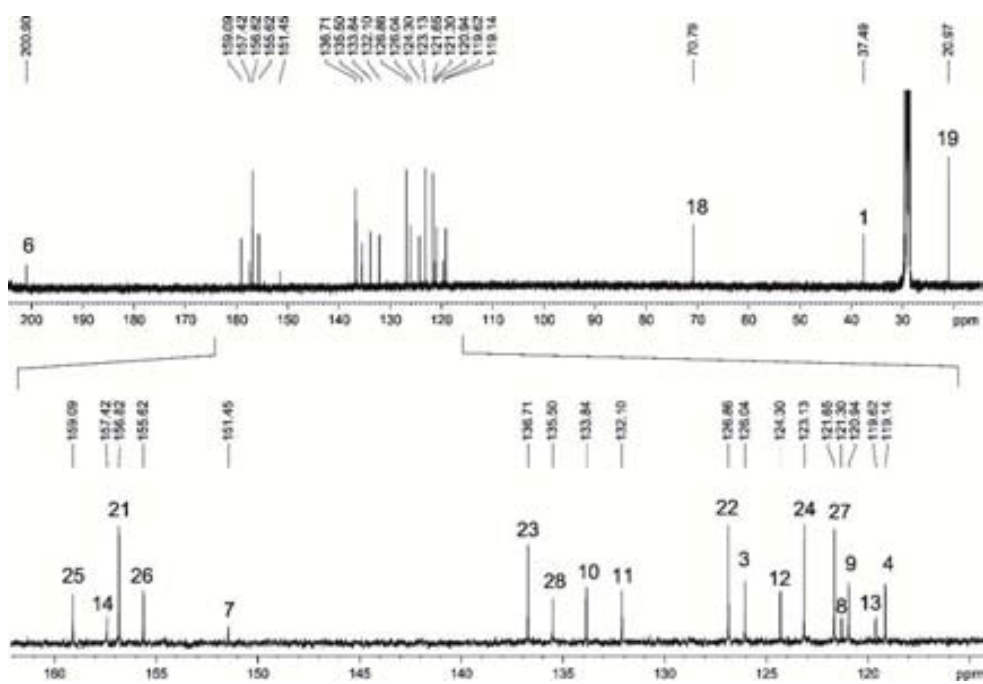


Figure S4. 1D and 2D NMR spectra of **C2-Cl** (600 MHz, 298K, acetone- $d_6$ ): a)  $^1\text{H}$  NMR, b)  $^{13}\text{C}$  NMR, c) HMBC, d) HSQC, e) ROESY, f) TOCSY

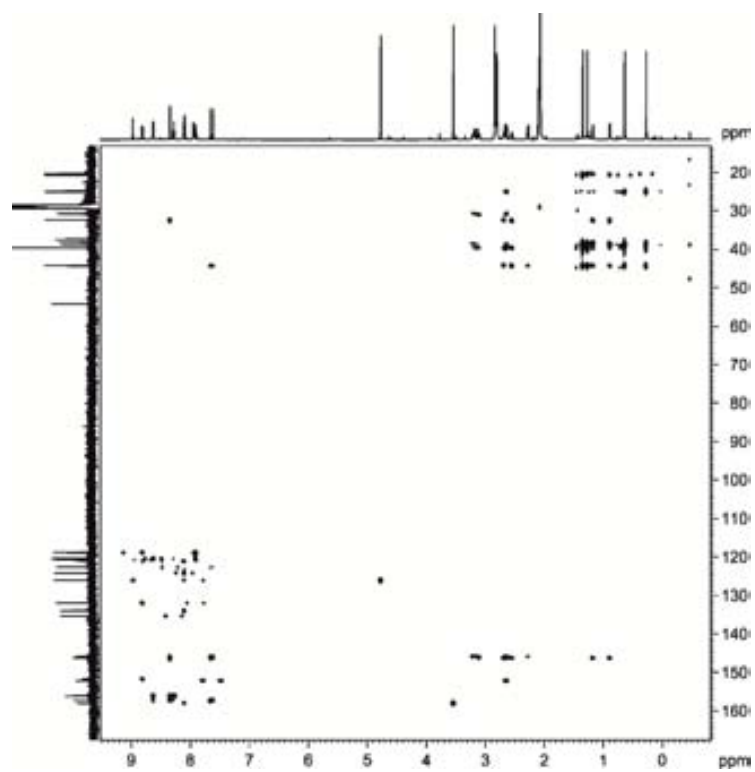
a)



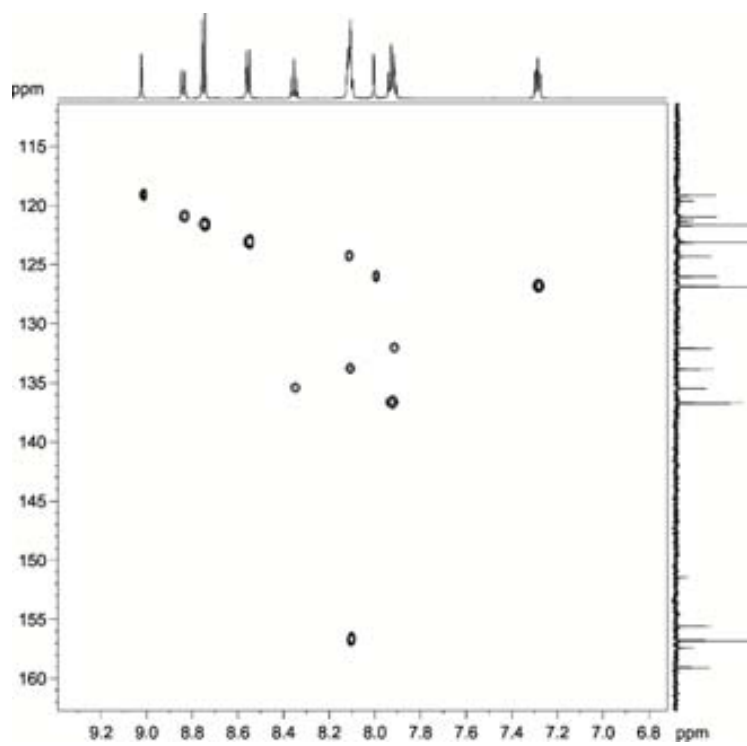
b)



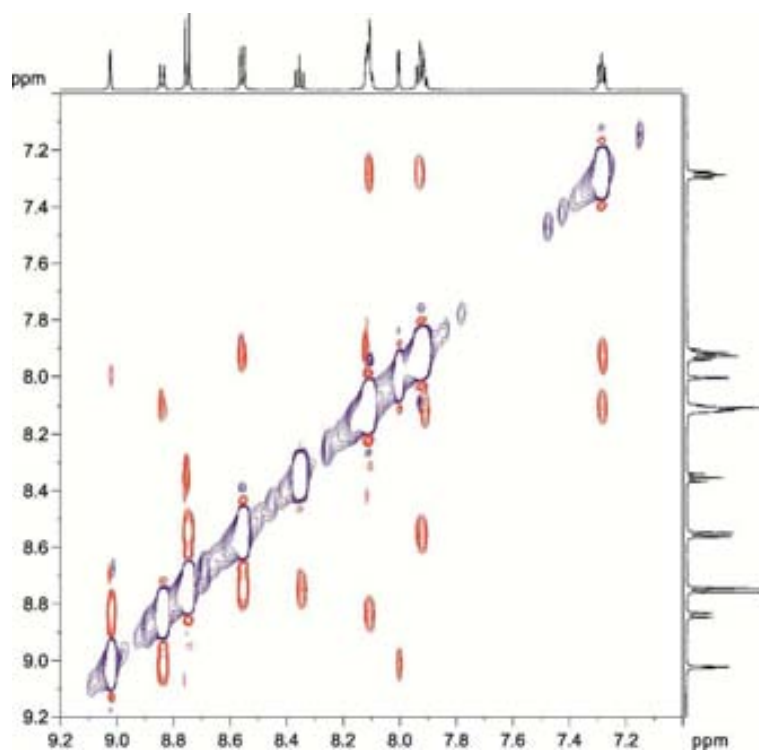
c)



d)



e)



f)

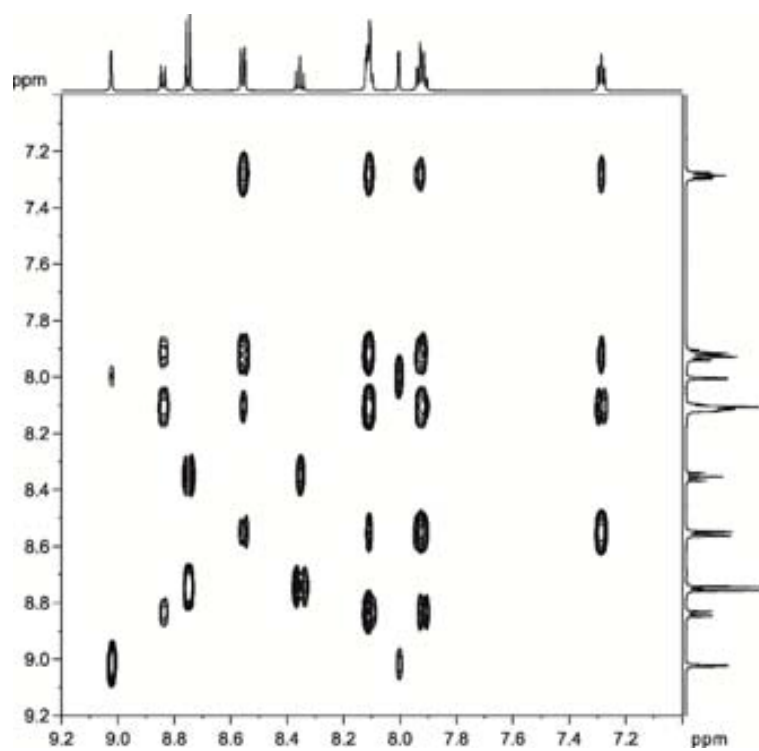
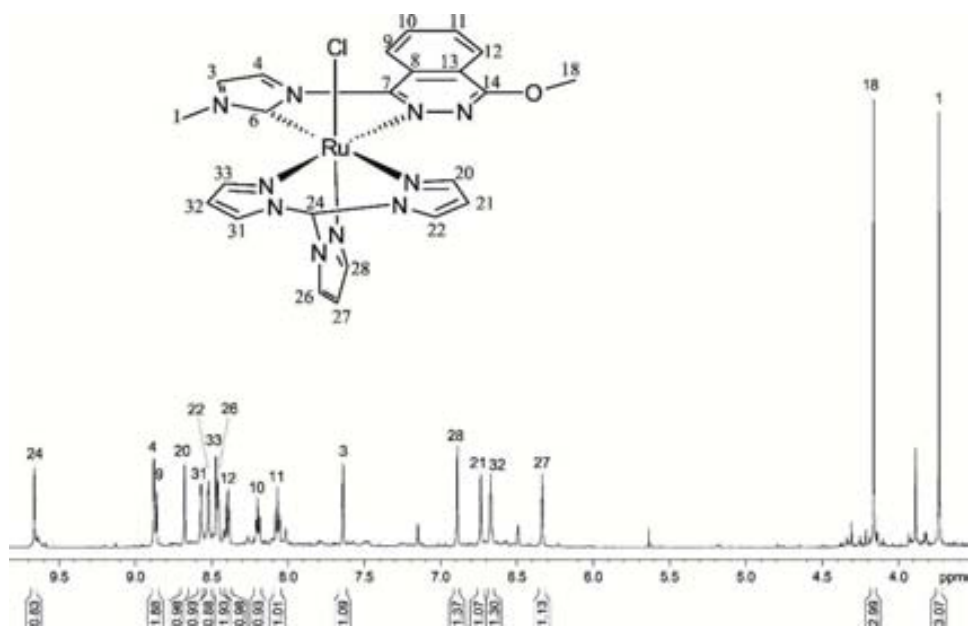
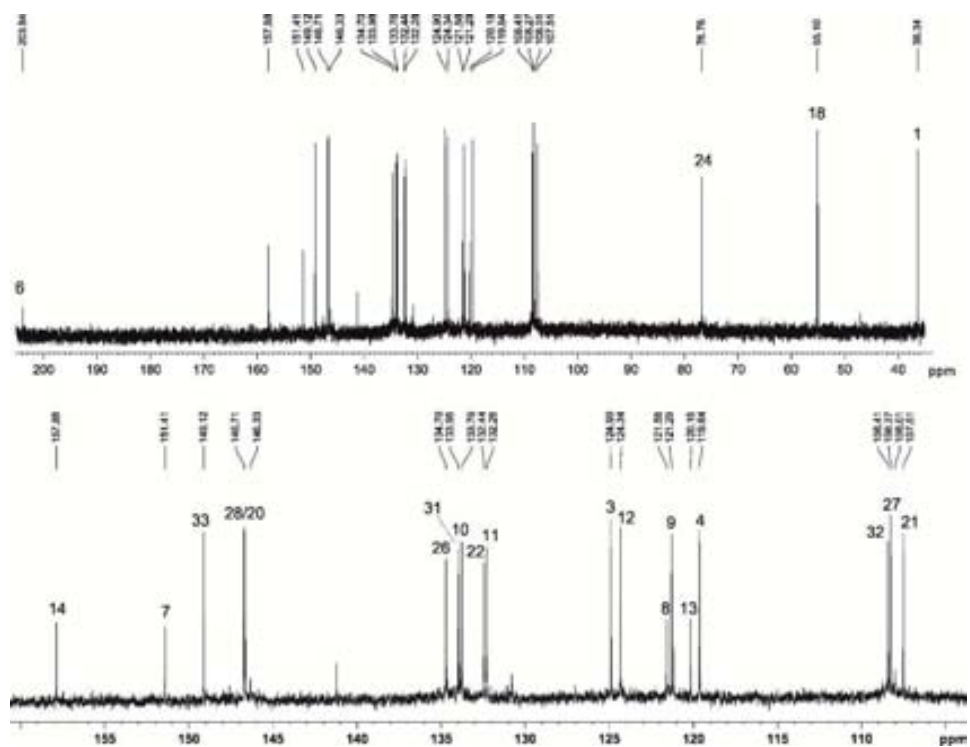


Figure S5. 1D and 2D NMR spectra of C3-Cl (600 MHz, 298K, acetone-d<sub>6</sub>): a) <sup>1</sup>H NMR, b) <sup>13</sup>C NMR, c) HSQC, d) HMBC, e) ROESY, f) TOSCY

a)

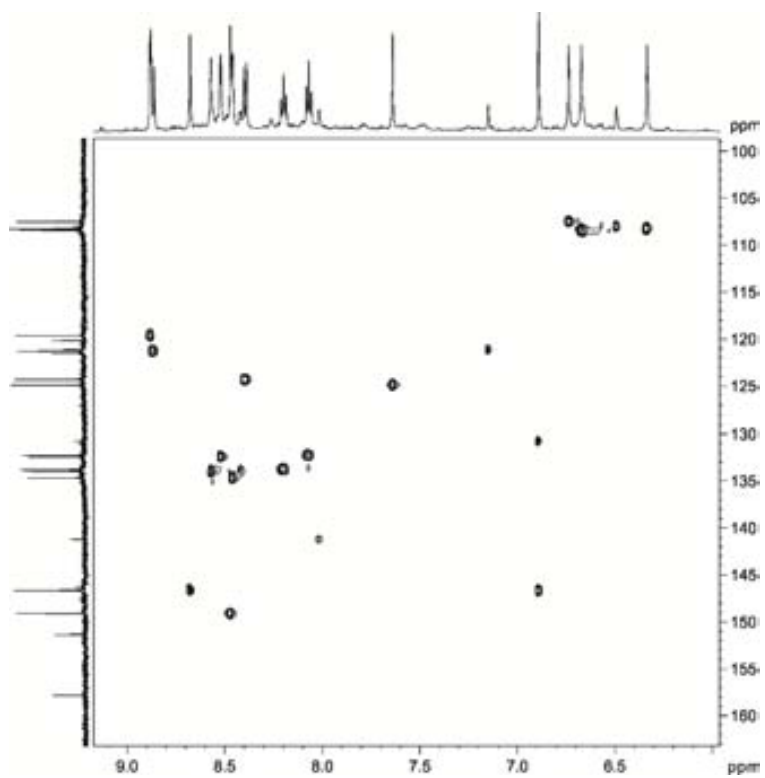


b)

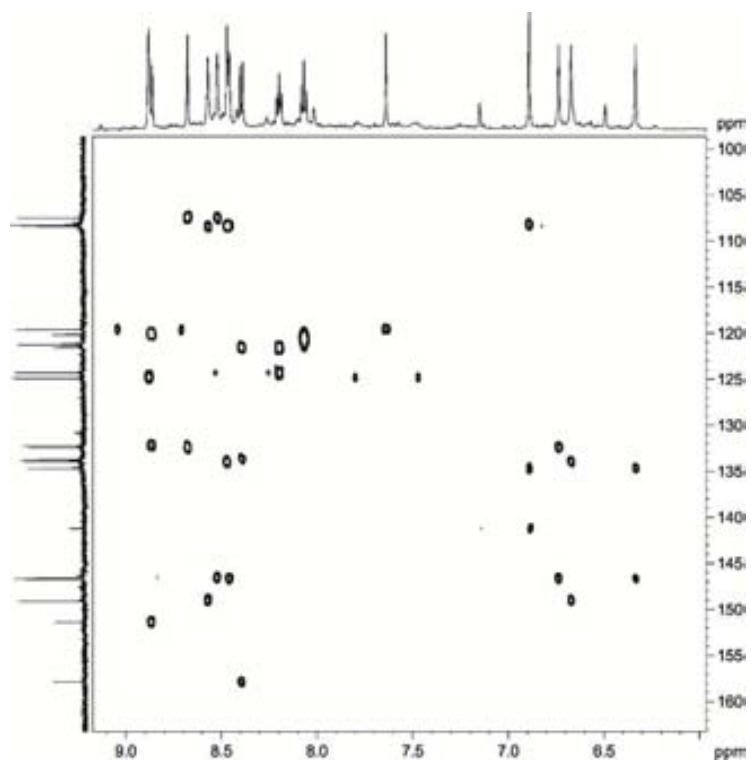




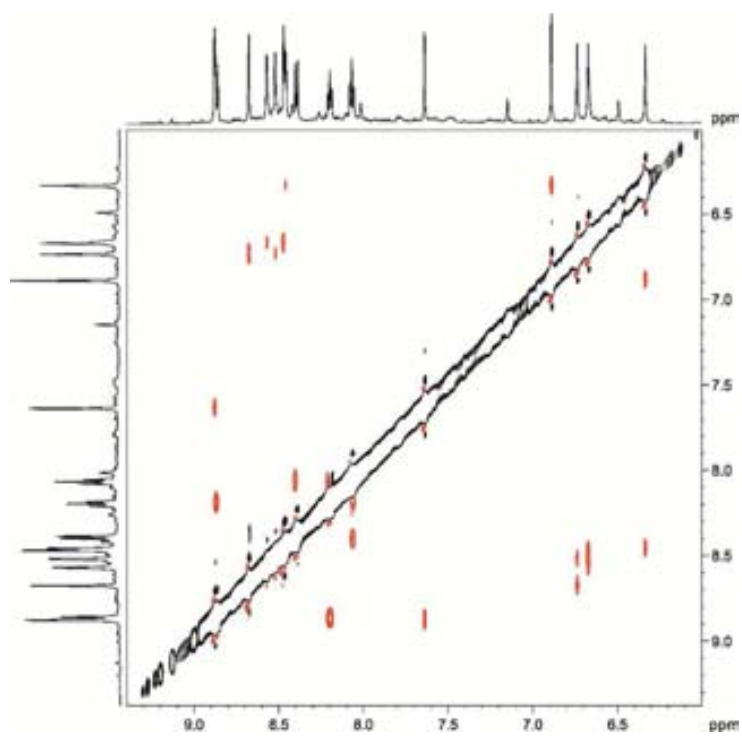
c)



d)



e)



f)

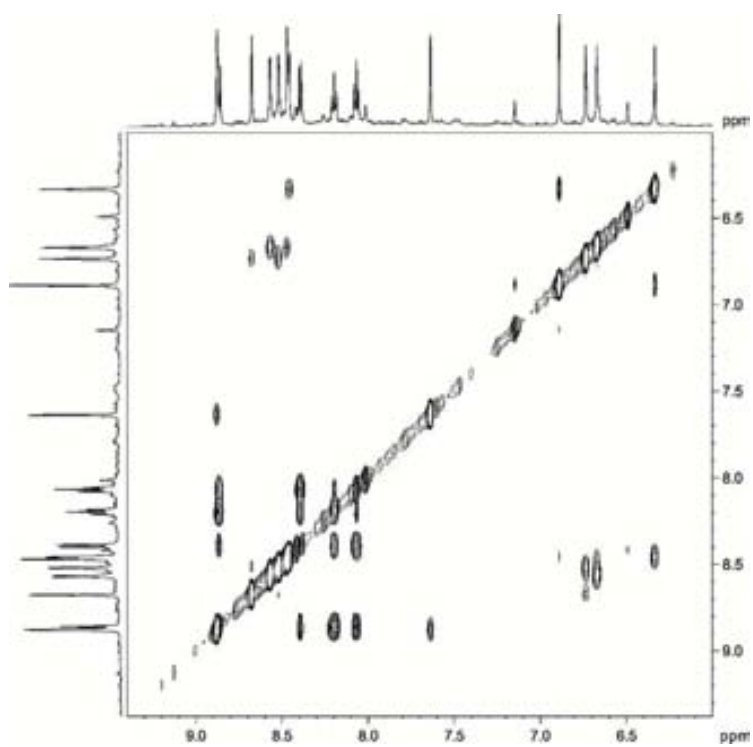
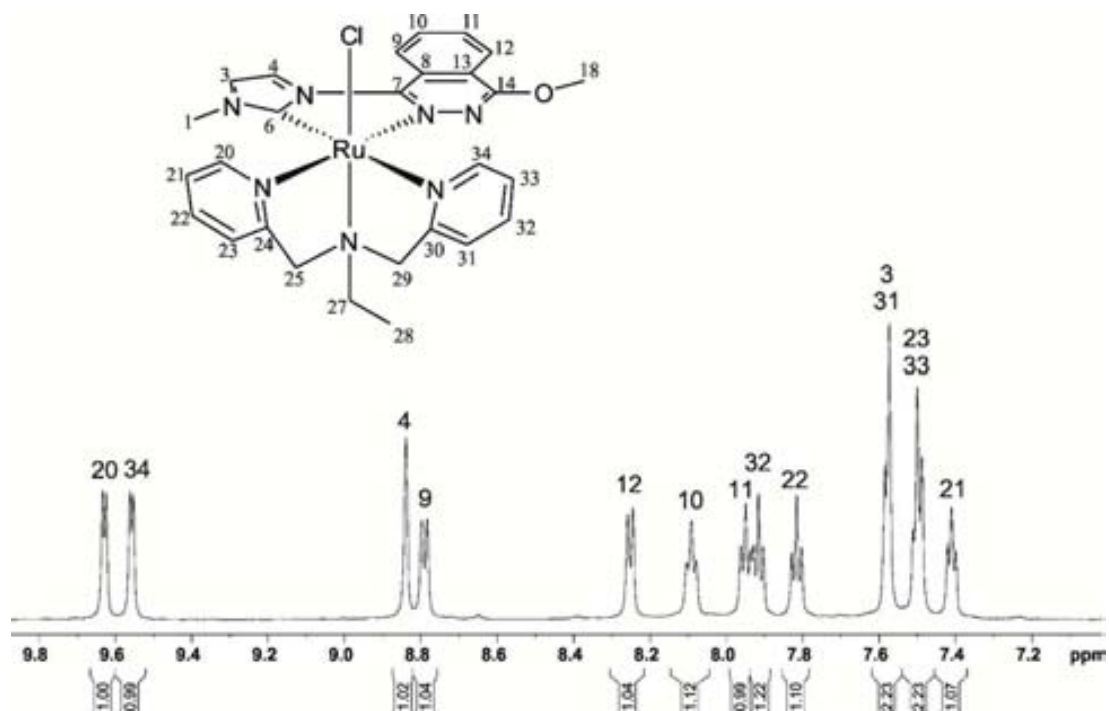
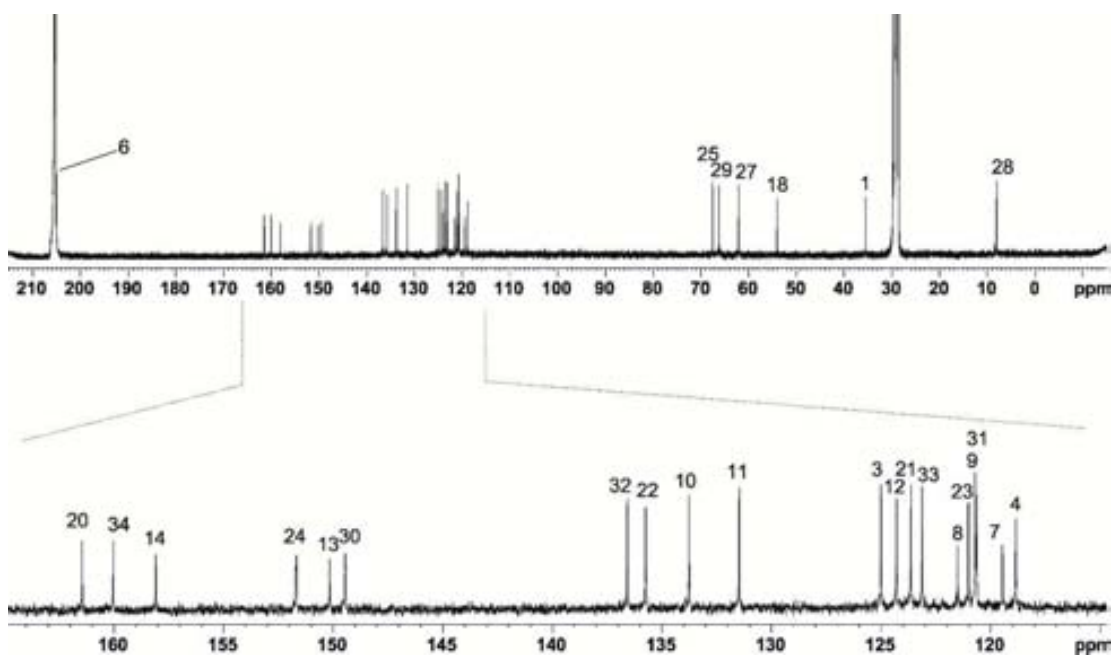


Figure S6. 1D and 2D NMR spectra of C4-Cl (600 MHz, 298K, acetone-d<sub>6</sub>): a) <sup>1</sup>H NMR, b) <sup>13</sup>C NMR, c) HSQC, d) ROESY, e) 1D selective NOESY

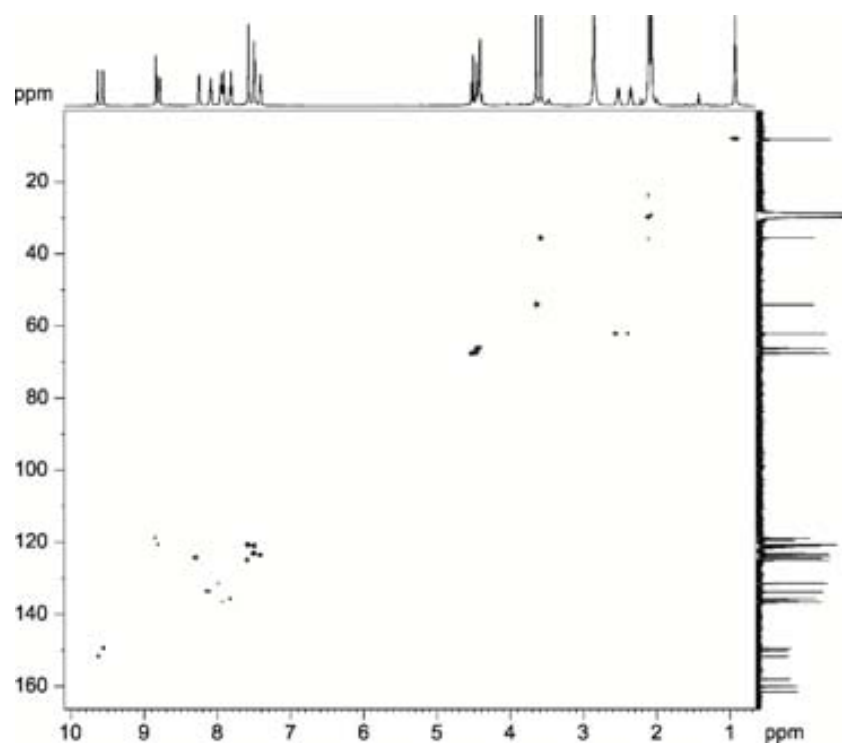
a)



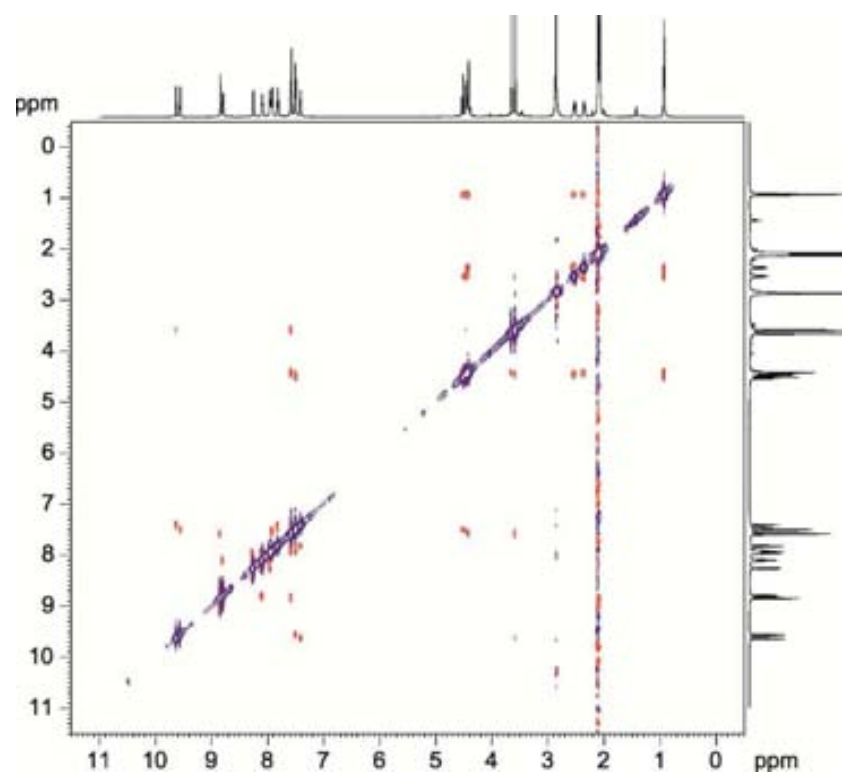
b)



c)



d)



e)

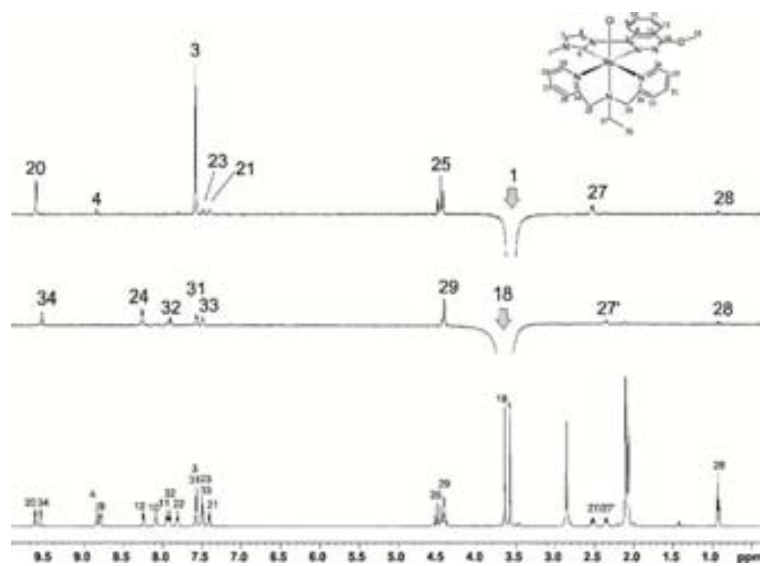
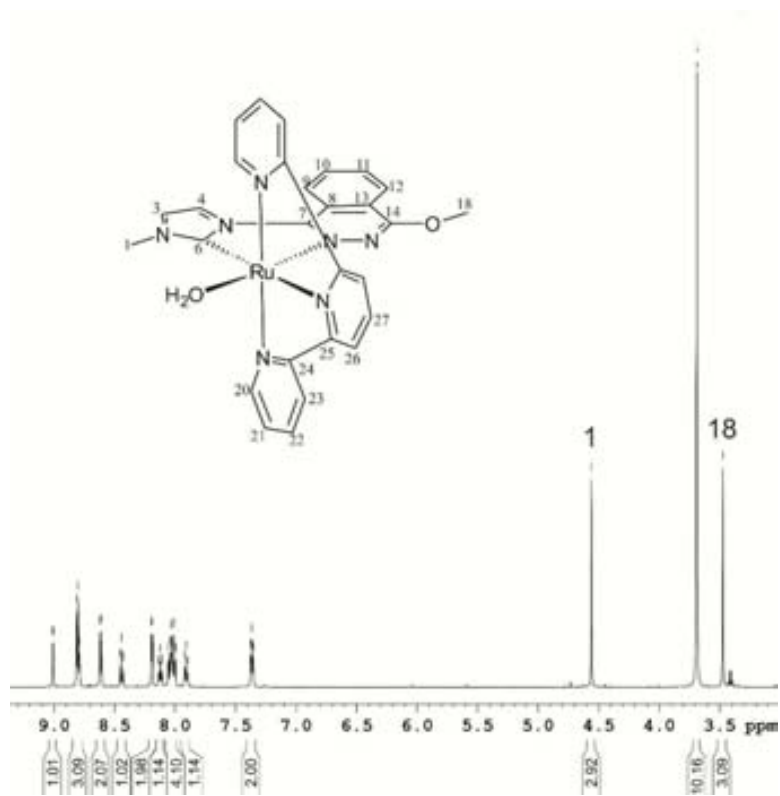
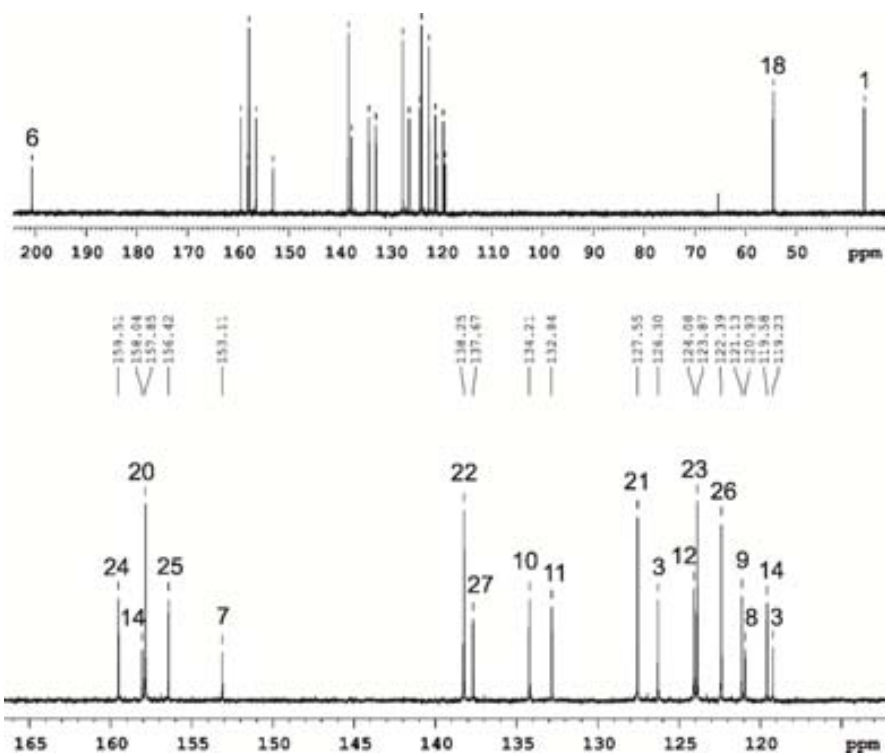


Figure S7. 1D and 2D NMR spectra of C1-OH<sub>2</sub> (600 MHz, 298K, acetone-d<sub>6</sub>): a) <sup>1</sup>H NMR, b) <sup>13</sup>C NMR, c) HSQC, d) HMBC

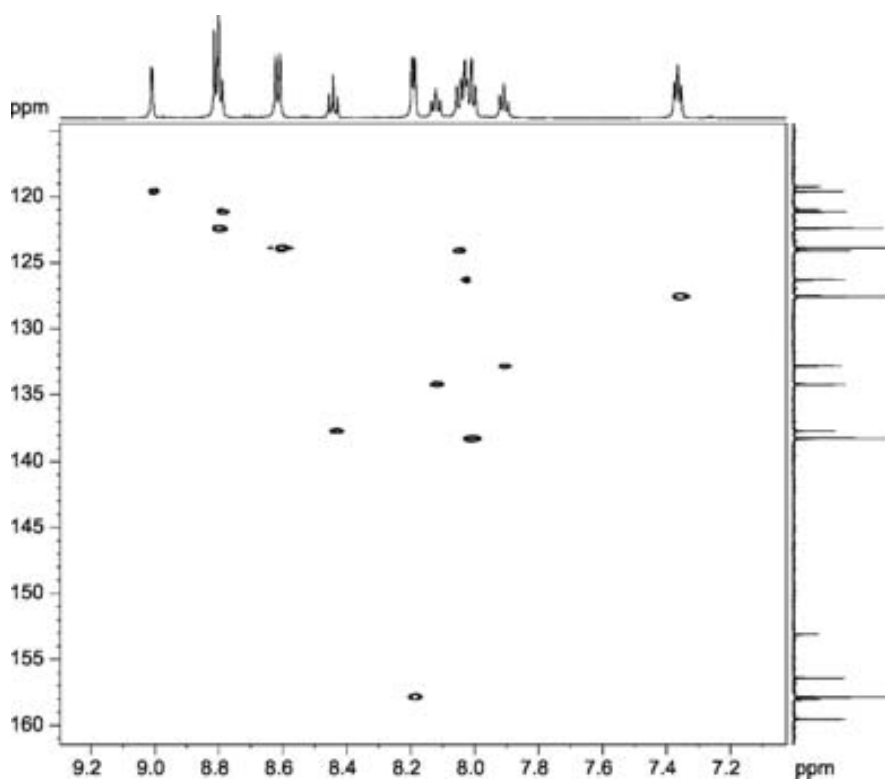
a)



b)



c)



d)

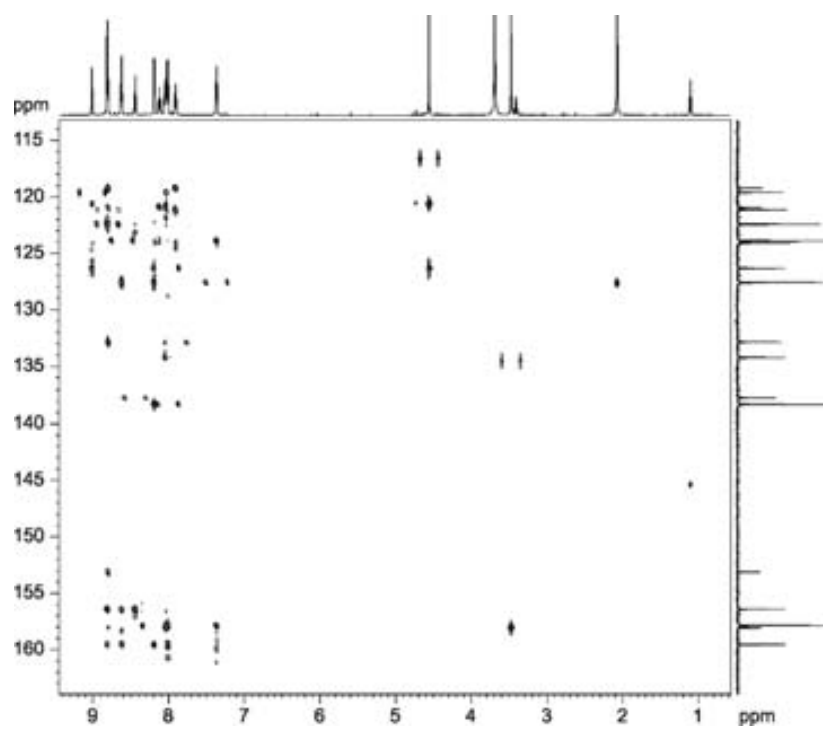
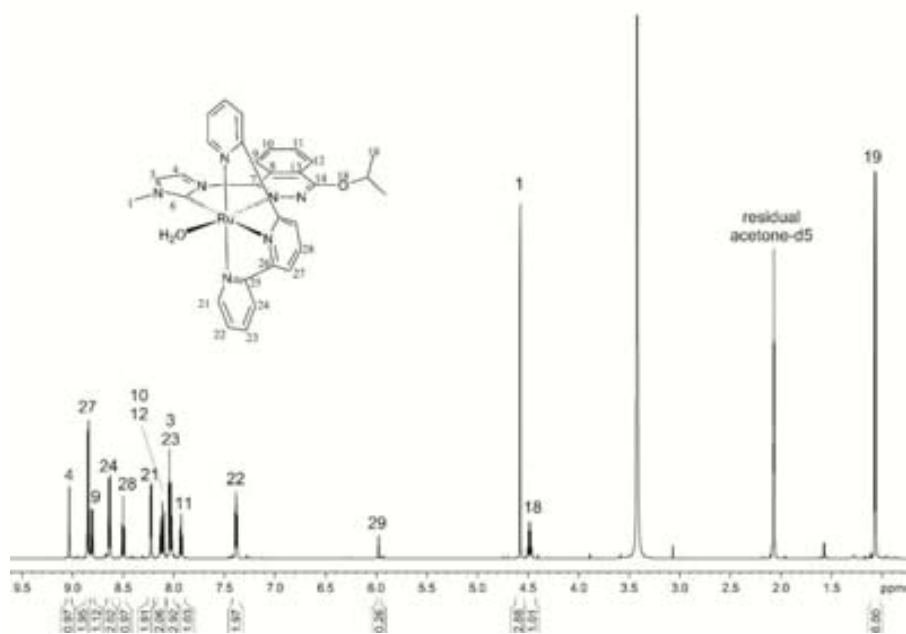
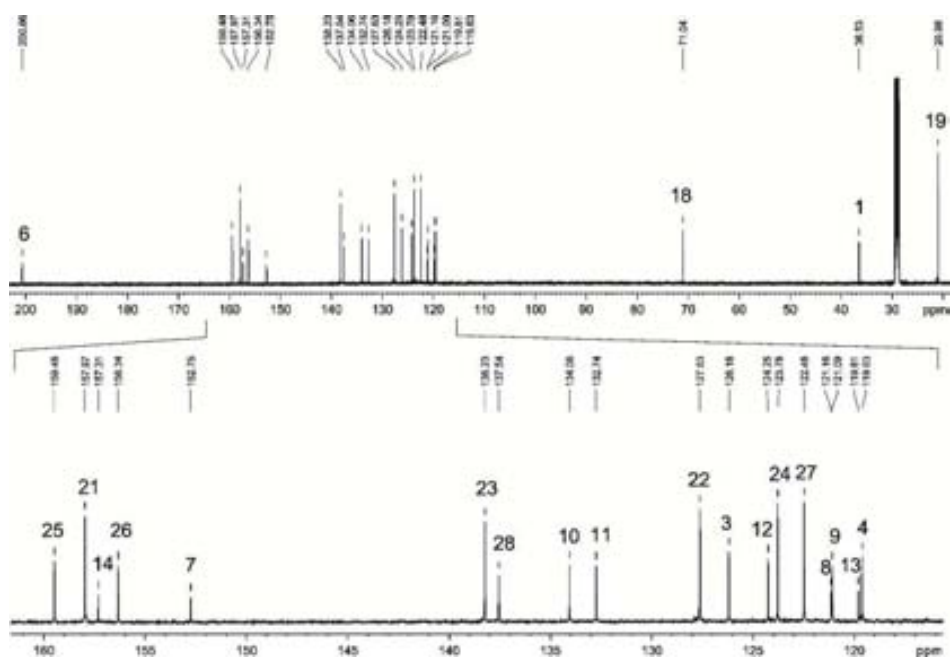


Figure S8. 1D and 2D NMR spectra of C2-OH<sub>2</sub> (600 MHz, 298K, acetone-d<sub>6</sub>): a) <sup>1</sup>H NMR, b) <sup>13</sup>C NMR, c) HSQC, d) HMBC, e) ROESY, f) TOCSY

a)

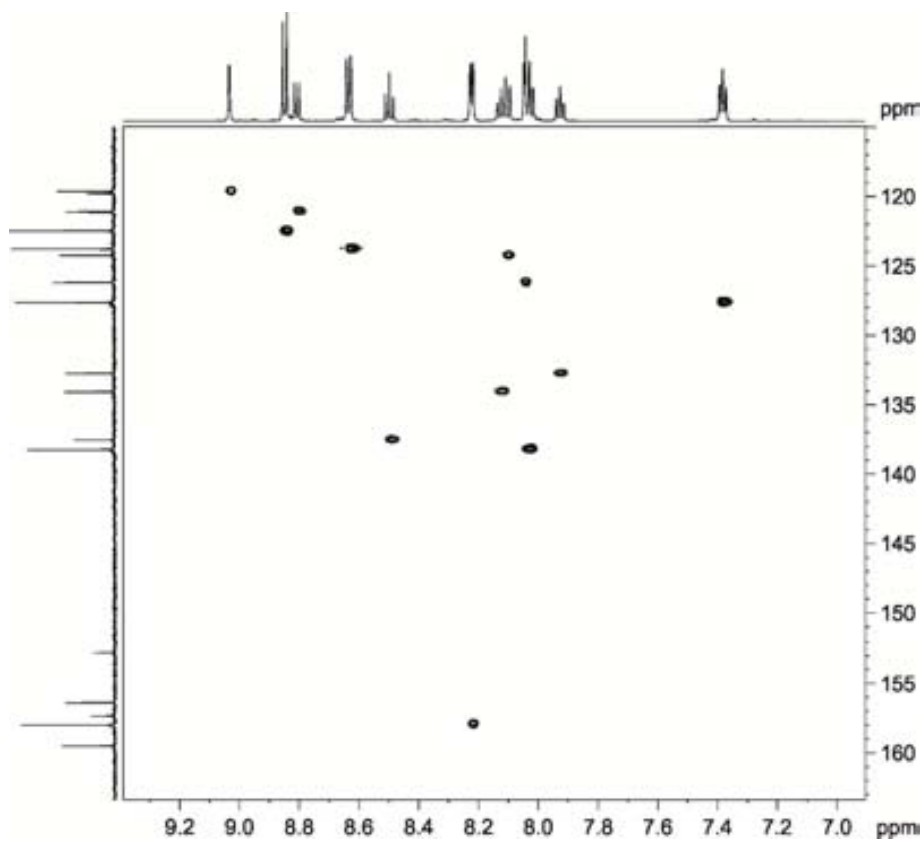


b)

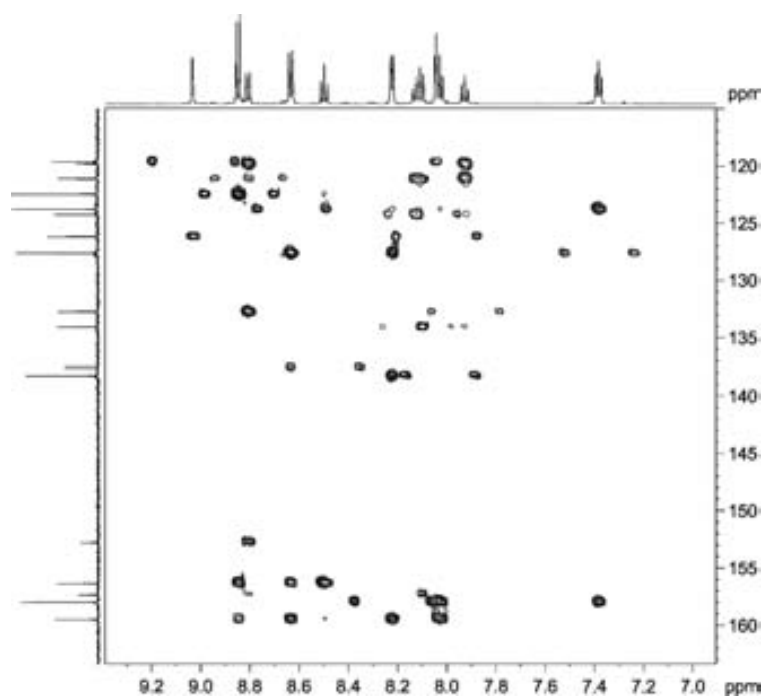




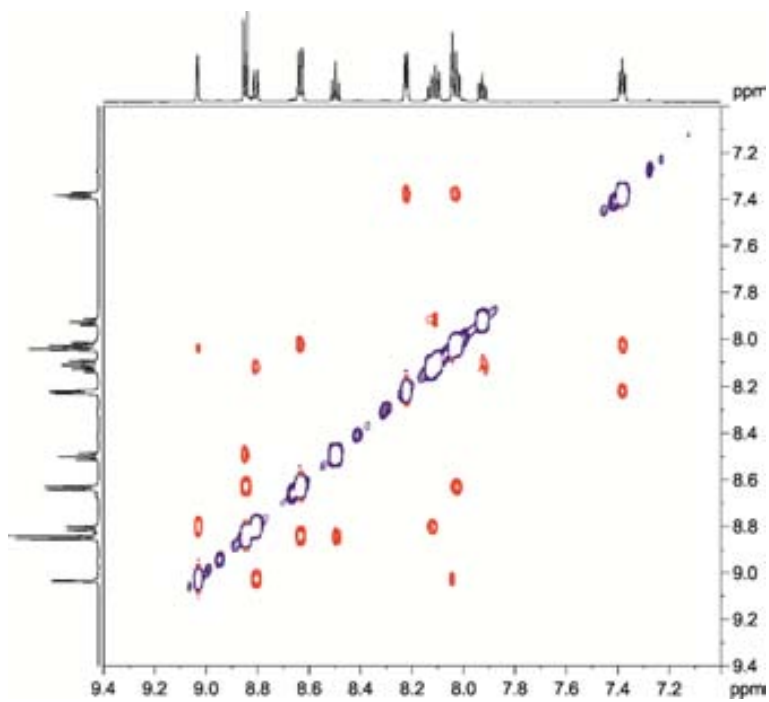
c)



d)



e)



f)

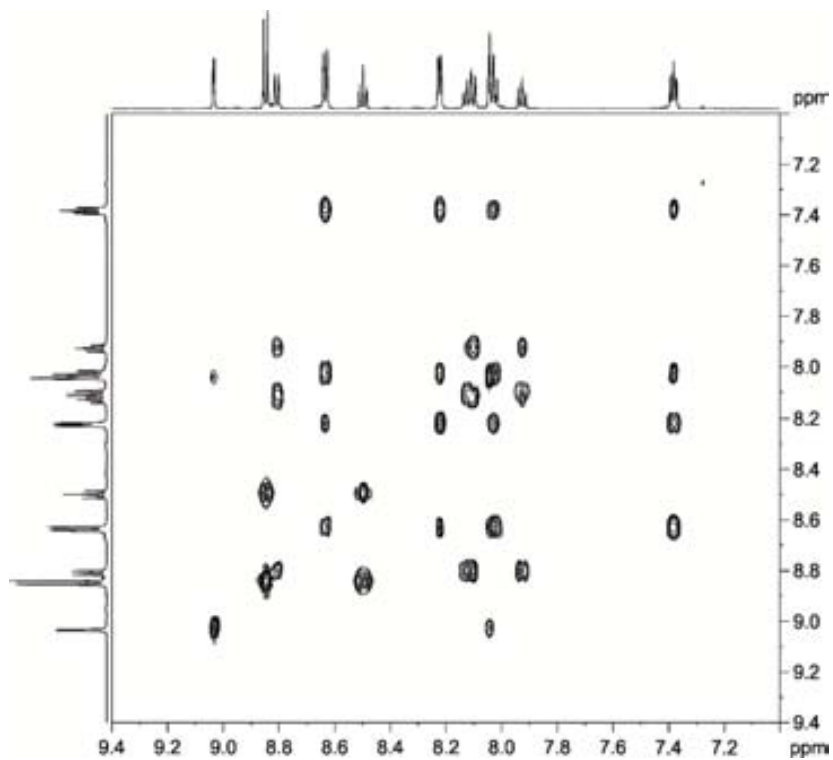
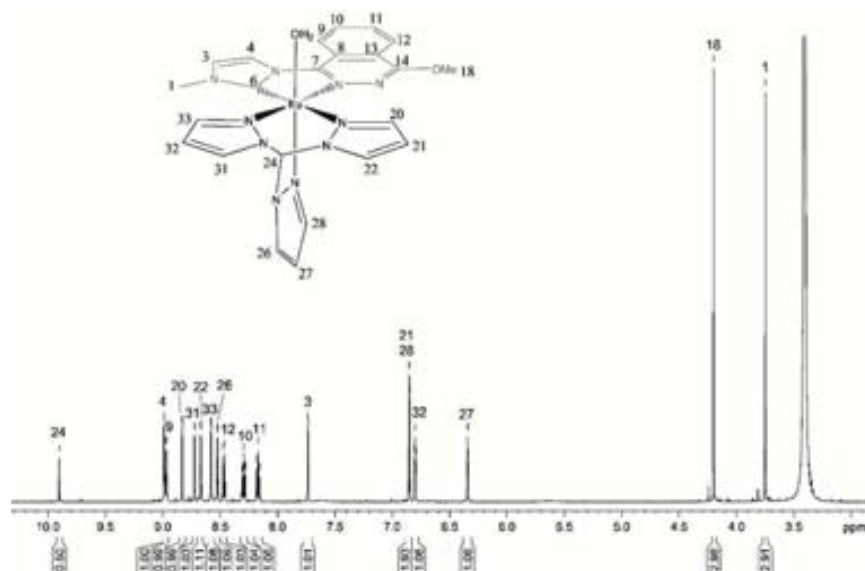
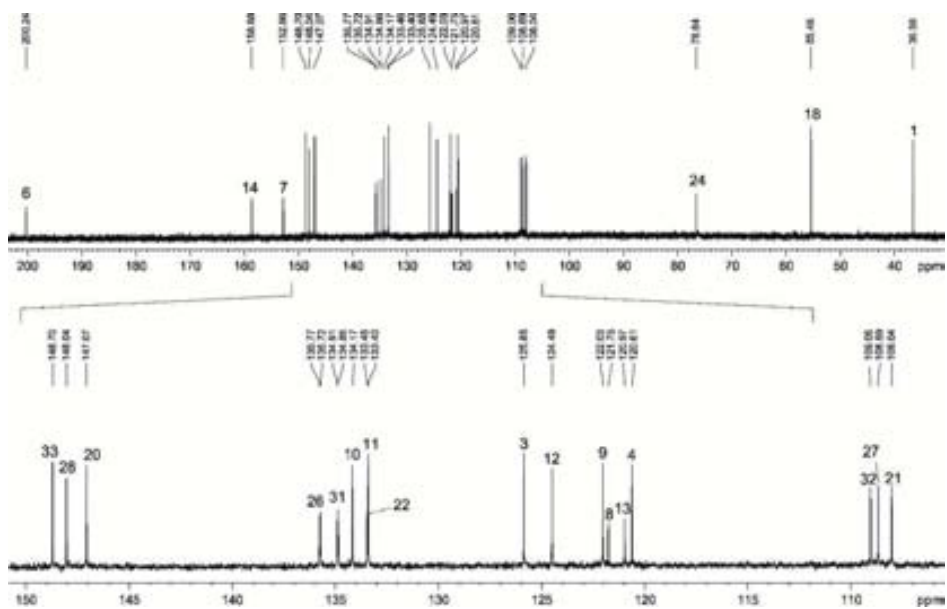


Figure S9. 1D and 2D NMR spectra of C3-OH<sub>2</sub> (600 MHz, 298K, acetone-d<sub>6</sub>): a) <sup>1</sup>H NMR, b) <sup>13</sup>C NMR, c) HSQC, d) HMBC, e) TOCSY

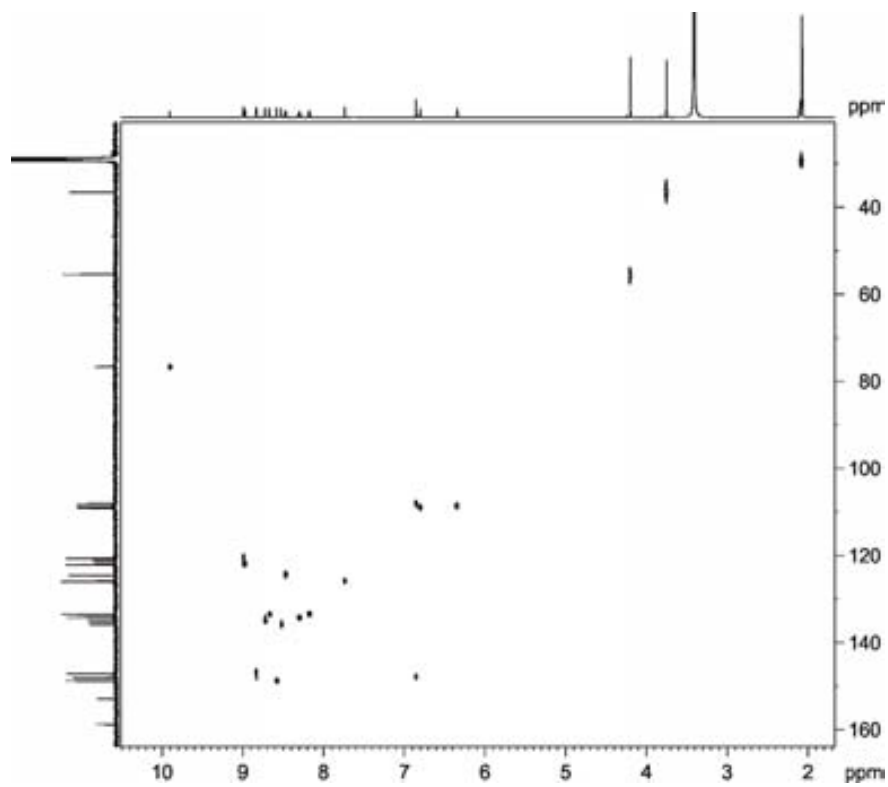
a)



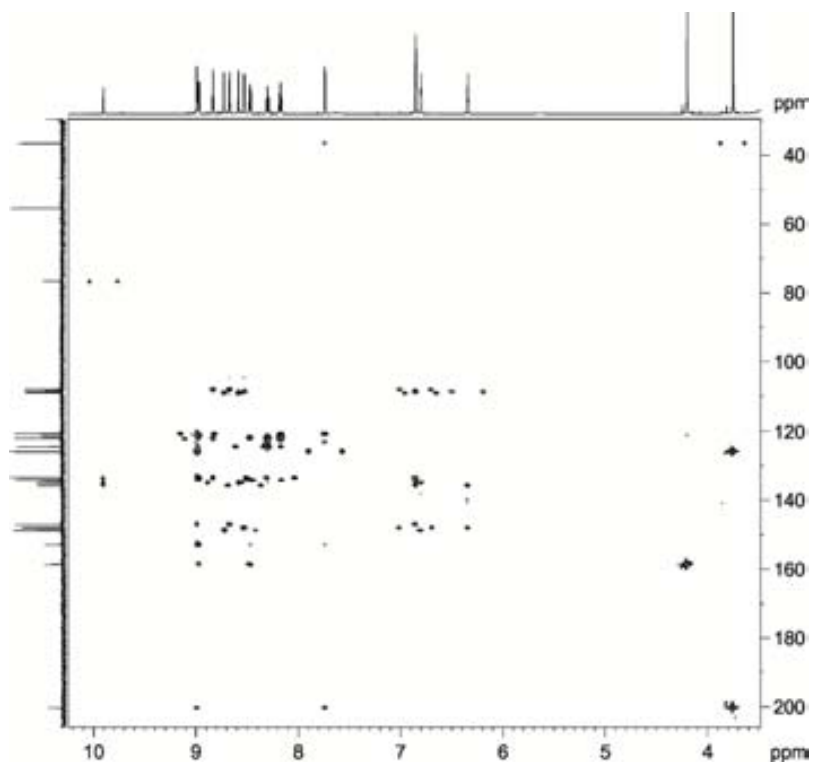
b)



c)



d)



e)

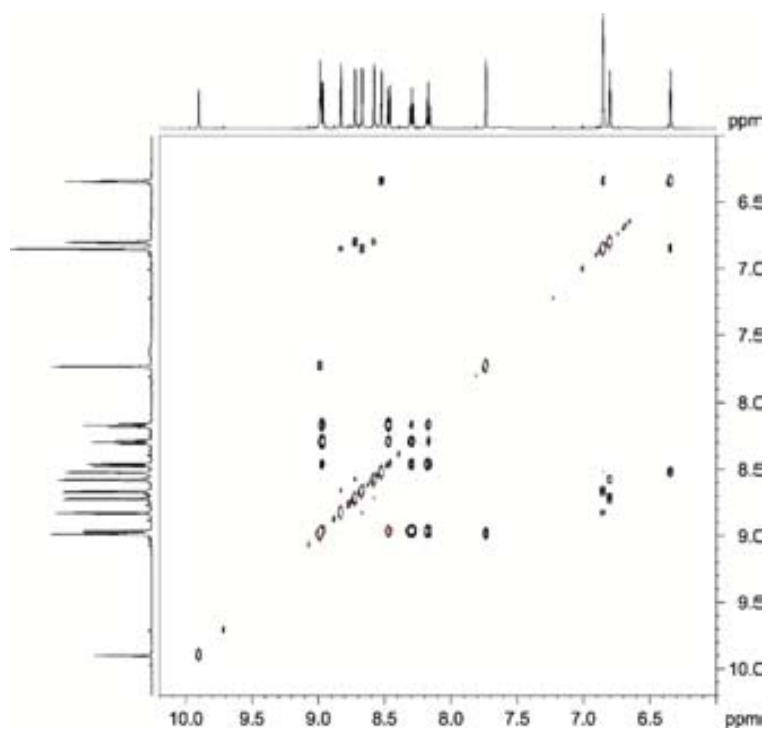
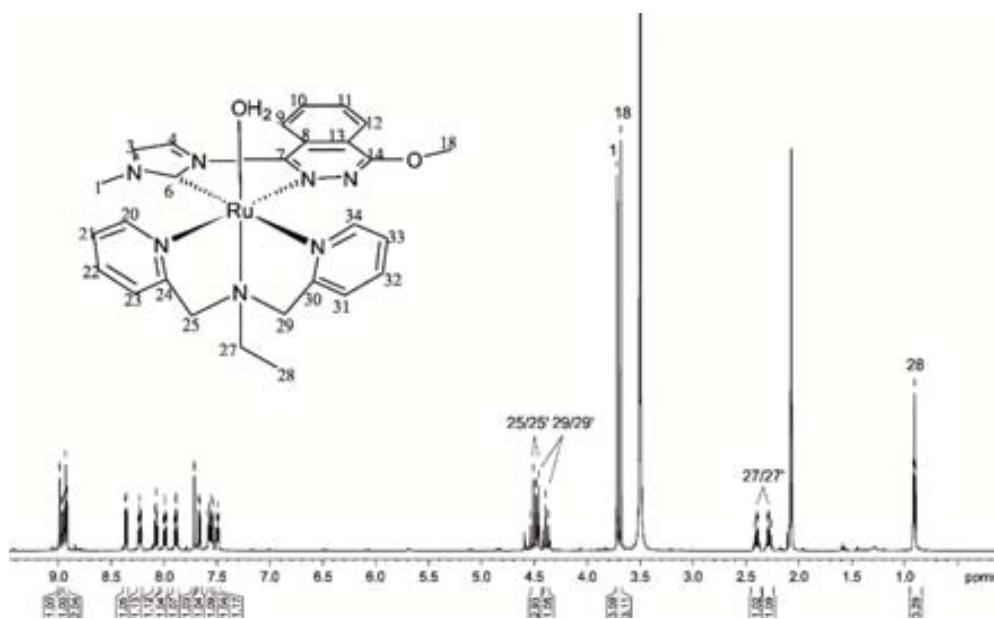
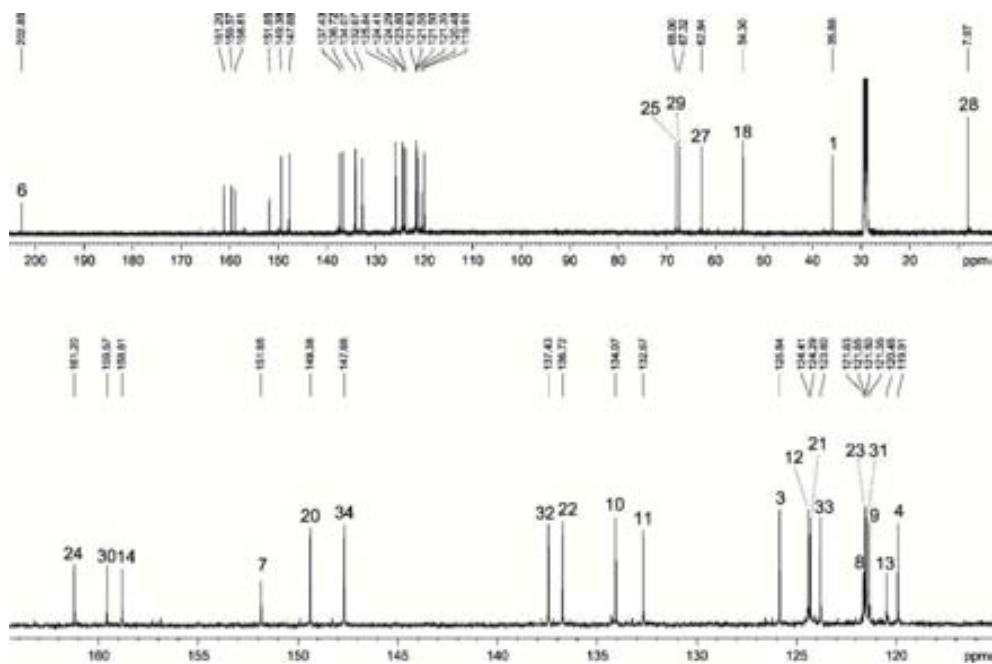


Figure S10. 1D and 2D NMR spectra of C4-OH<sub>2</sub> (600 MHz, 298K, acetone-d<sub>6</sub>): a) <sup>1</sup>H NMR, b) <sup>13</sup>C NMR, c) HSQC, d) HMBC, e) ROESY

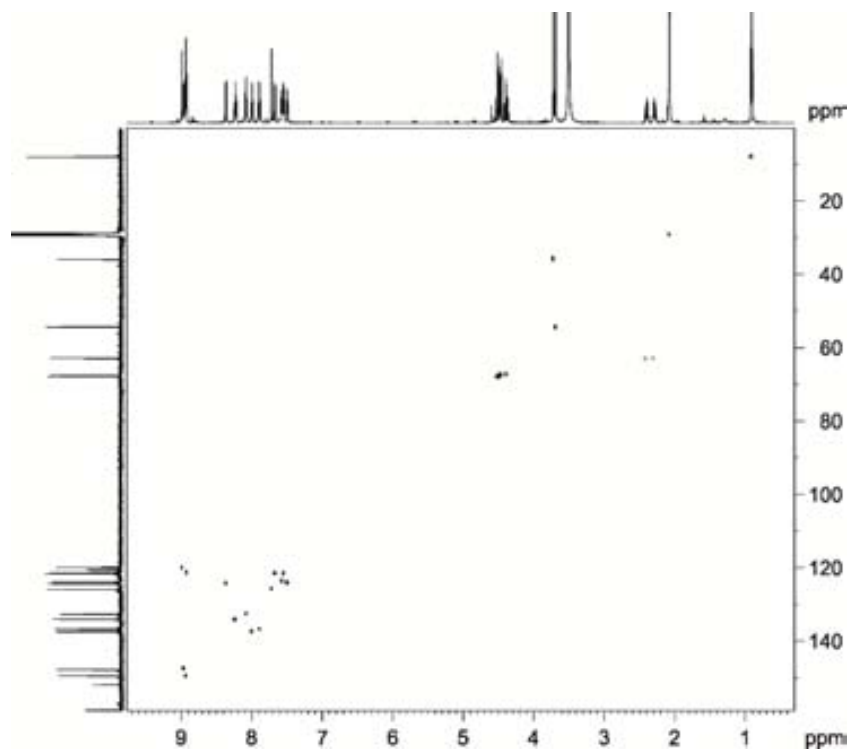
a)



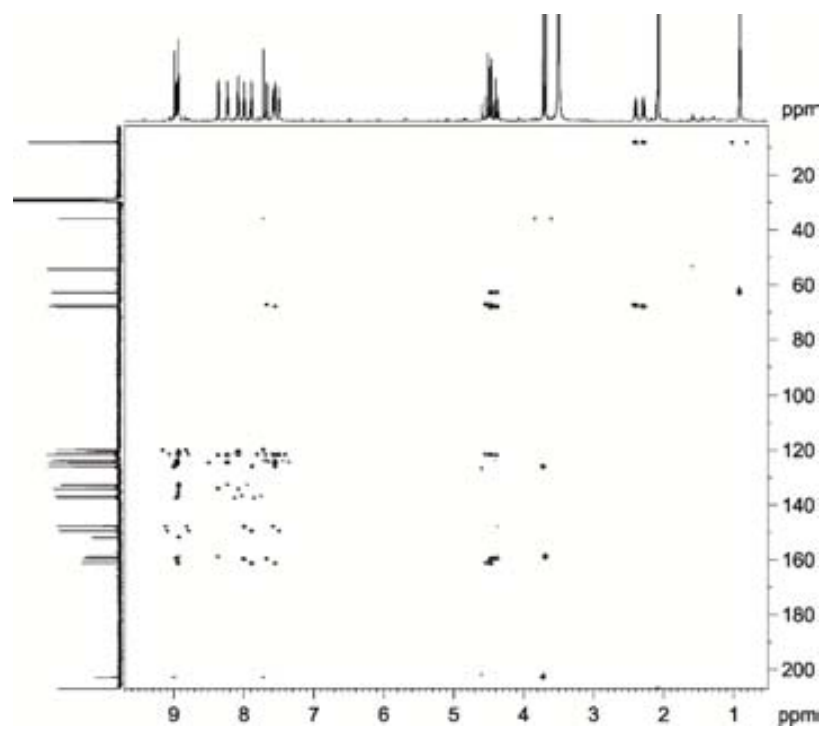
b)



c)



d)



e)

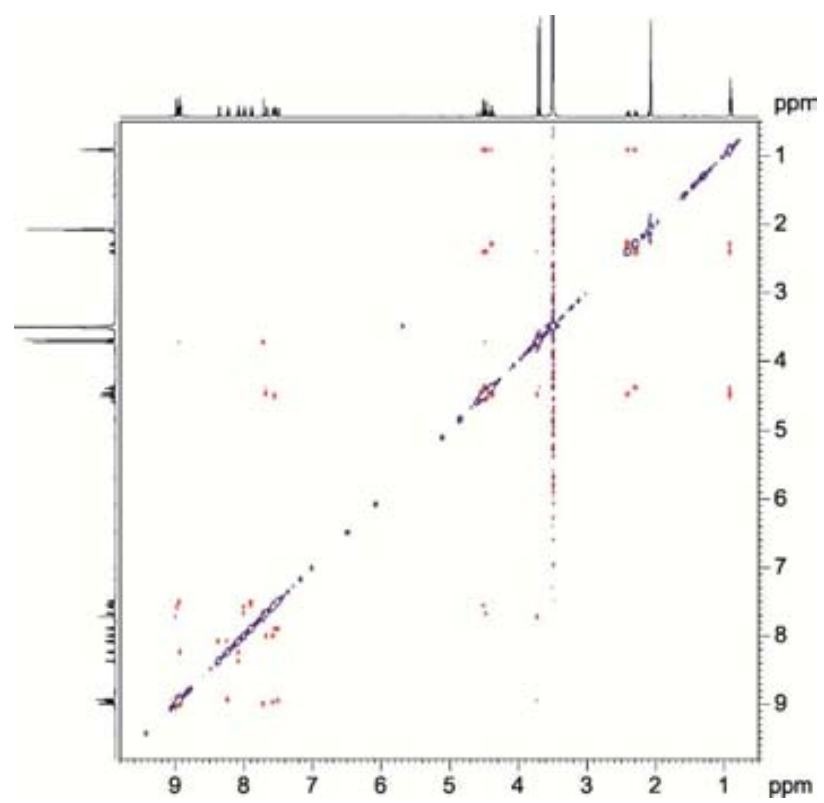
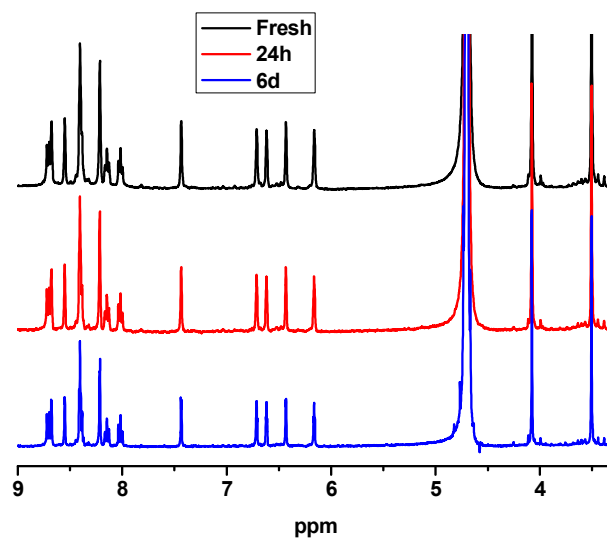


Figure S11.  $^1\text{H}$  NMR of complexes **C3-OH<sub>2</sub>** (a) and **C4-OH<sub>2</sub>** (b) freshly made, after 24 hours and after 6 days.

(a)



(b)

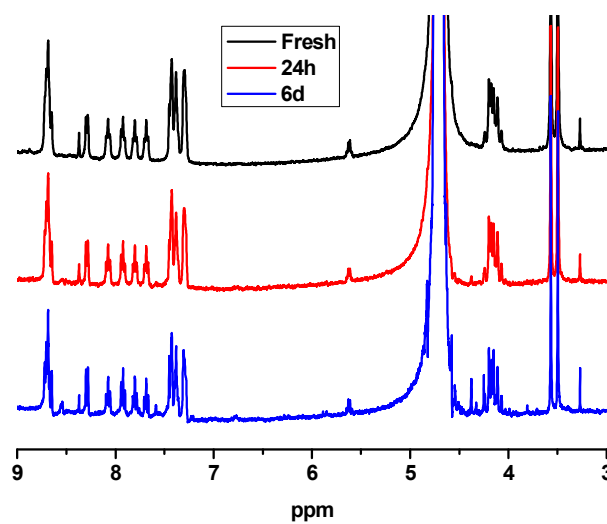




Table S2. Crystallographic data for C4-Cl.

Identification code	mo_HJCA4_0m	
Empirical formula	C <sub>27</sub> H <sub>29</sub> Cl F <sub>6</sub> N <sub>7</sub> O P Ru	
Formula weight	749.06	
Temperature	100(2) K	
Wavelength	0.71073 Å	
Crystal system	Triclinic	
Space group	P-1	
Unit cell dimensions	a = 7.8526(10)Å	α = 75.184(4)°.
	b = 12.5701(14)Å	β = 79.085(4)°.
	c = 16.1322(19)Å	γ = 77.741(4)°.
Volume	1488.9(3) Å <sup>3</sup>	
Z	2	
Density (calculated)	1.671 Mg/m <sup>3</sup>	
Absorption coefficient	0.744 mm <sup>-1</sup>	
F(000)	756	
Crystal size	0.15 x 0.05 x 0.03 mm <sup>3</sup>	
Theta range for data collection	1.701 to 25.968°.	
Index ranges	-9 ≤ h ≤ 9, -10 ≤ k ≤ 15, -19 ≤ l ≤ 19	
Reflections collected	18296	
Independent reflections	5655 [R(int) = 0.0588]	
Completeness to theta = 25.968°	97.00%	
Absorption correction	Empirical	
Max. and min. transmission	0.978 and 0.878	
Refinement method	Full-matrix least-squares on F <sup>2</sup>	
Data / restraints / parameters	5655 / 0 / 400	
Goodness-of-fit on F <sup>2</sup>	1.038	
Final R indices [I > 2σ(I)]	R <sub>1</sub> = 0.0493, wR <sub>2</sub> = 0.1162	

R indices (all data)

R1 = 0.0741, wR2 = 0.1293

Largest diff. peak and hole

1.123 and -0.578 e.Å-3

Figure S12. CV of C1-OH<sub>2</sub> in water pH=1 (triflic acid buffer) and pH=8 (phosphates buffer) at 100 mV/s scan rate. Glassy carbon is used as working electrode and the potential is measured vs.

SSCE.

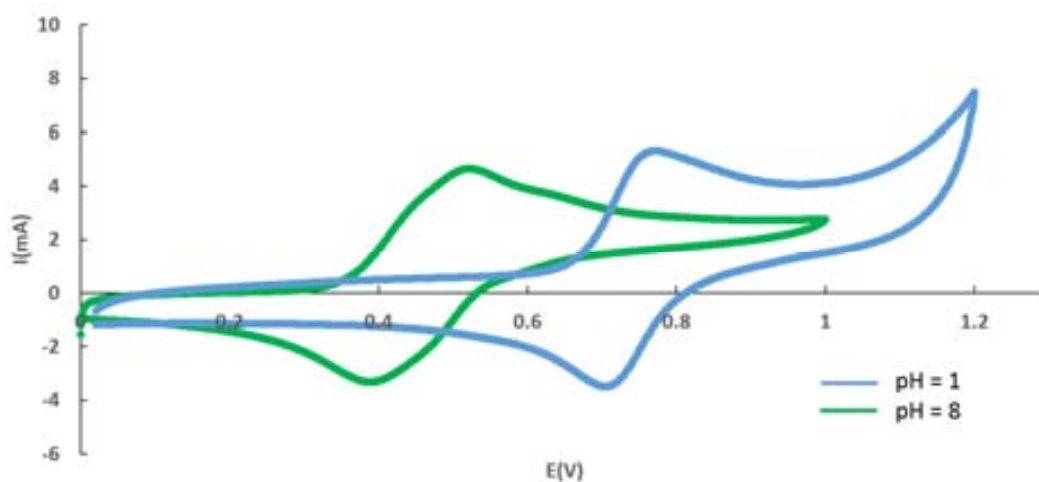


Figure S13. DPV of C1-OH<sub>2</sub> in water pH=1 (triflic acid buffer) and pH=8 (phosphates buffer) at 20 mV/s scan rate. Glassy carbon is used as working electrode and the potential is measured vs.

SSCE.

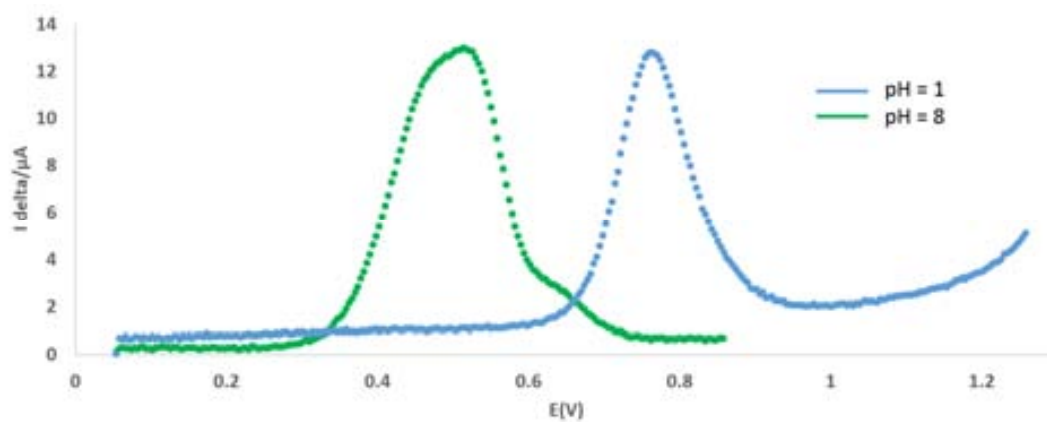


Figure S14. A plot of  $E_{1/2}$  vs. pH (Pourbaix Diagram) for complex C1-OH<sub>2</sub>. The pH/potential regions of stability for the various oxidation states and their dominant proton compositions are indicated by using abbreviations such as Ru<sup>III</sup>-OH<sub>2</sub>, for example, for [Ru<sup>II</sup>(CN-OMe)OH<sub>2</sub>(trpy)]<sup>2+</sup>.

The vertical solid lines in the various E/pH regions show the pKa values.

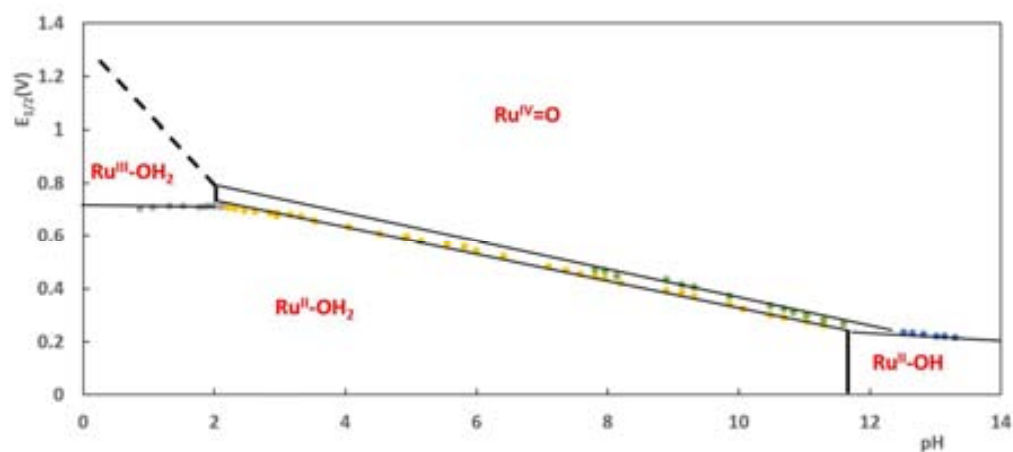
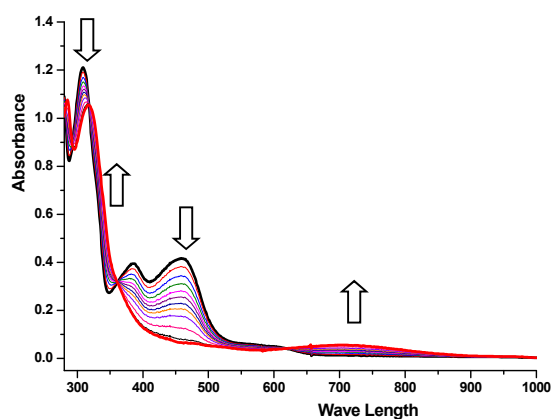


Figure S15. Spectrophotometric titration with Ce<sup>IV</sup> for C2-OH<sub>2</sub> (a) and C3-OH<sub>2</sub> (b) in pH=1 water solution. Two equivalents of Ce<sup>IV</sup> were added.

a)



b)

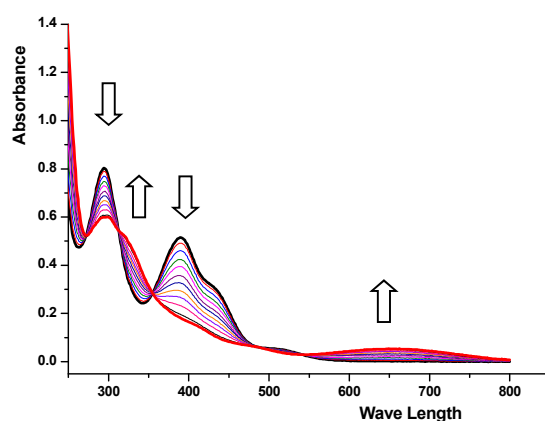
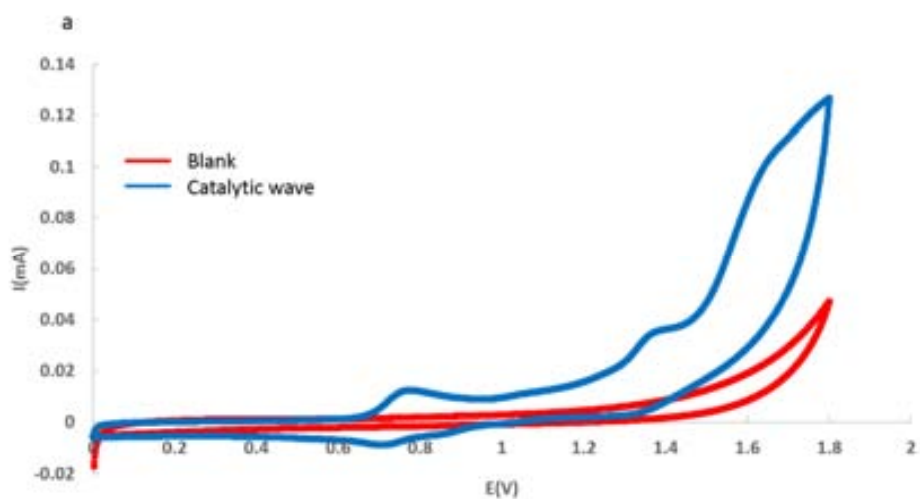
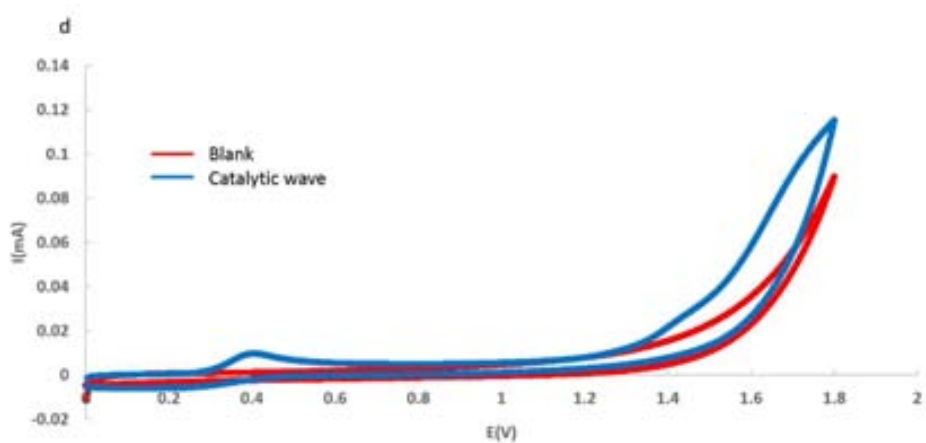
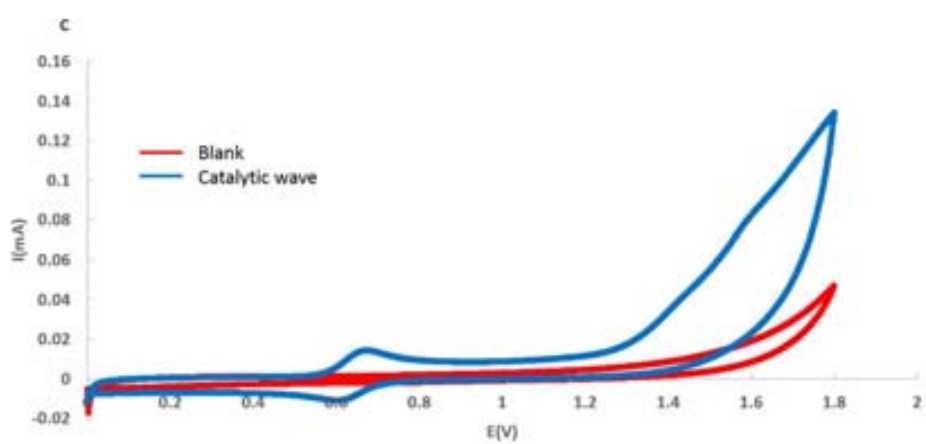
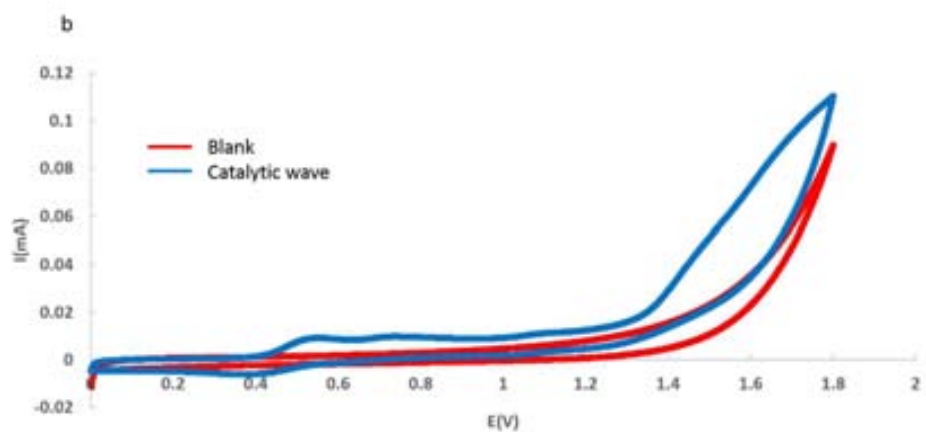


Figure S16. CV of the four complexes at different pH values. a) **C1-OH<sub>2</sub>** in a pH=1 solution, b) **C1-OH<sub>2</sub>** in pH=7 solution, c) **C3-OH<sub>2</sub>** in a pH=1 solution, d) **C3-OH<sub>2</sub>** in a pH=7 solution, e) **C4-OH<sub>2</sub>** in a pH=1 solution, f) **C4-OH<sub>2</sub>** in a pH=7 solution.





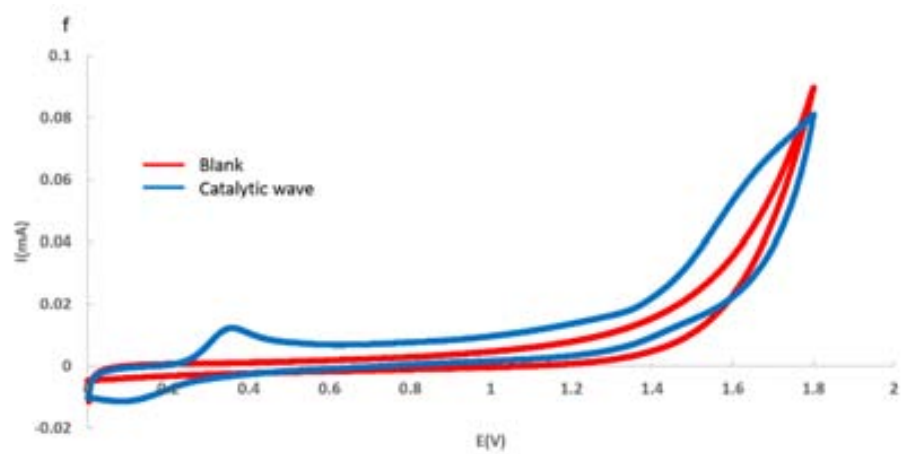
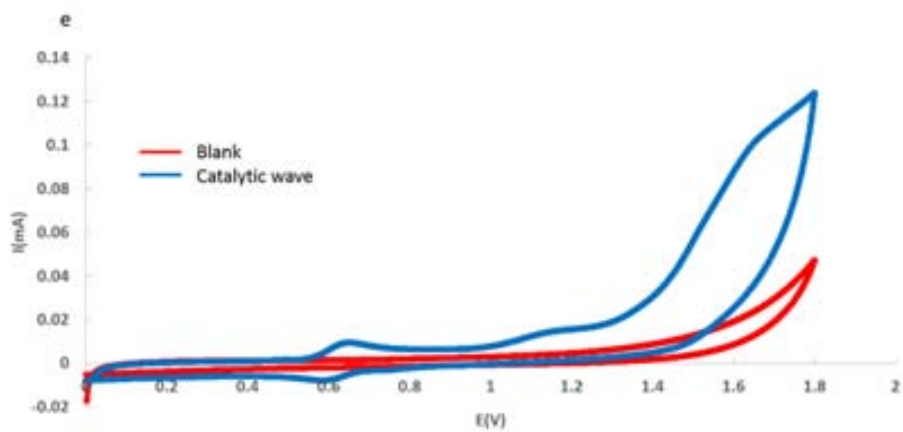


Figure S17. Successive cyclic voltammograms of 0.5mM solution of C3-OH<sub>2</sub> in DCM (0.1M TBAPF<sub>6</sub>) at increasing concentrations of *cis*- $\beta$ -methylstyrene. Working electrode: glassy carbon; counter electrode: Pt; reference electrode: Hg/Hg<sub>2</sub>SO<sub>4</sub>; scan rate: 100Mv. Starting at 0 V toward positive potential.

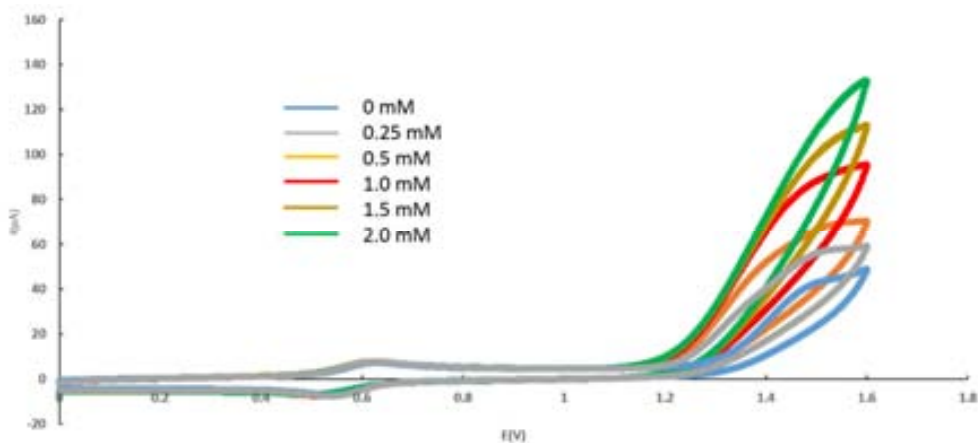


Figure S18. Dependence of  $i_{cat}$  vs. [sub]<sup>1/2</sup>. Experimental conditions: C3-OH<sub>2</sub> (0.5mM), [sub] = 0-2.0mM, DCM (0.1 M TBAPF<sub>6</sub>), working electrode: glassy carbon; counter electrode: Pt; reference electrode: Hg/Hg<sub>2</sub>SO<sub>4</sub>, scanning rate: 100mV/s.

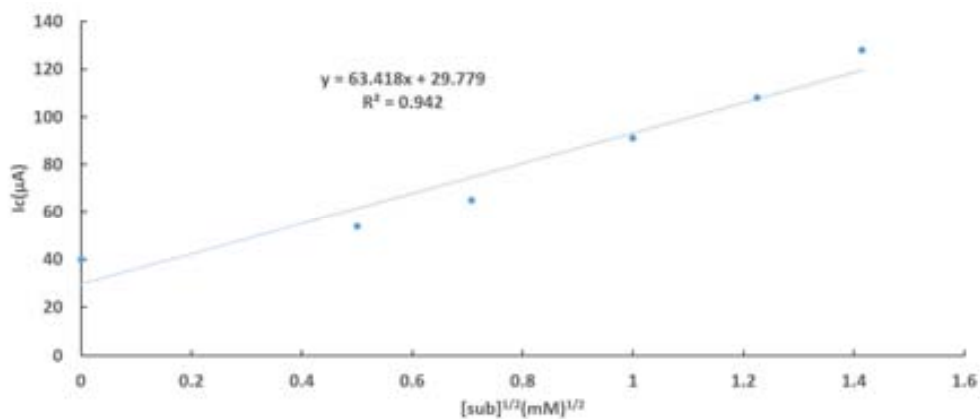


Figure S19. Dependence of  $i_p$  vs.  $v^{1/2}$ . Experimental conditions: C3-OH<sub>2</sub> (0.5mM)  $v = 20$ -200V/s, DCM (0.1 M TBAPF<sub>6</sub>), working electrode: glassy carbon; counter electrode: Pt; reference electrode: Hg/Hg<sub>2</sub>SO<sub>4</sub>.

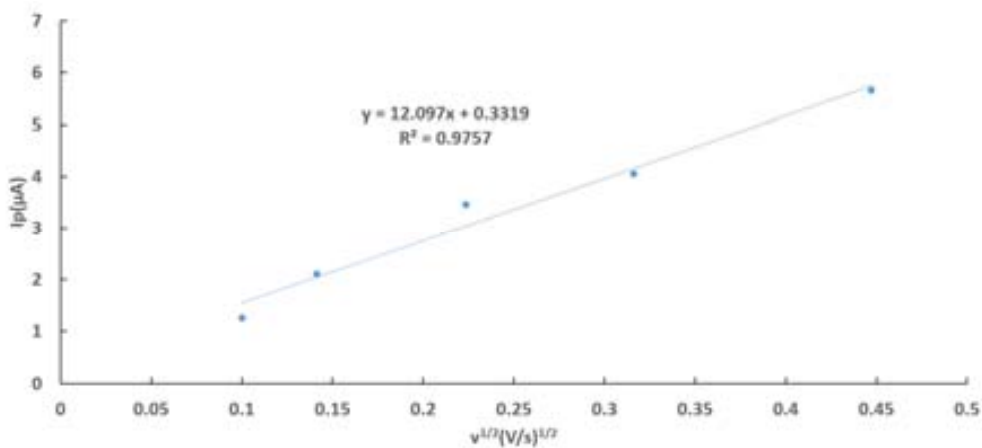


Figure S20. Successive cyclic voltammograms of 0.5mM solution of C4-OH<sub>2</sub> in DCM (0.1M TBAPF<sub>6</sub>) at increasing concentrations of *cis*- $\beta$ -methylstyrene. Working electrode: glassy carbon; counter electrode: Pt; reference electrode: Hg/Hg<sub>2</sub>SO<sub>4</sub>; scan rate: 100Mv. Starting at 0 V toward positive potential.

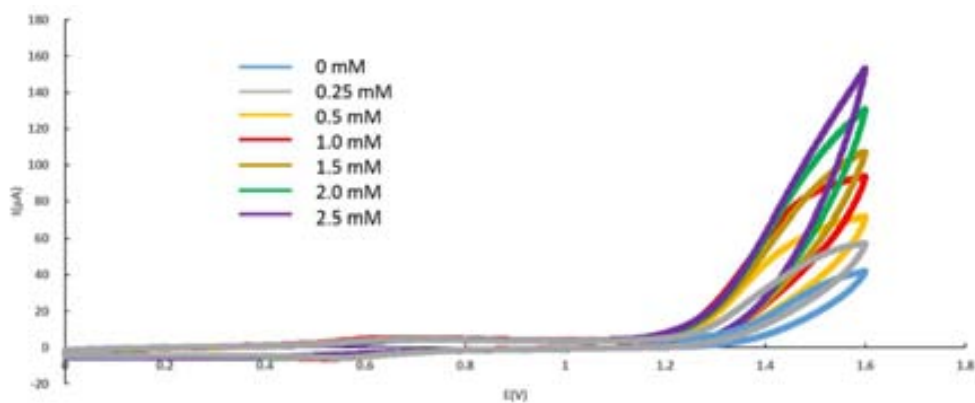




Figure S21. Dependence of  $i_{\text{cat}}$  vs.  $[\text{sub}]^{1/2}$ . Experimental conditions: **C4-OH<sub>2</sub>** (0.5mM),  $[\text{sub}] = 0$ -2.0mM, DCM (0.1 M TBAPF<sub>6</sub>), working electrode: glassy carbon; counter electrode: Pt; reference electrode: Hg/Hg<sub>2</sub>SO<sub>4</sub>, scanning rate: 100mV/s.

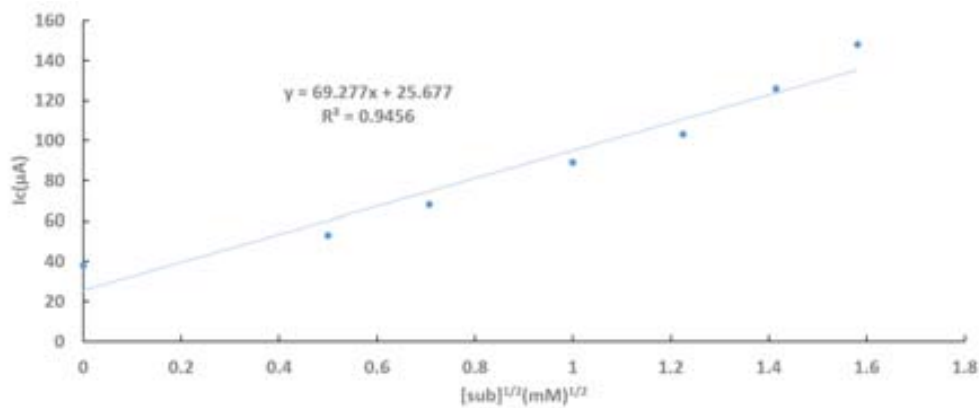
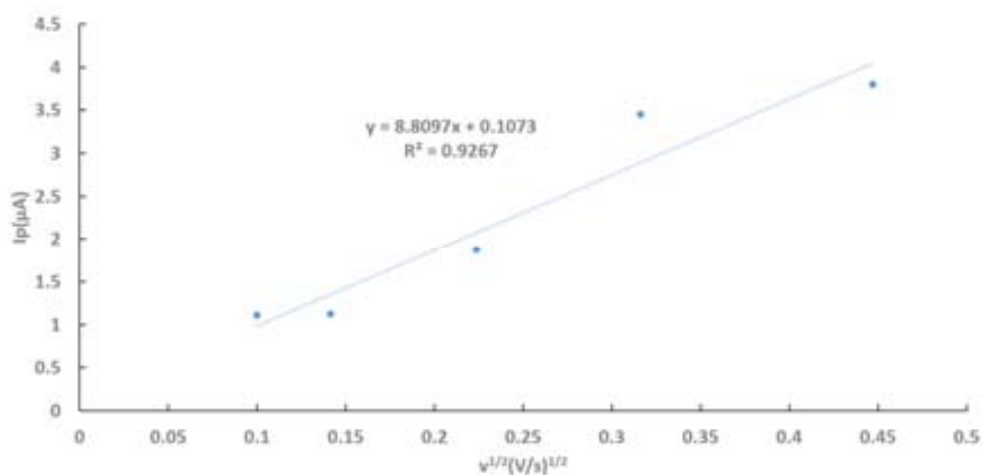


Figure S22. Dependence of  $i_p$  vs.  $v^{1/2}$ . Experimental conditions: **C4-OH<sub>2</sub>** (0.5mM)  $v = 20$ -200V/s, DCM (0.1 M TBAPF<sub>6</sub>), working electrode: glassy carbon; counter electrode: Pt; reference electrode: Hg/Hg<sub>2</sub>SO<sub>4</sub>.



## Chapter IV.

# Enantioselective Alkene Epoxidation Catalyzed by Ru Carbene Chiral Polypyridyl Complexes

### IV.1. Introduction

As highly versatile organic intermediates, chiral epoxides occupy a central position in the synthesis of enantiopure compounds, useful molecules for the preparation of advanced materials, biologically relevant compounds and pharmaceutical products.<sup>1</sup> During the nearly last 40 years the synthetic value of enantiopure epoxides has been well established and a substantial amount of investigation on the preparation of these oxygenated three-membered rings have been carried out. In 2001, Barry Sharpless was awarded the Nobel Prize as a reward for his great contribution to this field, which founded the grounds of asymmetric epoxidation.<sup>2,3</sup>

Traditional enantioselective alkene epoxidation catalysts are mainly based on the so-called “Sharpless system” or chiral metalloporphyrins. “Sharpless system” represented the transition metal compounds bearing multi-oxygen ligand<sup>4</sup>. Some of these catalysts gave excellent asymmetrical epoxidation capacity with enantiomeric excess (ee) more than 90%. However, the low turnover numbers (TONs) obtained came to be the main drawback of this system.<sup>5</sup> On the other hand, chiral metalloporphyrins have always been an important class of catalysts for the asymmetric epoxidation of alkenes since diverse chiral groups can be easily appended onto their macrocyclic rings. The ee values range from 30 to 90% when Fe or Ru is coordinated to the porphyrin centre.<sup>6</sup> The  $\pi$ -conjugated structure of the porphyrin ring precludes the presence of chiral carbons on

the main ligand skeleton close to the catalytic active sites, which prevents the attainment of higher enantioselectivities.<sup>7</sup>

As discussed in the former chapters, M-O species usually function as the catalytic active centers in oxidation catalysis. Ru-aqua/oxo species manifest particularly interesting properties thanks to proton coupled electron transfer (PCET), which convert Ru complexes in valuable tools in the field of hydrocarbon oxidation. Therefore, the combination of a Ru-aqua/oxo system with a chiral ligand environment has been also studied in asymmetric epoxidation reactions. Since 1980s, a wide range of chiral Ru complexes has been studied for this purpose. Several representative examples are presented in Figure 1.<sup>8,9,10</sup> The advances in this area were systematically reviewed by Chatterjee in 2008.<sup>11</sup>

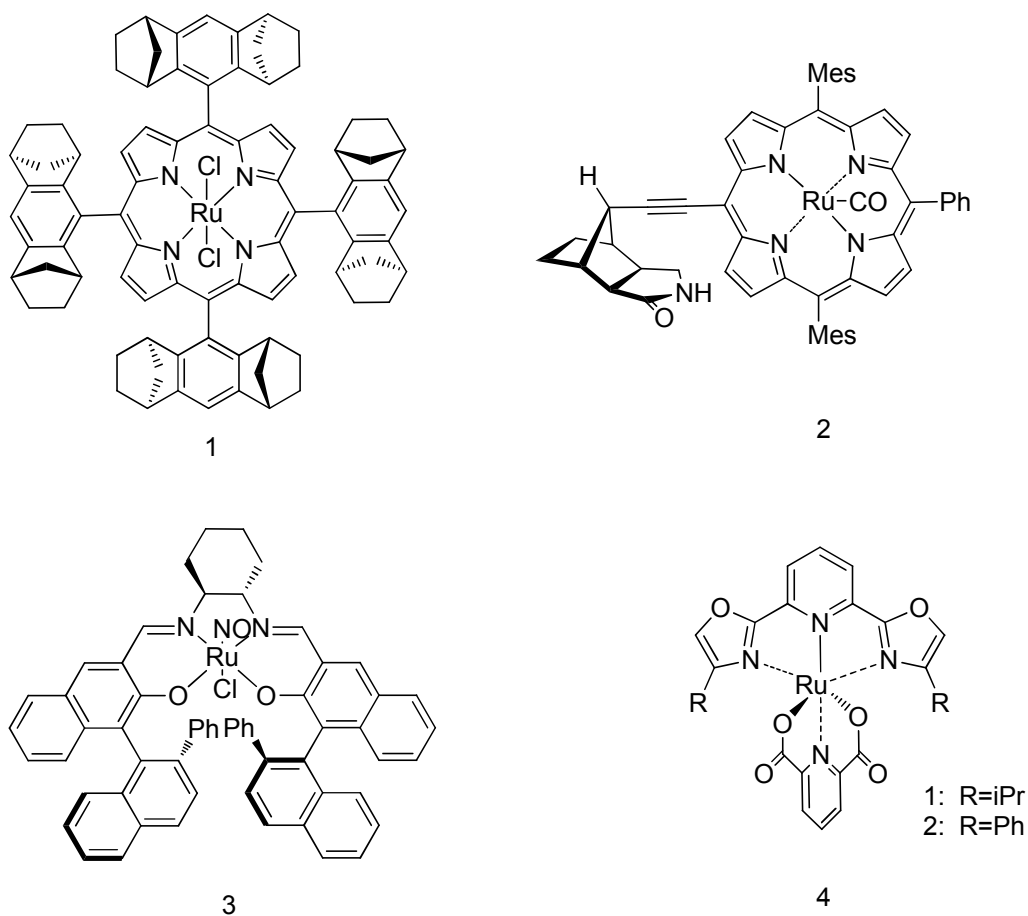


Figure 1. Representative chiral Ru complexes employed in asymmetric epoxidation processes.

Apart from the above-presented families, complexes bearing polypyridylic ligands with appended chiral substituents are also considered as promising chiral compounds.<sup>12</sup> However, despite their rich coordination chemistry, chiral polypyridylic ligands have not gathered much attention until Hayoz and co-workers introduced a chiral  $\alpha$ -pinene moiety into a pyridine ring in the 1990s.<sup>13,14</sup> Since then, a variety of pineno-annellated ligands have been described.<sup>15</sup> [4,5] and [5,6]pineno-fused ligands are easily accessible in their enantiomerically pure forms starting from the commercially available (-)- $\alpha$ -pinene or (-)-myrtenal monoterpenes, respectively. For example, in 2004 the group of Stefan Bernhard reported the chiral bridging ligand **1** (Figure 2)<sup>16</sup> and in 2006 Sala, Llobet and coworkers successfully synthesized the  $C_3$ -symmetric tripodal ligand **2** shown in Figure 1.<sup>17,18</sup> Based on this type of chiral ligands, a number of chiral pinene-containing complexes have been reported (**5**, **6** and **7** in Figure 1).<sup>19,20</sup>

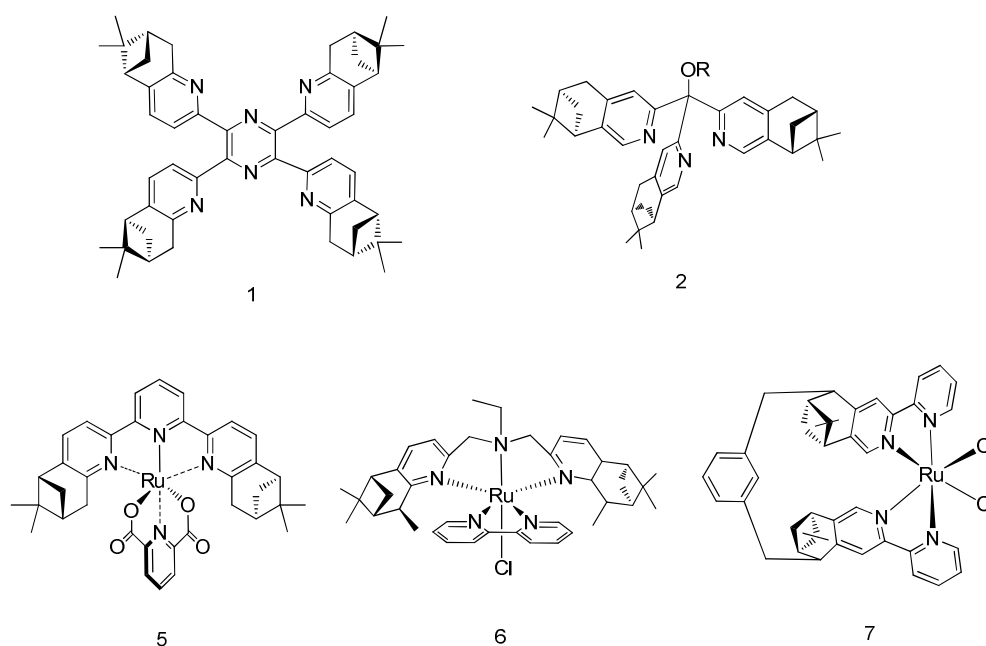


Figure 2. Examples of reported chiral pinene ligands (up) and Ru chiral pinene complexes (down).

In Chapter III of this PhD Thesis we have reported a new family of Ru-based epoxidation catalysts bearing NHC and polypyridylic ligands on their 1<sup>st</sup> coordination sphere, (see Chapter III for further details). Among them, **C1-Cl/OH<sub>2</sub>** and **C2-Cl/OH<sub>2</sub>**, bearing together with the NHC ligand a trpy scaffold were identified as the most interesting species given their capacity to stereospecifically epoxidize *cis* olefins such as *cis*- $\beta$ -methylstyrene. Therefore, here on we intend the introduction of chirality on the trpy ligand by means of Pinene moieties and the analysis of the resulting compounds in the stereo and enantioselective epoxidation of *cis* alkenes. Therefore, we present in this Chapter the synthesis of two complexes with general formula [Ru<sup>II</sup>(**L2**)(PhthaPz-Ome)X]<sup>n+</sup> (**L2** = [4,5]pinene-trpy; X = Cl, n = 1; X = OH<sub>2</sub>, n = 2), their structural and electrochemical characterization and the preliminary evaluation of their performance as asymmetric epoxidation catalysts.

## IV.2. Results and Discussion

### IV.2.1. Synthesis and characterization of [Ru<sup>III</sup>(L2)Cl<sub>3</sub>]

The chiral [4,5]pinene-trpy ligand **L2** (Scheme 1) was prepared according to the methodology presented by Balavoine and coworkers in 1999.<sup>21</sup> Using the chiral ligand, the precursor [Ru(L2)Cl<sub>3</sub>] was prepared following a slightly modified procedure also presented by the same research group.<sup>21</sup> Ethanol was chosen to be the best solvent for the synthesis of the [Ru(L2)Cl<sub>3</sub>] precursor.<sup>22</sup> RuCl<sub>3</sub>·3H<sub>2</sub>O and **L2** were refluxed together for 6h in ethanol and [Ru(L2)Cl<sub>3</sub>] was directly obtained as a reddish precipitate in a 65% yield. Given its paramagnetic nature that prevented NMR characterization, the presence of the desired compound was indicated by means of Cyclic Voltammetry (see Figure 3) and Mass Spectrometry (Figure S1 in Supporting Information). [Ru(L2)Cl<sub>3</sub>] was then employed for the next synthetic step without further purification.

As shown in Figure 3, the CV of the [Ru(L2)Cl<sub>3</sub>] precursor exhibits two reversible waves which can be assigned as the following electrochemical processes:



The two reversible waves observed at -0.09 and 1.35V correspond to the Ru(III/II) and Ru(IV/III) processes.

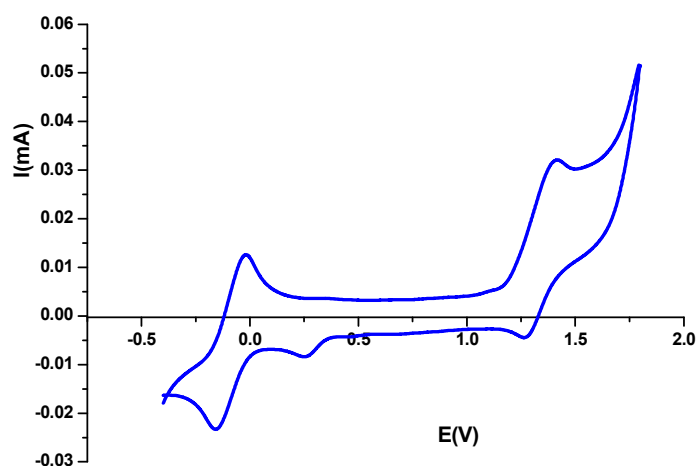


Figure 3. CV of the  $[\text{Ru}^{\text{III}}(\text{L}2)\text{Cl}_3]$  precursor.

## IV.2.2. Synthesis and Characterization of C5-Cl/OH<sub>2</sub>

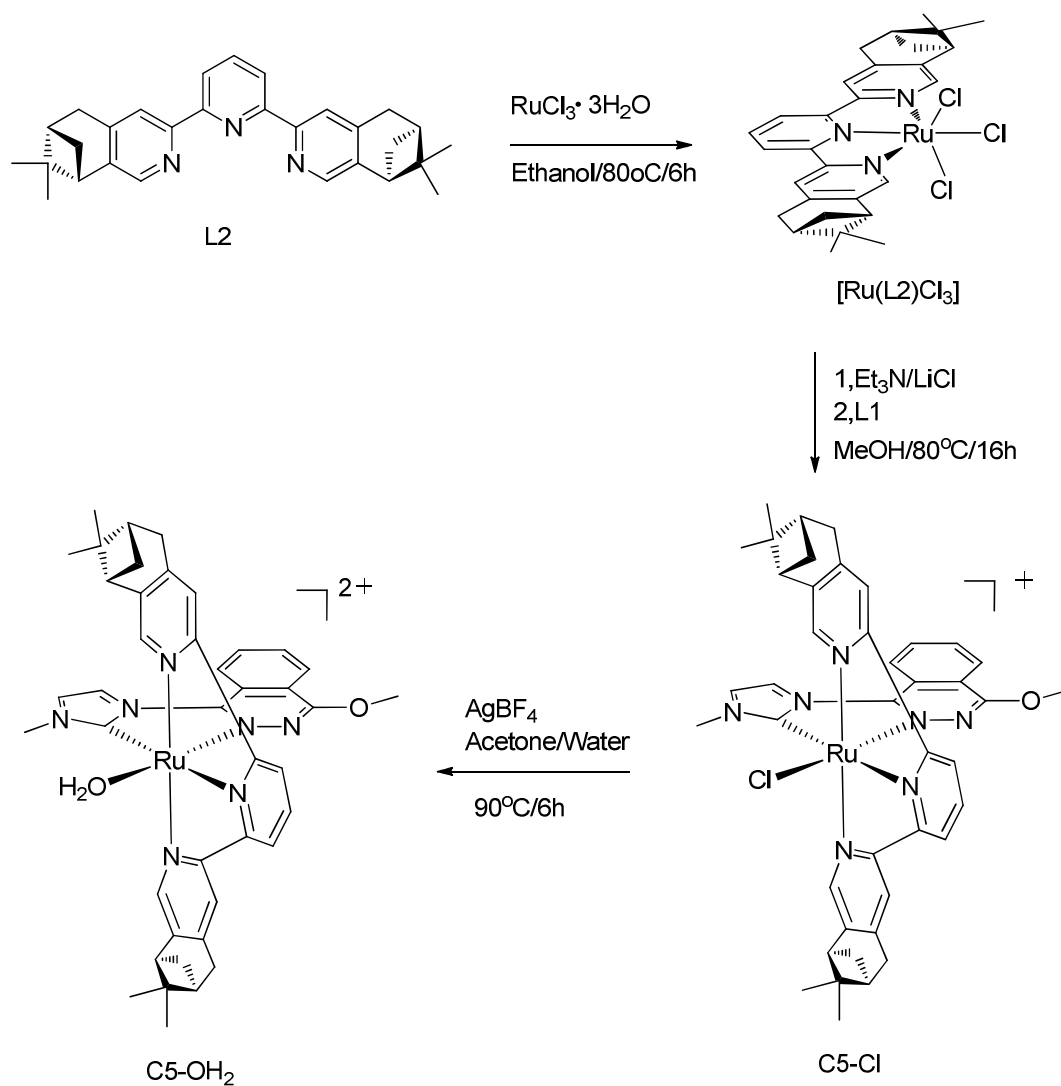
### IV.2.2.1. Synthesis of C5-Cl/OH<sub>2</sub>

The synthetic procedure of **C5** complexes (Scheme 1) is similar to the one employed for complexes **C1-C4-Cl/OH<sub>2</sub>** discussed in Chapter III.<sup>23,24</sup> Following a previously reported methodology reported by our group, 2 molar equivalents of  $[\text{Ru}(\text{L}2)\text{Cl}_3]$  were mixed with **L2**, Et<sub>3</sub>N as reducing agent and LiCl to ensure the presence of a labile site in the generated complex. After hot filtration, a few drops of aqueous NH<sub>4</sub>PF<sub>6</sub> were added to the crude solution and the solvent was evaporated to dryness under vacuum. Conversely to the trpy containing complexes reported in Chapter III that easily precipitate after counteranion addition, the increased aliphatic content in **L2** makes **C5-Cl** complexes highly soluble in organic solvents. Therefore, the brown solid obtained was purified by column chromatography in Alumina and the mononuclear complex **C5-Cl** was obtained as a red-brown powder in a final yield of about 30%. In analogy to **C1-Cl**, despite bimetallic species were expected, the mononuclear complexes **C5-Cl**

([Ru<sup>II</sup>(**L2**)(PhthaPz-Ome)Cl]<sup>+</sup>) was obtained under the reaction conditions employed. As commented in Chapter 3, the tetradentate dinucleating **L1** ligand decompose due to the nucleophilic attack of methanol to one of its C-N bonds that leading to a bidentate scaffold only able to form mononuclear complexes such as the ones shown in Scheme 1. The N-donor coordinating groups of the **L2** ligand are meridionally coordinated to the octahedral Ru metal center.

The aqua complex **C5-OH<sub>2</sub>** was attained by the addition of Ag<sup>I</sup> to a **C5-Cl** solution, which promoted the decoordination of the chlorido ligand and facilitated the entrance of an aqua group to the 1<sup>st</sup> coordination sphere of the Ru center. Since the solubility of **C5-Cl** was extremely low in water, the ratio of acetone: water was increased to 1: 2 (for **C1-OH<sub>2</sub>** in Chapter III the ratio was 1: 3). After AgCl filtration, acetone was slowly evaporated from the solvent mixture under vacuum. The counter ion could be easily exchanged from BF<sub>4</sub><sup>-</sup> to PF<sub>6</sub><sup>-</sup> by adding excess NH<sub>4</sub>PF<sub>6</sub>(aq) into the solution, thus obtaining [**C5-OH<sub>2</sub>**](PF<sub>6</sub>)<sub>2</sub> as a red precipitate. The synthetic procedure is depicted in Scheme 1.





Scheme 1. Synthesis of  $[\text{Ru}^{\text{III}}(\text{L2})\text{Cl}_3]$ , **C5-Cl** and **C5-OH<sub>2</sub>**.

#### IV.2.2.2. Characterization of **C5-(Cl/OH<sub>2</sub>)**

Complexes **C5-Cl/OH<sub>2</sub>** were spectroscopically (1D and 2D NMR and UV-vis) and electrochemically (CV) characterized in solution as detailed in the following subsections.

#### IV.2.2.2.1. NMR Spectroscopy

Nuclear Magnetic Resonance experiments have been carried out for the diamagnetic compound **C5-Cl** (See Figure 4 and Figure S2 in the Supporting Information). Both 1D ( $^1\text{H}$  and  $^{13}\text{C}$ ) and 2D (COSY, ROESY, HSQC and HMBC) experiments have proven to be mandatory tools in order to structurally characterize the compounds in solution. Both chlorido and aqua compounds (**C5-Cl**/ $\text{OH}_2$ ) display  $C_1$  symmetry in solution, with no symmetry elements present in the molecule. Therefore, two enantiomers are present in solution that remain indistinguishable in NMR. The symmetry plane present in the trpy containing complexes **C1** and **C2** in Chapter III is now not present due to the chiral pinene moieties present in **L2**. However, similarly to what is observed for **C1** and **C2** in Chapter III, only a single geometric isomer (the *cis* one) is obtained under the reaction conditions employed. The notation *cis* and *trans* refer to the relative position of the chlorido/aqua ligand with regard to the Ru carbene bond. The NMR spectra of complex **C5-OH<sub>2</sub>** are shown in the Supporting Information (Figure S3).

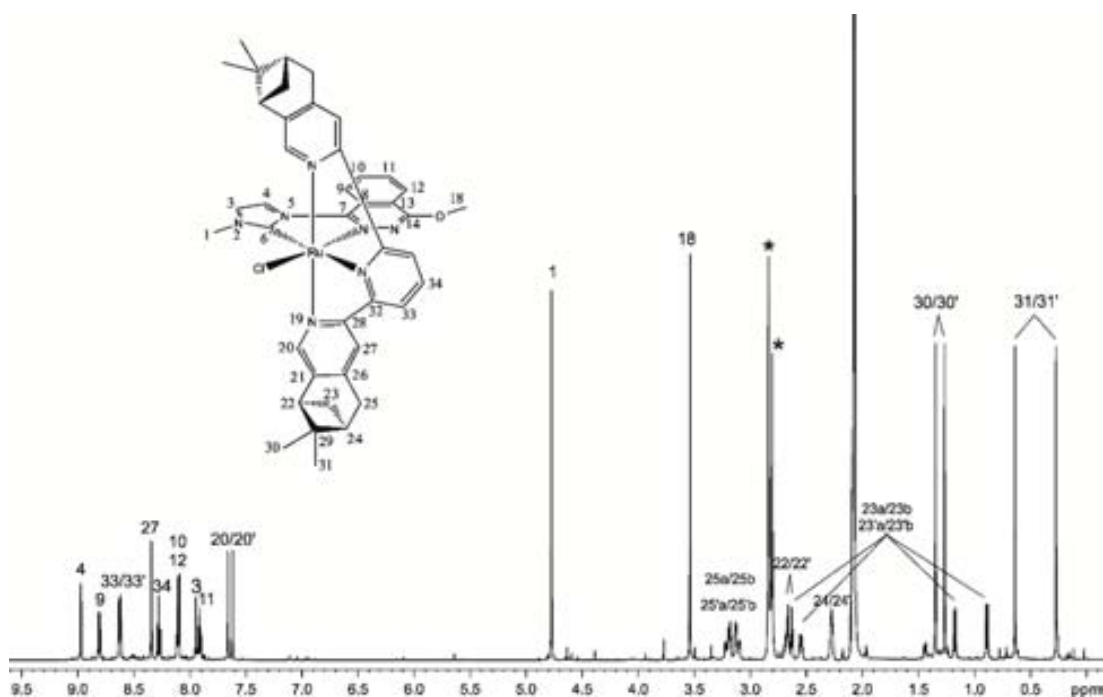


Figure 4.  $^1\text{H}$  NMR of **C5-Cl** in acetone- $d_6$  and its corresponding proton assignment.

#### IV.2.2.2.2. Electrochemistry

The redox properties of the chlorido and aqua complexes **C5-Cl**/**OH<sub>2</sub>** described in the present work have been investigated and their CVs are shown in Figure 5 and Figure 6, respectively.

The single reversible wave obtained for the chlorido complex is assigned to the following process:

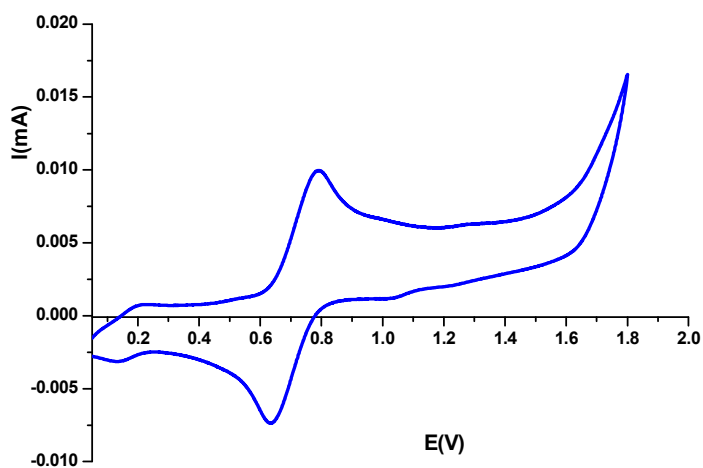


Figure 5. CV of **C5-Cl** in DCM at a scan rate of 100 mV/s and using glassy carbon as working electrode and SSCE as reference electrode.

As usual, Ru(III/II) processes are not observed for aqua complexes in DCM. Therefore, the reversible waves shown in Figure 6 correspond to the following Ru(IV/II) process:



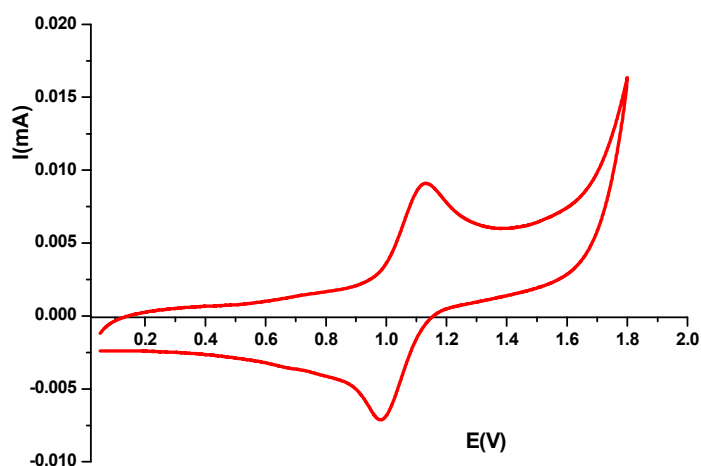


Figure 6. CV of **C5-OH<sub>2</sub>** in DCM at a scan rate of 100 mv/s and using glassy carbon as working electrode and SSCE as reference electrode.

In contrast to its non-chiral trpy-based counterpart [**C5-OH<sub>2</sub>**](PF<sub>6</sub>)<sub>2</sub> resulted to be totally insoluble in water, which precluded the analysis of its redox properties in this solvent.

#### IV.2.2.2.3. UV-vis

The UV-vis spectra of the complexes **C5-Cl/OH<sub>2</sub>** have been recorded in methanol and are displayed in Figure 7. Two regions could be observed for all the complexes; one region between 260 nm and 350 nm with very intense bands is due to intraligand  $\pi$  to  $\pi^*$  transitions of the coordinated ligands. A second region is between 350 nm and 550 nm where unsymmetrical broad typical MLCT (metal-to-ligand charge transfer) bands appear that could be tentatively assigned to  $d\pi(\text{Ru})$  to  $\pi^*$  N-ligands transitions.<sup>25,26</sup>

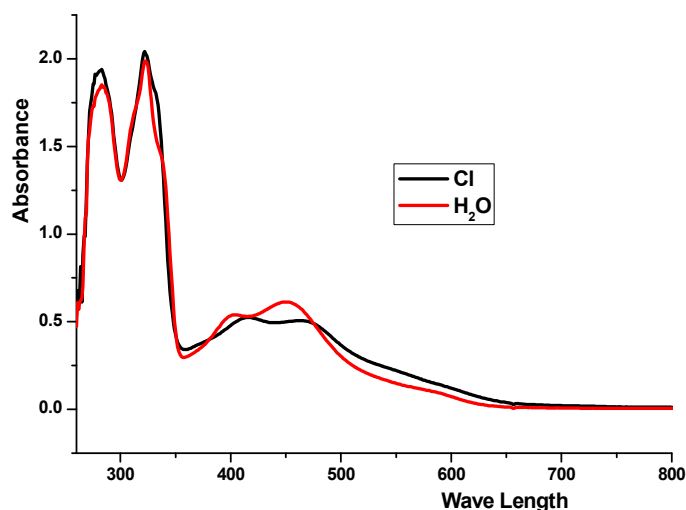
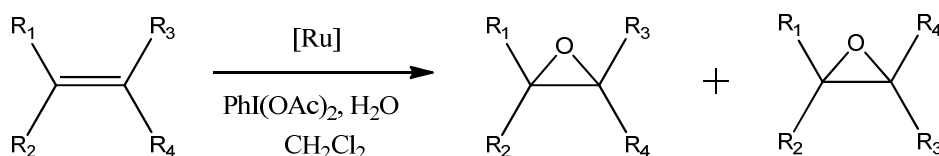


Figure 7. UV-vis spectra of **C5-Cl** and **C5-OH<sub>2</sub>** complexes in 50  $\mu$ M MeOH solutions.

The electronic nature of the monodentate ligand influences the energies of the transitions involving orbitals with d(Ru) character to some extent. The MLCT bands for the Ru-aqua complexes are slightly blue-shifted with regards to those of their Ru-Cl counterparts due to the relative stabilization of the  $d\pi(\text{Ru})$  levels provoked by the non- $\pi$ -donor character of the aqua ligand.<sup>27</sup>

### IV.2.3. Asymmetric Epoxidation of Different Alkenes

The aqua complex **C5-OH<sub>2</sub>** have been preliminarily tested with regards to its ability to asymmetrically epoxidize prochiral alkenes (Scheme 2) when chemically triggered with  $\text{PhI}(\text{OAc})_2$ . The catalytic reactions have been carried out following the conditions exposed in Table 1, while the most relevant results are displayed in Table 2.



Scheme 2. Enantioselective epoxidation of different alkenes catalyzed by chiral Ru complexes.

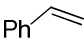
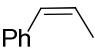
A vial containing 1 mL of 1,2-dichloroethane (DCE) as solvent, (diacetoxyiodo)benzene as co-oxidant, 1,1'-biphenyl as internal standard, the catalyst, and the alkene substrate was stirred at room temperature. The excess of water is mandatory to ensure the generation of PhIO from  $\text{PhI}(\text{OAc})_2$ .<sup>28,29</sup> The products of each catalytic reaction have been identified by GC ( $\beta$ -dex column) and identified by comparison of their reaction times with those of commercial samples of the pure enantiomers and GC-MS.

Table 1. Reaction conditions for asymmetric epoxidation of styrene and *cis*- $\beta$ -methylstyrene catalyzed by **C5-OH<sub>2</sub>**

Species	mmols	Concentration (M)	Ratio cat:X
<b>C5-OH<sub>2</sub></b>	2.5E-03	1.7E-03	—
Alkene	2.5	1.7	1000
1,1'-biphenyl	1	0.7	800
(diacetoxyiodo)benzene	5	3.4	2000
water	5	3.4	2000

The catalytic activity of **C5-OH<sub>2</sub>** towards the epoxidation of alkenes has been preliminary tested following the same methodology used in Chapter III for its non-asymmetric counterpart. The catalytic reaction was carried out at room temperature with a catalyst: substrate:  $\text{PhI}(\text{OAc})_2$  ratio of 1: 1000: 2500. The gathered results obtained for the two tested substrates are shown in Table 2.

Table 2. Enantioselective epoxidation of styrene and *cis*- $\beta$ -methylstyrene catalyzed by **C5**-OH<sub>2</sub>. Reaction conditions: **C5**-OH<sub>2</sub> ( $2.5 \cdot 10^{-3}$  mmols, final concentration 0.85 mM) in DCE (1mL), substrate (2.5 mmols, 1.7 M), PhI(OAc)<sub>2</sub> (5 mmols, 3.4 M), H<sub>2</sub>O (5 mmols, 3.4 M), 1,1'-byphenil (1 mmol, 0.68 M), final volume  $\approx$  1.47 mL.

Entry	Alkenes	Time (min)	Substrate Conversion (%) <sup>a</sup>	[Epoxide], M; (Selectivity, %) <sup>b</sup>	TON/TOFi <sup>c</sup>	ee%
1		480	100	0.27; (15)	154/0.3	20
2		420	100	1.32; (76) <sup>d</sup>	750/1.8	20

<sup>a</sup> Substrate conversion =  $\{([substrate]_i - [substrate]_f) / [substrate]_i\} \cdot 100$ . <sup>b</sup> Epoxide selectivity =  $\{[epoxide]_f / ([substrate]_i - [substrate]_f)\} \cdot 100$ . <sup>c</sup> TON with regard to epoxide; TOFi = TON/min. <sup>d</sup> *cis* epoxide.

After 7 hours reaction time, 1.29 M *cis*- $\beta$ -methylstyrene oxide is obtained with a moderate enantioselectivity (20% ee) together with benzaldehyde as main byproduct. Similar ee values are obtained for the epoxidation of styrene to styren oxide but, by far, with much lower product selectivity (Table 2, entry 2). While these results clearly manifest the capacity of Ru-complex, containing the pinene ligand, to enantiodifferentiate prochiral substrates such as styrene or *cis*- $\beta$ -methylstyrene, it is obvious that the enantiomeric excess obtained needs to be significantly improved in order to be able to have a meaningful synthetic application. Therefore, further work is in progress to optimize reaction conditions for this system in order to improve enantioselectivities.

### IV.3. Conclusions

In this chapter we presented the preparation, characterization and preliminary enantioselective alkene epoxidation capacity of a new family of nononuclear complexes with general formula  $[\text{Ru}^{\text{II}}(\text{PhthaPz-Ome})(\text{L2})\text{X}]^{n+}$  (**L2** is [4,5]pinene-trpy ligand;  $\text{X}=\text{Cl}$ ,  $n=1$ ;  $\text{X}=\text{OH}_2$ ,  $n=2$ ), **C5-Cl/OH<sub>2</sub>**. Initially, the chiral precursor  $[\text{Ru}^{\text{III}}(\text{L2})\text{Cl}_3]$  was synthesized and characterized by means of CV and MS. Reaction of this precursor with the dinucleating CNNC ligand **L1<sup>2+</sup>** (see Chart 1 in Chapter III) in MeOH lead to decomposition of **L1<sup>2+</sup>** due to C-N nucleophilic bond cleavage promoted by the solvent and, therefore, to the generation of the mononuclear species **C5**. Given the increased alkylic content supplied by the pinene groups appended to the trpy ligand this family of complexes show increased solubility in organic solvent but dramatically low solubility in water. **C5-OH<sub>2</sub>** was preliminary tested as a catalyst for the enantioselective epoxidation of styrene and *cis*- $\beta$ -methylstyrene in dichloroethane giving low ee values of about 20%. This result demonstrates the capacity of the ligand combination to enantiodifferentiate prochiral substrates. However, the remote position of the chiral pinene moieties with regard to the Ru-O active site is probably responsible for the low ee value observed.

### IV.4. Experimental Section

**Materials:** All reagents used in the present work were obtained from Sigma Aldrich Chemical Co. and were used without further purification. Reagent-grade organic solvents were obtained from Scharlab.  $\text{RuCl}_3 \cdot 3\text{H}_2\text{O}$  was supplied by Alfa Aesar and was used as received. The [4,5]pinene-trpy ligand **L2** was prepared as described in the literature.<sup>21</sup> The synthetic manipulations were routinely performed under nitrogen atmosphere using Schlenk tubes and vacuum-line techniques.



**Instrumentation and Measurements:** UV-Vis spectroscopy was carried out by a HP8453 spectrometer using 1 cm quartz cells. NMR spectroscopy was performed on a Bruker DPX 250 MHz, DPX 360 MHz, DPX 400 MHz, DPX 500 MHz or a DPX 600 MHz spectrometer. Samples were run in MeOD, DCM-d<sub>2</sub> or acetone-d<sub>6</sub> with internal references. Elemental analyses were performed using a Carlo Erba CHMS EA-1108 instrument from the Chemical Analysis Service of the Universitat Autònoma de Barcelona (CAS-UAB). Electrospray ionization Mass Spectrometry (ESI-MS) experiments were performed on an HP298s gas chromatography (GC-MS) system from the CAS-UAB. Cyclic voltammetry and Differential pulse voltammetry experiments were performed on the Bio Logic Science Instrument SP-150 potentiostat using a three-electrode cell. A glassy carbon electrode (2 mm diameter) was employed as working electrode while platinum wire as auxiliary electrode and a SSCE as a reference electrode. Working electrodes were polished with 0.05 micron Alumina paste and washed with distilled water and acetone before each measurement. The complexes were dissolved in methanol or dichloromethane solution of 0.1 M ionic strength containing the necessary amount of n-Bu<sub>4</sub>NPF<sub>6</sub> (TABH) as supporting electrolyte. E<sub>1/2</sub> values here presented were estimated from CV experiments from the average of the oxidative and reductive peak potentials (E<sub>p,a</sub> + E<sub>p,c</sub>)/2. The introduced alkenes and the corresponding chiral epoxides were separated and analyzed through Gas Chromatography HRGC-3000 KONIK INSTRUMENT.

### **Synthetic Preparations**

*[Ru(L2)Cl<sub>3</sub>]*: RuCl<sub>3</sub>·3H<sub>2</sub>O (523 mg, 2.0 mmol) and 2,6-bis((6S,8S)-7,7-dimethyl-5,6,7,8-tetrahydro-6,8-methanoisoquinolin-3-yl)pyridine (**L2**) (842 mg, 2.0 mmol) was suspended in 50 mL ethanol and refluxed for 4 hours while vigorous magnetic stirring was maintained. Then the reaction was cooled down to room temperature and the brown precipitate formed was filtered off and washed with 3×30 mL of first

methanol and then diethylether. Yield: 591 mg (47%).  $E_{1/2}$  (CV in DCM): Ru(III/II) = -0.09V, Ru(IV/III) = 1.35V. ESI-MS (MeOH):  $m/z$  = 593.1 ([M-Cl]), 559.1 ([M-2Cl+1]).

*cis*-[Ru<sup>II</sup>(PhthaPz-Ome)(L2)Cl]PF<sub>6</sub> (C5-Cl): [Ru(L2)Cl<sub>3</sub>] (130 mg, 0.3 mmol), 1,4-Bis(1-methylimidazolium-1-yl) phthalazine dichloride (L1(Cl)<sub>2</sub>) (73 mg, 0.2 mmol) and LiCl (38 mg 0.9 mmol) were placed together in a flask and dry methanol (20 mL) was added as solvent. Triethylamine (121 mg, 166  $\mu$ L, 1.2 mmol) was added to the solution and the mixture was refluxed at 80°C for 16 hours. The solution was filtered through celite<sup>®</sup> and to the residual solution 20 drops of saturated NH<sub>4</sub>PF<sub>6</sub> water solution were added. The solvent was removed under vacuum and the residual solid was purified by column chromatography with DMC: MeOH (98: 2) as eluent mixture. Yield: 62 mg (33%) <sup>1</sup>H NMR (600 MHz, acetone-d<sub>6</sub>, 298K)  $\delta$ =8.97 (d, 1H,  $J_{4-3}$  = 2.4 Hz, H4), 8.81 (d, 1H,  $J_{9-10}$  = 8.7 Hz, H9), 8.63 (d, 2H,  $J_{33-34}$  = 2.9 Hz, H33), 8.35 (s, 1H, H27), 8.28 (t, 1H,  $J_{34-33,33'}$  = 8.1 Hz, H34), 8.11 (m, 2H, H10, H11), 7.95 (d, 1H,  $J_{3-4}$  = 2.3 Hz, H3), 7.91 (t, 1H,  $J_{11-10,12}$  = 7.6 Hz, H11), 7.65 (d, 1H,  $J_{20-22}$  = 6.4 Hz, H20), 7.62 (d, 1H,  $J_{20'-22'}$  = 6.4 Hz, H20'), 4.77 (m, 3H, H1), 3.54 (s, 3H, H18), 3.20 (m, 4H, H25), 2.66 (ddt, 2H,  $J_{22-30,23,23'}$  = 23.0, 17.5, 5.6 Hz, H22), 2.55 (m, 4H, H23a), 2.28 (m, 2H, H24), 1.35 (s, 3H, H30), 1.27 (s, 3H, H30'), 1.18 (d, 1H,  $J_{23b-23a}$  = 9.4 Hz, H23b), 0.89 (d, 1H,  $J_{23b'-23a'}$  = 9.8 Hz, H23b'), 0.64 (s, 3H, H31), 0.27 (s, 3H, H31'). <sup>13</sup>C-NMR (600 MHz, acetone-d<sub>6</sub>, 298K) 157.95 (C13), 157.22 (C32), 157.17 (C32'), 156.05 (C28,28'), 152.14 (C20), 152.09 (C20'), 151.68 (C8), 146.23 (C21), 146.19 (C21'), 145.85 (C26), 145.82 (C26'), 135.33 (C34), 133.91 (C10), 131.93 (C11), 126.00 (C3), 124.16 (C12), 122.63 (C27), 122.58 (C27'), 120.70 (C9), 120.43 (C33), 120.40 (C33'), 118.86 (C4), 54.14 (C18), 44.26 (C22), 44.22 (C22'), 39.56 (C24,24'), 38.55 (C29), 38.38 (C29'), 37.44 (C1), 32.39 (C25,25'), 30.83 (C23), 30.63 (C23'), 25.00 (C30), 24.91 (C30'), 20.63 (C31), 20.34 (C31'). UV/vis (methanol):  $\lambda_{max}$  ( $\epsilon$ )= 283 (19400), 322 (20424), 417 (5238), 464 (5062). ESI-MS (MeOH):  $m/z$  = 798.2 ([M-PF<sub>6</sub>-1]).

*cis*-[Ru<sup>II</sup>(PhthaPz-Ome)(L2)(OH<sub>2</sub>)](PF<sub>6</sub>)<sub>2</sub> (C5-OH<sub>2</sub>): C5-Cl (120 mg, 0.13 mmol) was dissolved in a mixture of acetone and water (1: 2, 30 mL). AgBF<sub>4</sub> (109 mg, 0.56 mmol) was added into the solution. The mixture was refluxed at 90°C for 4 hours. 50 mL of acetone were then added to the reaction mixture and the solution was filtered through celite<sup>®</sup> to remove the AgCl formed. 20 drops of a saturated NH<sub>4</sub>PF<sub>6</sub> aqueous solution were then add to the filtrate. The solvent was removed under vacuum and the residual solid was purified by column chromatography in alumina with DMC:MeOH (95.5:1.5) as eluent mixture Yield: 49 mg (35%) <sup>1</sup>H NMR (600 MHz, acetone-d<sub>6</sub>, 298K) δ=9.00 (d, 1H, *J*<sub>4-3</sub> = 2.4 Hz, H4), 8.78 (d, 1H, *J*<sub>9-10</sub> = 8.7 Hz, H9), 8.71 (d, 2H *J*<sub>33-34</sub> = 7.4 Hz, H33), 8.45 (s, 2H, H27), 8.40 (t, 1H, *J*<sub>34-33,33'</sub> = 8.1 Hz, H34), 8.12 (dd, 1H, *J*<sub>10-9,11</sub> = 11.6, 4.2 Hz, H10), 8.10 (d, 1H, *J*<sub>12-11</sub> = 7.7 Hz, H12), 8.01 (d, 1H, *J*<sub>3-4</sub> = 2.4 Hz, H3), 7.93 (t, 1H, *J*<sub>11-10,12</sub> = 7.6 Hz, H11), 7.78 (s, 1H, H20), 7.74 (s, 1H, H20'), 4.53 (s, 3H, H1), 3.50 (s, 3H, H18), 3.16 (m, 4H, H25), 2.66 (m, 2H, H22, H23a), 2.52 (m, 1H, H23b), 2.25 (m, 2H, H25), 1.31 (s, 3H, H30), 1.22 (s, 3H, H30'), 1.14 (d, 2H, *J*<sub>23a'-23a</sub> = 9.5 Hz, H23a'), 0.84 (d, 1H, *J*<sub>23b'-23b</sub> = 9.9 Hz, H23b'), 0.62 (s, 3H, H31), 0.24 (s, 3H, H31'). <sup>13</sup>C-NMR (600 MHz, acetone-d<sub>6</sub>, 298K) 201.22 (C6), 157.87 (C13), 157.58 (C32), 157.50 (C32'), 156.75 (C28,28'), 153.12 (20), 153.00 (20'), 152.96 (C8), 147.56 (C21), 147.53 (C21'), 147.19 (C26), 147.18 (C26'), 137.40 (C34), 134.17 (C10), 132.67 (C11), 126.12 (C3), 124.14 (C12), 123.31 (C27), 123.27 (C27'), 121.20 (C33,33') 120.85 (C9), 119.35 (C4), 54.48 (C18), 44.22 (C22), 44.20 (C22'), 39.37 (C24,24'), 38.48 (C29), 38.27 (C29'), 36.49 (C1), 32.55 (C25), 32.52 (C25'), 30.78 (C23), 30.48 (C23'), 24.99 (C30), 24.86 (C30'), 20.63 (C31), 20.35 (C31'). UV/vis (methanol): λ<sub>max</sub> (ε)= 283 (18530), 323 (19872), 401 (5367), 451 (6123). ESI-MS (MeOH): m/z = 798.2 ([M-2PF<sub>6</sub>]).

## IV.5. References

---

- <sup>1</sup> a) Lane, B. S. and Burgess, K. *Chemical Reviews*, **2003**, 103(7), 2457. b) Simonneaux, G. and Le Maux, P. *Coordination Chemistry Reviews*, **2002**, 228, 43. c) Naota, T.; Takaya, H. and Murahashi, S. I. *Chem. Rev.* **1998**, 98, 2599. d) Barf, G. A.; Sheldon, R. A. *Journal of Molecular Catalysis A: Chemical*, 1995, 102, 23.
- <sup>2</sup> Schlingloff, G. and Sharpless, K. B. *Asymmetric Aminohydroxylation, in "Asymmetric Oxidation Reactions: A Practical Approach in Chemistry"*, Oxford University Press, London, **2001**.
- <sup>3</sup> Xia, Q. H.; Ge, H. Q.; Ye, C. P.; Liu, Z. M. and Su, K. X. *Chem. Rev.* **2005**, 105, 1603.
- <sup>4</sup> a) Sharpless, K. B. *Angew. Chem. Int. Ed.* **2002**, 41, 2024. b) Henbest, H. B.; Wilson, R. A. L. *J. Chem. Soc.* **1957**, 1958. c) Sharpless, K. B.; Michaelson, R. C. *J. Am. Chem. Soc.* **1973**, 95, 6136.
- <sup>5</sup> a) Michaelson, R. C.; Palermo, R. E. and Sharpless, K. B. *J. Am. Chem. Soc.* **1977**, 99, 1990. b) Berrisford, D. J.; Bolm, C. and Sharpless, K. B. *Angew. Chem., Int. Ed.* **1995**, 34, 1059. c) Murase, N.; Hoshino, Y.; Oishi, M. and Yamamoto, H. *J. Org. Chem.* **1999**, 64, 338. d) Hoshino, Y. and Yamamoto, H. *J. Am. Chem. Soc.* **2000**, 122, 10452. e) Bolm, C.; Kühn, T. *Syn. Lett.* **2000**, 899.
- <sup>6</sup> a) Meunier, B. *Chem. Rev.* **1992**, 92, 1411. b) Collman, J. P.; Zhang, X. M.; Lee, V. J.; Uffelman, E. S. and Brauman, J. I. *Science* **1993**, 261, 1404. c) Liu, W. S.; Zhang, R.; Huang, J. S.; Che, C. M. and Peng, S. M. *J. Organomet. Chem.* **2001**, 634, 34. d) Gross, Z.; Ini, S.; Kapon, M. and Cohen, S. *Tetrahedron Lett.* **1996**, 37, 7325. e) Srivastava, T. S. and Fleischer, E. B. *J. Am. Chem. Soc.*, **1970**, 92, 5518.
- <sup>7</sup> Le Maux, P.; Massonneau, V. and Simonneaux, G. *Tetrahedron*, **1988**, 44, 1409.
- <sup>8</sup> Berkessel, A.; Kaiser, P. and Lex, J. *Chem. Eur. J.*, **2003**, 9, 4746.
- <sup>9</sup> a) Fackler, P.; Berthold, C.; Voss, F. and Bach, T. *J. Am. Chem. Soc.*, **2010**, 132, 15911. b) Fackler, P.; Huber, S. M. and Bach, T. *J. Am. Chem. Soc.*, **2012**, 134, 12869.

- 
- <sup>10</sup> a) Nakata, K.; Takeda, T. Mihara, J. and Katsuki, T. *Chem. Eur. J.*, **2001**, 17, 7. b) Nishiyama, H.; Shimada, T.; Itoh, H.; Sugiyama, H. and Motoyama, Y. *Chem. Commun.*, **1997**, 1863.
- <sup>11</sup> Chatterjee, D. *Coordination Chemistry Reviews*, **2008**, 252, 176.
- <sup>12</sup> Chelucci, G.; Thummel, R. P.; *Chem. Rev. (Washington, DC, U. S.)* **2002**, 102, 3129.
- <sup>13</sup> Hayoz, P.; Von, Z. A. *Tetrahedron Lett.* 1992, 33, 5165.
- <sup>14</sup> Hayoz, P.; Von, Z. A. Stoeckli-Evans, H. *J. Am. Chem. Soc.* **1993**, 115, 5111.
- <sup>15</sup> a) Malkov, A. V.; Pernazza, D.; Bell, M.; Bella, M.; Massa, A.; Teply, F.; Meghani, P.; Kocovsky, P. *J. Org. Chem.* **2003**, 68, 4727. b) Malkov, A. V.; Baxendale, I. R.; Bella, M.; Langer, V.; Fawcett, J.; Russell, D. R.; Mansfield, D. J.; Valko, M.; Kocovsky, P. *rganometallics* **2001**, 20, 673. c) Loetscher, D.; Rupprecht, S.; Collomb, P.; Belser, P.; Viebrock, H.; von, Z. A.; Burger, P. *Inorg. Chem.* **2001**, 40, 5675. d) Langlotz, B. K.; Wadepohl, H.; Gade, L. H. *Angew. Chem., Int. Ed.* **2008**, 47, 4670.
- <sup>16</sup> Sauers, A. L.; Ho, D. M. and Bernhard, S. *J. Org. Chem.* **2004**, 69, 8910.
- <sup>17</sup> Sala, X. ; Rodríguez, A. M.; Rodríguez, M.; Romero, I.; Parella, T.; Von Zelewsky, A.; Llobet, A. and Benet-Buchholz, J. *J. Org. Chem.* **2006**, 71, 9283.
- <sup>18</sup> Sala, X.; Poater, A.; Von Zelewsky, A.; Parella, T.; Romero, I.; Solà, M.; Rodríguez, M.; and Llobet, A. et.al. *Inorganic Chemistry*, **2008**, 47, 8016.
- <sup>19</sup> Tse, M. K.; Klawonn, M.; Bhor, S. and Beller, M. *Org. Lett.*, **2005**, 7, 987
- <sup>20</sup> Vaquer, L.; De Tovar, J.; García-Antón, J.; Llobet, A.; Sala, X., *Inorg. Chem.* **2013**, 52, 4985.
- <sup>21</sup> Ziegler, M.; Monney, V.; Stoeckli-Evans, H.; Von Zelewsky, A.; Sasaki, I.; Dupic, G.; Daran, J. C. and Balavoine, G. A. *J. Chem. Soc., Dalton Trans.*, **1999**, 667.
- <sup>22</sup> Salierno, M.; Fameli, C. and Etchenique, R. *Eur. J. Inorg. Chem.* **2008**, 1125.
- <sup>23</sup> Sens, C.; Romero, I.; Rodríguez M.; Llobet A.; Parella, T. and Benet-Buchholz, J. *J. Am. Chem. Soc.* **2004**, 126, 7798.

- 
- <sup>24</sup> García-Antón, J.; Bofill, J.; Escriche, L.; Llobet, A. and Sala, X. *Eur. J. Inorg. Chem.* **2012**, 4775.
- <sup>25</sup> Rodríguez, M.; Romero, I.; Llobet, A. *Inorg. Chem.* **2001**, 40, 4150.
- <sup>26</sup> Takeuchi, K. J.; Thompson, M. S.; Pipes, D. W.; Meyer, T. J. *Inorg. Chem.* **1984**, 23, 1845.
- <sup>27</sup> Shriver, D. F. and Atkins, P. W. *Inorganic Chemistry*; Oxford University Press, **2012**.
- <sup>28</sup> Sala, X.; Serrano, I.; Romero, I. and Llobet, A. *Eur. J. Inorg. Chem.*, **2007**, 5207.
- <sup>29</sup> In, J. H.; Park, S. E.; Song, R. and Nam, W. *Inorg. Chim. Acta*, **2003**, 343, 373.

## **IV.6. Supporting Information**

NMR

ESI-MS

Figure S1. ESI-MS spectrum of [Ru(L2)Cl<sub>3</sub>]

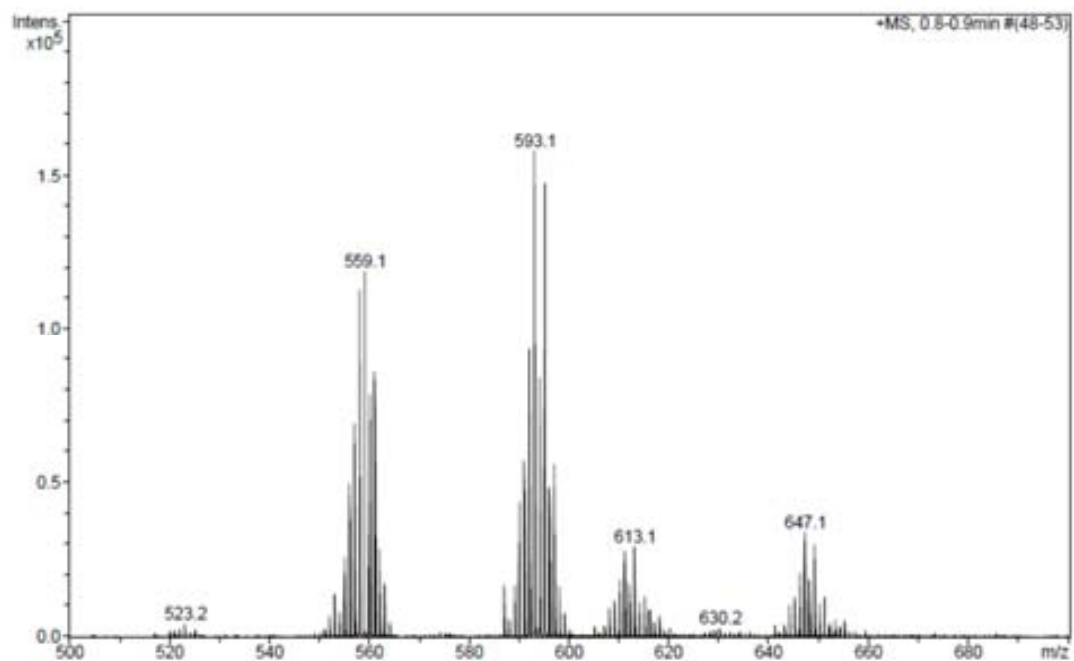
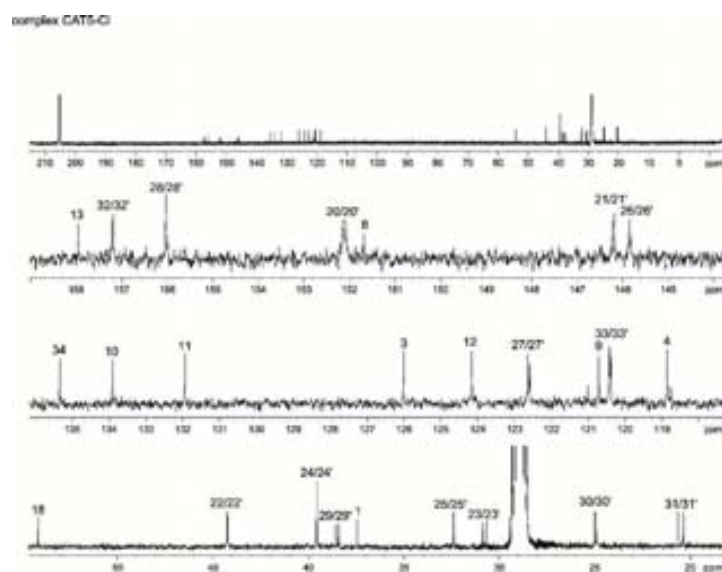


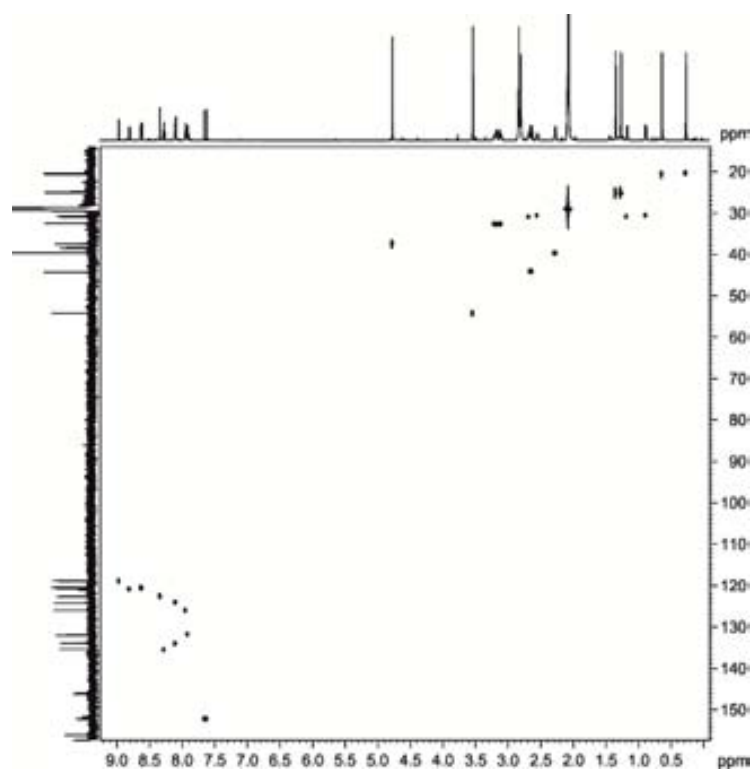
Figure S2. 1D and 2D NMR spectra of C5-Cl (600 MHz, 298K, acetone-d<sub>6</sub>): a) <sup>13</sup>C NMR, b) HSQC, c) HMBC, d) COSY, e) ROESY

a)

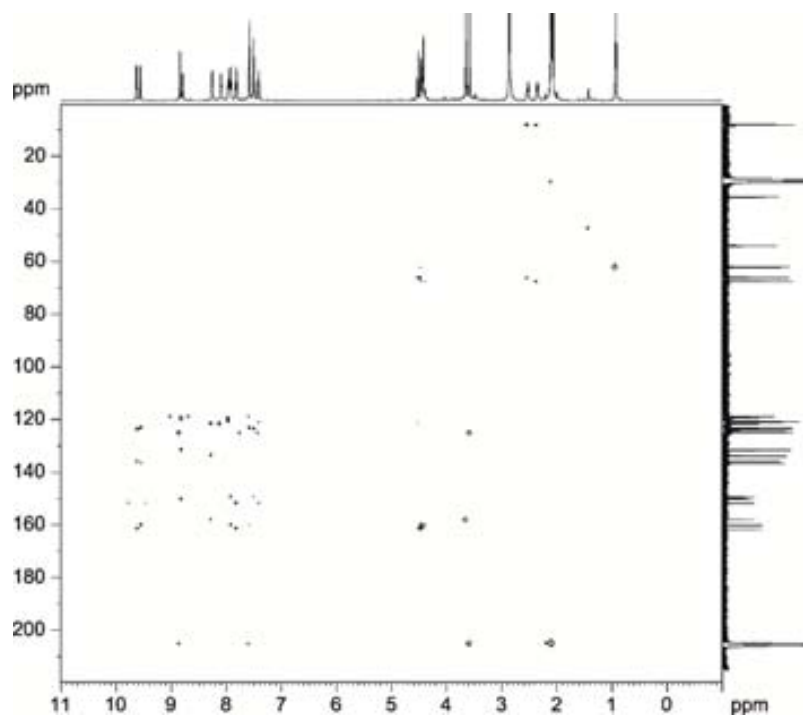




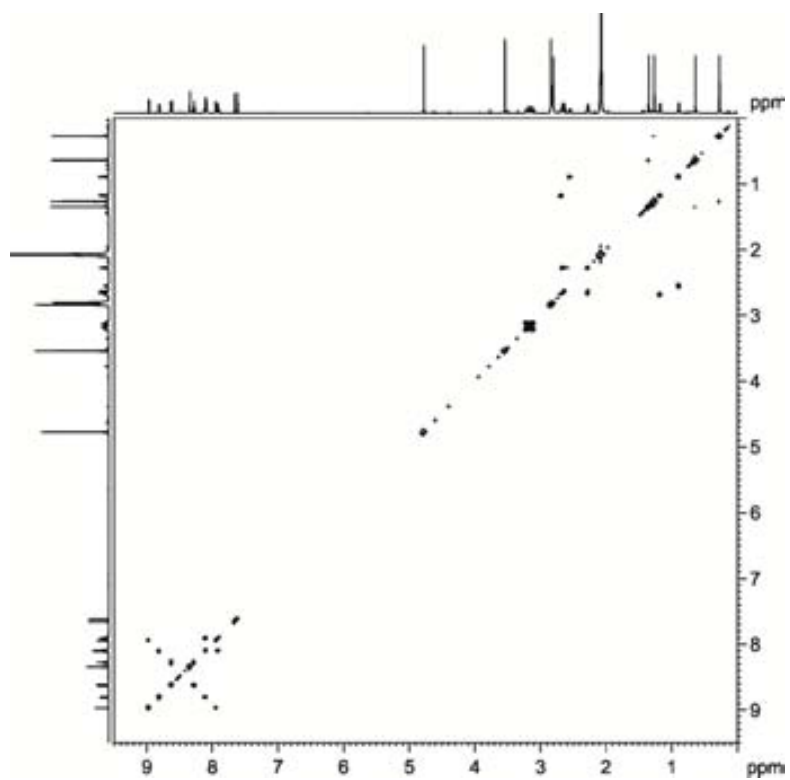
b)



c)



d)



e)

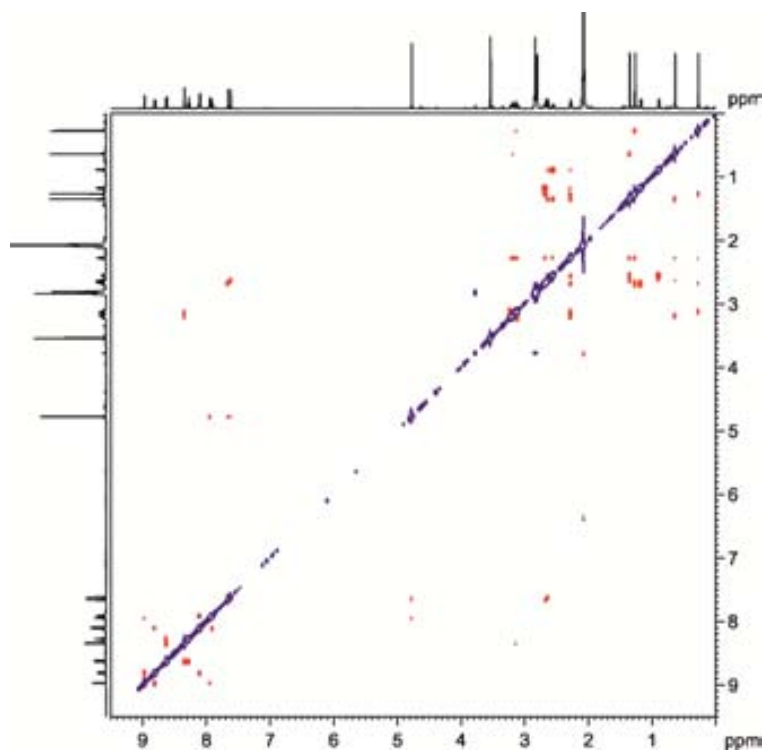
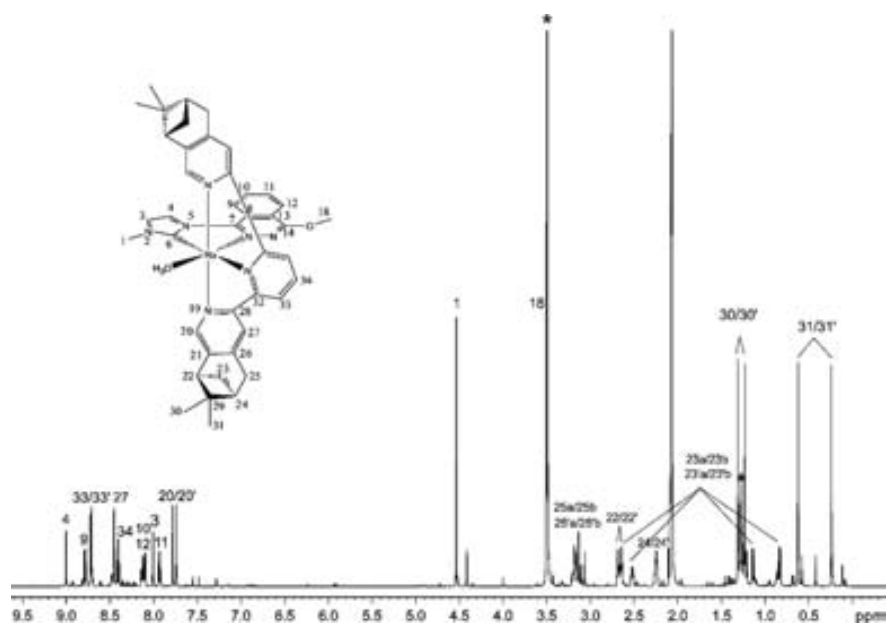
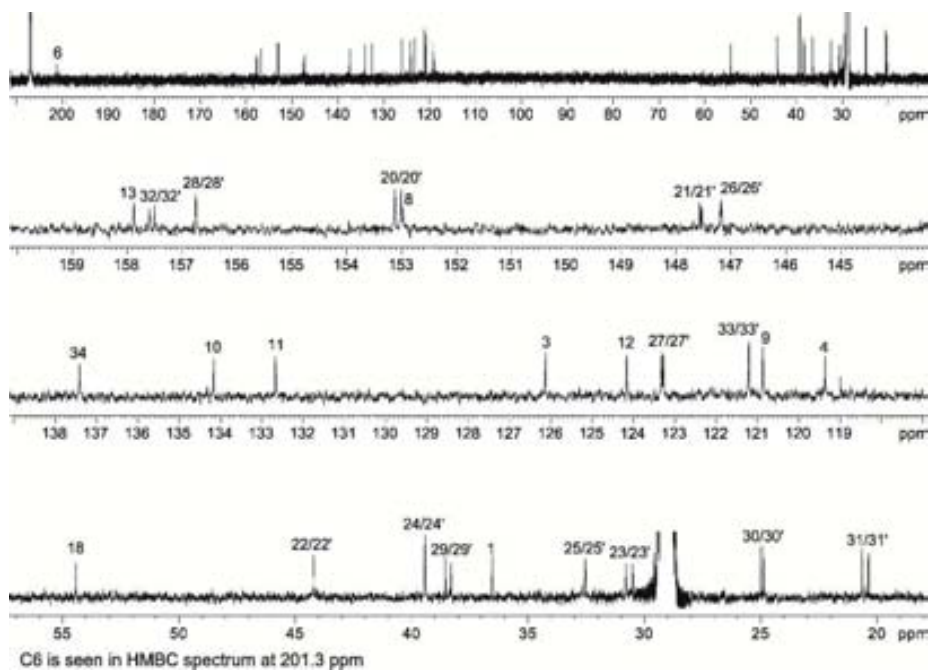


Figure S3. 1D and 2D NMR spectra of **C5-OH<sub>2</sub>** (600 MHz, 298K, acetone-d<sub>6</sub>): a) <sup>1</sup>H NMR, b) <sup>13</sup>C NMR, c) HSQC, d) HMBC, e) COSY, f) ROESY

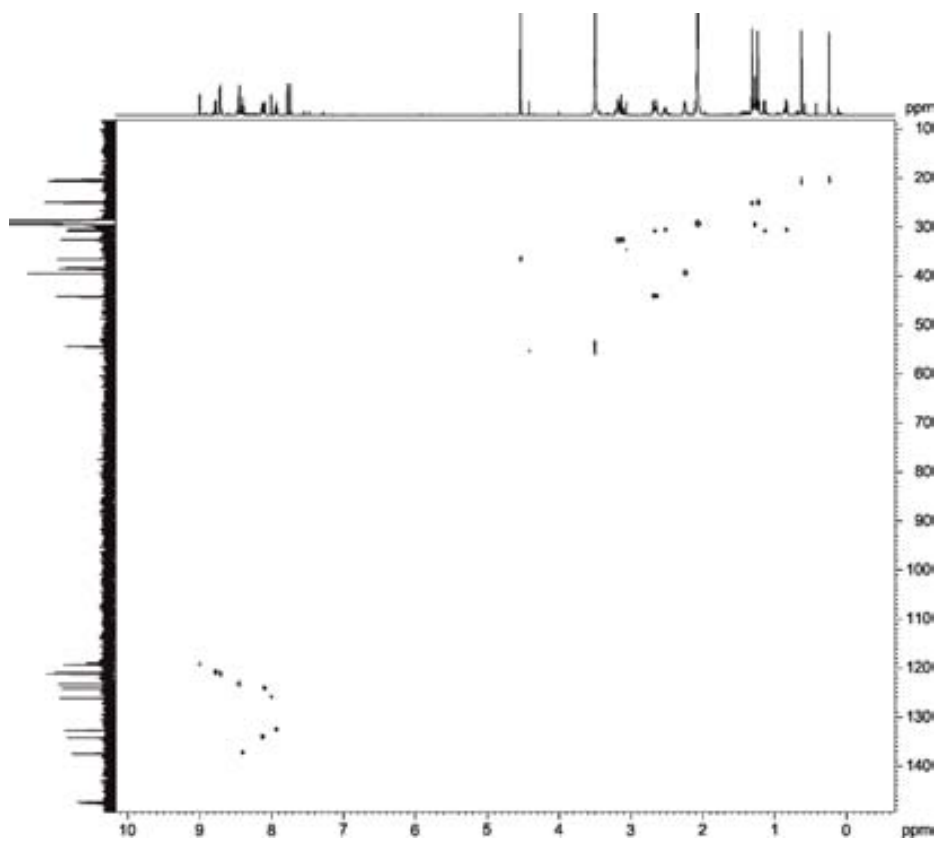
a)



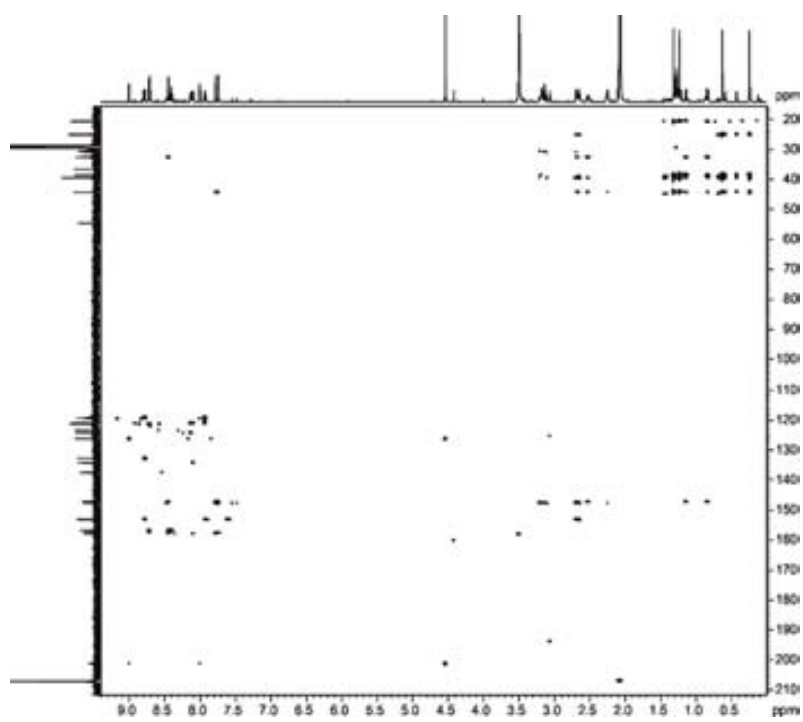
b)



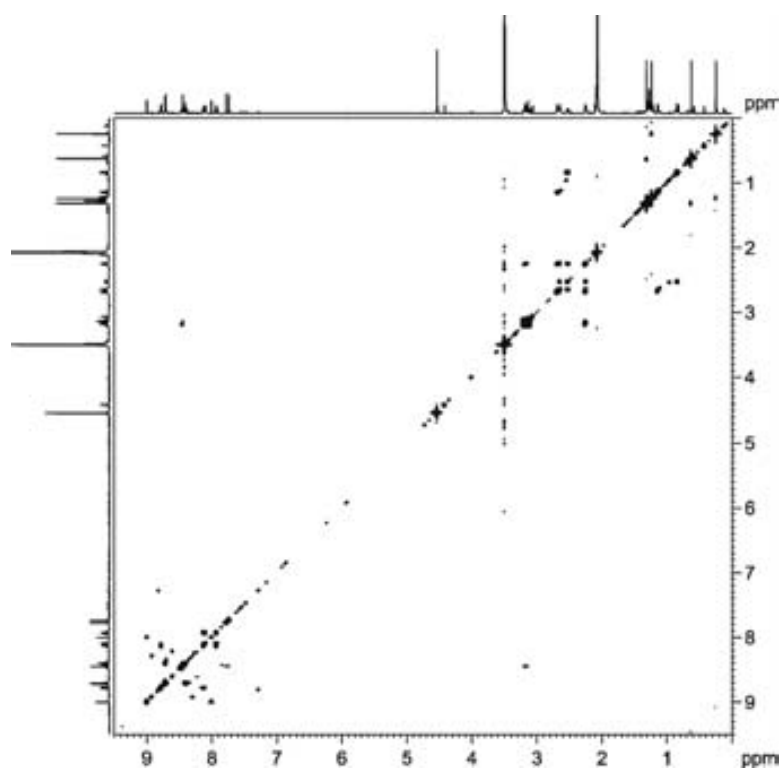
c)



d)



e)



f)

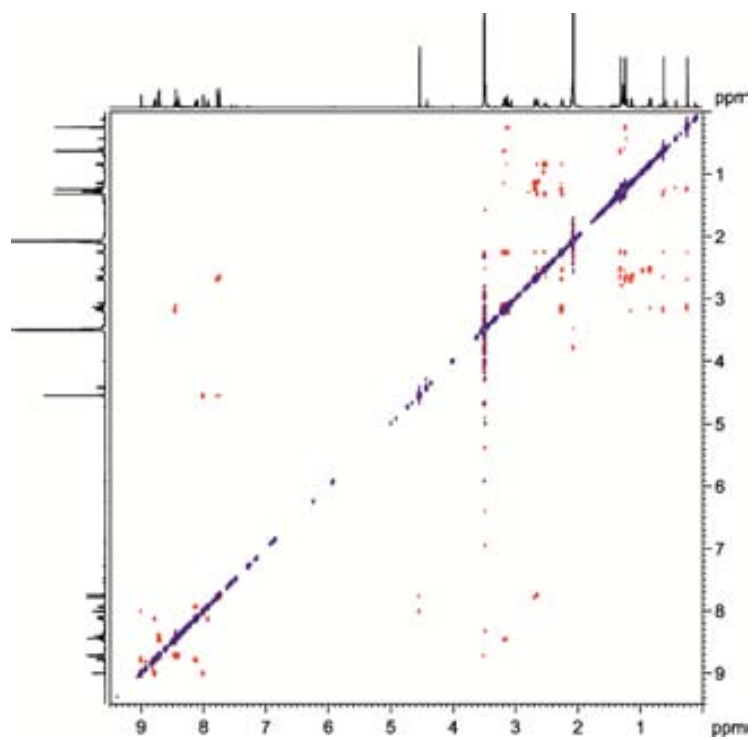


Figure S4. ESI-MS spectrum of C5-Cl

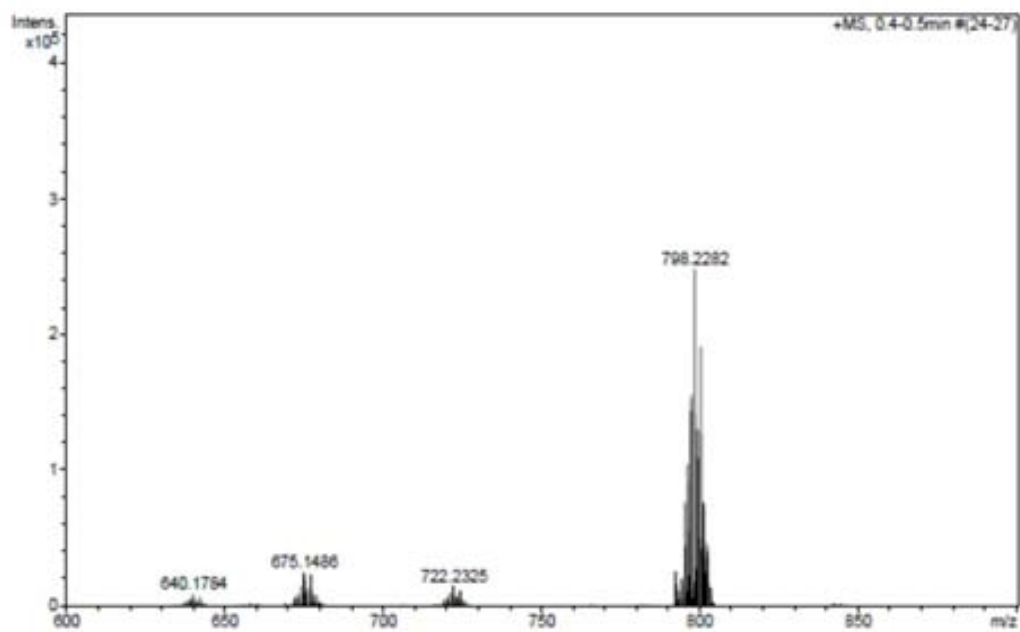
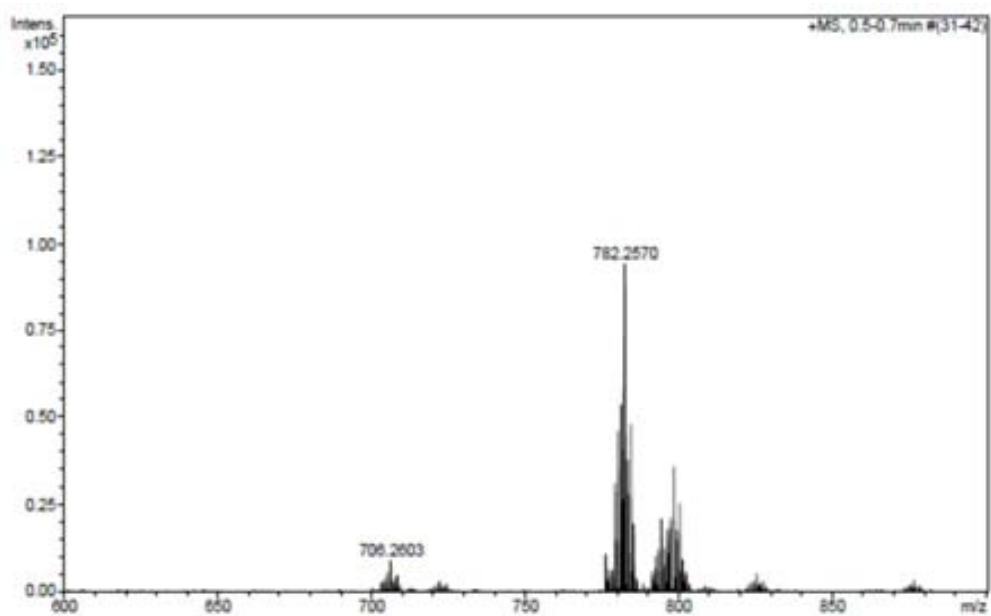


Figure S5. ESI-MS spectrum of C5-OH<sub>2</sub>



## Chapter V. Conclusions

### I.

#### Conclusions

1. A new tetradentate dinucleating NHC ligand, **L1**<sup>2+</sup>, has been synthesized and fully characterized by means of NMR spectroscopy and X-ray diffraction analysis.
2. Ligand **L1**<sup>2+</sup> partially decompose in nucleophilic protic solvents at high temperatures due to C-N bond scission.
3. Four ruthenium mononuclear chlorido and aqua complexes with general formula [Ru(PhthaPz-R)(T)X]<sup>n+</sup> (X = Cl, n = 1, X = H<sub>2</sub>O, n = 2 ; R = Methyl, Isopropyl; PhthaPz = 1,6-(1-methylimidazole)phthalene), T = trpy, bpea or tpm), have been successfully prepared by combining **L1**<sup>2+</sup> with [Ru(T)Cl<sub>3</sub>] type of precursors in nucleophilic protic solvents such as MeOH and iPrOH. Partial decomposition of the tetradentate NHC ligand to a bidentate scaffold takes place also in these conditions.
4. The spectroscopic and electrochemical properties of the eight prepared complexes have been thoroughly analyzed by means of NMR and UV-vis spectroscopy, CV and spectrophotometric titration with Ce<sup>IV</sup>.
5. A gradual destabilization of the Ru(III) oxidation state in aqueous media has been observed for the aqua complexes prepared: **C4**-OH<sub>2</sub> (bpea) increase its oxidation state through mono-electronic processes ( $\Delta E_{1/2} = 200$  mV) via Ru(III), **C1**-OH<sub>2</sub> and **C2**-OH<sub>2</sub> manifest quasi-bielectronic process ( $\Delta E_{1/2} = 40$  mV) and

complex **C3-OH<sub>2</sub>** is oxidized through bi-electronic processes ( $\Delta E_{1/2} \leq 0$  mV), being Ru(III) unstable with regards to disproportionation.

6. **C1-OH<sub>2</sub>** and **C2-OH<sub>2</sub>** are instable in aqueous media and progressively decompose/transform to other Ru-based species still unidentified.
7. The four aqua complexes show poor stability due to ligand oxidation under the harsh reaction conditions employed for the oxidation of water. The concomitant evolution of CO<sub>2</sub> and O<sub>2</sub> clearly reflects the weakness of the PhthaPz-OR family of ligands under oxidative conditions. Higher TON values are obtained for the trpy-based complexes **C1-OH<sub>2</sub>** and **C2-OH<sub>2</sub>** when compared with the bpea/tpm ones (**C3-OH<sub>2</sub>/C4-OH<sub>2</sub>**), which manifests the much less robust character of the latter with regards to oxidation.
8. Complexes where bi-electronic oxidative redox processes are favored show better performance and selectivity in the epoxidation of alkenes with  $\text{PhI}(\text{OAc})_2$ . The comparatively lower oxidation capacity of complex **C3-OH<sub>2</sub>** mainly originates from both; the easy oxidation of the tpm ligand under the reaction conditions and the much higher steric encumbrance of this facial ligand. When *cis*- $\beta$ -methylstyrene is employed as substrate, no *cis/trans* isomerization takes place, therefore leading to stereospecific epoxidation processes.

## II.

### Conclusions

1. The chiral ligand **L2** ([4,5]pinene-trpy) has been successfully coordinated to RuCl<sub>3</sub> leading to the chiral precursor [Ru<sup>III</sup>(**L2**)Cl<sub>3</sub>], which has been characterized by means of MS and CV.



2. Two chiral Ru complexes with general formula  $[\text{Ru}^{\text{II}}(\mathbf{L2})(\text{PhthaPz-Ome})\text{X}]^{n+}$  ( $\mathbf{L2} = [4,5]\text{pinene-trpy}$ ;  $\text{X} = \text{Cl}$ ,  $n = 1$ ;  $\text{X} = \text{OH}_2$ ,  $n = 2$ ) have been synthesized and fully characterized by means of NMR and UV-vis spectroscopies.
3. The aqua complex  $\mathbf{C5-OH}_2$  was preliminary tested as a catalyst for the enantioselective epoxidation of styrene and *cis*- $\beta$ -methylstyrene in dichloroethane giving low ee values of about 20%. This result demonstrates the capacity of the ligand combination to enantiodifferentiate prochiral substrates. However, the remote position of the chiral pinene moieties with regard to the Ru-O active site is probably responsible for the low ee value observed.